Energy CONSERVATION

DOE/CS/54209-18
(DE85000326)

HYBRID VEHICLE PROGRAM

Final Report

June 1984

Work Performed Under Contract No. AI01-78CS54209

General Electric Company
Schenectady, New York

Technical Information Center
Office of Scientific and Technical Information
United States Department of Energy

DISCLAIMER

DISCLAIMER

Available from the National Technical Information Service, U. S. Department of Commerce, Springfield, Virginia 22161.

Price: Printed Copy A10
Microfiche A01

Codes are used for pricing all publications. The code is determined by the number of pages in the publication. Information pertaining to the pricing codes can be found in the current issues of the following publications, which are generally available in most libraries: *Energy Research Abstracts (ERA); Government Reports Announcements* and Index *(GRA* and I); *Scientific and Technical Abstract Reports (STAR);* and publication NTIS-PR-360 available from NTIS at the above address.

THIS PAGE

WAS INTENTIONALLY

LEFT BLANK

ABSTRACT

This report summarizes the activities on the Hybrid Vehicle Program. The program objectives and the vehicle specifications are reviewed. The Hybrid Vehicle has been designed so that maximum use can be made of existing production components with a minimum compromise to program goals. This report presents the program status as of the February 9-10 Hardware Test Review and includes discussions of the vehicle subsystem, the hybrid propulsion subsystem, the battery subsystem, and the test mule programs. Other program aspects included are quality assurance and support equipment.

FOREWORD

This Final Report for the Hybrid Vehicle Program (Phase II) is submitted to the Jet Propulsion Laboratory of the California Institute of Technology to fulfill Data Requirement No. 23, Final Report, of Contract No. 955190 (Phase II).

This report is a comprehensive summary of the activities on the Hybrid Vehicle Program (Phase II). The following Work Breakdown Structure (WBS) levels are covered in the report:

100 Program Management
200 System Analysis and Design
300 Vehicle Subsystem
400 Hybrid Propulsion Subsystem
500 Battery Subsystem
600 Mule Program
700 Test and Evaluation
800 Quality Assurance
900 Manufacturing Studies and Evaluation (cancelled)
1000 Support Equipment

ACKNOWLEDGEMENTS

The Hybrid Vehicle Program has included inputs of many people. The list of names of the contributors is too extensive to attempt to include here. However, we do wish to acknowledge the following participating organizations:

- United States Department of Energy – Electric and Hybrid Vehicle Program
- Jet Propulsion Laboratory of the California Institute of Technology
- Triad Services, Inc.
- Research Division of Volkswagen A.G. (VW) (West Germany)
- Globe Battery Division of Johnson Controls
- Direct Current Motor and Generator (DCM&G) Department of the General Electric Company
- Audio-Video Corporation
- Daihatsu Motor Co., Ltd. (Japan)

TABLE OF CONTENTS

Section		Page
1	EXECUTIVE SUMMARY	1-1
	1.1 INTRODUCTION AND BACKGROUND	1-1
	1.2 OBJECTIVE OF HYBRID VEHICLE PROGRAM	1-1
	1.3 ENERGY CONSUMPTION CHARACTERISTICS	1-2
	1.3.1 Cost and Consumer Acceptance	1-2
	1.4 SUMMARY OF MAJOR TECHNICAL TASKS	1-3
	1.4.1 System Analysis and Design	1-3
	1.4.1.1 Characterization	1-3
	1.4.1.2 Operation	1-5
	1.4.1.3 Performance	1-7
	1.4.2 Mule Program	1-8
	1.4.3 Vehicle Subsystem	1-10
	1.4.4 Hybrid Propulsion Subsystem	1-10
	1.4.5 Battery Subsystem	1-11
	1.5 CONCLUSIONS	1-13
2	INTRODUCTION	2-1
3	PROGRAM MANAGEMENT	3-1
	3.1 PROGRAM ORGANIZATION	3-1
	3.2 WORK BREAKDOWN STRUCTURE	3-1
	3.3 PROGRAM SCHEDULE	3-1
	3.3.1 Summary Network Schedule	
	3.3.2 Summary Schedule of Deliverable and Performance Items	3-10
	3.4 PROGRAM CONTROL PLAN	3-11
	3.4.1 Program Scheduling	3-11
	3.4.2 Allocation of Resources	3-11
	3.4.3 Cost Control	3-14
	3.4.4 Performance Measurement System	3-14
	3.4.5 Configuration Control	3-14
	3.4.6 Subcontractor Management and Direction	3-14
4	SYSTEM ANALYSIS AND VEHICLE CHARACTERISTICS	4-1
	4.1 INTRODUCTION	4-1
	4.2 POWER TRAIN AND VEHICLE CHARACTERISTICS	4-2
	4.2.1 Weight Breakdown	4-2
	4.2.2 Road Load	4-4
	4.2.3 Acceleration and Gradeability Performance	4-6
	4.2.4 Fuel Economy and Energy Usage	4-8
5	DESIGN AND DEVELOPMENT	5-1
	5.1 INTRODUCTION	5-1
	5.2 VEHICLE SUBSYSTEM	5-1
	5.2.1 Vehicle Analysis	5-1
	5.2.1.1 Riding and Handling	5-1
	5.2.1.2 Tire Test	5-3
	5.2.1.3 Brakes	5-3

TABLE OF CONTENTS (Cont'd)

Section			Page
	5.2.1.4	Aerodynamic Testing	5-4
	5.2.1.5	Structural Design	5-5
	5.2.1.6	Front Structural Component Static Crush Tests	5-5
	5.2.1.7	Front End Crush Test	5-7
	5.2.1.8	Battery Box Dynamic Crush	5-8
	5.2.1.9	Computer Simulation Analysis	5-9
	5.2.1.10	Vehicle Weight and Distribution	5-11
5.2.2		Vehicle Design	5-11
	5.2.2.1	Vehicle Specifications	5-11
	5.2.2.2	Packaging	5-11
	5.2.2.3	Styling	5-12
	5.2.2.4	Body Structure	5-13
	5.2.2.5	Chassis	5-18
	5.2.2.6	Operator Controls	5-23
	5.2.2.7	Heating, Ventilation, Air-Conditioning, and Electrical Systems	5-25
5.3		HYBRID PROPULSION SUBSYSTEM	5-29
5.3.1		System Overview and Control Strategy	5-29
	5.3.1.1	Hybrid Propulsion System	5-29
	5.3.1.2	Overall Control Strategy	5-30
	5.3.1.3	Thermal Analysis	5-32
	5.3.1.4	Power Train Losses and Accessory Loads	5-34
5.3.2		Drive Motor	5-35
	5.3.2.1	Motor Description	5-36
5.3.3		Engine and Engine Clutch	5-37
	5.3.3.1	Engine	5-37
	5.3.3.2	Starting Clutch	5-40
5.3.4		Torque Transfer Unit and Transmission	5-42
5.3.5		Power Electronics	5-54
	5.3.5.1	Field Chopper	5-54
5.3.6		Controller	5-62
	5.3.6.1	HTV Controller Hardware	5-64
	5.3.6.2	Controller Software	5-67
5.3.7		HTV Sensors	5-68
5.3.8		Safety, Reliability, and Maintainability	5-74
	5.3.8.1	Safety	5-74
	5.3.8.2	Reliability	5-75
	5.3.8.3	Maintainability	5-75
5.4		BATTERY SUBSYSTEM	5-76
5.4.1		Battery (EV-1300)	5-76
	5.4.1.1	Design and Specifications	5-76
	5.4.1.2	Fabrication	5-80
	5.4.1.3	Battery Testing	5-82
	5.4.1.4	Battery Charging	5-87
	5.4.1.5	Battery Maintenance	5-88
5.4.2		Battery State-of-Charge	5-89
	5.4.2.1	Methodology	5-89

TABLE OF CONTENTS (Cont'd)

Section			Page
		5.4.2.2 State-of-Charge Unit and Its Use in the HTV	5-90
		5.4.2.3 Testing of the SOC System	5-91
	5.4.3	HTV On-board Microcomputer-Controlled Battery Charger	5-92
		5.4.3.1 Battery Charger Design	5-93
		5.4.3.2 Charger Control Strategy	5-95
		5.4.3.3 Battery Charger Operational Tests	5-97
	5.5	MULE PROGRAM	5-99
	5.5.1	Test Bed Mule	5-99
		5.5.1.1 Test Bed Mule Vehicle Design and Description	5-99
		5.5.1.2 Propulsion System Design and Fabrication	5-101
		5.5.1.3 Test Bed Mule Controller	5-105
		5.5.1.4 Engine Throttle Control System	5-109
		5.5.1.5 Power Train/Controller/Vehicle Integration	5-111
		5.5.1.6 TBM Vehicle Tests	5-112
	5.5.2	Structural Mule	5-117
		5.5.2.1 Base Vehicle Selection	5-117
		5.5.2.2 Body and Chassis Design	5-117
		5.5.2.3 Drive Components	5-118
		5.5.2.4 Fabrication Methods	5-118
		5.5.2.5 Scheduled Tests	5-118
	5.5.3	Mechanical Components Mule	5-118
		5.5.3.1 Base Vehicle Selection	5-118
		5.5.3.2 Body Modification	5-119
		5.5.3.3 Frame Modification	5-119
		5.5.3.4 Chassis Components	5-119
		5.5.3.5 Heating, Ventilating, and Air-Conditioning (HVAC)	5-120
		5.5.3.6 Fabrication Methods	5-121
		5.5.3.7 Instrumentation	5-122
		5.5.3.8 Transmission Development	5-123
		5.5.3.9 Clutch Development	5-123
		5.5.3.10 Ride and Handling Development	5-123
		5.5.3.11 Drive Train Mounting Development	5-123
	5.5.4	Hybrid Power Train Mule	5-124
		5.5.4.1 HPTM Development and Integration	5-124
		5.5.4.2 HPTM Vehicle Tests	5-126
6		HTV TEST AND EVALUATION	6-1
	6.1	INTRODUCTION	6-1
	6.2	TEST DESCRIPTION	6-1
	6.3	HYBRID TEST VEHICLE TEST RESULTS	6-3
	6.3.1	Performance Test Results	6-3
		6.3.1.1 Continuous Cruise	6-3
		6.3.1.2 Gradeability	6-3

TABLE OF CONTENTS (Cont'd)

Section		Page
	6.3.1.3 Acceleration	6-4
	6.3.1.4 On-Board Battery Charger	6-5
	6.4 SIGNATURE TEST RESULTS	6-6
7	QUALITY ASSURANCE	7-1
8	SUPPORT EQUIPMENT	8-1
	8.1 OVERVIEW	8-1
	8.2 DATA ACQUISITION SYSTEM	8-5
	REFERENCES	Refs-1

LIST OF ILLUSTRATIONS

Figure		Page
1.1-1	Hybrid Test Vehicle (HTV)	1-1
1.1-2	Hybrid Test Vehicle Schematic	1-2
1.4.1-1	Schematic of HTV Power Train	1-5
1.4.5-1	Cutaway View of the Hybrid Vehicle Battery Configuration	1-11
3.1-1	Relationship of GE Hybrid Vehicle Program to JPL and DOE	3-2
3.1-2	Relationship of the General Electric Company to the Hybrid Vehicle Program	3-3
3.1-3	Corporate Research and Development Hybrid Vehicle Program (Phase II) Organization	3-4
3.3.1-1	Summary Network Schedule	3-12
4.2-1	Schematic of HTV Power Train	4-3
4.2-2	Hybrid Test Vehicle (HTV) Weight Breakdown Based on Weight of Individual Components	4-5
4.2-3	HTV Road Load for Various Grades as a Function of Speed	4-7
4.2-4	Pulsed Power Characteristics of the Hybrid Vehicle Battery	4-9
4.2-5	Ampere-hour Capacity of the Hybrid Vehicle Battery for Constant Current Discharge	4-10
4.2-6	Hybrid Vehicle Battery State-of-Charge and Fuel Economy for Urban and Highway Driving	4-10
4.2-7	Average Energy Usage (kWh/mi) — Battery Electricity and Petroleum Equivalent	4-11
4.2-8	The Operating V-Mode Schedule in the HTV for VM-Starting Values of 60 mph and 40 mph	4-11
4.2-9	Hybrid Vehicle Fuel Economy (including petroleum used to generate electricity)	4-13
4.2-10	Average Annual Fuel Economy for the Hybrid Vehicle in Urban Driving	4-14
5.2-1	Hybrid Test Vehicle (HTV)	5-2
5.2-2	Scale Model in Wind Tunnel	5-6
5.2-3	Static Crush Test (overall view)	5-7
5.2-4	Static Crush Test (close-up)	5-8
5.2-5	Engine into Battery Box (force vs. displacement)	5-9

LIST OF ILLUSTRATIONS (Cont'd)

Figure		Page
5.2-6	Comparison of Predicted Hybrid Vehicle Deceleration With General Motors A-Body Test Results	5-10
5.2-7	Full-sized Clay Model (Hatchback)	5-13
5.2-8	HTV Full-sized Scale Model (Notchback)	5-14
5.2-9	General Arrangement of the Vehicle Body	5-14
5.2-10	Front Structure	5-15
5.2-11	Battery Box Mounted in HTV	5-17
5.2-12	Front Suspension	5-18
5.2-13	Rear Suspension	5-19
5.2-14	General Arrangement of Steering Gear and Linkage	5-20
5.2-15	Exhaust Route (top view)	5-21
5.2-16	Fuel Supply System	5-22
5.2-17	Accessory Drive (passenger side view)	5-24
5.2-18	Sectional View of Motor - Accessory Drive and Transmission Pump	5-25
5.2-19	Sectional View of Engine Accessory Drive	5-26
5.2-20	Instrument Panel	5-27
5.2-21	Sketch of Air-Conditioning Unit	5-28
5.2-22	Schematic of Heater Water Flow	5-28
5.2-23	Combustion Heater	5-29
5.3-1	Hybrid Vehicle Power Train Schematic (two-shaft, front-wheel drive)	5-30
5.3-2	Calculated Battery Temperature Change in Urban Driving	5-34
5.3-3	Battery Box Airflow for Cooling	5-35
5.3-4	HTV Loss/Accessory Load Breakdown	5-36
5.3-5	Power Required for HTV, HPTM, and TBM in Neutral with Accessories Operating	5-36
5.3-6	HTV Drive Motor	5-38
5.3-7	Electrical Connection Diagram for the HTV Drive Motor	5-39
5.3-8	Fuel-injected (CIS) Audi Engine (1.7 liter, unmodified engine)	5-40
5.3-9	Engine-starting Clutch	5-41
5.3-10	Heat Engine Drive Spline Shaft/Sprocket Assembly	5-43
5.3-11	Engine-Starting Clutch Characteristics	5-44
5.3-12	Schematic Diagram of HTV Drive	5-45

LIST OF ILLUSTRATIONS (Cont'd)

Figure		Page
5.3-13	Sectional View of Drive Clutch (C_2)	5-46
5.3-14	Transfer Case with Cover Removed	5-47
5.3-15	HTV High-Pressure Hydraulic Block Diagram	5-48
5.3-16	Final Drive	5-49
5.3-17	Hydraulic Pump	5-51
5.3-18	Schematic Diagram of Transmission Hydraulic Circuit	5-52
5.3-19	Power Control Circuit Block Diagram	5-54
5.3-20	Field Chopper Power Circuit	5-56
5.3-21	Field Chopper Logic/Base Drive Circuit Board	5-57
5.3-22	HTV Field Chopper	5-59
5.3-23	Block Diagram of Printed Circuit Coil Driver	5-60
5.3-24	Coil Driver Printed Circuit	5-61
5.3-25	HTV Electrical Interface Box	5-62
5.3-26	Schematic of the HTV Propulsion System	5-63
5.3-27	Simplified Propulsion Sequencing Diagram	5-64
5.3-28	Block Diagram of Motor Feedback Control System	5-65
5.3-29	Block Diagram of Heat Engine Feedback Control System	5-66
5.3-30	Simulated Dynamic Response of the Engine to a Step Change in Power Command	5-66
5.3-31	HTV Microcomputer Control	5-67
5.3-32	Block Diagram of HTV Controller Functions	5-68
5.3-33	Block Diagram of Sequencing Functions	5-69
5.3-34	Power Control Functions	5-69
5.3-35	Functional Block Diagram of Armature Current/Armature Voltage Board	5-72
5.3-36	IA-VA (Armature Current/Armature Voltage) Circuit Board	5-73
5.4-1	Cutaway View of the Hybrid Vehicle Battery Configuration	5-78
5.4-2	EV-1300 Battery	5-79
5.4-3	Acid Pump Schematic	5-80
5.4-4	Battery Pack Mounted In HTV	5-81
5.4-5	Battery Pack and Accessory Systems	5-82
5.4-6	Cell Cycle Performance Test Data	5-85

LIST OF ILLUSTRATIONS (Cont'd)

Figure		Page
5.4-7	Constant-Current Discharge Characteristics of the HTV Battery	5-87
5.4-8	Comparison of Expected and Measured Constant-Current Discharge Characteristics of the HTV Battery	5-89
5.4-9	Pulsed Power Characteristics of the HTV Battery	5-90
5.4-10	Battery State-of-Charge Meter and Microprocessor	5-91
5.4-11	Battery State-of-Charge Test Setup	5-92
5.4-12	Dual HTV Batttery Charger Block Diagram	5-93
5.4-13	HTV Battery Charger Power Circuit	5-94
5.4-14	HTV Battery Charger Control Circuit	5-95
5.4-15	Battery Charger Ground Continuity Detector	5-96
5.4-16	HTV Battery Charger	5-97
5.4-17	HTV Battery Charger Test	5-98
5.5-1	Test Bed Mule — Audi 5000	5-99
5.5-2	Drive Components of Test Bed Mule	5-101
5.5-3	Schematic Diagram of Test Bed Mule Driveline	5-102
5.5-4	Torsional Damper Components	5-103
5.5-5	Sectional View of Transfer Drive Unit	5-104
5.5-6	Transfer Drive Chain, Sprockets, and Housing	5-104
5.5-7	Vehicle Starting Clutch, Accessory Drive Flex Plate	5-105
5.5-8	Modified Transaxle	5-106
5.5-9	Test Bed Mule Propulsion System	5-107
5.5-10	Simplified TBM/HTV Propulsion Sequencing Diagram	5-107
5.5-11	Functional Block Diagram of TBM Controller Software	5-108
5.5-12	Controller Hardware Mounted in a Cabinet	5-109
5.5-13	TBM Custom Signal Conditioning Board	5-110
5.5-14	Block Diagram of Throttle Control System	5-110
5.5-15	Throttle Control Bench Test (front view)	5-111
5.5-16	Throttle Control Bench Test (rear view)	5-112
5.5-17	Response of Engine Throttle Control Unit to Step Changes in Acceleration Pedal	5-113
5.5-18	Transient Response of Throttle Control Unit	5-114
5.5-19	Comparison of TBM Fuel Economy Test Data and HYVEC Predictions for the EPA, Urban, and Highway Cycles	5-116

LIST OF ILLUSTRATIONS (Cont'd)

Figure		Page
5.5-20	Comparison of TBM Electrical Use Data and HYVEC Predictions for the EPA, Urban, and Highway Cycles	5-116
5.5-21	The Shortened Body of the Mechanical Components Mule	5-119
5.5-22	Front Structure and Battery Box of the Mechanical Components Mule	5-120
5.5-23	Rear Structure of the Mechanical Components Mule	5-121
5.5-24	Rear Suspension of the Mechanical Components Mule	5-122
5.5-25	Auxiliary Heater Installation in the Mechanical Components Mule	5-123
5.5-26	HPTM Parallel Shaft Hybrid Power Train	5-125
5.5-27	Hybrid Power Train Test Stand (Rickshaw) on the Dynamometer at General Electric	5-125
5.5-28	The Electronics and Vehicle Controller Packaged in the Trunk of the HPTM	5-126
5.5-29	The Engine and Battery Box under the Hood of the HPTM	5-127
6.3-1	HTV Gradeability Characteristics	6-4
6.3-2	HTV Maximum Effort Acceleration Response	6-5
6.3-3	Comparison of Maximum Effort Acceleration in Hybrid Mode — Test and HYVEC	6-6
8.1-1	IA/VA Card Exerciser	8-1
8.1-2	Coil Driver Card Exerciser	8-2
8.1-3	Field Chopper Card Exerciser	8-3
8.1-4	Debug Panel	8-4
8.1-5	HTV Controller Exerciser	8 5
8.1-6	Data Acquisition System	8-6

LIST OF TABLES

Table		Page
1.2-1	Hybrid Vehicle Design Goals Summary	1-3
1.3-1	Energy Consumption Characteristics	1-4
1.4.1-1	HTV Power Train Characteristics	1-6
1.4.1-2	Summary of Weight Differences Between Hybrid and Downsized (5/6 passenger) ICE Cars	1-6
1.4.1-3	HTV Performance	1-7
1.4.1-4	Comparison of Gasoline and Energy Usage for Hybrid and Conventional ICE Vehicles (50th-percentile owner)	1-8
1.4.1-5	Power Train Control Strategy	1-9
1.4.5-1	Hybrid Vehicle Battery Module Specifications and Final Battery Characteristics	1-12
3.2-1	Expanded Work Breakdown Structure for Near-Term Hybrid Vehicle, Phase II	3-5
3.3.2-1	Summary of Documentation Schedule	3-13
4.1-1	Hybrid Vehicle Minimum Performance Requirements	4-1
4.2-1	HTV Power Train Characteristics	4-4
4.2-2	Weight Breakdown of the Hybrid Power Train	4-6
4.2-3	Summary of Weight Differences Between Hybrid and Conventional ICE 5 Passenger Cars	4-6
4.2-4	HTV Road Load for Various Grades as a Function of Speed	4-7
4.2-5	Vehicle and Component Characteristics for the HTV	4-9
4.2-6	Calculation of Equivalent Fuel Economy of Hybrid Vehicle Including Petroleum Needed to Generate the Electricity Used	4-12
4.2-7	Comparison of Gasoline and Energy Usage for Hybrid and Conventional ICE Vehicles (50th-Percentile Owners)	4-15
5.2-1	Comparison of HTV and Typical Car Performance Parameters	5-3
5.2-2	Steady-State Rolling Resistance (30 mph)	5-4
5.2-3	Summary of Test Results from EPA Urban Cycle Tests	5-5
5.2-4	Front Suspension Specifications	5-19
5.2-5	Rear Suspension Specifications	5-20
5.2-6	Brake Specifications	5-21
5.3-1	Power Train Control Strategy	5-31
5.3-2	Special Operating Modes for the HTV	5-32

LIST OF TABLES (Cont'd)

Table		Page
5.3-3	Summary of HTV Heat Generation	5-33
5.3-4	HTV Drive Motor Design Parameters	5-37
5.3-5	Field Chopper Requirements	5-55
5.3-6	Hybrid Integrated Test Vehicle Sensors	5-70
5.4-1	Hybrid Vehicle Battery Module Specifications and Characteristics	5-76
5.4-2	Cell Constant-Current Discharges	5-83
5.4-3	Cell Pulse Power Tests	5-84
5.4-4	Cell Test Summary	5-84
5.4-5	Effects of Charging Conditions on Charging Times for the HTV Battery	5-85
5.4-6	Pulsed Profile Discharge Characteristics of the HTV Battery	5-88
5.4-7	HTV Onboard Battery Charger Ratings	5-93
5.5-1	Test Bed Mule Weight Breakdown	5-100
5.5-2	TBM Test Results-Cycle Emissions and Fuel Economies	5-115
6.2-1	Vehicle Parameters Used for GE Dynamometer Tests	6-2
6.2-2	HTV-1 Signature Test Summary	6-2
6.3-1	HTV Maximum Effort Acceleration Performance	6-6
6.3-2	Battery Charger Test Summary	6-7
6.3-3	HTV Signature Test Step Response Summary	6-7
6.3-4	Hybrid Mode Signature Test — 88 kW Step, Brake at BP = 0.5, VMode = 40 mph	6-8
6.3-5	Signature Test Summary Multiple EPA Cycles Followed by Step Accelerations (VM = 40 mph)	6-9
7-1	Quality Assurance/Inspection	7-1

Section 1

EXECUTIVE SUMMARY

1.1 INTRODUCTION AND BACKGROUND

The Electric and Hybrid Vehicle (EHV) Program was established in the U.S. Department of Energy (DOE) in response to the Electric and Hybrid Vehicle Research, Development, and Demonstration Act of 1976. Responsibility for the Hybrid Vehicle (HV) Program resides with the Hybrid Vehicle Program Office of DOE. Procurement and management responsibility for the Hybrid Vehicle Program has been assigned to the Jet Propulsion Laboratory (JPL) by DOE.

The hybrid test vehicle (HTV) (Figure 1.1-1) is a five-passenger vehicle utilizing two energy sources, electricity and gasoline fuel. A schematic of the HTV with various subsystems depicted is shown in Figure 1.1-2.

1.2 OBJECTIVE OF HYBRID TEST VEHICLE PROGRAM

The general objective of the Phase II program was to design, fabricate, and deliver to JPL a passenger vehicle which was projected to have the maximum potential for reducing petroleum consumption in the near term (commencing in 1985). The primary minimum vehicle requirements included:

- Capacity for five adult passengers
- Continuous cruise speed of at least 90 km/h (56 mph)
- Elapsed time for 0 to 90 km/h acceleration of 15 s or less
- Sustained speed of 90 km/h on a 3% grade, 1.0 km (.62 mi) long

Figure 1.1-1. Hybrid Test Vehicle (HTV)

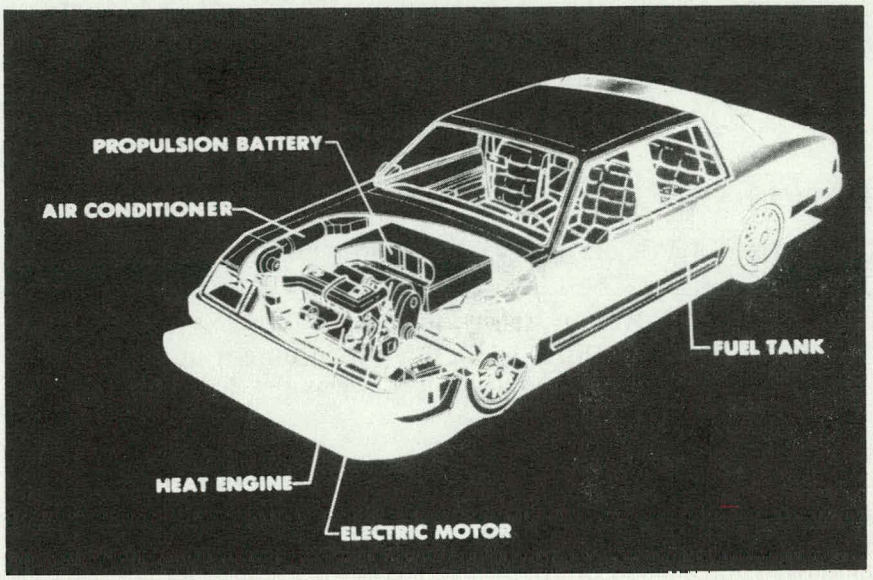

Figure 1.1-2. Hybrid Test Vehicle Schematic

- Compliance with applicable Federal Motor Vehicle Safety Standards (FMVSS), National Highway Traffic Safety Act (NHTSA) standards in effect September 25, 1978, and 1981 Federal Statutory emission standards

A summary of the design goals for the HTV is given in Table 1.2-1.

Under the Phase II program (per Contract Modification 17) two mule vehicles (Test Bed Mule and Hybrid Powertrain Mule) and a Hybrid Test Vehicle (HTV) were designed, fabricated and delivered to Jet Propulsion Laboratory.

1.3 ENERGY CONSUMPTION CHARACTERISTICS

The estimated energy consumption characteristics of the HTV are summarized in Table 1.3-1. Calculations show that for a mission of 11,852 mi/yr, consisting of 65% urban driving and 35% highway driving, the hybrid vehicle saves about 23% of the gasoline that would be used by the ICE reference vehicle having 1980 fuel economy (21 mpg urban, 29 mpg highway). The 1980 fuel economy of mid-size domestic cars is used as the reference because the HTV was built from a 1980 Buick Century using 1980 engine and transmission driveline components.

1.3.1 Cost and Consumer Acceptance

A second important goal of the hybrid vehicle design was to be competitive* with the ICE reference vehicle in first-cost, and equal or lower in total ownership cost. The hybrid vehicle sticker price is estimated at $10,500 in 1980 dollars compared with $7500 (in 1980 dollars) for the ICE reference vehicle. The ownership cost of the hybrid vehicle is about 30¢ per mile, including depreciation, insurance, and maintenance, and a gasoline price of $1.50 per gallon and 5¢/kWh for electricity. The corresponding ownership cost for the ICE reference vehicle is 25¢ per mile.

* Competitive means that the initial cost differential will not be so great as to discourage a potential buyer from purchasing the hybrid vehicle.

Table 1.2-1

HYBRID VEHICLE DESIGN GOALS SUMMARY

Capacity	
Passengers	5 Adults front – two (2) 95 percentile males rear – three (3) 95 percentile males
Cargo (luggage)	0.5m^3 (17.7 ft^3)
Payload (passengers and luggage)	430 kg (1147 lb)
Performance	
Continuous Cruise Speed	105 km/h (65 mph)
Accelerations	0-50 km/h (0-31 mph) in 5 s 0-90 km/h (0-56 mph) in 15 s 40-90 km/h (25-56 mph) in 10 s
Gradeability	Grade / Speed / Distance 3% / 105 km/h (65 mph) / 1.0 km (0.62 mi) 8% / 80 km/h (50 mph) / 0.3 km (0.19 mi) 15% / 40 km/h (25 mph) / 0.2 km (0.12 mi)
Cost	
Consumer Purchase Price	Within reasonable range of purchase price of reference conventional Internal Combustion Engine (ICE) vehicle
Consumer Life Cycle Cost	Same or less than average life cycle cost of the reference vehicle

1.4 SUMMARY OF MAJOR TECHNICAL TASKS

This executive summary describes the development process and significant accomplishments for each of the Hybrid Vehicle Program major technical areas: system analysis and design, the mule program, and the HTV major subsystems (Vehicle, Hybrid Propulsion and Battery).

1.4.1 System Analysis and Design

System analysis and design was concerned with the overall characterization, operation, and performance of the HTV as a system.

1.4.1.1 Characterization

The HTV is a parallel hybrid utilizing a two-shaft, transverse arrangement with the entire power train packaged under the hood. A schematic of the power train is shown in Figure 1.4.1-1. The power train characteristics of the HTV are summarized in Tables 1.4.1-1 to 1.4.1-4. As expected, the weight of the HTV is higher than comparable ICE vehicles. Table 1.4.1-2 indicates that the weight penalty for hybridizing the 5/6 passenger 1980 Buick Century using lead-acid batteries is 542 kg (1192 lb), of which 365 kg (800 lb) is due to the battery.

Table 1.3-1

ENERGY CONSUMPTION CHARACTERISTICS

Annual petroleum fuel energy consumption per vehicle compared to reference vehicle over contractor-developed mission[a]	14,720 MJ (14×10^6 Btu) SAVED[b]
Annual total energy consumption[c] per vehicle compared to reference vehicle over contractor-developed mission[a]	7757 MJ (7.4×10^6 Btu) ADDITIONAL[b]
Potential annual fleet petroleum fuel energy savings compared to reference vehicle over contractor-developed mission[d]	15×10^9 MJ (14.2×10^6 Btu)
Potential annual fleet total energy consumption compared to reference vehicle over contractor-developed mission[d]	7.8×10^9 MJ (7.4×10^{12} Btu) ADDITIONAL[b]
Average total energy consumption[c] over maximum nonrefueled range	
E5.1 FHDC (gasoline only)	3.0 MJ/km (27 mpg)
E5.2 FUDC[e]	5.4 MJ/km, (2.42 kWh/mi) 5.4 MJ/km, (2.42 kWh/mi) 3.8 MJ/km (1.70 kWh/mi)
E5.3 J227a (B) (electricity only)	2.8 MJ/km (1.25 kWh/mi)
Average petroleum-based fuel energy consumption over maximum nonrefueled range[a]	
E6.1 FHDC	3.0 MJ/km (27 mpg)
E6.2 FUDC[e]	0.92 MJ/km (90 mpg) 2.3 MJ/km (36 mpg) 3.3 MJ/km (25 mpg)
E6.3 J227a (B)	0 MJ
Total energy[c] consumed versus distance traveled starting with full charge and full tank over the following cycles	
E7.1 FHDC	3.0 MJ/km (1.34 kWh/mi) (Not a Function of Distance)
E7.2 FUDC	5.4 MJ/km at 27 km (2.42 kWh/mi)
E7.3 J227A (B)	2.8 MJ/km (1.25 kWh/mi) (Not a Function of Distance)
Petroleum fuel energy consumed versus distance traveled starting with full charge tank over the following cycles[f]	
E8.1 FHDC	3.0 MJ/km (1.34 kWh/mi) (Not a Function of Distance)
E8.2 FUDC	2.3 MJ/km at 27 km (1.03 kWh/mi)
E8.3 J227a (B)	0 MJ/km (Not a Function of Distance)
Life cycle energy consumption - not analyzed	

1MJ = 0.278 kWh = 948 Btu (0.00758 gal gasoline equivalent)

10^9 MJ/yr (equivalent to 452 barrels crude oil/day)

a) Mission is 11,852 mi/yr: 65% EPA urban cycle, 35% EPA highway cycle.
b) The annual fuel and energy usages of the Reference ICE Vehicle (1980 model) are 490 gallons of gasoline and 64,644 MJ. A fleet of one million Reference ICE Vehicles would use 64×10^9 MJ.
c) Includes energy needed to generate the electricity at the power plant (35% efficiency)
d) For one million hybrid vehicles replacing one million Reference ICE Vehicles (1980 model).
e) The first number corresponds to the first 10 km; the second number to 27 km, the third number to 400 km, at which the gasoline tank is empty.
f) Does not include energy consumption for generating the wall plug electricity.

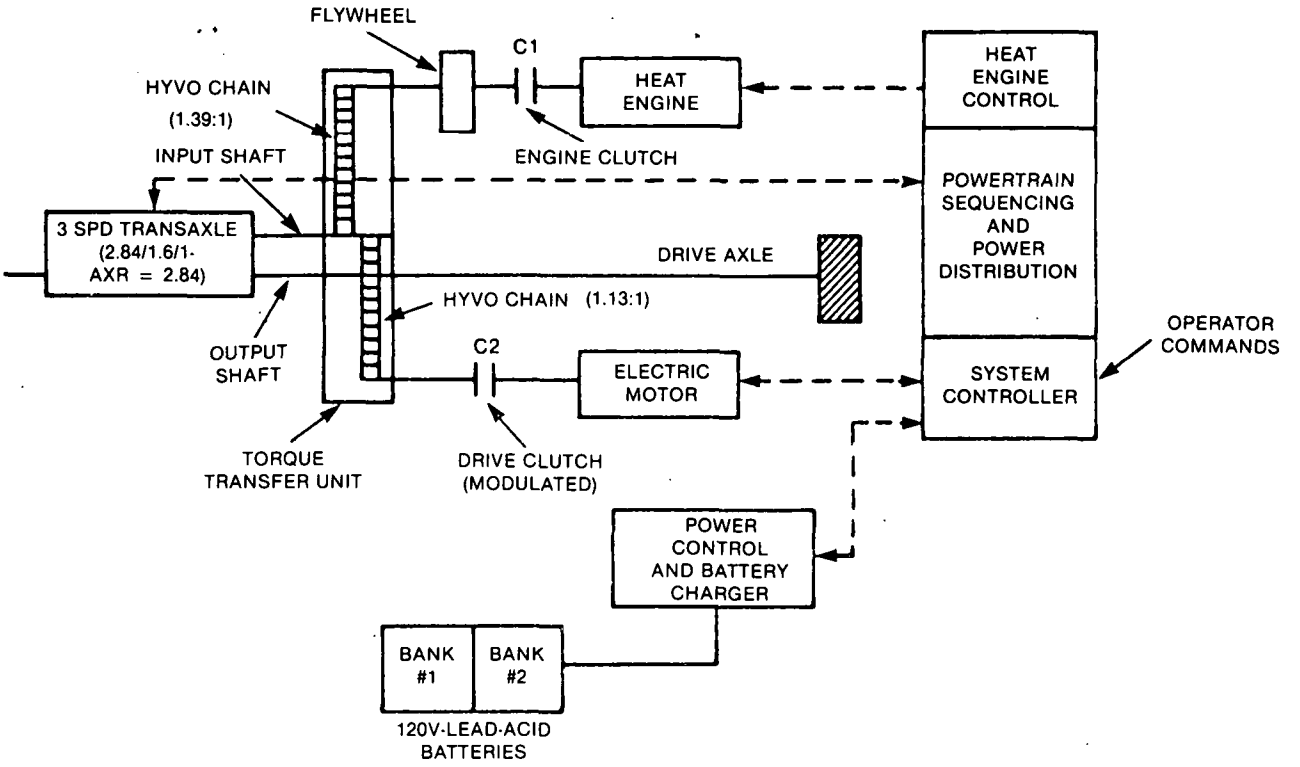

Figure 1.4.1-1. Schematic of HTV Power Train

1.4.1.2 Operation

The control strategy for the HTV has been devised so that the fraction of gasoline saved (compared to the ICE reference vehicle) will be maximized. This requires that the HTV utilize battery-stored electrical energy to power the vehicle whenever possible. Hence, in urban driving, the electric drive system is used alone unless the power demanded exceeds the electric drive system capability and/or the battery state-of-charge falls below 20%. In that event, the heat engine is turned on and it shares the load with the electric motor. When the power demand falls below that which can be provided by the electric motor alone, the heat engine is turned off and the HTV is driven as an electric vehicle. Hence, the heat engine is operated in an on/off mode and is on only when it is providing power. The heat engine never idles.

The two-shaft mechanical arrangement of the hybrid power train permits the electric motor to be decoupled from the driveline when it is not energized by opening the vehicle drive clutch C_2. This avoids all losses due to the motor shaft turning. Development tests of the HPTM and the HTV indicated that there were driveability problems (lags and jerks) associated with the coupling and decoupling of the electric motor into and out of the driveline when the vehicle was accelerating or braking. For that reason, the HTV as delivered does not decouple the electric motor from the driveline when it is de-energized (when the vehicle is operating on the heat engine only). Hence the HTV power train operates essentially as a single-shaft unit from a control point-of-view even though it is a two-shaft mechanical arrangement. The electric motor is, of course, decoupled (the drive clutch C_2 is opened) when the vehicle comes to a stop and the electric motor is idling.

The vehicle speed (V_{MOD}) below which the HTV is operated as an electric vehicle (power demand permitting) is gradually reduced as the battery state-of-charge (SOC) decreases.

Table 1.4.1-1

HTV POWER TRAIN CHARACTERISTICS

Parallel Configuration

- Complete propulsion system under-the-hood
- Transverse, two-shaft arrangement

Electric Drive

- DC separately excited motor (34 kW peak)
- Battery switching, 60 V and 120 V
- Field control

Heat Engine

- Four-cylinder, gasoline, fuel-injected (55 kW peak)
- On/Off operation
- Two-step, starting clutch action

Transmission/Torque Transfer

- Three-speed automatic without torque converter
- Hy-Vo chain drives
- Modulated drive (EM) clutch

Batteries

- Lead-acid, 760 lb (10 modules)
- 12 V, 106 Ah modules
- Electrolyte circulation
- Active cooling

Microcomputer Control

- Propulsion system sequencing
- Transmission shifting
- Electric motor and heat engine control
- Power distribution and blending
- Battery charging

Table 1.4.1-2

SUMMARY OF WEIGHT DIFFERENCES BETWEEN HYBRID AND DOWNSIZED (5/6 PASSENGER) ICE CARS

Vehicle	Curb Weight (kg)	Weight Difference (kg)
HTV (as delivered)	2032	+577
1980 Buick Century (V-6)*	1455	0

Table 1.4.1-3

HTV PERFORMANCE[1]

Acceleration[2]	
0 – 48 km/h (0-30 mph)	8.4 s
0 – 90 km/h (0-56 mph)	18.0 s
40 – 90 km/h (25-56 mph)	10.7 s
Gradeability	
Percent grade	Speed[2] (km/h)
3	>100 (3rd gear)
8	80 (2nd gear)
15	20 (1st gear)
30 (max.)[4]	10
Maximum Speed (km/h)	
100 – electric motor only	
>120 – heat engine only	
>120 – electric motor and heat engine	

1) HTV Performance based on Dynamometer tests of delivered vehicle
2) Electric motor and heat engine combined, battery state-of-charge >30%
3) Heat engine alone
4) Electric motor alone, T_{max} = 140 ft-lb (191 N-m)

When the SOC reaches 20%, the V_{MOD} is set at its minimum value of 12 mph. At this condition, the heat engine is used to recharge the batteries until the SOC reaches at most 30%. The V_{MOD} is then maintained at 12 mph and the electric drive system is used primarily only at low vehicle speeds (less than 12 mph). For highway driving, the heat engine is primary with the V_{MOD} set at 40 mph. The electric drive system is used only to provide peak power for passing and to recover energy in regenerative braking. For the EPA Highway Cycle, using the electric drive system in this way (using 0.3 kWh/cycle*) permits a highway range of about 300 mi before the batteries must be recharged from the heat engine. For easy reference, the HTV power train control strategy is summarized in general terms in Table 1.4.1-5.

The control strategy summarized in Table 1.4.1-5 is that for normal operation of the HTV. There are, however, a number of circumstances in which it is desirable to have the vehicle operate in special ways. Hence, a number of special operating modes have been built into the vehicle controller. These modes can be attained by simply positioning a knob on the outside of the controller panel. Some of the modes are intended primarily for test purposes (e.g., inhibiting regenerative braking) and others would be used primarily in the event of a malfunction in the power train (e.g., electric drive only). Maintenance modes are also provided to permit adjustments of the electric motor and heat engine with the vehicle at rest.

1.4.1.3 Performance

The actual performance of the HTV based on dynamometer tests of the delivered vehicle is summarized in Table 1.4.1-3. The fuel economy and energy usage of the HTV have been calculated using the GE simulation computer program (HYVEC). An overall comparison of

* Based on HYVEC simulation.

Table 1.4.1-4

COMPARISON OF GASOLINE AND ENERGY USAGE FOR HYBRID AND CONVENTIONAL ICE VEHICLES (50th-PERCENTILE OWNER)

	Gasoline Used (Gal)	Electricity Used at Wall Plug (kWh)	Total Energy at Power Plant (kWh)	Petroleum Used* (kWh)
Hybrid Vehicle (HTV)				
Urban driving (32.5 mpg) (7400 mi)	228 (35% saved)	1974	14,610	9,190
Highway driving (27 mpg) (4000 mi)	148	---	5,417	5,417
Total	376 (23% saved)		18,111 (12% greater)	9,605 (18% saved)
Conventional ICE Vehicle (1980 Buick Century)				
Urban driving (21 mpg) (7400 mi)	352	---	12,883	
Highway driving (29 mpg) (4000 mi)	138	---	5,051	
Total	490		17,934	

Energy Cost Saving

Cost Saving = Gasoline 1980 Buick Century − Gasoline HTV-electric HTV
= \$735 − \$564 − \$99 = \$72/yr

Calculation made for gasoline at \$1.50/gal and electricity at 5¢/kWh

*Assuming 13.5% of electricity generated from petroleum.

the hybrid test vehicle and the 1980 ICE vehicle on which the HTV is based is presented in Table 1.4.1-4. The gasoline savings and total energy usage are critically dependent on the usable battery capacity in the hybrid vehicle application. Tests of the test bed mule (TBM) and HTV vehicles have shown that the usable capacity of the lead-acid batteries is much less than expected at the outset of Phase II (see Section 5.4.4). Hence, the fuel savings of the HTV are significantly less than the 50% projected at the beginning of the program.

1.4.2 Mule Program

The mule programs comprise three mule vehicles − the test bed mule (TBM), the mechanical components mule (the role of this vehicle was changed by Contract Modification 17 and the vehicle was renamed the hybrid power train mule), and the structural mule.

The TBM is a modified Audi 100 Avanti, which is the hatchback model of the Audi 5000 marketed in the U.S. The heat engine, clutch, and electric drive components used in the TBM are essentially the same used in the HTV. Integration and checkout of the hydrid

Table 1.4.1-5

POWER TRAIN CONTROL STRATEGY

- On/Off Engine Operation
- Regenerative Braking
- Electric Motor Idling When Vehicle is at Rest
- Electric Drive System Primary -- Battery State-of-Charge Permitting and Vehicle Speed Less Than V_{MODE}*
- Sharing of Load Between Motor and Heat Engine When Both are Needed
- Batteries Recharged by Heat Engine in a Narrow Range (20% < SOC < 30%)
- Electric Motor Dominant in Determining Shift Logic When it is Operating
- Heat Engine Primary for Highway Driving
- Electric Motor Always Used to Initiate Vehicle Motion from Rest and in Low-Speed Maneuvers (e.g., parking)

*V_{MODE} is the vehicle speed above which the heat engine is used to power the vehicle if the power demanded is less than the heat engine peak power capability.

power train, the power electronics, and the controller hardware and software in the test bed mule vehicle were started in December 1980. By the end of February 1981, integration and checkout were completed and the TBM was functioning satisfactorily on a chassis dynamometer in the EHV Laboratory at VW, Wolfsburg, West Germany. Test data indicated good agreement with computer simulations of TBM performance and fuel economy. The vehicle was delivered to JPL in September 1981.

The mechanical components mule was used to check function and fit of the components which make up the suspensions, steering, brakes, drive train, heating, ventilating and air conditioning (HVAC), and hydraulic system of the HTV. The GM E-body Toronado was selected as the base vehicle for the mechanical components mule because it required a minimum of conversion. It was instrumented to provide visual as well as recorded information about the operation of the subsystems in the vehicle. Per Contract Modification 17, the mechanical components mule was retrofitted (summer 1981) with the HTV vehicle controller, and a prototype hybrid power train. This retrofit allowed for a preliminary checkout and debug of the final HTV power train prior to installation in the HTV. With the hybrid power train installed, the vehicle was renamed the Hybrid Power Train Mule (HPTM).

A structural mule was built with the intention of evaluating the overall structural performance of the hybrid vehicle with sufficient leadtime to benefit the final HTV design. Budget cuts in early 1981 (Contract Modification 17) resulted in cancellation of the 30 mph barrier tests of the structural mule. The structure and running gear of the structural mule were then used as vehicle subsystem components for the final HTV. Contract Modification 17 also reduced the number of HTV's to be delivered from two to one.

1.4.3 Vehicle Subsystem

The hybrid vehicle was designed so that maximum use could be made of existing production components with the minimum compromise in program goals. The body center section and the interior were taken from a GM A-body Buick Century. The hybrid vehicle features front-wheel drive, independent front suspension, power rack and pinion steering, lightweight trailing arm and beam rear suspension, low rolling resistance steel-belted radial tires, power brakes, an automatic three-speed transmission (torque converter removed), and air conditioning. The propulsion batteries are packaged under the hood to maximize passenger space.

The chassis front suspension (GM E-body) is independent double wishbone with torsion bars. The rear suspension (GM X-body) is a beam axle controlled by trailing arms and a panhard rod. A modified Chrysler K-car power rack and pinion gear was used. The braking system is disc front and drum rear with hydraulic assist. Tires are extra-load Goodyear P205/75-R15 on 15 in. by 6 JJ wheels from the GM E-body. The exhaust three-way catalytic converter is a VW unit which is part of the certified Audi 4000 system. The fuel supply system is also from the Audi 4000.

The accessory system includes a 12 V alternator, high- and low-pressure hydraulic pumps, and an air-conditioning compressor driven by either the gasoline engine or the electric motor. Operator controls consist of the steering wheel, the brake pedal, and the accelerator pedal, along with the instruments and warning lights. Heating of the passenger compartment is by a conventional hot water system and an auxiliary gasoline heater. The air conditioner makes use of standard GM components. A 12 V, deep-discharge type battery is used for the vehicle and electronic equipment power requirements.

1.4.4 Hybrid Propulsion Subsystem

The HTV utilizes a parallel hybrid power train (Figure 1.3.1-1) in which the heat engine and/or the electric motor are used to transmit torque to the wheels. The electric motor for the hybrid vehicle is a modification of the electric motor used in the ETV-1. The field windings have been redesigned and the voltage has been increased to 120 V to deliver a continuous 24 hp, compared with 20 hp in the ETV-1. The same armature design and frame size are used for both motors. Electric power control in the HTV uses a combination of battery switching and field control. The vehicle drive clutch modulates the power from the electric motor to the vehicle drive wheels. Modulation of the drive clutch is controlled by the microprocessor.

The 1.7-liter, fuel-injected (CIS) gasoline engine is a modification of that used in the Audi 4000. The engine produces 74 SAE hp at 5000 rpm. A new flywheel clutch was designed so that the engine could be operated in an on/off mode. The engine clutch was developed for the Hybrid Vehicle Program by LUK of West Germany. Closing and opening of the engine clutch can be accomplished in less than 0.5 s.

Morse Hy-Vo type-2300 chains are used to transfer torque from the heat engine and the electric motor to the wheels. The transaxle used is the three-speed automatic unit (with torque converter removed) used in the GM X-body vehicles. It is shifted using a system of electrically operated hydraulic valves.

The hybrid power train is completely microprocessor (two Intel 8086 boards) controlled with the only driver inputs being those from the accelerator and brake pedals. The vehicle controller commands the operation of the electric motor and heat engine and the shifts of the transmission as well as the opening and closing of the vehicle drive and engine clutches. The power train control strategy is dependent on the battery state-of-charge. Battery charging by the heat engine is commanded when the state-of-charge decreases to 20%.

A transistorized battery charger operating under micro-computer command is used to charge the two 60 V banks of lead-acid batteries from the wall plug. The battery state-of-charge is determined by the use of a resistive shunt and a battery state-of-charge unit based on the columbic approach.

1.4.5 Battery Subsystem

The HTV battery pack consists of ten modules. Figure 1.4.5-1 shows a schematic of the EV-1300 battery. The pack has two strings, each of which has five modules wired in series. The two strings can be connected in series or in parallel. This is controlled by the vehicle microprocessor. Two of the ten batteries in the pack (one in each bank) have temperature probes which provide measurements of electrolyte temperature. In addition, each battery bank contains thermostats that control operation of the battery pack cooling fan.

Prototype cells were tested at Globe prior to the fabrication of the 12 V modules. The 12 V modules have been tested by Globe, General Electric, and the National Battery Test Laboratory (NBTL) at Argonne. The complete battery pack has been tested by General Electric during dynamometer tests of the HPTM and HTV. HTV battery module characteristics and specifications have been summarized in Table 1.4.5-1.

Vehicle design considerations set the energy storage requirement and constraints on battery weight and volume. The volume (size) constraint was the most critical because the batteries were placed under the hood in the HTV. The design approach for the EV-1300 battery

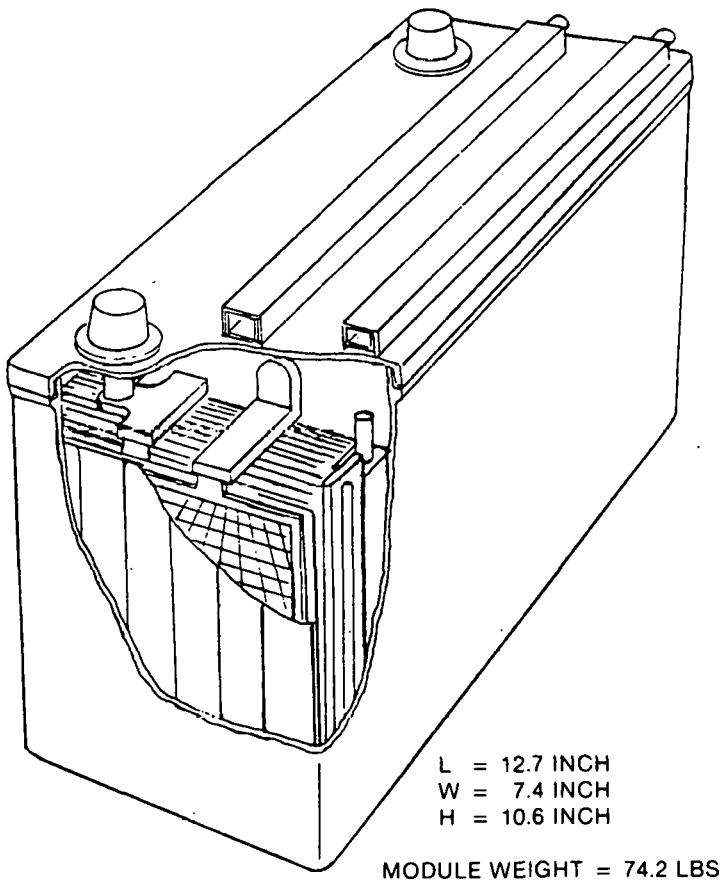

Figure 1.4.5-1. Cutaway View of the Hybrid Vehicle Battery Configuration

Table 1.4.5-1

HYBRID VEHICLE BATTERY MODULE SPECIFICATIONS AND FINAL BATTERY CHARACTERISTICS

	Specifications			Final
	Minimum	Target	Maximum	Battery Modules*
Module Voltage, V		12		12
Weight of Module, kg (lb)		34.0 (75.0)	36.5 (80.0)	33.3 (73.4)
Weight of Accessory Systems for Battery Pack, kg (lb)	4.5 (10.0)	5.5 (12.0)	6.7 (14.9)	
Module Dimensions				
Length, cm (in.)			32.38 (12.75)	32.3 (12.7)
Width, cm (in.)			18.92 (7.45)	18.8 (7.4)
Height, cm (in.)			27.43 (10.80)	26.9 (10.6)
Performance 3 h rate, to 10.5 V				
Capacity Ah	105	110		107
Energy storage, Wh	1250			1267
Energy density, Wh/kg (Wh/lb)	36.1 (16.4)			37.4 (17.0)
Power Characteristics, Voltage (V) after 15 s at 50% state of charge				
200 A pulse	10.5	10.8		10.8
300 A pulse	9.8	10.2		10.3
400 A pulse	9.0	9.5		9.8
Cycle Life at 80% DOD, 3 h Rate (cycles)		800**		

*Based on tests of delivered 12 V modules

**Battery life cycle tests were not conducted as part of this program

involved the utilization of all of the Globe electric vehicle battery developments existing in 1980. These included most of those in use in the Globe Improved State-of-the-Art (ISOA) battery which was developed with the assistance of DOE funding under Contract No. 31-109-38-4205 with Argonne National Laboratory.

In order to achieve the attractive cycle life goal shown in Table 1.4.5-1, the battery pack utilizes an electrolyte circulation system similar to the one used for Globe's ISOA battery (U.S. Patent No. 4,221,847).

The advantages of the electrolyte circulation system are

1. Increased cycle life

2. Improved charging efficiency resulting in increased round-trip energy efficiency and decreased water loss and hydrogen generation
3. Improved power density at low states of charge
4. Improved energy density
5. Improved thermal management

The EV-1300 battery also features a single-point watering system which significantly reduces maintenance time. This system also provides for venting of the hydrogen and oxygen gases through a pair of flame arrestors located on the hood of the HTV.

1.5 CONCLUSIONS

In this section, the total experience (design, development, and testing) gained in the Hybrid Vehicle Program is summarized in terms of a number of conclusions concerning the feasibility and attractiveness of hybrid passenger cars and the technical areas in which additional work is needed before the hybrid car could be marketed in the event of future petroleum crises (availability and/or rapid price increases). Each conclusion is stated and discussed briefly.

- *A Microcomputer-Controlled, Dual-Mode Hybrid Vehicle Having Performance and Driveability Comparable to that of a Conventional ICE Car is Feasible*

Dynamometer, track, and road tests of the HTV and mule vehicles (TBM and HPTM) have shown that a car powered by a hybrid (dual-mode electric/heat engine) power train can have acceleration and top-speed performance comparable to a conventional car. The use of advanced microcomputer hardware and software permits the design and development of a hybrid car which has the same ease of operation and smooth driveability as a conventional car. Further development of the HTV power train should result in improvements in acceleration compared to the vehicle (HTV) delivered to JPL.

- *The Gasoline and Electrical Energy Usage of the HTV is Close to that Predicted in Computer Simulations, and the Fuel Economy on the EPA Urban Cycle is Attractive (~ 90 mpg) as Long as the Battery State-of-Charge Remains Above 50%*

Tests of the TBM and HTV on the chassis dynamometer over the EPA cycles have shown that the gasoline and electrical energy usage of the hybrid vehicles are within 10-15% of those predicted using the GE computer simulation program (HYVEC). All the hybrid vehicles (TBM, HPTM, HTV) tested were able to negotiate the EPA test cycles with no difficulty. For an initial Vmode of 40 mph, the fuel economy inferred from the emissions data is about 90 mpg* for the full-sized HTV as long as the battery state-of-charge is above 50%. For battery state-of-charge above 50%, the heat engine is used to provide peak power at speeds below Vmode, and therefore the vehicle is driven by the electric motor most of the time.

- *The On/Off Engine Operation Utilized in the HTV Functions* Satisfactorily, and the Resultant Emissions (HC, CO, NO_x) *Should Meet 1981 Standards (0.4 gm/mi HC, 3.4 gm/mi CO, and 1.0 gm/mi NO_x) Over the Complete Range of Vehicle Operating Modes with Little Further Development*

Emissions tests of the TBM and HTV (preliminary data) indicate that HC and CO emissions are close to or below the 1981 standard and NO_x emissions are well below the 1981 standard. In most tests, the NO_x emissions are less than the EPA research standard for NO_x of 0.4 gm/mi. Additional work is required to perfect the cold-start procedures for an engine

* For our initial Vmode of 60 mph, the fuel economy would be in excess of 100 mpg.

operating in the on/off mode. Further development of engine clutch actuation is needed to improve both durability and reliability. However, the feasibility of on/off engine operation has been demonstrated.

- *The Lead-Acid Batteries Designed and Fabricated by Globe Meet All Target Specifications for the C/3 Capacity (106 Ah) and Voltage Droop at High Pulse Currents, but the Batteries had only a 35 Ah Usable Capacity in the Hybrid Application on the EPA Urban Cycle*

The lead-acid battery modules designed and fabricated by Globe for use in the HTV have a C/3 capacity 106 Ah. Dynamometer tests of the HTV on the EPA urban cycle showed that the usable capacity of the battery pack was only 35 Ah which is about 1/3 of the C/3 capacity. The useful capacity of 35 AH was much less than the 65 AH capacity expected based on pulsing (15 s, 400 A pulses) the cells intermittently during a 65 A average current discharge. In both the cell pulse tests and the vehicle dynamometer tests using the complete battery pack (ten 12V modules), the test was terminated when the battery voltage drooped to 1.3V/cell during the high current pulse. The new Globe battery (12 V module) met the voltage droop specifications* (V/cell for specified pulse currents) at selected state-of-discharge and yielded a peak power density of 164 W/kg for the standard NBTL (Argonne) peak power test. Hence, even though the new battery had low internal resistance and high peak power density, it demonstrated unsatisfactory capacity performance in the hybrid vehicle application. The question of how to optimize the design of lead-acid batteries, whose capacity is inherently discharge-rate profile dependent, for use in hybrid vehicles requires further study.

- *The Weight Penalty of a Hybrid Car Compared to a Conventional ICE Car of the Same Interior Size is Significant, and Careful Design is Required to Reduce the Penalty*

The curb weight of the HTV as delivered to JPL is 2032 kg (4470 lb) compared with 1455 kg (3200 lb) for the 1980 Buick Century and 1282 kg (2820 lb) for the downsized 1983 Buick Century. It is estimated that a ground-up HTV design would have a curb weight of about 1800 kg (3960 lb). Further weight reductions in the hybrid car are undoubtedly possible as more development is done on the power train. Nevertheless, it appears that even with careful design, the weight penalty in a full-size hybrid vehicle would be at least 450 kg (1000 lb) unless the battery pack weight can be significantly reduced from the 375 kg (825 lb) used in the HTV. Both the petroleum savings and economic attractiveness of the hybrid car are highly dependent on the weight, because weight affects both initial cost and energy usage.

- *Advanced Microcomputer Hardware and Software and Complex Mechanical Arrangements have made the HTV Simple to Operate from the Driver's Point of View, but Relatively Complicated and Expensive from the Maintenance and Economic Viewpoints. Future Development Should Emphasize Making the Power Train Less Complex and Control Techniques as Simple as Possible*

The present HTV was designed and built to demonstrate the feasibility of the hybrid power train concept. From that point of view, it was a success. Future developments should emphasize making both the hardware and operating strategies as simple as possible, with a minimum compromise in vehicle driveability and power train efficiency.

- *The Petroleum Saving Potential of a Hybrid Passenger Car is Attractive if the Effective Electrical Energy Storage Capacity of the Battery is a Reasonable Fraction of the C/3 Capacity Yielding a Usable Energy Density of at Least 25 Wh/kg for the Hybrid Application*

An annual petroleum savings potential of 70% in urban driving and at least 50% in combined urban/highway driving is attainable for a hybrid car, compared with a reference 1985 ICE car *if* the usable capacity of the battery in the hybrid car is at least 25 Wh/kg. In the case

* Specified by GE at the outset of Phase II.

of the HTV, the effective energy density of the lead-acid battery was only about 12 Wh/kg, resulting in a projected annual fuel savings of 35% in urban driving and 23% in combined urban/highway driving compared with the 1980 reference car (21 mpg urban, 29 mpg highway). The usable capacity of the battery does not affect the utility of the hybrid vehicle; but the petroleum savings attractiveness of the hybrid is critically dependent on the effective Wh/kg of the battery. In this respect, battery types, whose usable capacities are not highly discharge-rate profile dependent, may be better suited for hybrid vehicles than lead-acid batteries.

Section 2

INTRODUCTION

The Electric and Hybrid Vehicle (EHV) Program was established in DOE in response to the Electric and Hybrid Vehicle Research, Development, and Demonstration Act of 1976. The EHV Program is the responsibility of the Hybrid Vehicle Program Office of DOE. The Hybrid Vehicle Program was an element of the EHV Program. The Department of Energy has assigned procurement and management responsibility for the Hybrid Vehicle Program to the California Institute of Technology, Jet Propulsion Laboratory (JPL).

The overall objective of the DOE EHV Program is to promote the development of electric and hybrid vehicle technologies and to demonstrate the viability of these systems as transportation options which are less dependent on petroleum resources.

As part of the Hybrid Vehicle Program, General Electric and its subcontractors completed studies leading to the preliminary design of a hybrid passenger vehicle which was projected to reduce petroleum consumption in the near term (commencing in 1985). This work was done under JPL Contract 955190, Modification 3, Phase I of the Hybrid Vehicle Program. The Phase I Final Report summarized all of the effort in Phase I and is included in Appendices A, B, C, and D.

General Electric was awarded the Hybrid Vehicle Program (Phase II) in November 1979. The overall goal of Phase II (Contract Modifiction 17) was to design, develop and fabricate one Hybrid Test Vehicle (HTV). This was accomplished through a mule program under which two prototype vehicles were developed – Test Bed Mule (TBM) and Hybrid Power Train Mule (HPTM). Throughout the total program, system performance and fuel economy projections were revised based on current design and hardware inputs. A HTV Hardware Review was held in February 1983 after which this vehicle was shipped to JPL. JPL formally accepted the vehicle in April 1983 and a vehicle test program began.

Section 3

PROGRAM MANAGEMENT

3.1 PROGRAM ORGANIZATION

The relation of the JPL Electric and Hybrid Vehicle Project to the DOE Electric and Hybrid Vehicle Program and to the General Electric Hybrid Vehicle Program is given in Figure 3.1-1.

General Electric Corporate Research and Development (CRD) was the prime contractor for the Phase II Program. Corporate Research and Development reports directly to the Corporate Executive Staff of the General Electric Company (Figure 3.1-2). Within CRD, research and development activities in the field of hybrid and electric vehicles are carried out by the Electronics Laboratories under the management of Dr. K.A. Pickar. The Hybrid Vehicle Program was executed within the Power Electronics Laboratory, headed by Dr. J.W.A. Wilson (acting) and within the Power Circuits and Systems Branch headed by Dr. J.W.A. Wilson. Mr. M.F. Ciccarelli was the Program Manager for Phase II of the Hybrid Vehicle Program. It should be noted that prior to Mr. Ciccarelli, two previous Program Managers were responsible for the Hybrid Vehicle Program at General Electric, Mr. E.A. Rowland (November 1979−February 1981) and Dr. T.R. Haller (February 1981−May 1982).

Mr. M.F. Ciccarelli, Program Manager, was responsible for Phase II of the Hybrid Vehicle Program. All contributing organizations within the General Electric Company, as well as major subcontractors, received technical and programmatic direction from the Program Manager and were responsible to him for their performance. The "solid line" elements of Figure 3.1-3 denote those personnel who reported administratively to Mr. Ciccarelli, while the "dotted line" relationships indicate those organizations which reported administratively to other managers, but were accountable to Mr. Ciccarelli for their responsibilities on this program.

3.2 WORK BREAKDOWN STRUCTURE

The original work breakdown structure (WBS) for Phase II is presented in Table 3.2-1. Beginning with the task level breakdown furnished by the Jet Propulsion Laboratory, each task was further expanded into subtasks (Level 4) and, in some cases, to work items (Level 5). Exceptions to this rule are level-of-effort tasks (such as program management) which were not expanded, thereby following the guidelines of Jet Propulsion Laboratory-Performance Management Systems (JPL-PMS). An effort was made in constructing the expanded WBS to strike a balance between good management visibility of the required work and a reasonable number of discrete work elements which had to be scheduled, monitored, and reported.

3.3 PROGRAM SCHEDULE

The program schedule was based on the work breakdown structure. The schedule was the pivotal point of the performance measurement system upon which the baseline estimate was established. To aid in schedule interpretation, a detailed network and a summary network schedule was supplied. These items graphically interpret the schedule to the work item level and, in summary, depict the key events of the program.

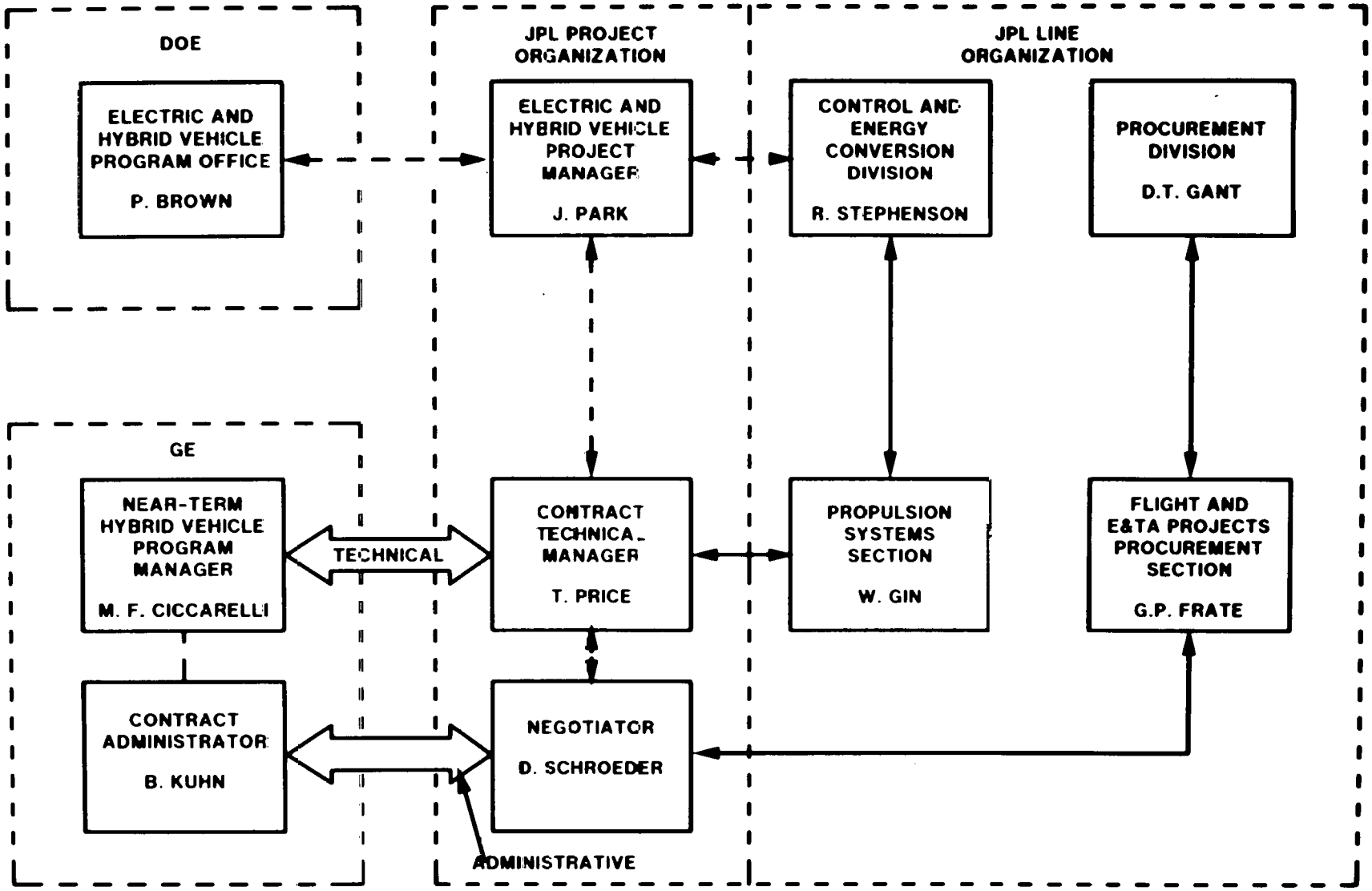

Figure 3.1-1 Relationship of GE Hybrid Vehicle Program to JPL and DOE

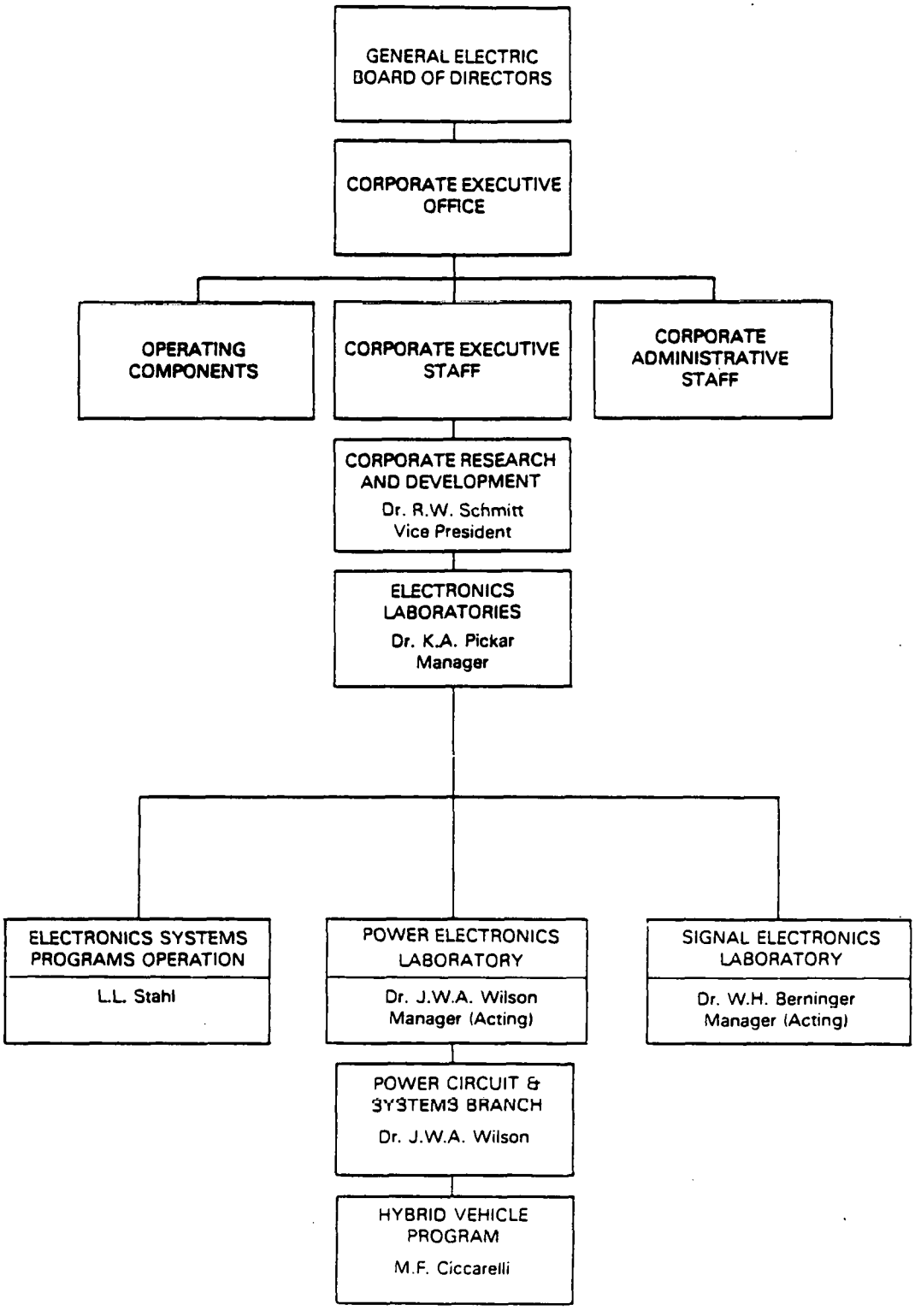

Figure 3.1-2. Relationship of the General Electric Company to the Hybrid Vehicle Program

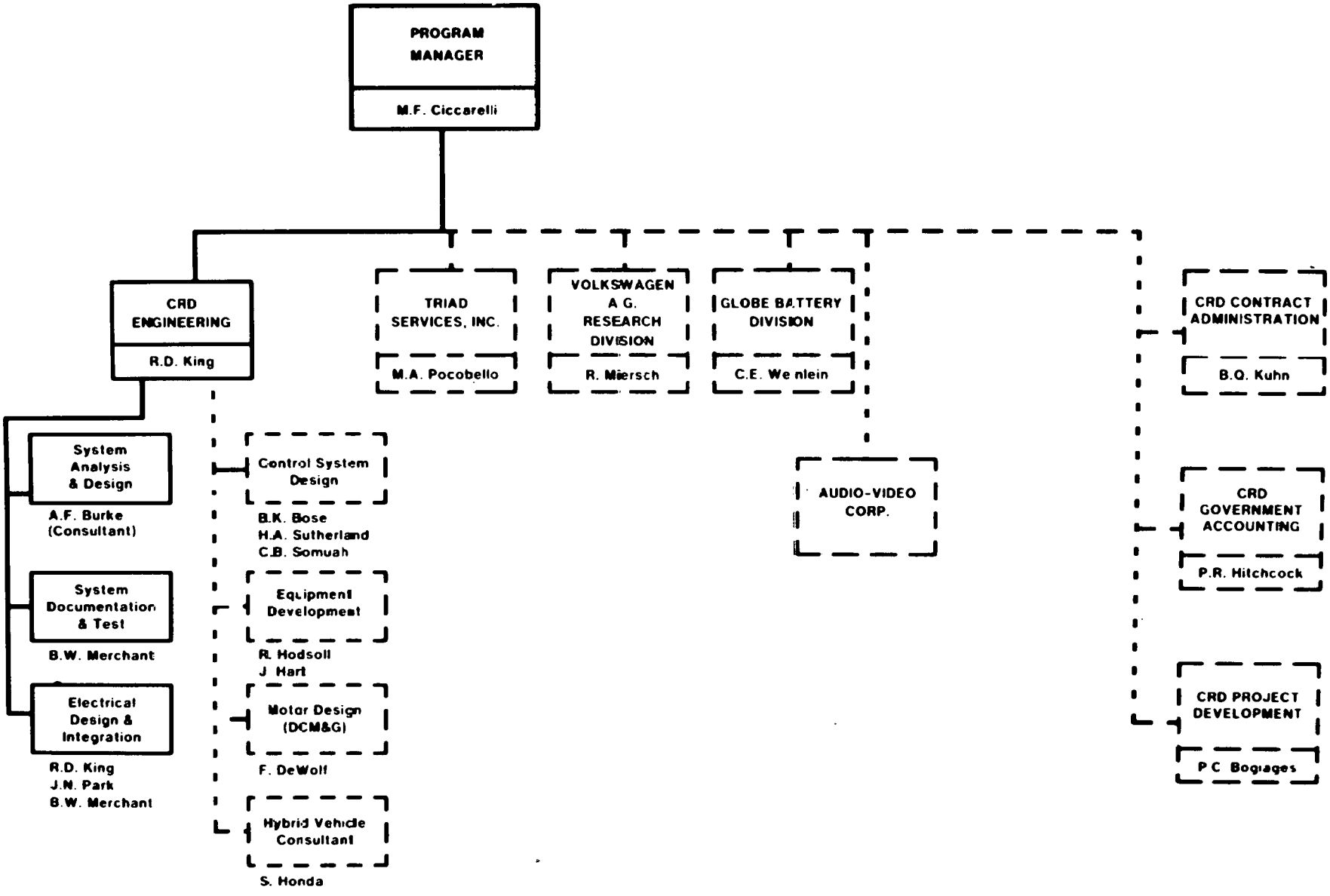

Figure 3.1-3. Corporate Research and Development Hybrid Vehicle Program (Phase II) Organization

Table 3.2-1

EXPANDED WORK BREAKDOWN STRUCTURE FOR NEAR-TERM HYBRID VEHICLE, PHASE II

100	Program Management*
	110 Program Management
	120 Financial Planning and Analysis
	130 Configuration and Data Management
	140 Safety
	150 Scheduling
	160 Performance Measurement
	170 Subcontract Liaison
200	System Analysis and Design*
	210 Technology Transfer
	220 Preliminary Design
	221 Design Studies
	222 Design Data Package Update
	230 Performance Analysis Model
	231 Math Modeling
	232 Computer Program Updates
	233 ELVEC Analysis
	234 Performance Prediction and Analysis
	240 System Design and Specifications
	241 System Requirements Analysis
	242 Subsystem Requirements Allocation
	243 System and Subsystem Specifications
	244 Interface Specifications
	245 Subsystem Design Criteria
	246 Design and Analysis Documentation
	247 Design Supervision (LOE)
	248 Thermal Analysis and Design
	250 Design Reviews
	251 Preliminary Design Review
	252 Interim Design Review
	253 Critical Design Review
	260 Safety, Reliability, and Maintainability
	261 Safety Reviews
	262 Failure Modes and Effects Analysis
	263 Maintainability Analysis
	270 Test Reviews
	271 Test Bed Mule Review
	272 Ride and Handling Demo
	273 Barrier Test Review
	274 HTV Test Review
	275 HTV Hardware Reviews
	276 Battery Test Review

*Reporting Level

Table 3.2-1 (Cont'd)

EXPANDED WORK BREAKDOWN STRUCTURE FOR NEAR-TERM HYBRID VEHICLE, PHASE II

300	Vehicle Subsystem*
	310 Preliminary Design
	311 Design Studies
	312 Design Data Package Update
	320 Analysis
	321 Chassis Components
	322 Vehicle Handling
	323 Structures
	324 Aerodynamic Testing and Analysis
	330 Design
	331 Body/Structure
	332 Chassis
	333 Heating, Ventilating, and Air-Conditioning
	334 Controls and Instruments
	340 Fabrication
	341 Tooling
	342 Fixtures
	343 Sheet Metal Parts
	344 Mechanical Components
	345 Body in White
	346 Vehicle Assembly
	347 Finish and Trim
	350 Test Requirements
	351 Hybrid Test Vehicle – Integration
	352 Hybrid Test Vehicle – Performance
	360 Component Assembly and Test
	361 Static Crush Structure
	362 Transmission and Final Drive
	363 Front Compartment
	364 Tire Testing
400	Hybrid Propulsion Subsystem*
	410 Preliminary Design
	411 Design Studies
	412 Design Data Package Update
	420 Design Analysis and Control Strategy
	421 Analysis of Operating Modes
	422 Control Strategy Simulation
	430 Detail Design
	431 Component Specifications - TBM
	432 Component Specifications - HTV
	433 Interface Control Drawings
	434 Design Supervision (LOE)
	435 Dynamometer Evaluation of Propulsion Subsystem
	440 Drive Motor
	441 Procure Prototype Motors
	442 Vibration Tests
	442 Procure HTV Motors
	443 Dynamometer Tests

*Reporting Level

Table 3.2-1 (Cont'd)

EXPANDED WORK BREAKDOWN STRUCTURE FOR NEAR-TERM HYBRID VEHICLE, PHASE II

	450 Engine and Clutch
	451 Design
	452 Fabrication and Assembly
	453 Dynamometer Tests
	454 Project Supervision and Technical Support
	460 Power Electronics
	461 Electrical Design
	462 Electrical Breadboard
	463 Thermal Analysis and Design
	464 Mechanical Design
	465 Fabrication
	466 Test Fixtures
	467 Electrical, Thermal, and Mechanical Tests
	470 Controller
	471 Control System Development
	472 Control System Analysis
	473 Control System Simulation
	474 Hardware Design
	475 Software Design
	476 Breadboard Assembly and Evaluation
	477 TBM Controller Design and Test
	478 Packaging Design and Fabrication
	4781 Packaging Design
	4782 Fabrication
	4783 Functional Tests
	479 Hardware/Software Integration and Test
	480 Battery Charger
	481 Electrical Design
	482 Electrical Breadboard
	483 Thermal Analysis and Design
	484 Mechanical Design
	485 Fabrication
	486 Test Fixtures
	487 Electrical, Thermal, and Mechanical Tests
	490 Sensors
	491 Engine Sensors
	492 Electrical Sensors
	493 Vehicle Sensors
500	Battery Subsystem*
	510 Design
	511 Battery Design Concepts
	512 Battery Production Drawings
	513 Battery Design Revisions
	514 Support Items Design
	515 Support Items Design Revisions
	520 Development
	521 Procure Polypropylene and Grid Molds
	522 Design and Procure Fabrication Tooling
	523 Debug Fabrication Tooling
	524 Design and Procure Assembly Tooling
	525 Debug Assembly and Support Item Tooling
	526 Debug Container and Cover Molds

*Reporting Level

Table 3.2-1 (Cont'd)

EXPANDED WORK BREAKDOWN STRUCTURE FOR NEAR-TERM HYBRID VEHICLE, PHASE II

	530 Fabrication 531 Fabricate Cells 532 Fabricate Battery and Components 533 Assemble Batteries 534 Fabricate Temperature Probes 540 Test 541 Cell Tests 542 Battery Tests 543 Technical Support 5431 Charging Procedure 5432 Thermal Control 5433 Watering Procedure 5434 Battery Pack Installation 5435 EV2-13 Power Testing 5436 Cycling Batteries 5437 1H, 2H – Rate Discharge Tests
600	Mule Program* 610 Test Bed Mule 611 Design 612 Vehicle Modification 613 Propulsion Subsystem Integration 614 Controller Integration 615 Functional Test 616 Project Supervision and Technical Support 617 Transfer Case 620 Dynamics Mule 621 Mechanical Components Mule 6211 Design 6212 Vehicle Modification - Toronado 6213 Component Fabrication 6214 Vehicle Assembly 6215 Development Program 6216 Control Strategy Development 622 Structural Mule 6221 Design 6222 Component Fabrication 6223 Assembly - Century 6224 Nondestructive Testing 6225 Structural Update 6226 Instrumentation 623 Prototype Hybrid Power Train Dynamics Mule
700	Test and Evaluation* 710 Test Planning and Integration 711 Master Test Requirements 712 Propulsion Subsystem 713 Test Bed Mule 714 Dynamics Mule 715 HTV – Integration and Performance Tests

*Reporting Level

Table 3.2-1 (Cont'd)

EXPANDED WORK BREAKDOWN STRUCTURE FOR NEAR-TERM HYBRID VEHICLE, PHASE II

	720 Test Bed Mule 721 Vehicle Shakedown Tests 722 Control Strategy Verification Tests 723 Energy Consumption and Emission Tests 724 Test Analysis 725 Project Supervision and Technical Support 730 Dynamics Mule 731 Ride and Handling Tests 732 30-mph Barrier Test 740 Hybrid Propulsion Subsystem Tests 741 Subsystem Integration (Bench) Tests 742 Subsystem Performance (Mule) Tests 743 Test Analysis 750 Hybrid Vehicle Tests 751 Vehicle Integration 752 HTV Performance Tests
800	Quality Assurance* 810 Quality Plan 820 Quality Assurance (LOE)
900	Manufacturing Studies and Evaluation* 910 Producibility Study 911 Vehicle Subsystem 912 Hybrid Propulsion Subsystem 913 Battery Subsystem 920 Cost Study 921 Vehicle Subsystem 922 Hybrid Propulsion Subsystem 923 Battery Subsystem 924 Hybrid Vehicle 930 Consumer Acceptance Study 931 Styling and Human Factors Analysis
1000	Support Equipment* 1010 Design 1011 Vehicle Instrumentation 1012 Portable Test Equipment 1013 Battery Handling Equipment 1014 Assembly Level Test Aids 1020 Procurement Activities 1021 Parts and Materials 1031 Vehicle Instrumentation 1032 Portable Test Equipment 1033 Battery Handling Equipment 1034 Assembly Level Test Aids

*Reporting Level

Table 3.2-1 (Cont'd)

EXPANDED WORK BREAKDOWN STRUCTURE
FOR NEAR-TERM HYBRID VEHICLE, PHASE II

1100	Documentation*		
	1110	Management	
		1111	Program Plan
		1112	Network Schedule
		1113	Baseline Estimate
		1114	Work Breakdown Structure
		1115	Weekly Status Report
		1116	Financial and Management Report
		1117	Contract Status Report
		1118	Documentary Film
		1119	Schedule Accomplishment Report
	1120	Technical	
		1121	Design Review Materials
	1122	Test Plans	
		1123	Test Reports
		1124	Detailed Design Drawings
		1125	Mid-Term Report
		1126	Final Report
		1127	Photographs
		1128	Studies and Evaluation
		1129	Brochure
	1130	Operational	
		1131	Safety Report
		1132	Operation and Maintenance Manual
		1133	Scale Models
1200	Field Support*		

*Reporting Level

3.3.1 Summary Network Schedule

The summary network schedule is shown in Figure 3.3.1-1. All delivery dates specified in the contract schedule have been included along with the key decision dates, such as design reviews, test reviews, and design releases.

3.3.2 Summary Schedule of Deliverable and Performance Items

A summary schedule of the deliverable and performance items follows:

Item	Date
• Documentation	As specified in pp. 2 and 3 of Exhibit III of the RFP and summarized in Table 3.3.2-1
• Design reviews	
Preliminary design (PDR)	3-4-80

Interim design (IDR)	10-15-80
Critical design (CDR)	5-12-81
• Hardware and test reviews	
Test bed mule (TBM)	9-14-82
Ride and handling demonstration (HPTM)	4-15-82
Hybrid test vehicle hardware review	2-9-83
• Test vehicles	
– Test bed mule	9-15-81
– Hybrid power train mule	4-15-82
– Hybrid test vehicle	2-9-83
One set of selected spare hardware	2-9-83
• Support Equipment	
First set	6-1-82
Second set	2-9-83

3.4 PROGRAM CONTROL PLAN

Included in the program control plan are program scheduling, allocation of resources, cost control, design reviews, performance measurement and reporting, and configuration control.

3.4.1 Program Scheduling

A detailed network schedule was used to provide a roadmap for the entire program. Each task of the WBS was scheduled in sufficient detail to show interrelations between activities and to identify key milestones for measuring the progress of each task.

To aid in establishing and furnishing data required by the performance measurement system, a computerized scheduling and financial reporting system was developed. This system was used by the Program Office to generate schedules and schedule accomplishments reports, monthly financial reports, and computer-drawn detail network schedules.

All subcontractors and key engineers (task responsibility) at CRD received a weekly status report. This report contained a listing of open tasks for which each engineer was responsible. The key engineer updated the listings as to actual start or completion dates for a particular task. In the event of delayed start or completion, the key engineers supplied a "delay date" for management review. The computer data-base was then updated accordingly. The weekly status report provided the basis for weekly and monthly schedule reporting. During monthly program reviews at the subcontractor facility, discussions were held to determine the progress in each task.

Particular attention was given to critical paths when reviewing the weekly report. Critical paths are those activities which pace the total program effort because they represent the longest time interval between two key milestones. It was the responsibility of each key engineer to take corrective action when potential delays were recognized.

3.4.2 Allocation of Resources

The allocation of program funds was controlled by the GE-CRD Program Manager and administered by the Program Office. A funding allocation plan was developed to distribute the contract funds. A part of these funds was held as a management reserve by the Program Manager to deal with unforeseen problems.

THIS PAGE

WAS INTENTIONALLY

LEFT BLANK

GENERAL ELECTRIC

Contract Start 11-9-79 210A

12-10-79 210B

Technology Transfer

Performance Simulation Started 12-10-79 231A

System Requirements Analysis Completed 1-12-80 241B

Vehicle Preliminary Design Completed 4-11-80 310B

System Design & Specifications Complete 9-5-80 243B

Preliminary Design Review (PDR) 3-20-80 2511B

Start Prel. Design of • Subsystems • TBM • Dynamics Mule

Prel. Design Completed Hybrid Propulsion Subsystem 3-7-80 410B

Drive Motor Spef. Completed 9-17-80 4421B

Structural-Mule Start Design 6-7-80 822A

Static Cruh Tests Completed 12-1-80 3818

Structural Mule Fabricated 3-9-81 673B

Structural Mule Tested & Updated 3-17-81 6225B

Start Conversion of Mule to HTV 3-17-81 6225B

Start Vehicle Component Fabrication 10-1-80 344A

Vehicle Retrofarl Design Complete 2-27-81 3311B

Start Structural Design Modifications 4-1-81 3317A

Complete Vehicle Component Fabrication 8-17-81 344B

HTV Buoy in White 9-11-81 3463B

Interm Design Review (IDR) 10-15-80 2521B

Critical Design Review (CDR) 5-12-81 2531B

Performance Simulation Completed 8-31-81 232B

Controlled Hardware Design Completed 7-22-80 4745B

Engine Sensors & Electrical Sensors Design Completed 9-15-80 4921B

Engine Design Completed 9-25-80 451B

Controller Software Design Completed 12-12-80 4753B

Engine Sensors & Electrical Sensors Fabricated & Tested 10 23-80 491B

Dynamic Mule Controller Fabricated and Tested 3-30-81 476428

Mule-Drive Waters Fabricated & Tested 5-1-81 440B

Controller Hardware Design Fabricated 3-21-81 476B

Controller Software Update 7-31-81 4723B

CDR 2531B

HTV Controller Fabricated & Tested 8-15-81 47111B

HTV Engine Fabricated & Tested 2-10-81 45321B

Prototype Pnwer Electronics Completed 2-28-81 465328

Power Electronics Design Completed 5-30-81 4642B

CDR 2531B

HTV Pnwer Electronics Fabricated 7-30-81 461228

Battery Charger Design Completed 8-30-81 841B

CDR 2531B

HTV Battery Charger Fabricated & Tested 11-15-81 483B

Start Vehicle Sensor Desing 2-25-81 493A

CDR 2531B

HTV Vehicle Sensors Fabricated & Tested 7-7-81 493B

TBM Test Preview 8-12-81 273B

TBM Deliver 9-15-81

HTV Propulsion Subsystem Integration 10-25-82 740B

HTV Trimmed and Painted 11-15-82 3742B

HTV Track and Emission Tests 1-31-83 750B

HTV Hardware Review 2-9-83 274A

Deliver • HTV • Selected Spares • Support Equipment (Set 2) 2-9-83

TBM Drive Motor Procured 7-22-80 441B

TBM Engine Fabricated & Tested 8-5-80 453IB

TBM Design Completed 7-1-80 6113

TBM Power Electronics Fabricated & Tested 10-29-80 467128

TBM Controller Fabricated & Tested 11-25-80 478318

TBM Vehicle Modified 10-15-80 612B

TBM Integrated 12-21-80 614B

TBM Shakedown Test 3-10-81 721B

Engine Complete Developed 4-15-81

CDR 2521B

TBM Transfer Case Assembly 9-10-80 6173B

Mechanical Component Mule-Drive Motor Procured 7-22-80 441B

Mechanical Components Mule-Engine Fabricated & Tested 8-25-80 4521B

Mechanical Component Mule-Components Complete 12-5-80 6213B

Vehicle Assembly Completed 12-5-80 6214B

Mechanical Component More Developed Completed 4-20-81 6151B

Hybrid Power Train Mule Controller Integration 8-15-81 622B

Ride & Handling Tests 2-19-82 272B

HPTM Delivery 4-15-82

PDR 2511B

Battery Subsystem Preliminary Design Completed 12-10-79 511B

Battery Subsystem Final Design Completed 9-26-80 513B

CRD 2531B

Battery Tooling Completed 5-12-81 525B

HTV Battery S/S Fabricated & Tested 7-15-81 541B

Battery Test Review 10-1-81 276B

Support Equipment Fabricated & Tested (Set 2) 2-9-83 10322B

Start Design of Support Equipment 9-1-80 1010A

Start Fabrication of Support Equipment 12-10-80 1030A

Support Equipment Fabricated & Tested (Set 1) 6-1-82 10321B

Progam Plan Submitted 1-15-80

Interim Report 6-30-81

Brochure 11-25-81

Mid Program Documentary Film 1-6-82

Safety Report Submitted 9-15-82

Deliver Detail Design Drawings 3-17-83

Deliver • Final Report (Draft) 6-30-83

△ Deliver Item or Contract Due Date

Figure 3.3.1-1. Summary Network Schedule

THIS PAGE

WAS INTENTIONALLY

LEFT BLANK

Table 3.3.2-1

SUMMARY OF DOCUMENTATION SCHEDULE

Deliverable Item	Title or Description	Date Due
8A	Program Plan	1-15-80
9	Network Schedule	1-29-80
10	Baseline Estimate	1-29-80
11	Work Breakdown Structure (WBS)	1-29-80
12	Weekly Status Report (TWX)	Tuesday of week following reporting period
13	Financial and Management Report	15th of the following month
14	Contract Status Report	With line item 13
15	Design Review Materials	10 working days before review
16	Test Plans	30 days prior to test
17	Test Reports	30 days after test
18	Detailed Design Drawings	5-9-82
19	Safety Report	10-28-81
20	Operation and Maintenance Manual	3-31-82
21	Documentary Film Midprogram Final	 5-6-81 5-5-82
22	Mid-Term Report	5-6-81
23	Final Report	5-9-82
24	Photographs	Monthly
25	Studies and Evaluation	3-31-82
26	Brochure	6-18-81
27	Schedule Accomplishment Report (SAR)	15th of the following month

Within CRD, allocation of funds to individual tasks was accomplished by means of a shop order structure which provided a unique account number for each major activity. The allocation of resources was managed at Level 3 of the WBS, which is one level below the reporting level. Financial reports were received weekly for each shop order and listed labor and material dollars expended for the previous week, as well as cumulative expenditures for the current year and the total program.

3.4.3 Cost Control

The process of controlling contract expenditures was a logical extension of the allocation of resources and the reporting process described in Section 3.3.2. Each week the Program Office reviewed expenditures for each task and plotted expenditures versus plan values. Any significant discrepancies uncovered by the Program Office were reported immediately to the Program Manager and to the individual responsible for the task.

The schedule accomplishment report (SAR) was prepared and submitted as part of the initial report. The initial SAR listed planned start dates and completion dates for each report item and work item of the WBS along with the baseline cost estimate for each task. Subsequent (monthly) submittals reported actual start and completion dates and incorporated changes as a result of contract modifications. Monthly financial and management reports were submitted in accordance with the contract data requirements. These reports provided the required financial data and a narrative assessment by the Program Manager of the progress made during the reporting period toward meeting the technical requirements. Weekly status (TWX) reports were submitted to both JPL and the subcontractors' management. These weekly reports included information on schedule progress and manpower expenditures.

3.4.4 Performance Measurement System

General Electric implemented a system for performance measurement and reporting which satisfied the requirements and intent of the JPL-PMS. The same information which was supplied to JPL for performance measurement was also used by CRD to measure and control the performance of internal groups and subcontractors. A variance analysis was performed each month to identify those tasks which were behind schedule and/or overexpended.

3.4.5 Configuration Control

The objective of this step of the program was to control the vehicle design configuration. Following approval of the vehicle preliminary design at the preliminary design review (PDR), any changes affecting the basic design concept or performance were reviewed by JPL at each monthly status review meeting. At the design reviews, the design was reviewed and specifications were updated.

The system documentation function maintained control of and storage for all drawings, specifications, and test plans. Any changes affecting the basic vehicle styling, performance, or cost required JPL concurrence. Changes to the HTV that affected the test bed mule, structural mule, or mechanical components mule (hybrid power train mule) test results also required JPL concurrence.

3.4.6 Subcontractor Management and Direction

Those subcontractors selected by CRD (and approved by JPL) received subcontracts which contained all of the flow-down requirements of the JPL contract. Work statements, contract schedules, and data requirement descriptions were prepared, which included specific excerpts from the Phase II contract modification along with supplementary information developed by CRD.

Each subcontractor selected for the Phase II program was required to identify a Program Manager to interface with the GE-CRD Program Manager. Each subcontractor was also required to supply a baseline plan which clearly defined the subcontractor's performance plans. Weekly status reports from each subcontractor served to record technical progress, manpower expenditures, and problem areas. By means of monthly technical, financial, and management reports, CRD closely measured each subcontractor's performance.

All formal contractual interfaces with the subcontractors were administered at CRD by the Program Office. Technical and programmatic interfaces with each subcontractor were managed by the GE-CRD Program Manager. Engineering issued specifications, interface control documents, and design criteria which were incorporated by reference into the subcontract schedule of work.

Section 4

SYSTEM ANALYSIS AND VEHICLE CHARACTERISTICS

This section presents a discussion of system analysis activities and reviews the program objectives and vehicle specifications. The power train and vehicle characteristics are summarized and a weight breakdown is given. The HTV road load as a function of speed and grade is discussed along with the acceleration and gradeability performance.

4.1 INTRODUCTION

The objective of the Phase II program (per Contract Modification 17) was to design, fabricate, and deliver to JPL two mule vehicles and a hybrid test vehicle (HTV). The HTV was projected to have a maximum potential for reducing petroleum consumption in the near term. At the onset of the program, components had to be available for vehicle testing in 1982 and the vehicle was to be marketable in 1985. Based on the results of the Mission Analysis Task (Reference 1) of Phase I, the ICE reference vehicle selected was the 1979 Chevrolet Malibu. In terms of utility, performance, and passenger comfort, the HTV was designed to be equivalent to the ICE reference vehicle. The petroleum savings of the HTV were determined relative to a 1980 GM mid-size car, especially the 1980 Buick Century.

The general program objectives were translated into vehicle specifications, which are given in detail in Reference 2. Those specifications for the HTV characteristics were based on Phase I simulation results. For the most part, the specifications for vehicle performance exceeded the minimum requirements set by JPL at the outset of the Hybrid Vehicle Program. The JPL minimum requirements are summarized in Table 4.1-1. Current power train and predicted vehicle characteristics for the HTV are discussed in some detail in subsequent sections of this report.

The following tasks were included in the systems analysis activity:

1. Preparation of detailed vehicle and component specifications

Table 4.1-1

HYBRID VEHICLE MINIMUM PERFORMANCE REQUIREMENTS

Speed			
Continuous cruise	90km/h (56 mph)		
Maximum (1 min)	100km/h (62 mph)		
Acceleration			
0 - 50 km/h	6 s		
0 - 90 km/h	15 s		
40 - 90 km/h	12 s		
Gradeability			
Grade		Speed	Distance
3%		90 km/h	1.0 km
8%		50 km/h	0.3 km
15%		25 km/h	0.2 km

2. Tracking of the vehicle weight during design
3. Computer simulation of vehicle operation as a means of projecting vehicle performance and making design trade-offs
4. Continuous update of projected hybrid vehicle fuel economy, energy-use, and emissions, as well as component design and test data
5. Coordination of component interface activities, especially as they relate to power train control strategy and vehicle controller hardware, and software development
6. Vehicle overall thermal analysis as it relates to packaging the hybrid power train under the hood
7. Development of test procedures and plans for the testing of components, mule vehicles, and the final HTV

4.2 POWER TRAIN AND VEHICLE CHARACTERISTICS

The HTV is a parallel hybrid utilizing a two-shaft, transverse arrangement with the entire power train packaged under the hood. A schematic of the power train is shown in Figure 4.2-1. The power train characteristics are summarized in Table 4.2-1. Detailed descriptions of each of the components and the control strategy employed in the HTV to operate the power train are discussed in this section.

4.2.1 Weight Breakdown

The weight breakdown for the HTV is shown in Figure 4.2-2. The component weights shown were obtained from a variety of sources. When possible, final component hardware was weighed. In other cases, weights obtained from the component suppliers were used. In any case, the weights shown in the breakdown are thought to be quite accurate. The final projected HTV weight of 1969 kg (4332 lb) was reasonably close to the 2032 kg (4470 lb) value determined when the completed HTV was weighed.

A weight breakdown of the hybrid power train is shown in Table 4.2-2. The weight of the mechanical and electrical components in the hybrid power train can likely be reduced somewhat after more experience with their operation in a vehicle is gained. However, there would still continue to be a significant weight penalty associated with the hybrid power train compared to the conventional ICE power train.

Considerable attention was given to weight reduction and control during the design and fabrication of the HTV. The effective chassis weight (vehicle minus power train) for the HTV is 1180 kg (2600 lb) compared with 1160 kg (2550 lb) for the baseline 1980 Buick Century. Further weight reductions in the HTV chassis weight would have been possible if the passenger compartment from the Buick Century had not been used intact and the front and underbody structures of the HTV had not been assembled by welding together numerous smaller simpler sections.

The weight of a hybrid vehicle can be expected to be considerably heavier than a comparable ICE vehicle. The weight differences are summarized in Table 4.2-3. The information given in Table 4.2-3 indicates that the weight penalty for hybridizing the 1980 Buick car using lead-acid batteries was 577 kg (1269 lb) with the battery subsystem weighing 375 kg (825 lb). The 1983 down-sized Buick Century is 173 kg (380 lbs) lighter than the 1980 Buick Century which is likely to make reducing the weight penalty for hybridizing difficult.

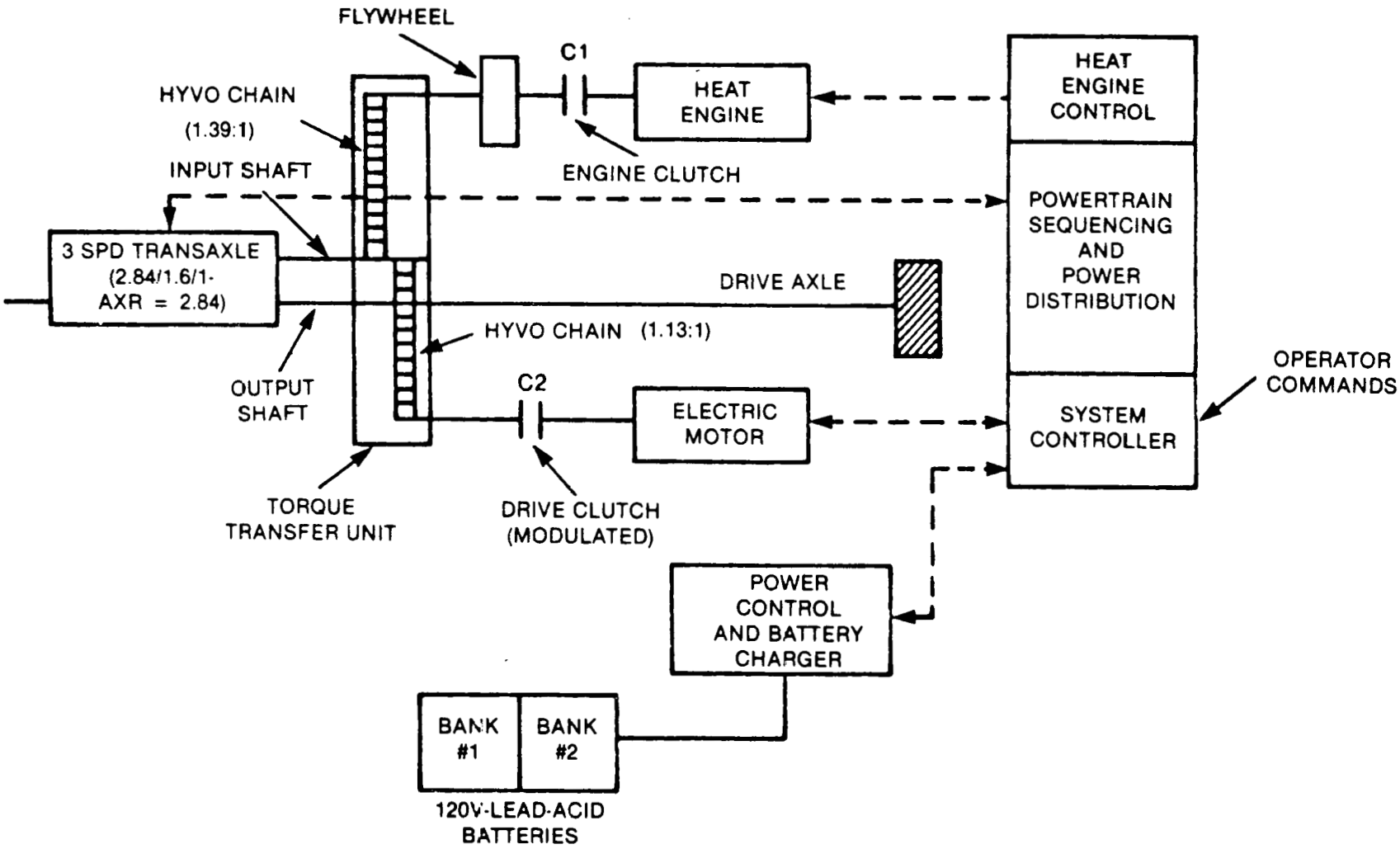

Figure 4.2-1. Schematic of HTV Power Train

Table 4.2-1

HTV POWER TRAIN CHARACTERISTICS

Parallel Configuration
Complete propulsion system under the hood
Transverse, two-shaft arrangement
Electric Drive
DC separately excited motor (34 kW peak)
Battery switching, 60 V and 120 V
Field control
Heat Engine
Four-cylinder, gasoline, fuel-injected (55 kW peak)
On/Off operation
Two-step, starting clutch action
Transmission/Torque Transfer
Three-speed automatic without torque converter
Hy-Vo chain drives
Modulated drive (EM) clutch
Batteries
Lead-acid, 760 lb
12 V, 106 Ah modules
Electrolyte circulation
Active cooling
Microcomputer control
Propulsion system sequencing
Transmission shifting
Electric motor and heat engine control
Power distribution and blending
Battery charging

4.2.2 Road Load

The HTV road load as a function of speed and grade (percent) is shown in Figure 4.2-3. The calculations were made using the following vehicle characteristics:

$$C_D A = 0.922\ m^2,$$

$$f_r = 0.011\ kgf/kgf,$$

$$w_v = 2168\ kg\ (test\ weight)$$

Also shown in Figure 4.2-3 are the peak powers attainable at the wheels from the electric motor and heat engine operating alone and the combined peak power when both are operating together. A transaxle efficiency of 92% was used in the peak power calculations. The drag coefficient (wind-weighted) of 0.45* was based on wind tunnel tests of a 3/8-scale model of

* The drag coefficient of 0.45 was used because the HTV is a notchback rather than the hatchback tested.

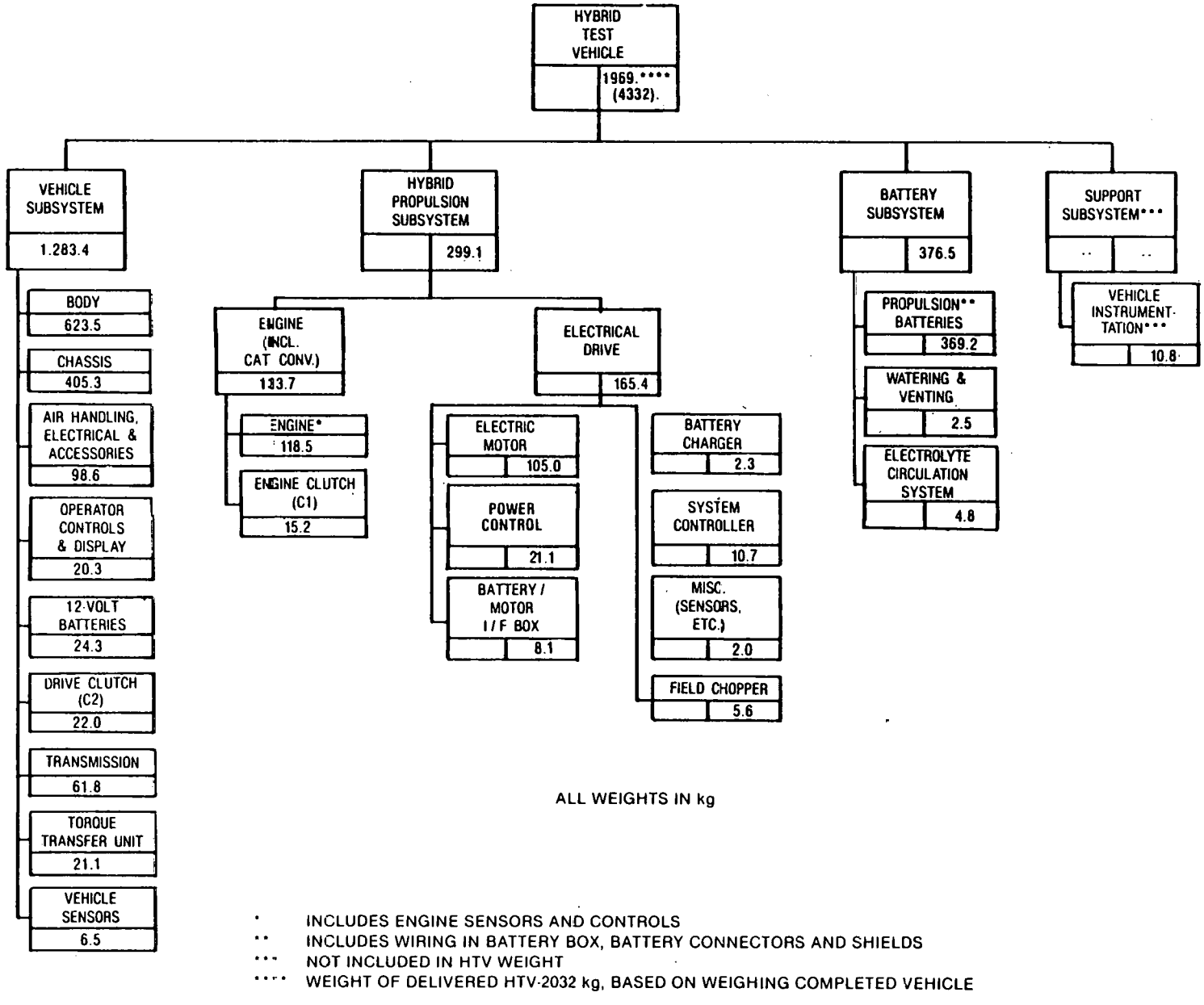

Figure 4.2-2. Hybrid Test Vehicle (HTV) Weight Breakdown Based on Weight of Individual Components

Table 4.2-2

WEIGHT BREAKDOWN OF THE HYBRID POWER TRAIN

Component	Weight (kg)
Engine and Starting Clutch	175
Mechanical Drive	117
Electric Motor	105
Power Electronics	40
Controller (microcomputer)	14
Battery Charger	23
Batteries Including Box	375
Subtotal	849 (1868 lb)

Table 4.2-3

SUMMARY OF WEIGHT DIFFERENCES BETWEEN HYBRID AND CONVENTIONAL ICE 5 PASSENGER CARS

Vehicle	Curb Weight (kg)	Weight Difference (kg)
HTV (as designed)	2032	+577
1980 Buick Century (V-6)	1455	0
1983 Buick Century (V-6)	1282	-173

the HTV (hatchback) in the University of Michigan wind tunnel. The rolling resistance of 0.011 kgf/kgf was based on tests of the P205/75R15 Goodyear tires at the Calspan Tire Research Facility (TIRF). The tire tests showed a steady-state (80 km/hr) rolling resistance of 0.00865 kgf/kgf. Based on recent studies (Reference 3) of the effect of road surface texture and roughness on rolling resistance, the measured rolling resistance values were increased by about 20& to obtain the 0.011 kgf/kgf value used to project the road-load characteristics of the HTV.

4.2.3 Acceleration and Gradeability Performance

The projected performance of the HTV (based on GE HYVEC simulations) is summarized in Table 4.2-4. The acceleration times shown require the combined output of the electric motor and heat engine, but the latter is not started until the drive clutch (C_2 in Figure 4.2-1) between the motor and the transmission is closed. This occurs at about 12 mph. The acceleration performance of the HTV is comparable to a conventional diesel-powered 5 passenger car. That performance can be maintained until the battery state-of-charge drops to about 30%. At lower states-of-charge, the peak power of the electric drive system is less than 34 kW and as a result, the acceleration times are longer.

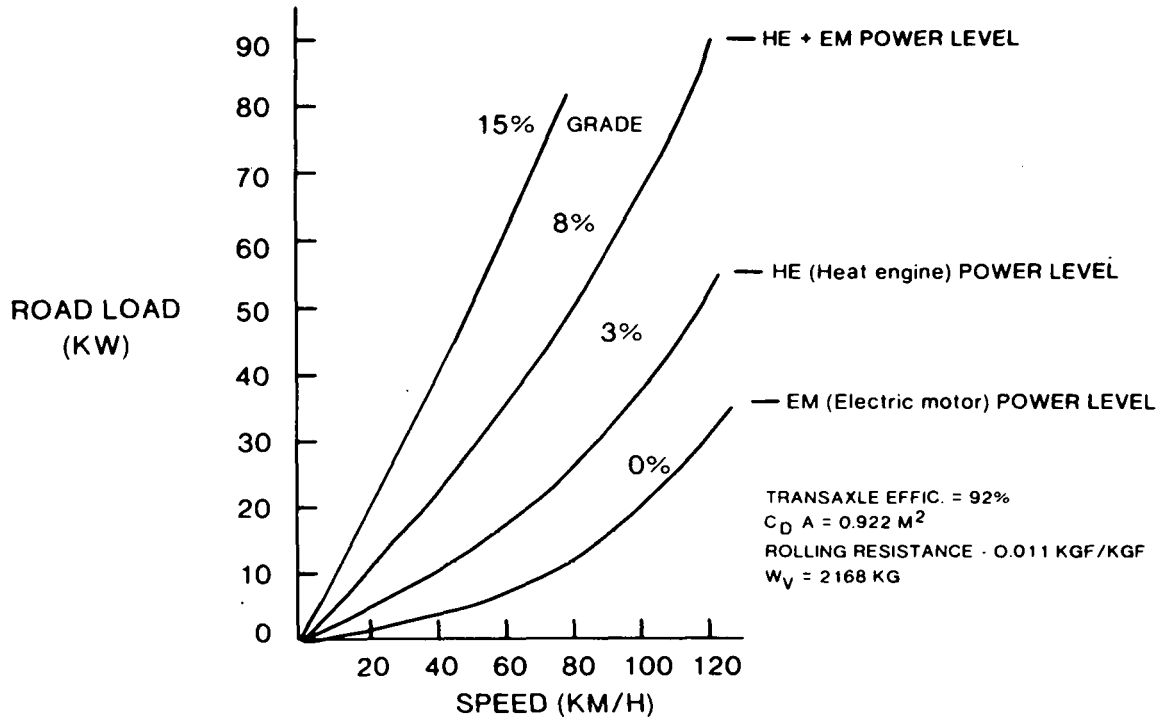

Figure 4.2-3. HTV Road Load for Various Grades as a Function of Speed

Table 4.2-4

PROJECTED HTV PERFORMANCE[1]

Acceleration[2]	
0 - 48 km/h (0 — 30 mph)	6.5 s
0 - 90 km/h (0 — 56 mph)	18.0 s
40 - 90 km/h (25 — 56 mph)	13.0 s
Gradeability	
Percent grade (sustained)	Speed[3] (km/h)
3	100 (3rd gear)
8	40 (2nd gear)
15	22 (1st gear)
Maximum Speed (km/h)	
120	— electric motor only
150	— heat engine only
>160	— electric motor and heat engine

(1) Based on computer simulations using the GE HYVEC Program
(2) Electric motor and heat engine combined, battery state-of-charge >30%.
(3) On heat engine alone

The gradeability characteristics (3 to 15% grades) shown in Table 4.2-4 can be achieved using only the heat engine. Hence the speeds indicated can be sustained continually, independent of battery state-of-charge. Higher speeds can be attained using both the electric motor and heat engine, but the resulting high battery currents will rapidly deplete the battery charge if the speeds are sustained for more than a minute or so. A maximum gradeability of 30% at low speeds (less than 15 mph) requires a torque of 195 N-m (140 ft-lb) from the electric motor. For the HTV motor, that torque can be produced using an armature current of 500 A and field current of 17.5 A. Higher torques (up to 240 N-m) can be produced by increasing the field current to its maximum value of 24 A. This cannot be done on a continuous basis, however, because the field windings would overheat. Hence, at sustained electric motor operating limits of 400 A armature current and 13.3 A field current, the HTV maximum gradeability is expected to be 20-25%.

The maximum speed of the HTV is comparable to conventional ICE cars and is in excess of 150 km/h (93 mph). These high speeds are attainable because of the relatively low final drive ratio (2.84) and the use of the three-speed transmission. The HTV is geared similarly to a conventional vehicle because of the desire to reduce the vehicle speed at which the drive clutch is closed to as low a value as possible and to have good highway fuel economy on the heat engine alone. Maximum speed for the HTV will ultimately be determined by power limitations, not motor or heat engine speed.

4.2.4 Fuel Economy and Energy Usage

The fuel economy and energy usage of the HTV have been calculated using the GE simulation program (HYVEC). The calculations were updated a number of times during Phase II as more refined information became available concerning the vehicle weight and component characteristics. For a given control strategy, critical factors affecting urban fuel economy are vehicle test weight, peak power from the electric motor, and the battery characteristics. Vehicle aerodynamic drag and rolling resistance, have a more significant effect on highway fuel economy than on urban energy usage. The final vehicle and component characteristics used to simulate the operation of the HTV are summarized in Table 4.2-5. The battery characteristics shown in Figures 4.2-4 and Figures 4.2-5 are based on tests of cells and 12 V modules developed by Globe for use in the HTV.

The fuel economy and electrical energy usage of the HTV are given in Figures 4.2-6 and 4.2-7 for both urban and highway driving. The EPA urban and highway cycles have been used throughout the program because they are the cycles used to rate the fuel economy of conventional ICE passenger cars. It is clear from Figure 4.2-6 and Figure 4.2-7 that the urban fuel economy of the HTV is strongly influenced by the distance traveled since the battery was last charged from the wall plug. This occurs because the VM* schedule used in the HTV (see Figure 4.2-8) is such that the heat engine is used as the primary power source at lower and lower vehicle speeds as the battery state-of-charge decreases. Both battery cell and module tests have shown that the effective energy storage capacity of the battery pack as used in the HTV for the EPA urban cycle is less than 5 kWh rather than the nominal 12.5 kWh corresponding to the C/3 discharge rate. Thus, as shown in Figure 4.2-6, the battery state-of-charge is about 50% at the end of the first EPA urban cycle (7.5 mi) for a starting VM of 40 mph. At a starting VM of 60 mph, the battery state-of-charge is 30% at the end of the first EPA urban cycle. This primarily electric range** is much less than was expected at the

* VM (V mode) is the vehicle speed below which the electric motor is the primary power source when the battery is fully charged; the operating VM is decreased from at maximum starting value as the battery is discharged (see Figure 4.2-8).

** Primary electric range is the distance driven on the EPA urban cycle before the operating VM is reduced significantly from the maximum starting value. The hybrid fuel economy remains constant for driving distances less than the primary electric range.

Table 4.2-5

VEHICLE AND COMPONENT CHARACTERISTICS FOR THE HTV

Vehicle Characteristics	
Test weight	2168 kg
Drag coefficient	0.45 (Notchback)
Frontal area	2.05 m^2
Rolling resistance	0.011 kgf/kgf
Component Characteristics	
Maximum motor power	33.6 kW
Maximum engine power	55.0 kW
Electrical energy storage	12.5 kWh (c/3 rate)
Battery characteristics	(see Figures 4.2-4 and 4.2-5)
Operating V-mode Schedule	(see Figure 4.2-A)

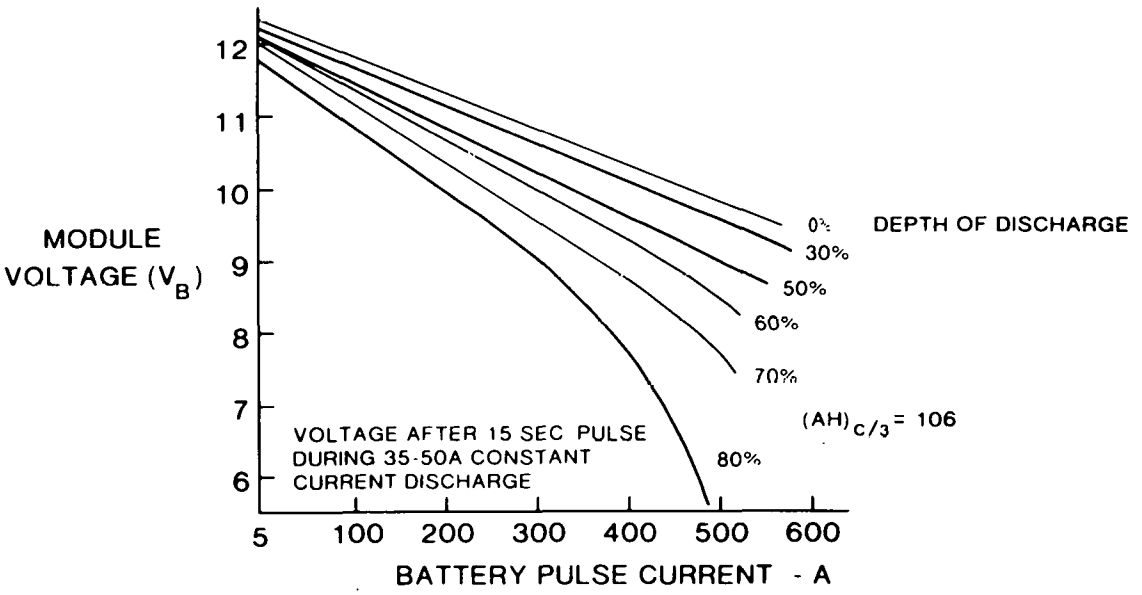

Figure 4.2-4. Pulsed Power Characteristics of the Hybrid Vehicle Battery

initiation of the Phase II program. In the hybrid vehicle application, the battery pack experiences high currents during the time that the vehicle is operated primarily in the electric-drive-mode. Hence the useable capacity of lead-acid batteries, whose capacity is strongly dependent on discharge rate, is only a fraction of the C/3 nominal rated capacity. This factor is the principal reason for the less favorable than expected gasoline saving results discussed in the following paragraphs.

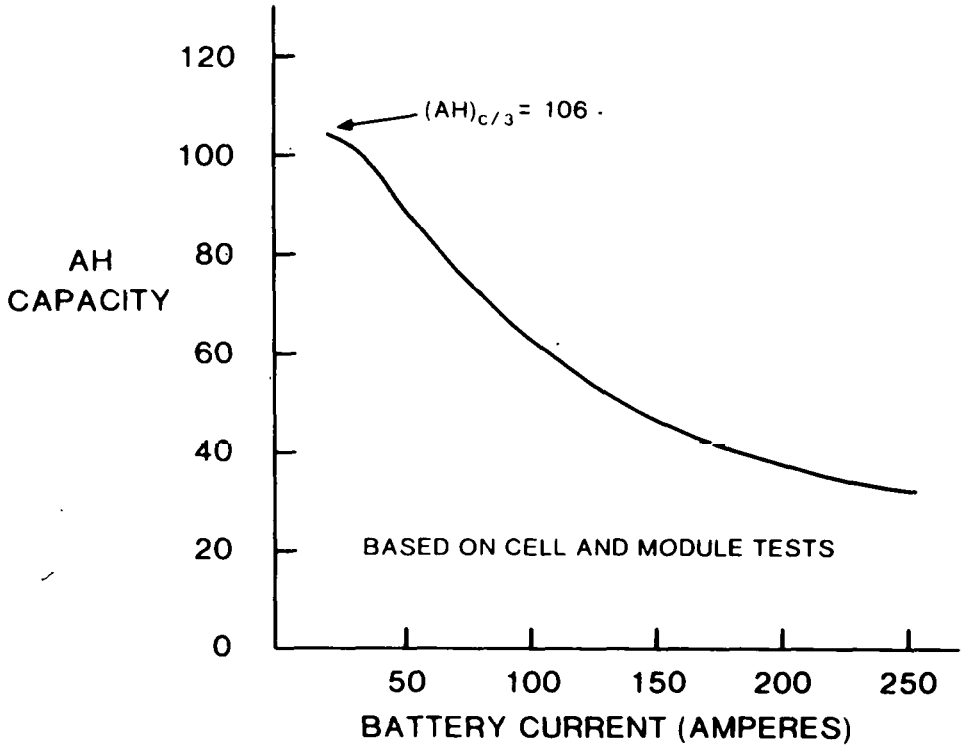

Figure 4.2-5. Ampere-hour Capacity of the Hybrid Vehicle Battery for Constant Current Discharge

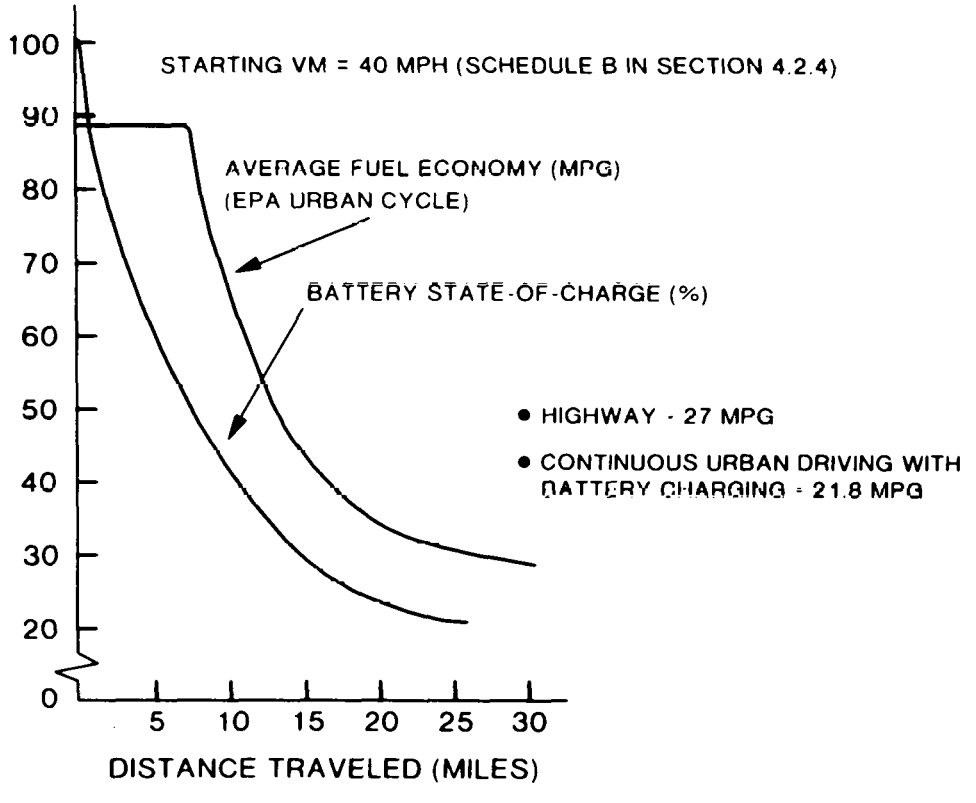

Figure 4.2-6. Hybrid Vehicle Battery State-of-Charge and Fuel Economy for Urban and Highway Driving

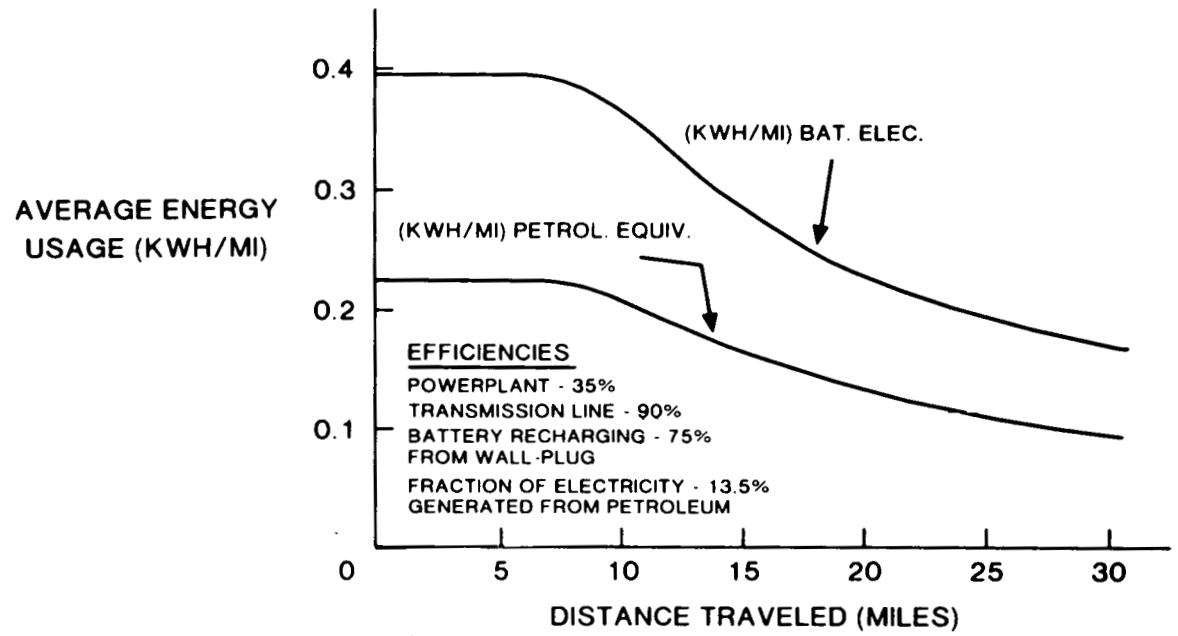

Figure 4.2-7. **Average Energy Usage (kWh/mi) - Battery Electricity and Petroleum Equivalent**

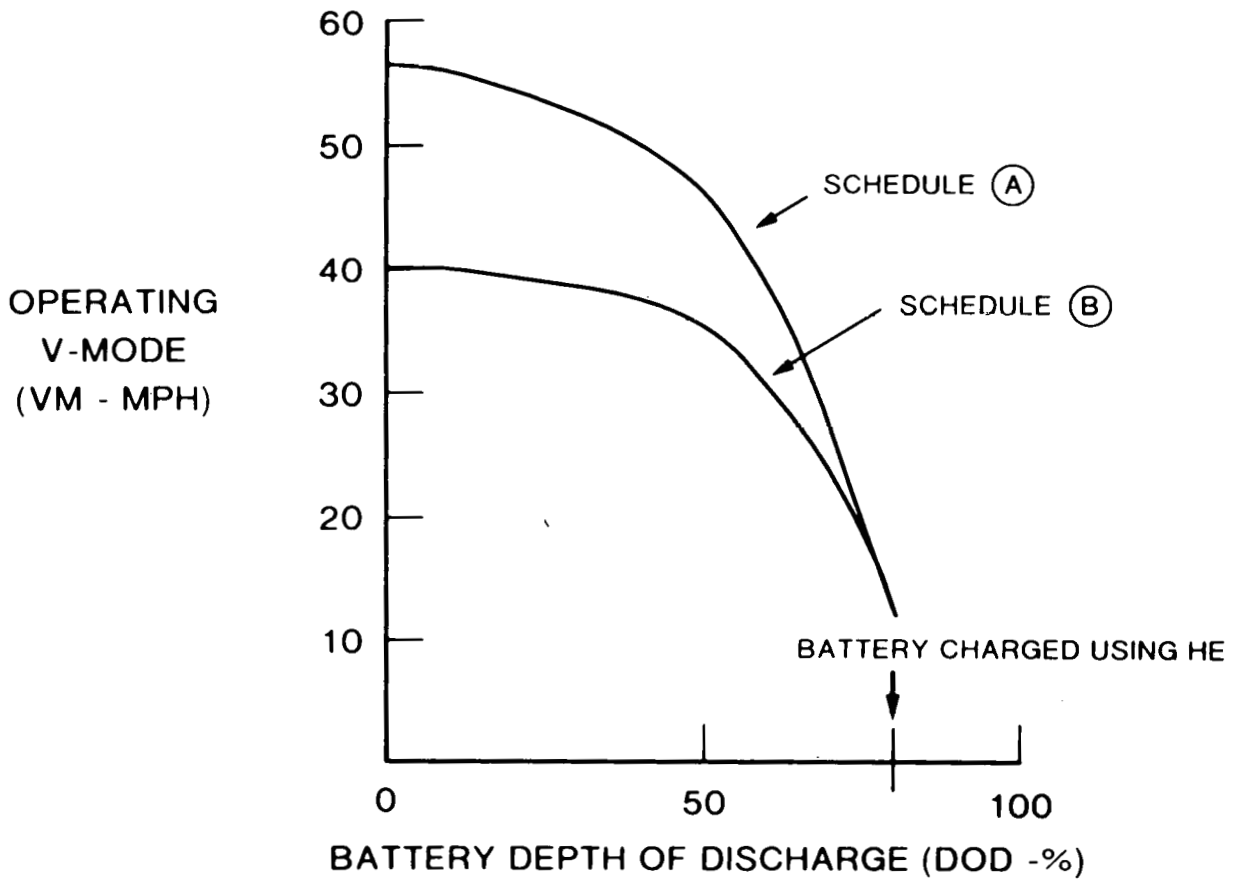

Figure 4.2-8. **The Operating V-Mode Schedule in the HTV for VM-Starting Values of 60 mph and 40 mph**

The primary electric range of the HTV is projected to be between 5-10 mi in urban driving. Hence the very high fuel economy potential (90-200 mpg for VM between 40 and 60 mph) of the HTV can be realized for only a driving range of 10 mi or less. For longer driving ranges the fuel economy decreases rapidly, i.e., 43 mpg at 15 mi and 29 mpg at 30 mi. For continuous urban driving in which the battery is charged intermittently by the heat engine a fuel economy of 21.8 mpg is projected (Figure 4.2-6). As shown in Figure 4.2-7, the corresponding electrical usage (kWh/mi) from the wall-plug decreases rapidly with range for ranges in excess of 10 mi. The restricted primarily electric range of the HTV is due to the characteristics of the lead-acid batteries. The very high fuel economy potential of the hybrid power train could be attained for ranges in excess of 20 mi if it were possible to utilize 10-12 kWh from the battery pack in the hybrid application.

The highway fuel economy of the HTV is projected to be 27 mpg over the EPA highway cycle. Preliminary dynamometer tests of the HTV indicate this may be a conservative estimate. For highway driving, the power train control strategy is such that the HTV is primarily powered by the heat engine except when power demand exceeds the capability of the engine alone. In those instances, the electric drive system is utilized together with the heat engine. The projected highway fuel economy of 27 mpg for the HTV is somewhat less than the 33 mpg projected at the outset of Phase II because the final vehicle weight is about 10% higher than initially estimated, the body styling was changed from a fastback to a notchback, increasing the estimated drag coefficient from 0.42 to 0.45, and the power train losses, including accessory loads, are somewhat larger than expected.

The fuel economy values discussed in the previous paragraph refer to gasoline from the pump and do not include petroleum used at the electric power plant to generate the electricity stored in the battery. In 1980*, on a national average, 13.5 % of the electricity used is generated from oil. When that petroleum is included, as is shown in Table 4.2-6, the effective fuel economy of the HTV is lower than the values previously cited. The pump-based and effective (petroleum equivalent) fuel economies are compared for various daily distances in Figure 4.2-9.

* The fraction of electricity generated using petroleum decreased to 10% in 1981.

Table 4.2-6

CALCULATION OF EQUIVALENT FUEL ECONOMY OF HYBRID VEHICLE INCLUDING PETROLEUM NEEDED TO GENERATE THE ELECTRICITY USED

Cycle No.	Distance (mi)	Battery State-of-Charge (%)	Net Energy Out of Battery (kWh)	Elec. kWh[4] / mi	Petroleum Equivalent Electricity[2] kWh / mi	Gasoline From Pump (mpg)[4]	Effective Fuel Economy Including Generation of Electricity[3] (mpg)
1	7.5	51	2.98	0.397	0.227	88.9	57.3
2	15.0	31	4.28	0.285	0.162	43.4	32.4
3	22.5	24	4.75	0.21	0.120	33.0	29.8
4	30.0	22	5.18	0.17	0.097	29.4	27.3
5	37.5	22	5.18	0.14	0.086	27.5	25.8
6	45.0	22	5.18	0.12	0.074	26.4	25.1

(1) Battery charged by heat engine
(2) Efficiencies used $\eta_{Gen} = 0.35$, $\eta_{Trans} = 0.9$, $\eta_{Bat} = 0.75$; 13.5% of electricity generated from petroleum
(3) 1 gallon gasoline = 36.6 kWh
(4) Average values based on total distance traveled

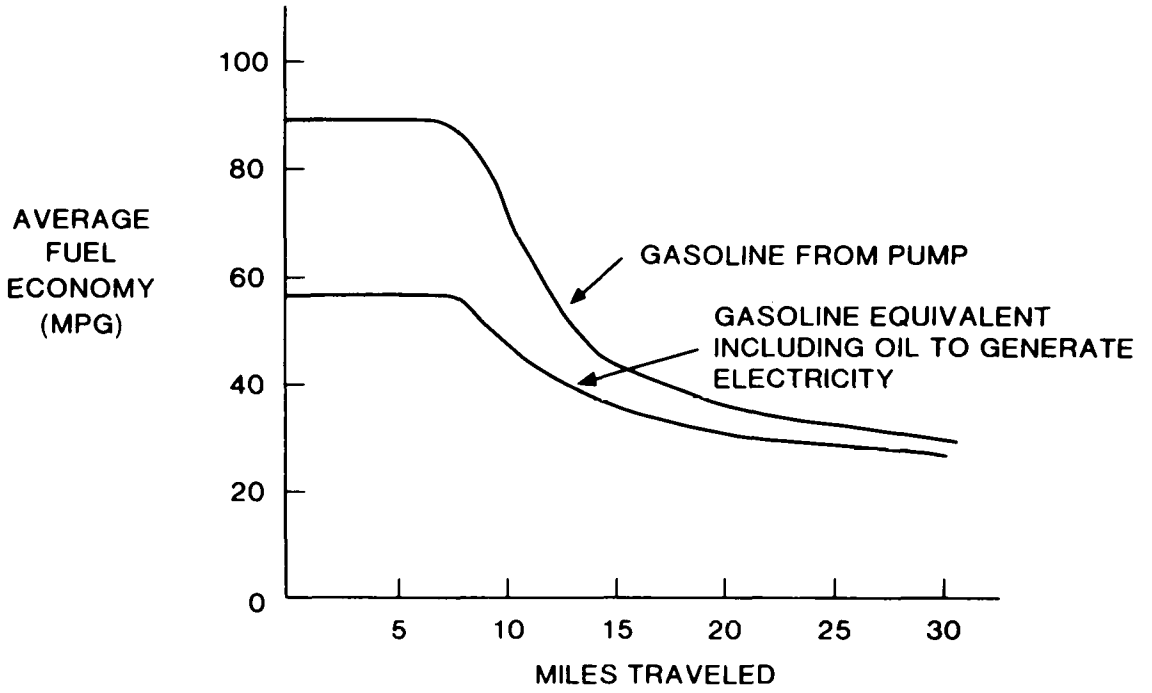

Figure 4.2-9. Hybrid Vehicle Fuel Economy (including petroleum used to generate electricity)

It is clear from Figures 4.2-6 and 4.2-9 that the attractiveness of the hybrid vehicle is a strong function of daily driving distance. For daily ranges of 10 mi or less, the use of the HTV would result in saving a large fraction of the fuel used by an ICE car of the same passenger carrying capacity. For much longer daily urban distances and highway driving, the HTV is less attractive. Hence, in order to properly evaluate hybrid vehicles, it is necessary to include the use statistics as they apply to potential owners. Methods have been developed (Reference 4) to do this in which potential owners have been categorized in terms of annual mileage. For example, 50th-percentile owners are assumed to live 7.5 mi from their work and to use their cars 11,400 mi on an annual basis (7400 mi for urban driving and 4000 mi for highway driving). The pump and effective (petroleum equivalent) fuel economy of the HTV are given in Figure 4.2-10 for a wide range of potential users. For 50th-percentile owners, the pump and effective annual average fuel economies are 32 and 29 mpg, respectively.

Further, it is of interest to compare the total energy (gasoline plus electricity) used by the HTV and a reference 1980 5/6 passenger ICE car. The comparison is made in Table 4.2-7 for 50th-percentile owners. The results indicate a gasoline saving of 23% and a petroleum saving of 18% compared to a 1980 Buick Century; however, the HTV would use 12 % more total energy than the conventional 1980 ICE vehicle. This additional total energy use of the HTV is due to its heavier weight (577 kg). Table 4.2-7 indicates that the HTV is a much more efficient vehicle (i.e., a greater fraction of the energy input to the power train is ultimately applied at the wheels to power the vehicle) than the conventional ICE vehicle, but this does not compensate for the greater energy demand due to the higher weight of the HTV for a powerplant efficiency of 35%. Considering only the energy utilized from the gasoline pump and wall plug, the HTV requires .585 $\frac{kWh}{ton-mi}$ on an annual basis (11,400 mi) while the 1980 Buick Century requires 1.01 kWh/ton-mi on the same basis. Note that the energy usage has been

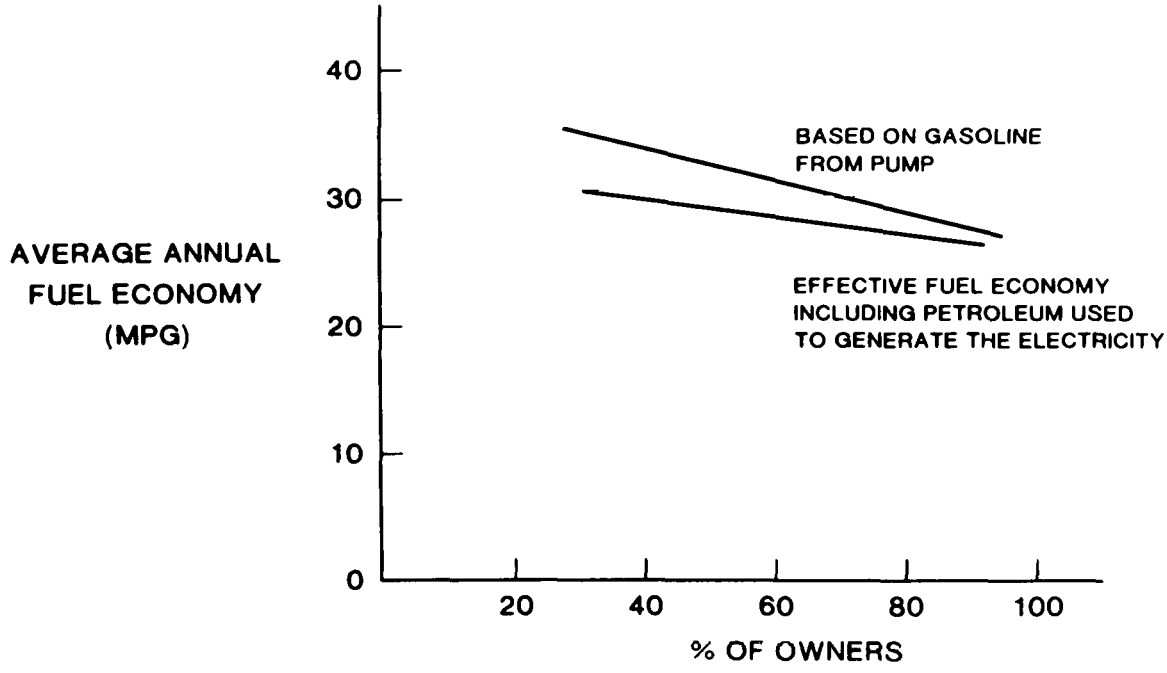

Figure 4.2-10. Average Annual Fuel Economy for the Hybrid Vehicle in Urban Driving

normalized using the respective weights of the two vehicles. Hence it follows that the hybrid power train is more efficient per pound of vehicle for the same mission than the ICE vehicle power train. As shown in Table 4.2-7, the energy cost (gasoline* plus electricity**) for operating the HTV is $72/yr less than that for the 1980 Buick Century on which it is based.

* Gasoline price - $1.50 gal

** Electricity - 5¢/kWh

Table 4.2-7

COMPARISON OF GASOLINE AND ENERGY USAGE FOR HYBRID AND CONVENTIONAL ICE VEHICLES (50th-PERCENTILE OWNERS)

	Gasoline Used (gal)	Electricity Used at Wall Plug (kWh)	Total Energy at Power Plant (kWh)	Petroleum Used* (kWh)
Hybrid Vehicle (HTV)				
Urban Driving (32.5 mpg) (7400 mi)	228 (35% saved)	1,974	14,610	9,190
Highway Driving (27 mpg) (4000 mi)	148	---	5,417	5,417
Total	376 (23% saved)		20,029 (12% greater)	14,608 (18% saved)
Conventional ICE Vehicle (1980 Buick Century)				
Urban Driving (21 mpg) (7400 mi)	352	---	12,883	
Highway Driving (29 mpg) (4000 mi)	138	---	5,051	
Total	490		17,934	

Energy Cost Savings

Cost Saving = Gasoline 1980 Buick Century − Gasoline HTV - electricity HTV
= \$735 − \$564 − \$99 = \$72/yr

Calculation made for gasoline at \$1.50/gal and electricity at 5¢/kWh

*Assuming 13.5% of electricity generated from petroleum

Section 5

DESIGN AND DEVELOPMENT

5.1 INTRODUCTION

In this section of the report, the design and development of the hybrid test vehicle and its power train are discussed in detail. The major subsections of this section are the following: 5.2 - Vehicle Design and Analysis; 5.3 - Hybrid Propulsion System; 5.4 - Battery System; and 5.5 - Mule Vehicle Programs. Each subsection is further divided, treating in detail the design, development, and testing of the components of each of the vehicle/power train subsystems.

5.2 VEHICLE SUBSYSTEM

The hybrid vehicle (body, chassis, and accessories) was designed so that maximum use could be made of existing production components with a minimum compromise in program goals. For this reason, the major portions of the body center section and interior were taken from a General Motors A-body Buick Century. Therefore, the hybrid vehicle offers space and comfort levels equal to other current models. This choice dictated compromises in the exterior shape but achieved an economical vehicle design and build program.

The hybrid vehicle design includes front-wheel drive; independent front suspension; power rack and pinion steering; lightweight trailing arm and beam rear suspension; low-rolling resistance, steel-belted, radial tires; power brakes; automatic three-speed transmission; and air-conditioning. The propulsion batteries are packaged under the hood for easy maintenance and passenger space maximization. A photograph of the HTV as delivered to JPL is shown in Figure 5.2-1.

The vehicle is designed to meet the requirements of all Federal Motor Vehicle Safety Standards (FMVSS) and the applicable Department of Transportation (DOT) recommended practices for electric vehicles.

5.2.1 Vehicle Analysis

5.2.1.1 Riding and Handling

Front-wheel drive and high front weight bias, coupled with the desire to use currently available major components, led to use of the General Motors E-body front suspension. Numerous rear suspensions in the load capacity required were available. The General Motors X-body rear suspension was selected due to its low weight, simplicity, and packaging requirements.

Ride quality is dependent upon the ride frequencies of both the front and rear suspension systems and the relationship of one to the other. A number of vehicles were tested and suspension frequencies were measured. The 1980 Eldorado was selected as offering the most desirable ride. Hence, the hybrid test vehicle spring rates were selected to match the 1980 Eldorado frequencies. Front and rear stabilizer bars limit the vehicle roll to 8°/g.

Vehicle handling reflects the effect of many parameters. Among these are weight distribution, tire characteristics, steering system arrangement, suspension geometry, and compliances. Computer simulations were run after all the above inputs were determined. Calculations showed the vehicle to understeer heavily and be responsive. Table 5.2-1 shows a comparison of the HTV with typical sub-compact and full-size passenger cars. Handling tests of the HPTM at the TRC test track indicated the HTV would have understeer comparable to a large car and response comparable to a small car.

Figure 5.2-1. Hybrid Test Vehicle (HTV)

Table 5.2-1

COMPARISON OF HTV AND TYPICAL CAR PERFORMANCE PARAMETERS

Performance Parameter	Full-size	Sub-compact	HTV	
			Calc.	Test
Understeer Factor, degrees/g	5.84	2.84	11.87	6.55
Lateral Acceleration Gain, g/rad				
30 mph	3.7	5.4	2.8	–
60 mph	6.9	12.0	4.01	8.88
Yaw Velocity Gain, rad/rad				
30 mph	2.72	3.98	2.05	–
Body Slip-Angle Sensitivity, degrees/g	5.0	4.9	2.81	–

A quantitative evaluation of the handling of the hybrid power train mule (see Section 5.5 for a description of that vehicle) during track tests at the Transportation Research Center of Ohio (TRC) showed that the handling of the vehicle was quite close to that calculated and was better in all respects than the baseline 1980 Buick Century. Road tests of the hybrid power train mule (HPTM) in Schenectady utilizing a ride jury indicated the HPTM had ride characteristics comparable to those of the 1980 Buick Century and the 1980 Buick Riviera, which were included in the HPTM ride tests for comparison purposes.

5.2.1.2 Tire Test

In keeping with the need for an energy-efficient vehicle, low-rolling resistance tires are used. The tires, manufactured by Goodyear, are designated P205/75-R15 extra load and are capable of running at 50 psi.

Tire tests were conducted at the Calspan Tire Research Facility. In the tests, rolling resistance at steady speeds and on a simulated EPA urban test cycle were measured. Table 5.2-2 shows the results of the steady-state rolling resistance tests. The EPA cycle tests were run at various temperatures. Table 5.2-3 shows the results of the EPA cycle tests. Cornering tests were also made at various slip and camber angles. The data was used in the handling simulation calculation given in Table 5.2-1.

5.2.1.3 Brakes

Computer simulations of brake balance and bulk temperatures were made using factors accepted in the auto industry. Delco-Moraine cooperated in supplying test results for vehicles using the same brake components. Data were used to validate the computer program and the appropriateness of the factors used. Calculations showed the brake system to be capable of meeting the fade requirements of the brake standard. Brake temperatures predicted for the fade test were 1305 °F for the front and 709 °F for the rear. These temperatures compared favorably with 1337 °F measured by GM on the Seville.

With modification of the rear brake wheel cylinders to 11/16 in. diameter, incorporation of a 0.27:1 proportioning valve and an early trip pressure of 250 psi, the system produces 82% front braking, which is required to eliminate premature wheel lockup. This calculation did

Table 5.2-2

STEADY-STATE ROLLING RESISTANCE
(30 mph)

Normal Load (lb)	Tire Pressure (psi)	Rolling Resistance Force (lb)	Rolling Resistance Coefficient fr(lb/lb)
1623	49.4	12.73	0.0078
1586	50.0	12.05	0.0076
1590	40.1	13.46	0.0085
1404	30.0	14.28	0.0100
1098	50.1	8.32	0.0076
821	30.1	8.14	0.0100
1610	49.1	12.14	0.0075
1591	50.1	12.19	0.0077
1589	40.1	13.96	0.0088
1402	30.1	14.38	0.0102
1098	50.1	8.60	0.0078
800	30.1	8.06	0.0101

not include the effect of regenerative braking. Therefore, it was concluded that the hydraulic braking system capacity was adequate and that, with further development of the proportioning, good balance was achievable.

Road tests of the hybrid vehicle braking system were conducted following the FMVSS procedures for brake fade and recovery. The tests were run in Schenectady using the Hybrid Power Train Mule (HPTM) with the hybrid power train operational. The vehicle met all the requirements of the FMVSS standard. Driving experience with both the HPTM and HTV on public roads in Schenectady indicated that the braking system, including regeneration, operates satisfactorily with the driver having a safe and secure feeling for a wide range of driving conditions.

5.2.1.4 Aerodynamic Testing

Aerodynamic testing of the HTV shape was limited to "slicking-up." Tests were conducted using the University of Michigan wind tunnel. A 3/8 scale model of the hatchback configuration* was tested. Figure 5.2-2 shows the model in the wind tunnel. Oil trace, smoke, and tufting were used to identify turbulent areas. The effects of headlamp covers, rearview mirrors, and a rear spoiler were examined. The drag coefficient, C_D, was determined at zero yaw and at yaw angles up to 30 degrees. The results were windweighted for an

* The final notchback configuration was not wind-tunnel tested.

Table 5.2-3

SUMMARY OF TEST RESULTS FROM EPA URBAN CYCLE TESTS

Tire Pressure[1,2] (psi)	Ambient Temperature (°F)	Total Distance Traveled (miles)	Integrated Energy Parameter[3] ER $\left(\frac{ft-lb}{ft}\right)$ mi	Average Rolling Resistance Coefficient fr[4] (lb/lb)
30	55	7.45	113.46	0.010
45	58	7.44	97.91	0.0088
30	89	7.45	128.31	0.0115
45	89	7.45	89.83	0.0080
45	86	7.47	133.09	0.0114

(1) Tire Normal Load N_L: 1500 lb

(2) Capped tire pressure varies with temperature during run

(3) $ER = \sum_{cycle}$ [(energy used per ft) Δ m_i cycle]

$ER = \sum_{cycle}$ [(tire resistance force) Δ m_i cycle]

(4) $fr = \frac{ER}{7.45\ (N_L)}$ (follows from (3))

8 mph average cross windspeed. The hatchback configuration produced a C_D of 0.363 at zero yaw and 0.39 windweighted. Since the test model was not representative of the underbody or radiator opening areas, the C_D of an actual full-scale hatchback vehicle would be expected to be slightly higher than the test value of 0.39. A C_D of 0.42 was used for the hatchback HTV design.

Partway through the Phase II Program, it was decided by JPL and DOE to change the rear styling of the HTV from the hatchback to a notchback styling. The notchback styling will result in a higher drag coefficient than the hatchback styling. It is estimated that the C_D of the notchback HTV is 0.45 rather than 0.42 for the hatchback design.

5.2.1.5 Structural Design

This subsection describes the front structural component static crush tests, front-end crush tests, battery box dynamic crush, and the computer simulation analysis of crash effects.

5.2.1.6 Front Structural Component Static Crush Tests

During frontal collisions, a vehicle's major structural energy-absorbing members tend to be loaded along the longitudinal axis. The structural collapse then approximates the post-buckling behavior of short columns. A series of static, force-deflection crush tests were con-

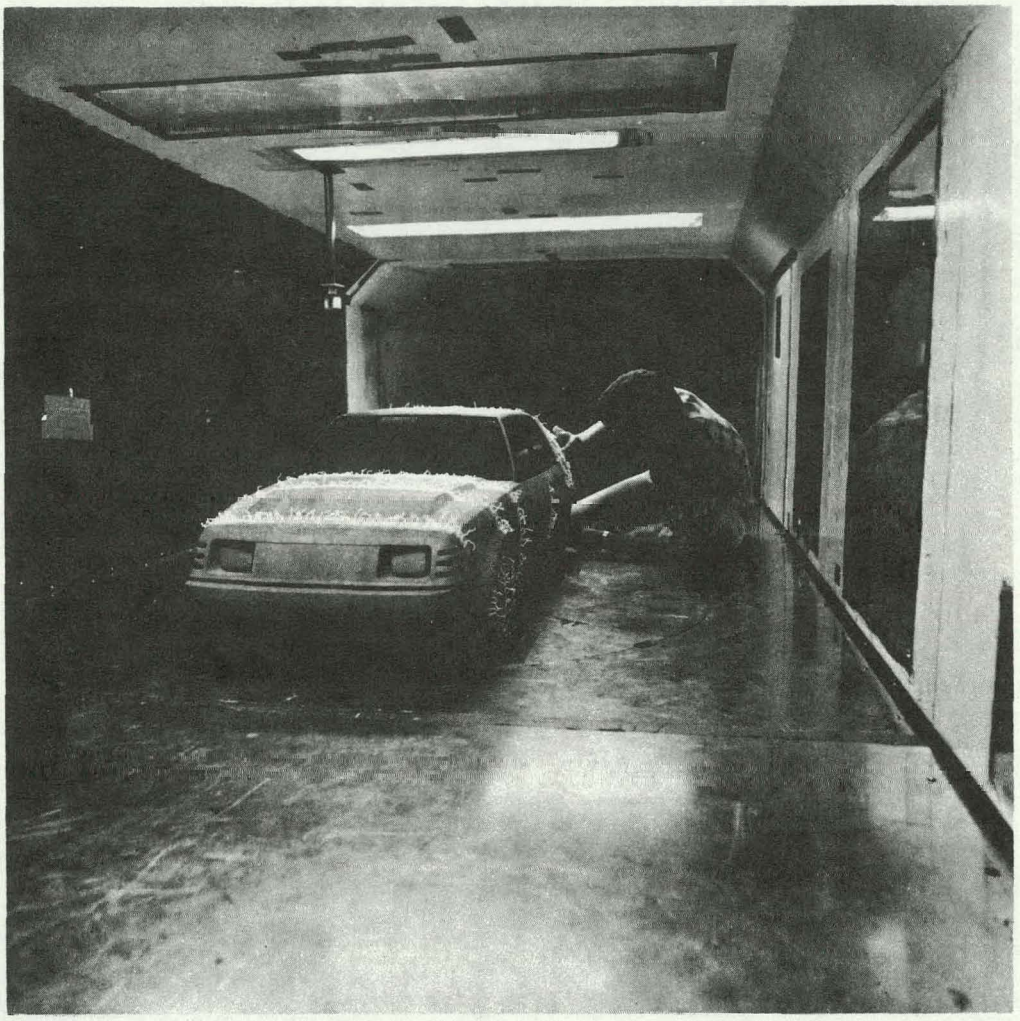

Figure 5.2-2. Scale Model in Wind Tunnel

ducted on the prototype frontal members in order to determine peak collapse forces and energy absorption capabilities. These tests were utilized to size the structural members as to section construction, fabrication technique, and material gauge. These tests also provided an indication of the failure mechanism which could be expected during dynamic barrier testing.

A vehicle's front structural members must meet two often conflicting requirements. First, they must provide the vehicle's structural support for road-load inputs, component attachment, and the structural integrity of the vehicle in torsional and beaming stiffness. Second, they must provide energy absorption capability which allows a safe crash deceleration for the occupants. The two major frontal members were fabricated in 24 in. sections and crushed statically in a Tinus Olson test machine (Figures 5.2-3 and 5.2-4).

Several variations of section design, material thicknesses, and welding techniques were evaluated. The final configuration for the upper catwalk member is a 2-1/2 in. by 2-1/2 in. square section with overlapping flanges spot welded. An internal diagonal web attached at the upper and lower skin flange provided the stiffness for controlled collapse rather than major column buckling. The material chosen is mild steel, 0.060 in. thick. The lower frame

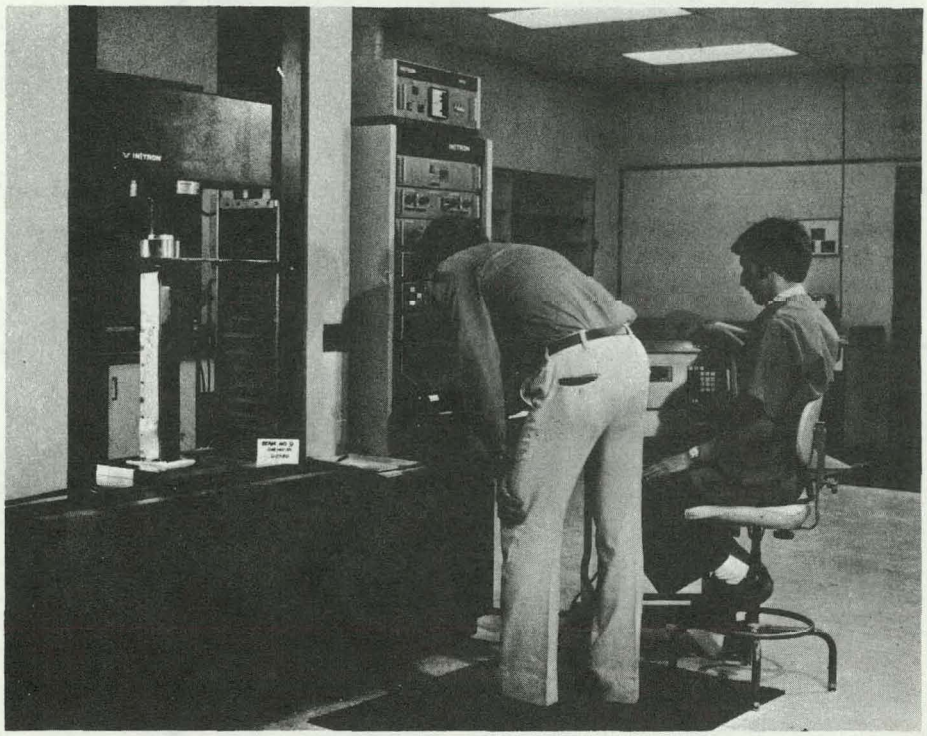

Figure 5.2-3. Static Crush Test (overall view)

member exhibiting the best force levels and controlled collapse is a 2 in. by 5 in. section constructed from overlapping C-sections skip welded along the outer surface.

In order to initiate crush, darts were formed on the beam sides forward of the vehicle front crossmember. It is interesting to note that the crush behavior initiated by the ribbed beam repeatedly continued through the nonribbed portion once the crush sequence had been established. These beam sections were then integrated into the front module test structure for full-scale testing.

5.2.1.7 Front End Crush Test

The barrier crash computer simulation analysis, done to establish the optimum hybrid drive system component arrangement, was conducted using available automotive static crush data. Due to the unique front packaging configuration of the HTV, a better data base was necessary to predict, with confidence, the crash performance of the structural mule.

A front structural test module was constructed using a Buick front cowl and pillar section. The front-end members were fabricated identical to the beam sections previously tested. The test module was constructed utilizing the fabrication and assembly techniques which would be employed in the HTV.

The module was statically crushed, element by element, at Calspan in order to establish the force deflection properties of the front structure. Static crush testing has proven to be a useful development tool in understanding vehicle barrier performance. Although the individual elements are crushed separately, a computer simulation is used to time phase these results and apply the correct strain-rate sensitivity. It was assumed that the crushing of the front structural members and the pushing of the battery box and electric motor into the firewall

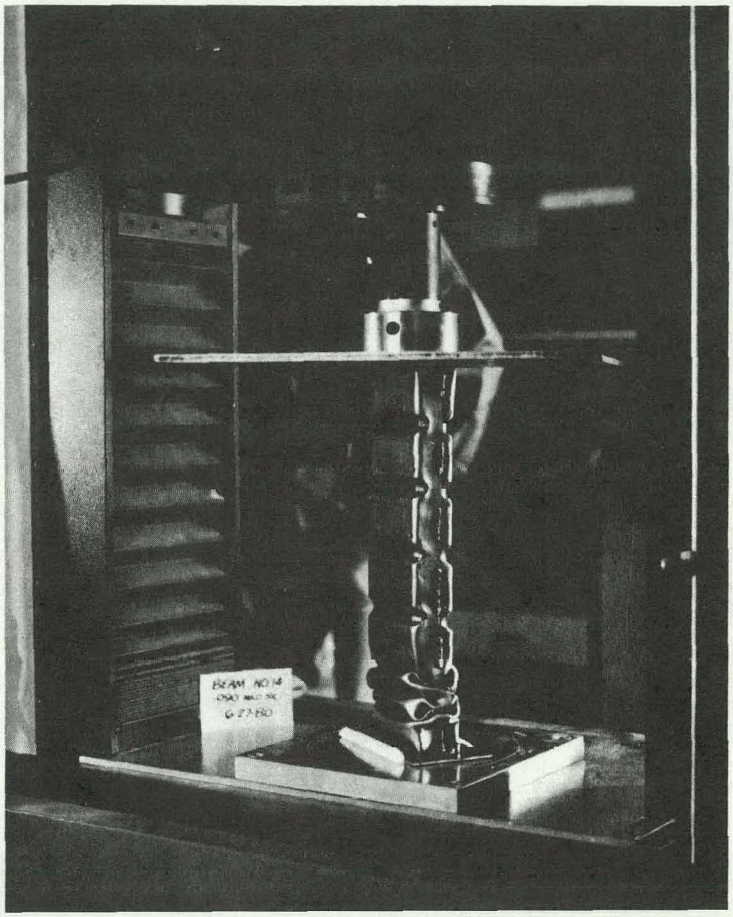

Figure 5.2-4. Static Crush Test (close-up)

and toe-board panels occurred simultaneously. This led to some uncertainty in the force-deflection properties of the rear rail and the dynamic interaction of the battery box with the ICE engine and the firewall. Due to the complexity of the hybrid vehicle power train package, time phasing of the crash and mass displacement of the components greatly affected deceleration and crash performance of the vehicle.

The static data obtained were used as input into the MGA Research Corporation computer simulation. It became apparent that the interaction of the engine and the battery box was critical to the vehicle crash performance. The decision was made to dynamically test crash a battery box module into a fixed engine block in order to establish the actual force levels and the mode of failure. Controlled, low force-level crush of the battery box face would ensure minimum firewall intrusion, thus eliminating electrolyte spill into the passenger compartment and ensuring windshield retention.

5.2.1.8 Battery Box Dynamic Crush

The battery box test module consisted of an operational battery box including the outer case, lid, and wiring circuit. The module was mounted on a moving barrier framework consisting of the hybrid vehicle's lower members and battery box support crossmembers. The module was set up to discharge through a resistor bank at 200 A during impact.

The VW engine was dressed and outriggered from the Calspan rigid barrier face. The engine was impacted by the battery box at 20 mph, a speed established from previous simulations at the predicted relative velocity. Barrier load cells and onboard accelerometers were employed to obtain the dynamic force deflection profile.

The impact resulted in force levels which were higher than those predicted from static data using the established strain rate factors. These are plotted in Figure 5.2-5. The failure mode which resulted was similar in nature to that observed statically. The ICE crushed through the battery box, resulting in failure of seven of the ten batteries. The large inertia of the battery mass prevented rearward displacement or upward motion. The engine crushed the lower leading edge of the box, damaging the batteries from the underside. Even though the battery pack was discharging, there was no evidence of terminal contact or flashing of the hydrogen atmosphere.

Based on these test results, the battery box and the mounting system were used as designed in the structural mule. The force levels generated by this interaction should be reacted by the battery mounting system, the firewall, and the inertia of the mass. Firewall intrusion should be minimal during the barrier crash.

5.2.1.9 Computer Simulation Analysis

The results of the static force deflection tests and the battery box dynamic test were employed in the SMDYN - Spring Mass Simulation by the MGA Research Corporation. The

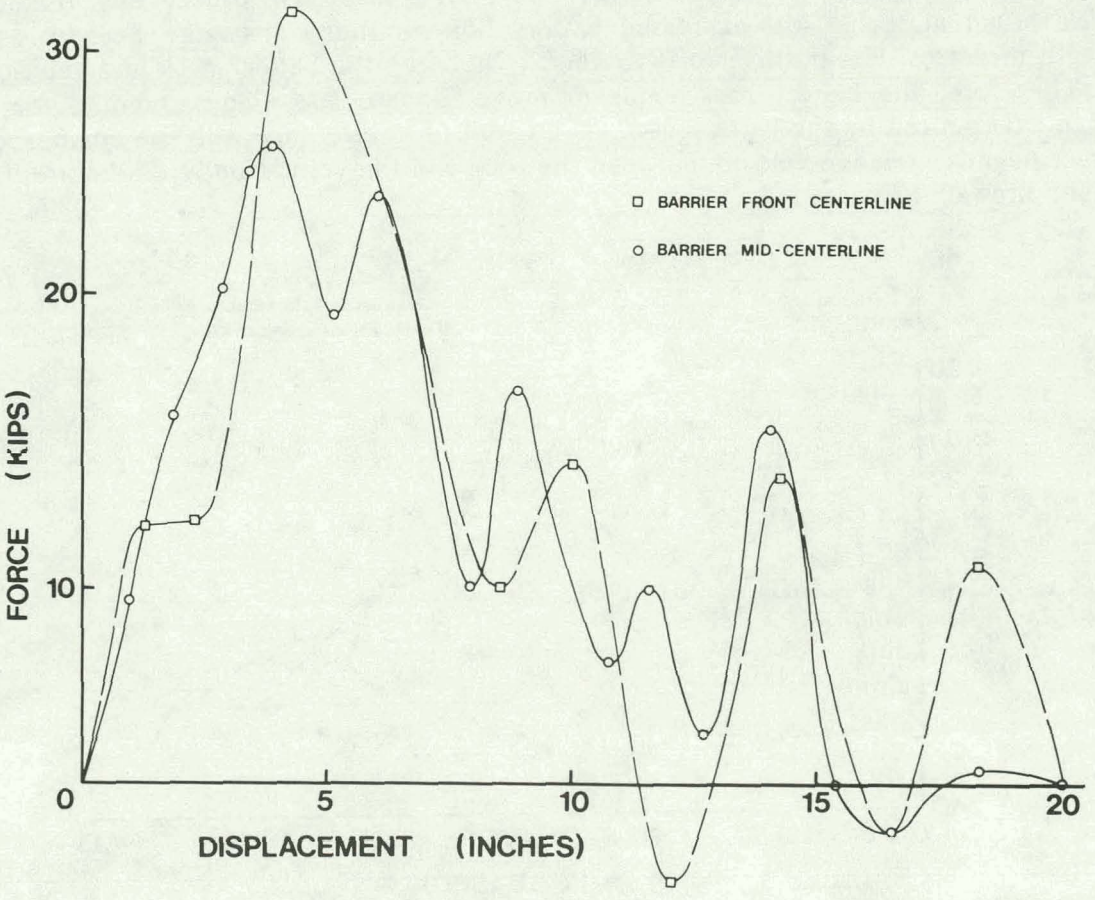

Figure 5.2-5. Engine into Battery Box (force vs. displacement)

model treats the physical automotive structure as a one-dimensional representation, idealized in the form of discrete lumped masses interconnected by massless deformable elements characterized by force-deflection properties. Since automotive collisions are dynamic, a method was used in the model to account for the dynamic overstresses by the use of a strain-rate factor.

A series of 40 computer runs was made to establish the baseline barrier prediction. The effects of changes to key elements of interest were also studied in order to demonstrate variations from the baseline and to establish confidence in the structure.

A comparison of the deceleration time-history of the baseline structural design with a measured General Motors A-body response is shown in Figure 5.2-6. The results of this baseline run are considered to be satisfactory as the peak deceleration of the passenger compartment and the duration are similar to the GM A-body car. Maximum passenger toeboard intrusion of 5 in. occurred due to rearward displacement of the electric motor. The battery box was not displaced rearward and the overall vehicle crush was 26.1 in.

Various structural parameters for the rear frame rail, the battery box mount, the engine mount, and the engine/firewall crush were evaluated. Only an increase in rear frame rail strength had an effect on the peak deceleration. It is interesting to note that an increase in battery box mounting rigidity caused a decrease in peak deceleration. This was apparently due to the increase in the effective mass of the passenger compartment due to stronger coupling of the two masses. However, this increase in mount strength also tended to increase the intrusion into the passenger compartment. Two factors may have caused this. First, overall vehicle crush increases with increased battery box mounting strength. Second, as mount strength increases, less-positive relative velocity between the battery pack and vehicle is built up. Therefore, the battery pack tends to move forward less. Consequently, the velocity change experienced by the battery pack, as a result of interference with the engine, results in a larger negative relative velocity between the pack and the vehicle body. Therefore, intrusion into the firewall increases.

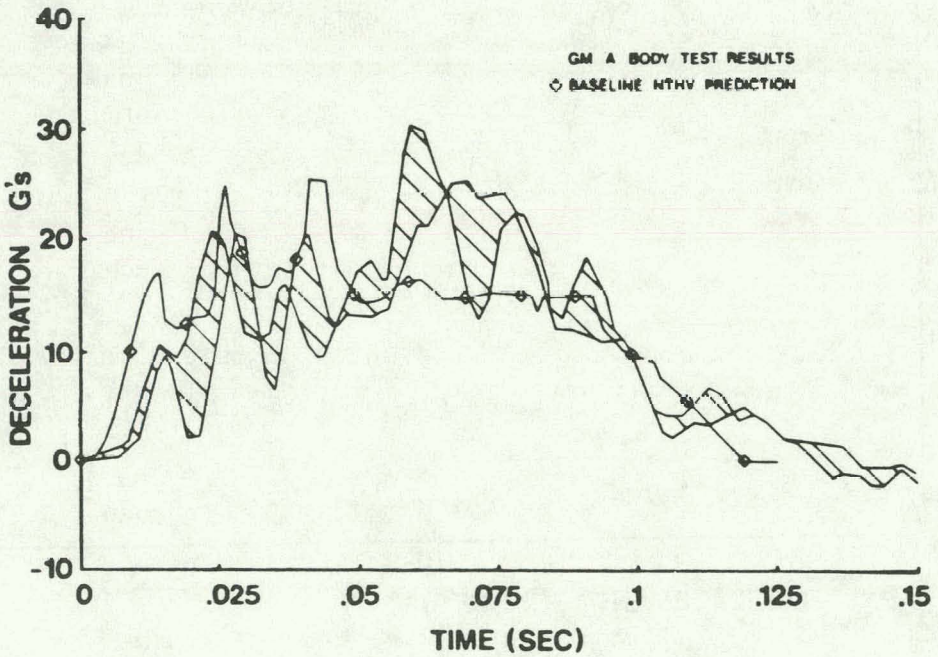

Figure 5.2-6. Comparison of Predicted Hybrid Vehicle Deceleration with General Motors A-Body Test Results

5.2.1.10 Vehicle Weight and Distribution

Estimates of the vehicle curb weight and its distribution early in Phase II projected a total vehicle curb weight of 1834 kg with a distribution of 68% front. As the vehicle design developed, better component definition allowed a more accurate weight analysis to be developed. The weight of each component was determined, or, if necessary, estimated, and its location within the vehicle grid system was measured. This information was input into the computer and the total vehicle weight and distribution, sprung and unsprung center of gravity, location, and polar moment of inertia were calculated. The final weight of the HTV was 2032 kg with 1409 kg on the front wheels.

5.2.2 Vehicle Design

The vehicle design approach was to use current production components where possible; where unique parts were required, the designs were made using industry accepted standards. The design of each component was such that fabrication of the parts required for testing and for building the vehicle could be completed without extensive tooling and machinery.

5.2.2.1 Vehicle Specifications

Overall Length	200.1 in.
Overall Width	71.5 in.
Overall Height	55.1 in.
Wheelbase	108.1 in.
Front Tread	59.3 in.
Rear Tread	57.8 in.
Body Style - 4-door Sedan	(5 passengers)

5.2.2.2 Packaging

The general packaging arrangement of the major components and the rationale for it are contained in the Phase I Final Report (Reference 1). Except for a small number of minor components, the configuration has not changed since that time. A brief description of the general arrangement follows:

• Body	4-door (5 passengers)
• Engine	4-cylinder, 1700 cc gasoline engine front-mounted transverse connected to the transmission by a chain
• Transmission	Three-speed automatic gear box with a concentric differential driving the front wheels
• Drive Motor	Transversely mounted behind the transmission; connected by a chain
• Drive Batteries	Ten 12 V batteries in a fiberglass container positioned under the hood above the transmission and the electric motor
• Steering Gear	Rack and pinion placed behind the wheels

• Radiator	Inclined in front of the engine, air is ducted in from under the bumper
• Air Conditioner	Mounted in the front right-hand corner of the engine compartment with air ducted to and from the passenger compartment
• Heater	Located under the instrument panel inside the passenger compartment
• Auxiliary Heater	Positioned under the trunk floor on left-hand side
• 12 V Battery	Placed in the trunk on the left-hand side
• Battery Charger	Situated in the trunk on the right-hand side
• Spare Wheel	Recessed in the trunk floor
• Power Contactors	Located under the fender on the front left hand side
• Field Chopper	Located in front of the console
• Controller	Located in the rear of the console

5.2.2.3 Styling

Concept Development. Having selected the General Motors mid-size car as the base vehicle (specifically the 1980 Buick Century), styling objectives were established to guide the development of specific tasks. An individual and positive identity was required to distinguish the HTV from the base vehicle image. Maximum utilization of the original equipment was sought to maintain a reasonable level of effort. Finally, aerodynamic optimization was sought in keeping with the practical goals of the project.

Analysis of a Buick Century indicated that the objectives could be achieved by maintaining the original vehicle components in the "glass house" area of the vehicle (i.e., windshield, roof, doors, A, B, and C pillars, and most of the passenger compartment). The areas revised in the re-styling were the front fenders, hood, bumpers, rear quarters, and rear deck. The following styling/design activities were undertaken:

- Lower the hoodline of the vehicle as much as possible consistent with the constraints caused by batteries and power train
- Narrow the front and rear appropriately
- Incorporate large plan view radii

These tasks were initially approached using design concept sketches. The original sketches were reviewed with engineering and design personnel for packaging coordination as well as subjective visual reaction. Consensus was reached on an original concept sketch, which was then converted to surface drawings to assure that the visual effect could be maintained in concert with mechanical limitations.

Scale Clay Model. After completion of the conceptual design, the work on a 3/8-scale clay model was started. This model allowed a much more realistic impression of how the final vehicle would appear, and was also utilized for aerodynamic testing. As discussed in Section 5.2.1.4, aerodynamic tests were performed on the model at the University of Michigan and, after minor development work, the aerodynamic objective was achieved.

Full-Size Clay Model. A full-size clay model was then constructed. This step was executed to incorporate refinements for body tooling. At the time of completion of the full-size clay model (Figure 5.2-7), it was perceived that the market place was undergoing a change in attitude toward the hatchback style, particularly on a vehicle of this size. Hence, the vehicle styling was reconsidered.

Detailed discussion and review of alternate styling sketches indicated that the program would be better served by restyling the rear portion of the vehicle to a notchback configuration. A sketch which complemented the entire vehicle most effectively was selected, and the clay model was revised accordingly. A full-scale clay model of the final HTV syling is shown in Figure 5.2-8.

5.2.2.4 Body Structure

This subsection describes the general body structure, the front structure, the underbody, the rear structure, the interior trim and seats, the battery container, the exterior lighting, the body front-end exterior, the body rear-end exterior, and the body hardware.

General Approach. The approach taken in the packaging of hybrid-related components did not necessitate major changes to the conventionally accepted vehicle interior space. Therefore, it was possible and desirable to utilize the passenger compartment of the General Motors A-body base vehicle. However, the A-body is a frame vehicle. This is not a weight efficient method of construction and was not in keeping with the program goals. A fully unitized structure was realized by adding structure to the body floor area and extending it to form the front and rear structure for both the suspension and the power train support and energy absorption. Front and rear exterior surfaces were fabricated from fiberglass and attached directly to the surface. Figure 5.2-9 shows the general arrangement of the body.

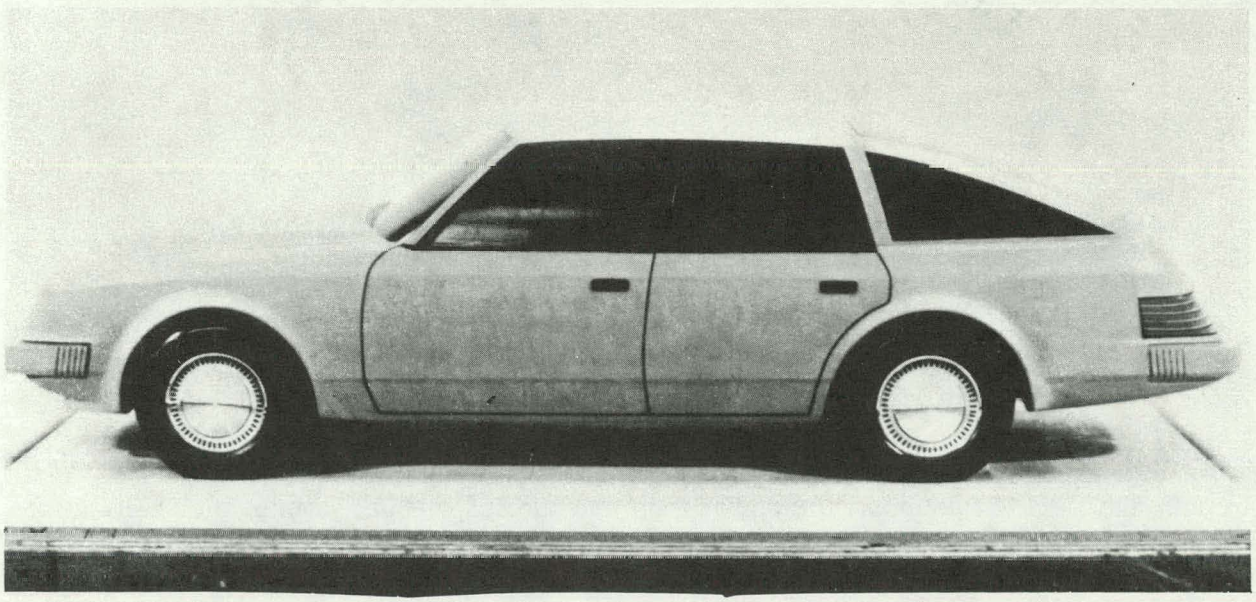

Figure 5.2-7. Full-Sized Clay Model (Hatchback)

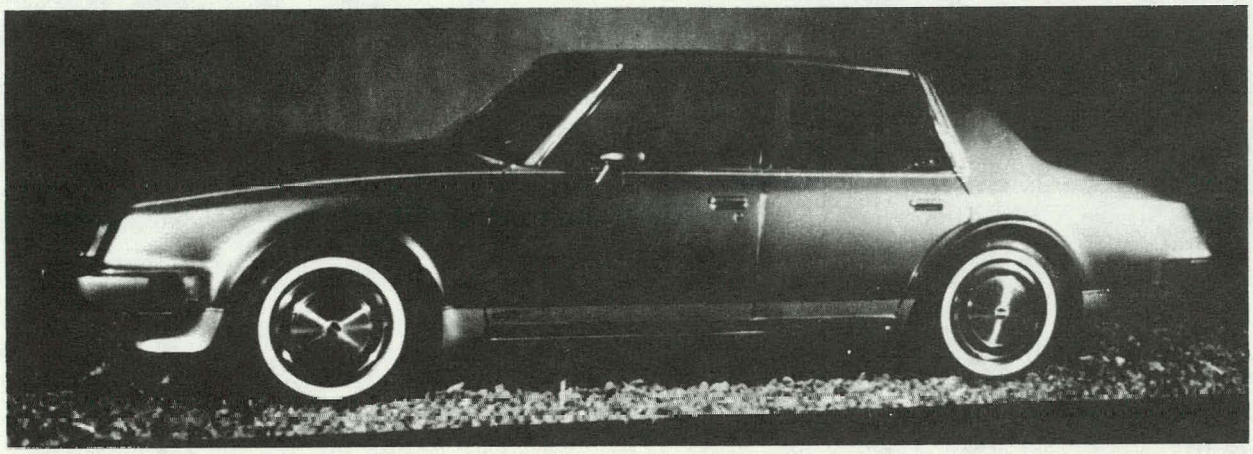

Figure 5.2-8. HTV Full-Sized Scale Model (Notchback)

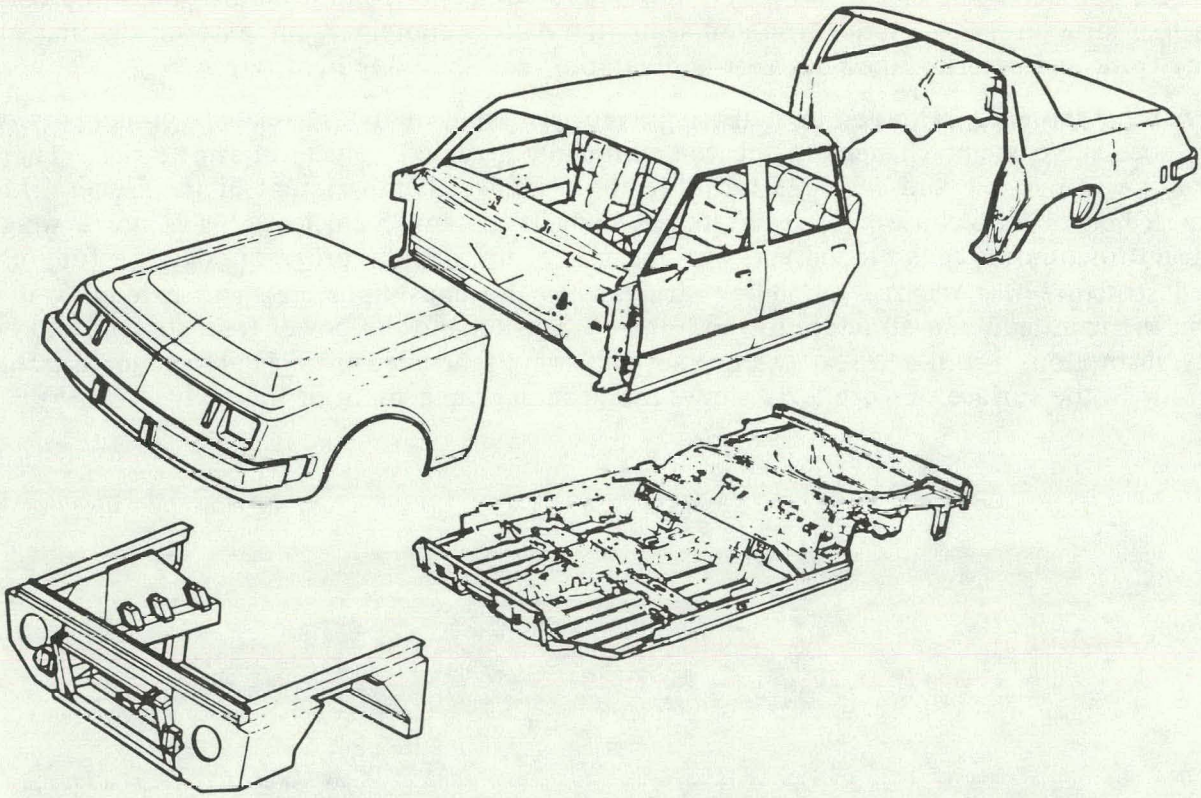

Figure 5.2-9. General Arrangement of the Vehicle Body

Front Structure. The front structure arrangement was dictated by two requirements: first, strength and rigidity to support the power train and the suspension; second, the ability to absorb energy in an impact. The energy absorption requirements have been discussed elsewhere in this report. However, the results of that analysis proved to be the dominant factor in formulating a front-end structure.

The basic structure consists of upper and lower longitudinal members joined at the front by vertical and transverse members which also support the radiator and the headlamps. Front bumper loads are also taken directly by the lower beams. The rear end of the upper member is married directly into the "A" pillar and the lower end into the rockers by way of a torque box and crossmember. The cross-car suspension loads are reacted by two crossmembers which tie into the suspension lower control arm. These crossmembers are also utilized to support the power train and steering system. The propulsion battery container is mounted directly onto the lower longitudinal beams and is positioned rearward to clear the engine. This rearward location could not be achieved without a complete redesign of the Buick cowl and dash panel. Figure 5.2-10 shows the front structure arrangement.

Underbody. The underbody offers a flat floor in the front and a small tunnel in the rear for exhaust pipe clearance. The Buick rocker panels are formed in an open channel to provide clearance for the frame. This channel was transformed into a box to increase the section strength. An analysis of the structure was made in order to determine the optimum sections to produce a vehicle with the same bending and torsional stiffness as others using unitized construction. As much as possible of the base vehicle underbody was kept to simplify fabrication and to facilitate use of existing interior trim.

Rear Structure. The rear floor of the Buick has been retained up to the rear of the wheelhouse. Behind this point, the floor continues to a rear bulkhead which, together with the outside skin, serves as a cross-car support. Below the floor, two longitudinal members add structure for supporting and locating the rear suspension. These members are tied into the rockers at the front and run rearward to pick up the bumper attachments. The rear floor contains a well for spare wheel storage.

Interior Trim and Seats. All interior trim, with the exception of the carpet, was taken directly from the Buick Century. The carpet was made to follow the floor contour resulting

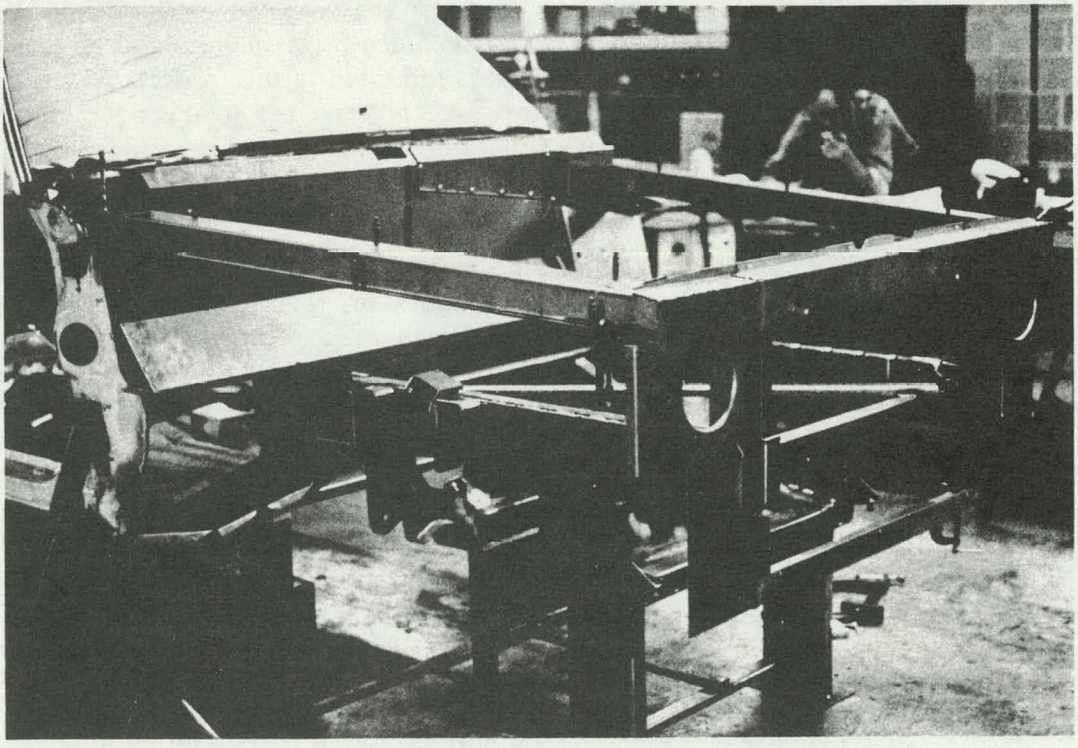

Figure 5.2-10. Front Structure

from the elimination of the tunnel. The rear seat is also Buick Century unmodified. The front seats are bucket type due to the inclusion of a console to house the electronic components. As Buick does not offer bucket seats in the Century but does offer a 60/40 arrangement, it was possible to fit two 40% seats with a slight modification for the passenger side.

Battery Container. The propulsion batteries are housed under the hood above the electric motor. The container was fabricated from fiberglass with three steel supporting beams. The container has a foam-cored cover which seals around its periphery. The batteries are separated by ridges in the container floor and are held down by hard rubber blocks attached to the cover. The cover is insulated by the foam core, which also adds rigidity for the hold-down arrangement. Lifting straps are built into the unit to allow removal from the car. To remove the unit, three bolts are removed from each wheel house. Inside the container, the batteries are wired in two banks of five each. Central watering and electrolyte circulation systems are attached to the container and are removed intact when the batteries are removed.

Provision has been made for ducting of air through the battery box. The air is blown into a plenum in the front left corner of the box and is allowed to escape at the rear through openings on both sides. Testing has shown an even flow of air between all of the batteries and an adequate air flow at both 60 V and 120 V to cool the cells. Figure 5.2-11 shows the battery container.

Exterior Lighting. All electrical systems are 12 V and designed for industry practice. In all cases, production parts from vehicles produced in the past four years are used. The front lamps are AMC 7.5 in. by 5.2 in. rectangular, the rear lamps are taken from a 1978 Chevette. Parking lamps are VW, and the side marker lamps are from Ford. As the 12 V system is charged from the alternator, all electrically operated accessories offered by GM for the base vehicle have been retained.

Body Front End Exterior. The front end of the vehicle is fabricated from fiberglass. Therefore, it was possible to design the entire unit as one piece with the exception of the hood. This method of construction offers the lightest possible design, as flanges and returns are not required at the connection points. The entire unit is mounted to the front structure along the front and sides of the hood opening and to the "A" pillars close to the door hinges. The lower front edge fastens to the radiator support lower beam, resulting in a very rigid structure. The hood is also fiberglass with a fiberglass inner panel. Weak areas have been designed into the inner member to ensure that the hood folds during impact.

Body Rear End Exterior. The rear end, like the front end, is constructed as one piece with the exception of the trunk lid. The rear-end configuration retains use of the base vehicle roof, the backlight, and the cross-car structure beneath the backlight. The fiberglass panel "gloves over" the rearmost 6 in. of the retained structure and butts up to the backlight. The rear of the panel attaches to the rearmost structural bulkhead and forms a cross-car beam. The fiberglass panel fits into the door opening at the reardoor shut face which eliminates the need for any exposed joining of steel and fiberglass. Across the roof, at the point where the rear panel ends, is a strip of trim which hides the surface-level change. The trunk lid is also fabricated from fiberglass. However, since the lid must be counterbalanced so that it self-opens and holds itself open, the load must be present at all times. Fiberglass under constant load tends to creep and will result in the lid bowing out of position. Consequently, the lid inner panel, although being fabricated from fiberglass, is also reinforced between the hinge and the latch with aluminum tubing.

Body Hardware. Door hinges and latches, seat adjusters, seat belts, and all other passenger compartment hardware are carried over from the base vehicle. Hood and trunk hinges and

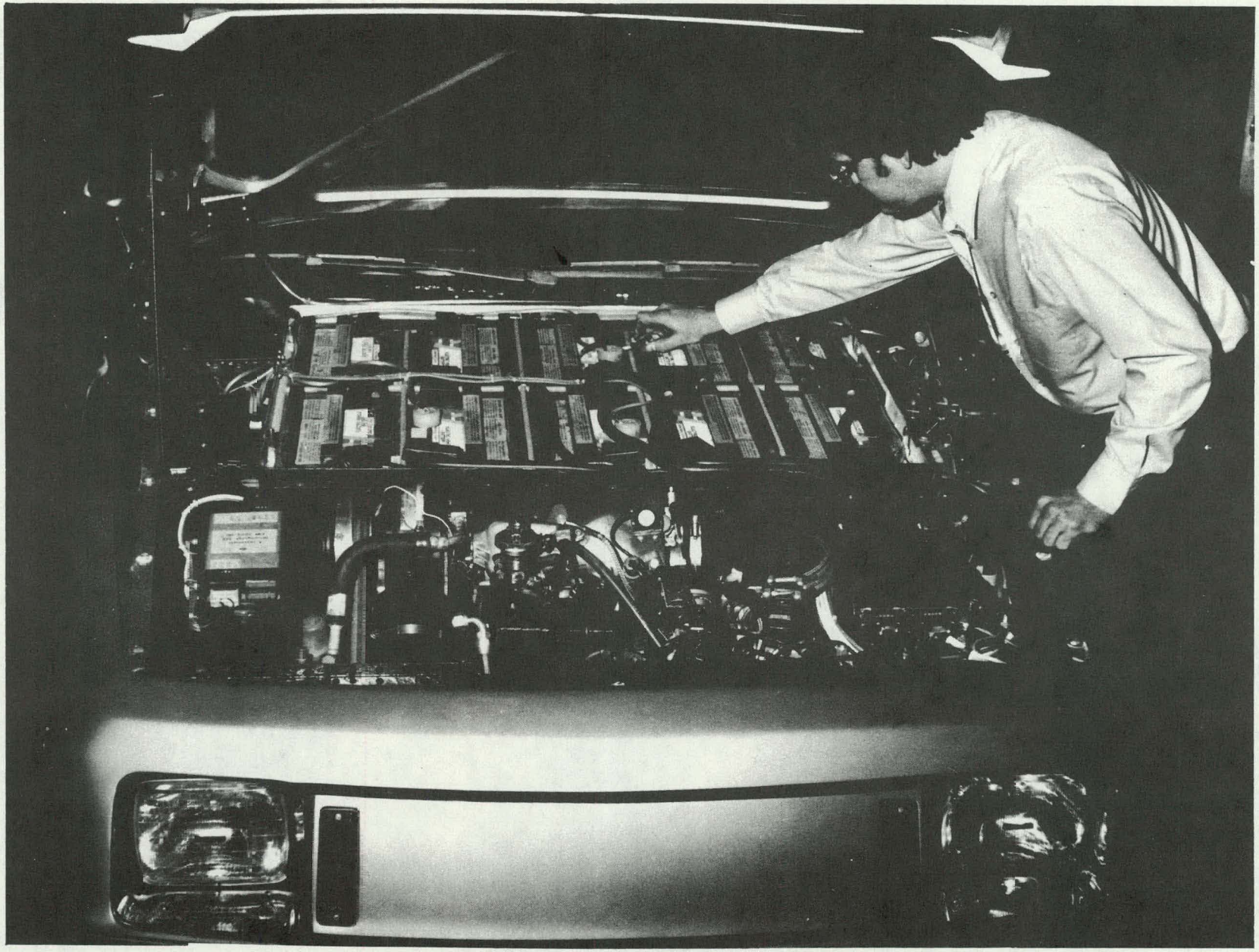

Figure 5.2-11. Battery Box Mounted in HTV

latches are also carried over from the base vehicle. However, these are used in a slightly different configuration. The hood is held open by use of a prop rather than the struts, which are retained for the trunk.

5.2.2.5 Chassis

This subsection discusses the front suspension, the rear suspension, the steering gear and linkage, the brakes, the wheels and the tires, the exhaust system, the fuel system, the bumpers, the chassis electrical system, the cooling system, the accessory system, and the hydraulic system.

Front Suspension. Front suspension is an independent double wishbone with torsion bars, as shown in Figure 5.2-12. The components are taken from the General Motors E-body, which offers a front-wheel drive arrangement designed to carry similar loads. However, the E-body is a "front" steer system while the HTV needed to be a "rear" steer system for packaging reasons. Therefore, the E-body right- and left-hand sides were switched, and new steering arms were added to the knuckle. A stabilizer bar is included to control roll and roll-couple distribution. Table 5.2-4 shows the front suspension specifications.

Rear Suspension. The rear suspension is a beam axle controlled by trailing arms and a panhard rod. Coil springs are mounted above and forward of the axle, as shown in Figure 5.2-13. The axle beam torsional stiffness controls the roll and is tuned by use of an additional bar installed concentric with the beam. Wheel tread is adjusted by the addition of spacers to the axle beam and the plates.

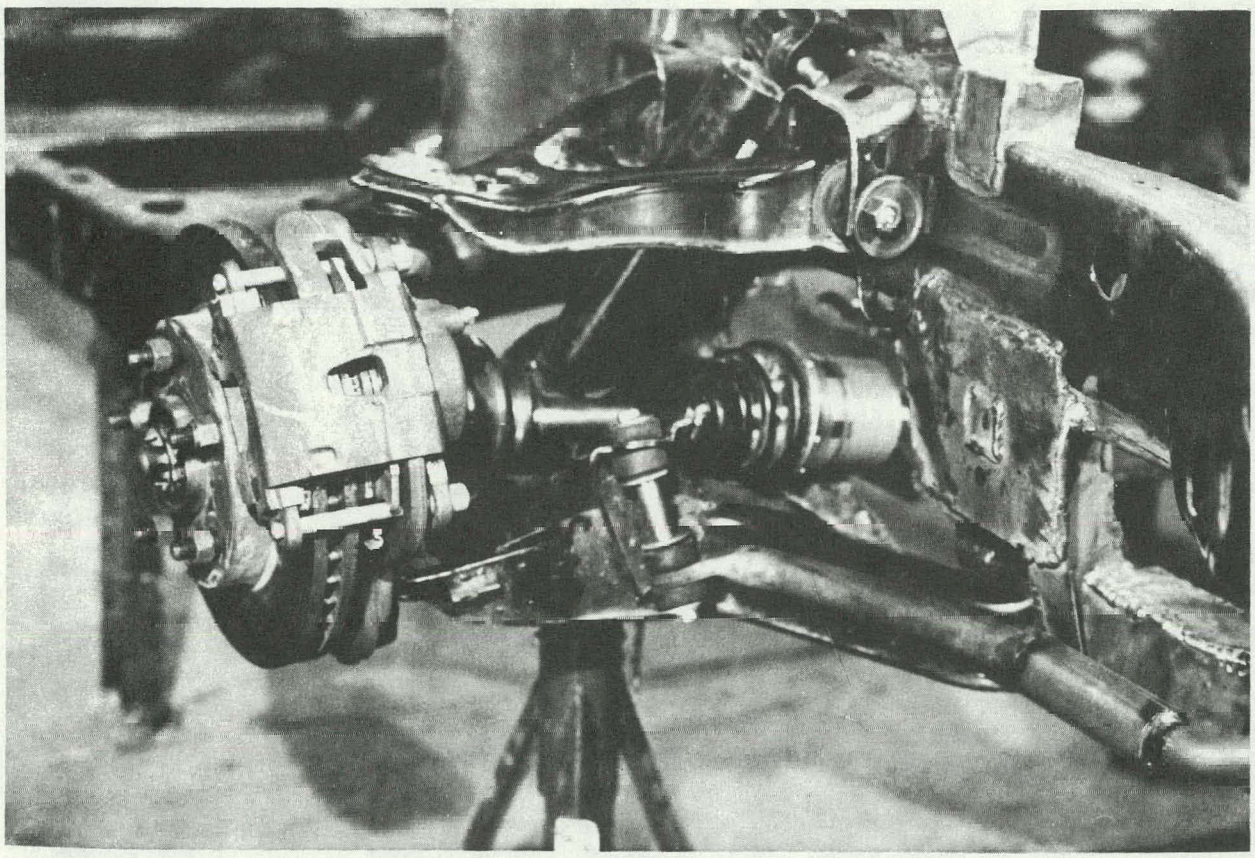

Figure 5.2-12. Front Suspension

Table 5.2-4

FRONT SUSPENSION SPECIFICATIONS

Jounce at Design	3.5 in.
Rebound at Design	4.25 in.
Wheel Rate	294 lb/in.
Ride Frequency	1.20 Hz
Caster	0.0 degree
Toe	0.0 in.
Scrub Radius	0.0 in.
Roll Center Height	2.33 in.

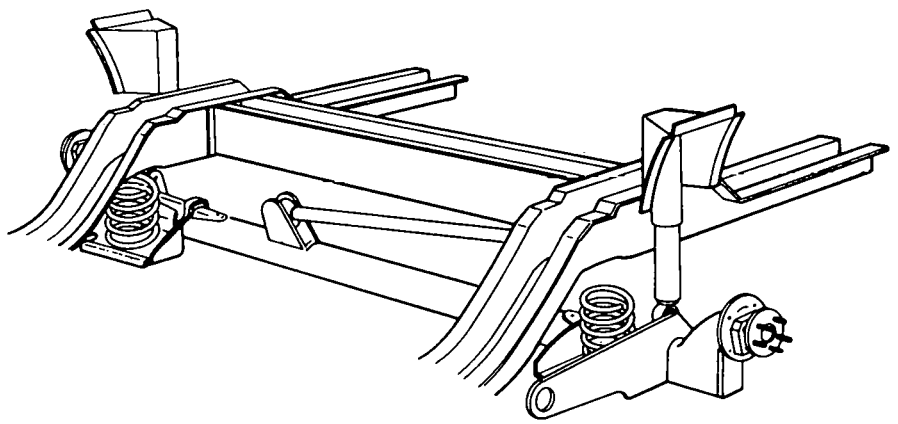

Figure 5.2-13. Rear Suspension

The major components are taken from the General Motors X-body vehicles. The axle beam is reinforced in the high-stress points. Braking forces are not increased over those experienced on the X-body due to the HTV's high front weight bias and weight transfer experienced under maximum braking.

The concentric antiroll bar has been increased in diameter over the X-body to produce the required roll-couple distribution. The wheel bearings, the hub, and the spindle are from the E-body in order to mate with the brakes and the wheels from that vehicle. Table 5.2-5 shows the rear suspension specifications.

Steering Gear and Linkage. Packaging of the power train eliminated the possibility of using the recirculating ball gear and centerlink-type steering linkage. A location, behind the wheel centerline and beneath the electric motor, was found for a power rack and pinion gear, which is itself the centerlink of the linkage. TRW produces a similar unit for the Chrysler K-car. TRW modified this gear by increasing its overall length and travel to meet the needs of the HTV. In this location, the tie rods required severe bends in order to clear the tire in full lock conditions. The overall steering ratio obtained was 20:1, and the roll steer effect was understeer. Figure 5.2-14 shows the general arrangement.

Table 5.2-5

REAR SUSPENSION SPECIFICATIONS

Jounce	4.12 in.
Rebound	3.75 in.
Wheel Rate	194.8 lb/in.
Ride Frequency	1.22 Hz
Camber, Caster, and Toe	0.0 degree
Roll Center Height	12.8 in.

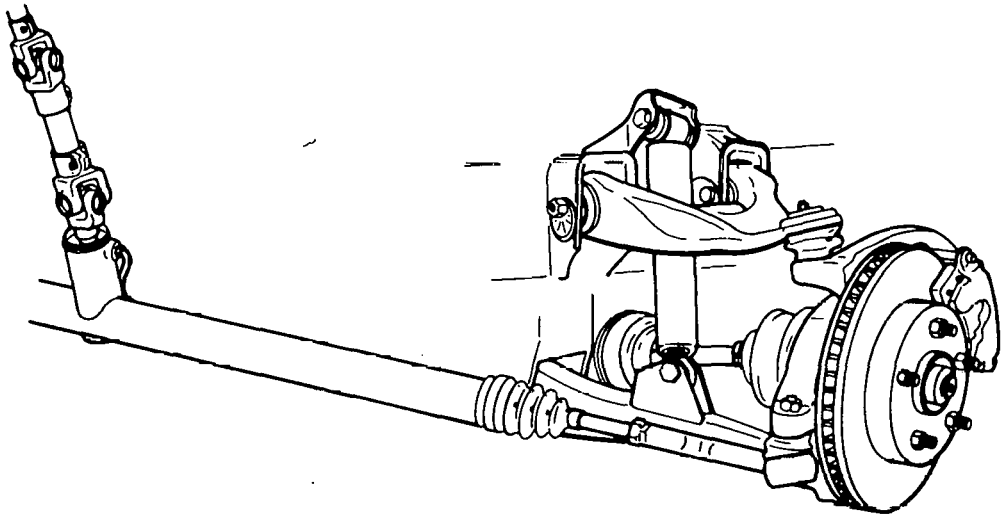

Figure 5.2-14. General Arrangement of Steering Gear and Linkage

Brakes. The braking system is disc front and drum rear with hydraulic power assist. The front calipers and the rotor are taken from the E-body. The rear brakes are E-body with an 11/16 in. diameter wheel cylinder and aluminum drums.

The hydraulic system is split diagonally and is proportioned so that the rear brakes are reduced by 0.27:1, commencing at a 250 psi line pressure. The effect of the regenerative braking could affect the balance of the system, and further reduction of the rear brake output may be found necessary as development proceeds. Table 5.2-6 shows the brake specifications.

Wheels and Tires. The road wheels are 15 in. by 6 JJ taken from the General Motors E-body, including a mini-type spare wheel. Tires are specially constructed, extra load, Goodyear P205/75-R15, steel-belted radials. These tires can be operated at 50 psi in order to reduce rolling resistance.

Exhaust. Figure 5.2-15 shows the exhaust pipe routing from the manifold to the catalytic converter. The converter is positioned 34 in. from the engine. This is as close as possible, consistent with the overall power train packaging. The three-way catalytic converter is a VW

Table 5.2-6

BRAKE SPECIFICATIONS

Front Caliper	2.5 in. diameter
Rotor	10.5 in. by 1.0 in., vented
Rear Brake	9.5 in. x 2 in. aluminum drum 11/16 in. wheel cylinder
Master Cylinder	0.945 in. diameter by 1.38 in. stroke Tandem
Booster	Hydraulic, run from power steering pump
Valve	Diagonal split, 0.27:1 proportioning trip pressure 250 psi pressure differential

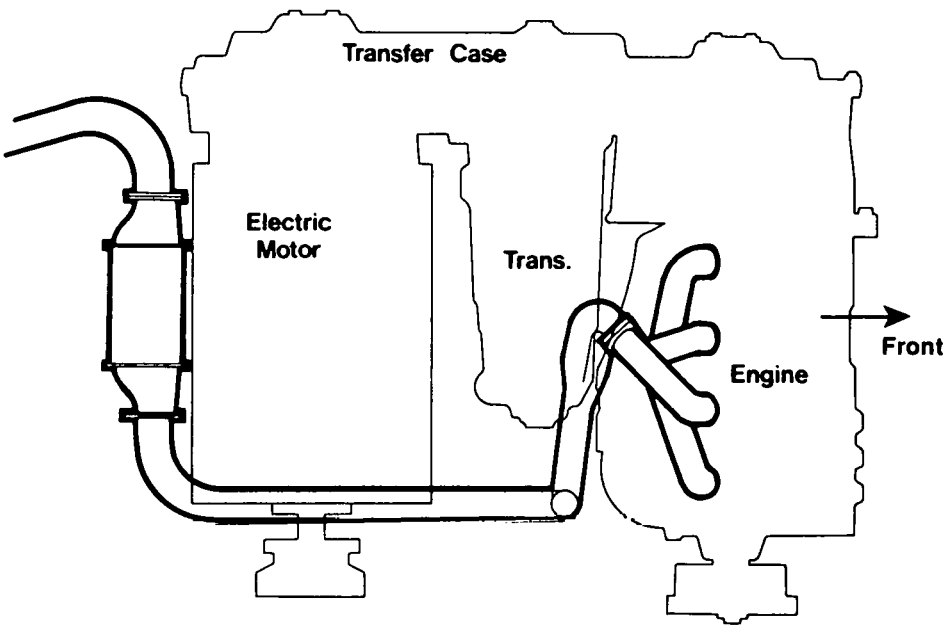

Figure 5.2-15. Exhaust Route (Top View)

unit which is certified in the Audi 4000 system. From the catalytic converter, the pipe is routed rearward down the tunnel. Under the rear seat, it moves to the right-hand side, then rearward to a VW muffler mounted alongside the spare wheel well.

Fuel. The fuel tank is located in front of the rear axle under the floor pan and seat. The filler is routed to the left-hand rear quarter where the cap is concealed with a flush fitting door. The tank is fabricated from aluminum and incorporates a GM-style level indicator and fuel pickup. The fuel supply system is taken from the Audi 4000 and is designed as part of the Bosch K Jetronic fuel-injection system. A high-pressure pump (70 psi) is positioned close

to the tank and is close-coupled to an accumulator with a check valve between. The fuel passes through a filter to the fuel distributor. There is a return line to the fuel tank. Figure 5.2-16 shows the fuel system arrangement.

Bumpers. Front and rear bumpers are designed using the same method. A high-strength, low-alloy (HSLA) steel beam is mounted on hydraulic energy absorbers (EA). The EAs have a stroke of 3.5 in. and clearance behind the bumpers has been provided for the full stroke. The steel beam is covered with a fiberglass skin which is styled to match the vehicle exterior. Rubber-covered steel bumperettes protrude through the skin. In the 5 mph barrier and front pendulum tests, they are the only part of the bumper to make contact. The corner pendulum test exerts a lower impact load and makes contact with the skin at a point where the skin is fully supported by the beam. Additional structure has been added to the bumpers to produce the crush rate desired for the front structure. This extends the crush length of the vehicle by 3 in.

Cooling. Engine cooling is achieved by a radiator positioned in front of the engine which is inclined forward at the top. The radiator is a cross-flow type and is oversize for the engine. The radiator size has been dictated by the air-conditioning condenser, which is positioned in front of the radiator. The cooling requirements of the radiator are less than a conventional automatic vehicle system because the engine does not idle, and the automatic transmission does not have a torque converter to cool. Air is ducted into the radiator from beneath the bumper where an air dam has been built into the body surface. An electric fan is used to assist the air flow at low speed. The fan is operated when coolant temperature is above a set value.

Accessory System. The accessory system consists of the 12 V alternator, the hydraulic pumps, and the air-conditioning compressor. This section deals with the mechanical drive system developed to drive these accessories. The individual component functions are covered in later sections.

Accessory power requirements for the hybrid vehicle were derived from early measurements on the ICE reference vehicle. Additional loads were added to account for the 100 A, 12 V alternator needed to deliver the extra current required for the solenoid coils which operate the valves in the transmission and clutch systems. Maximum accessory power was determined to be 7.4 hp at idle speed and 16 hp at maximum speed. The maximum torque required from the accessory drive is approximately 358 in.-lb and occurs at idle speed.

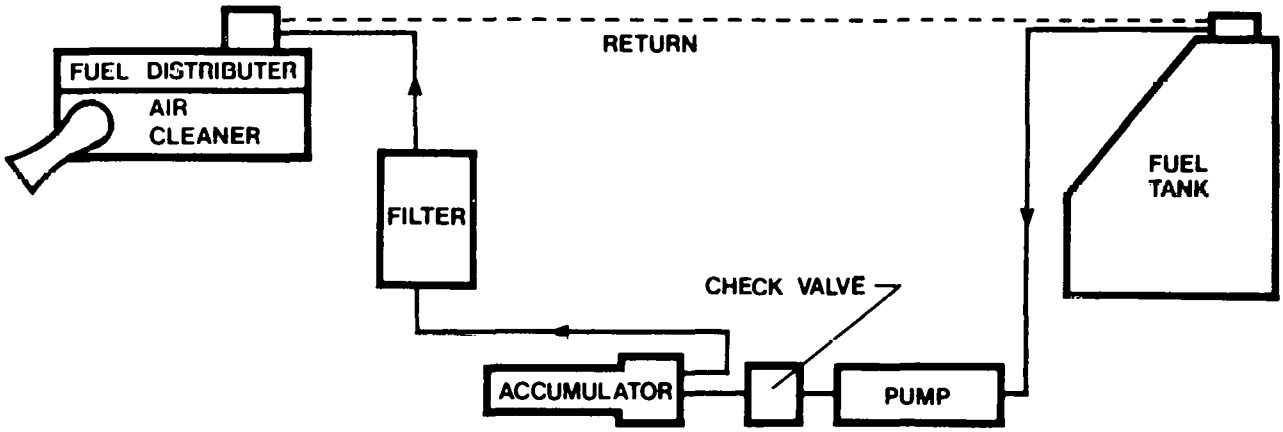

Figure 5.2-16. Fuel Supply System

Since the hybrid vehicle control strategy allows the gasoline engine or the electric motor alone to drive the vehicle, a means of driving the accessories during either mode of operation had to be developed. This was accomplished through the use of a pair of over-running clutches, one on the accessory drive end of the engine and one on the commutator end of the electric motor. This permits the accessories to be driven from either the motor or engine shaft. The drive ratio between the engine and the motor was selected to permit the engine to drive the accessories during times of simultaneous operation. Hence when the hybrid power train is operated as a single-shaft arrangement (that is the electric motor is not decoupled from the driveline when it is de-energized) the gasoline engine drives the accessories just as it would if the power train were operated as a two-shaft arrangement with the electric motor decoupled (drive clutch open) when it is de-energized.

The mechanical drive selected for the accessories was the Gates Micro-V belt employed in a serpentine fashion like the drive currently used on the Ford Thunderbird. This singular belt drives all of the accessories, except the engine water pump, and connects the engine and the motor together at the accessory drive end. A computer analysis of belt durability and tension requirements conducted by the Gates Rubber Company yielded a projected life of 9600 hr of operation when driven over simulated city and highway cycles in a ratio of 55% to 45%. This long life is a result of the generous contact arcs and low span tension requirements of only 31.2 lb. Tension is provided by a spring-loaded idler pulley operating on the back side of the belt.

Figure 5.2-17, a drawing of the accessory drive, illustrates the belt path and the location of the accessories. Figure 5.2-18 depicts a sectional view through the motor commutator end and shows the over-running clutch and the transmission hydraulic pump drive. Figure 5.2-19 is a sectional view through the engine accessory drive end and illustrates the over-running clutch and the water pump drive. The water pump is only driven during engine operation.

Hydraulic System. The power steering, the power brakes, the vehicle drive clutch, and the engine starting clutch, require a high-pressure hydraulic system. A completely closed-center system which utilizes a hydraulic accumulator and operates the hydraulic pump only when hydraulic fluid is needed would be desirable in order to minimize the power delivered to the hydraulic pump. Budget and schedule considerations did not permit implementation of the complete closed-center system. Only the clutches are operated in a closed-center manner from the hydraulic accumulator. The hydraulic pump is from an Audi 4000 and is driven by the accessory belt. Details of the hydraulic circuit are provided in Section 5.3.4.

5.2.2.6 Operator Controls

Included in this subsection are the steering column and wheel, the brake, the accelerator pedals, and the instrument cluster.

Steering Column and Wheel. The steering column consists of the main column and an intermediate shaft. The main column is taken from a General Motors X-body, which incorporates all of the required energy absorbing and collapsing features. This column required modification at the lower end for packaging and maintaining acceptable universal joint angles. The intermediate shaft has two universal joints, a slip joint to adjust the length, and a rubber isolator to reduce the noise from the power steering.

The steering wheel is from the base car and therefore will match the interior trim. Transmission gear selection is made by a column-mounted lever operating microswitches located at the base of the column. A cable to the transmission engages and disengages "Park."

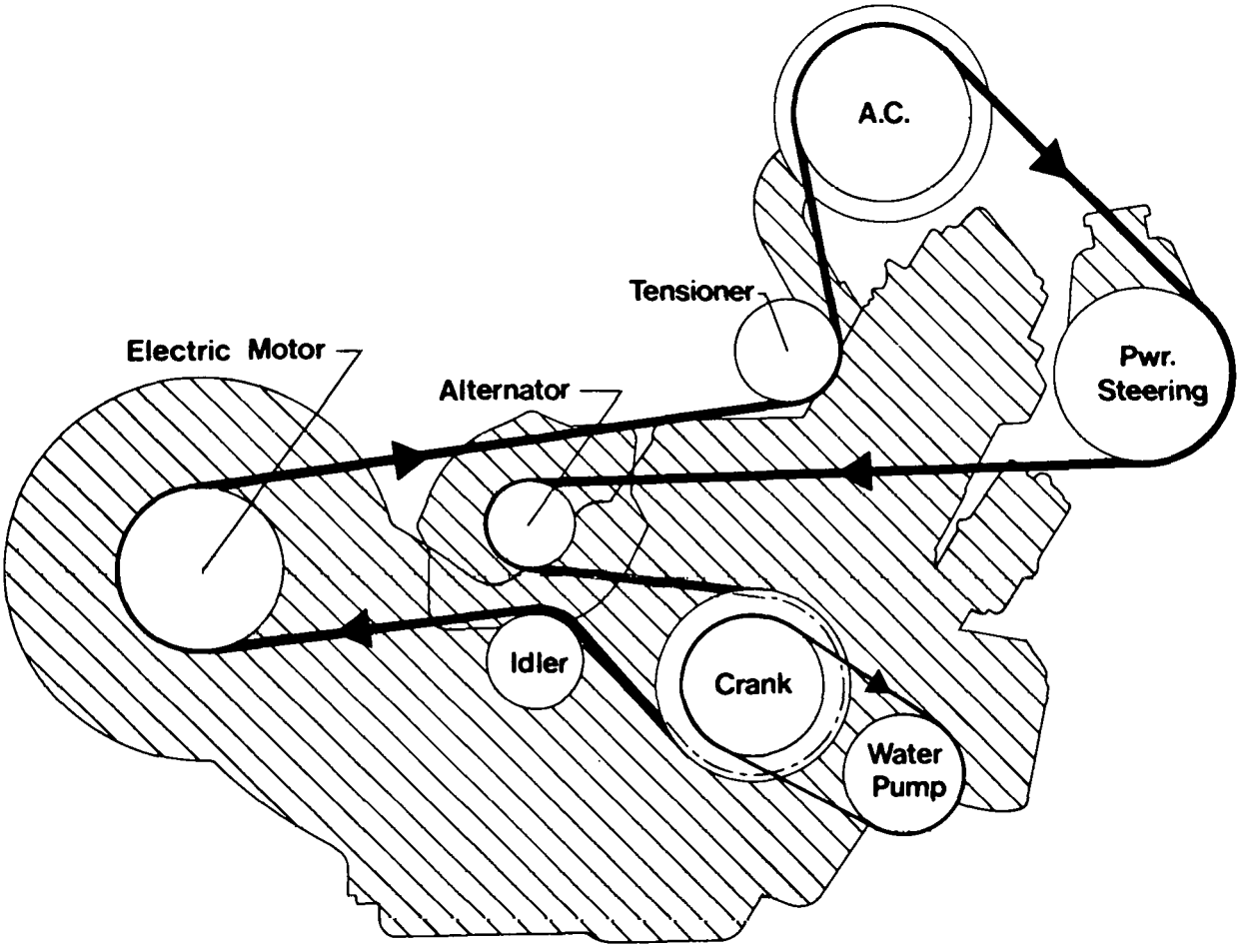

Figure 5.2-17. Accessory Drive (Passenger Side View)

Brake Pedal. The position of the propulsion battery box forced the brake booster and master cylinder to be positioned much further outboard than is customary. The brake pedal, therefore, is offset and relies on a stiff shaft and auxiliary lever to actuate the brake push rod. The pedal position is maintained in essentially the same location as in the base car. The brake pedal is connected to a potentiometer which interfaces with the vehicle controller to set the level of regenerative braking. Switches are mounted to the pedal support bracket to actuate the brake lights and the regenerative braking system.

Accelerator Pedal. The accelerator pedal is connected to a potentiometer which interfaces with the vehicle controller. The pedal and its position are the same as that in the base car. Deletion of the tunnel and replacement with a console provides more foot room for the driver than that offered in the base car.

Instrument Cluster. Figure 5.2-20 shows the general arrangement of the instruments and the warning lights for the HTV. The base car instrument panel together with an auxiliary warning light panel available from General Motors offers sufficient space for all of these instruments. The battery charge mode selector is positioned in the console, and the emergency power "OFF" button is located on the lower edge of the panel.

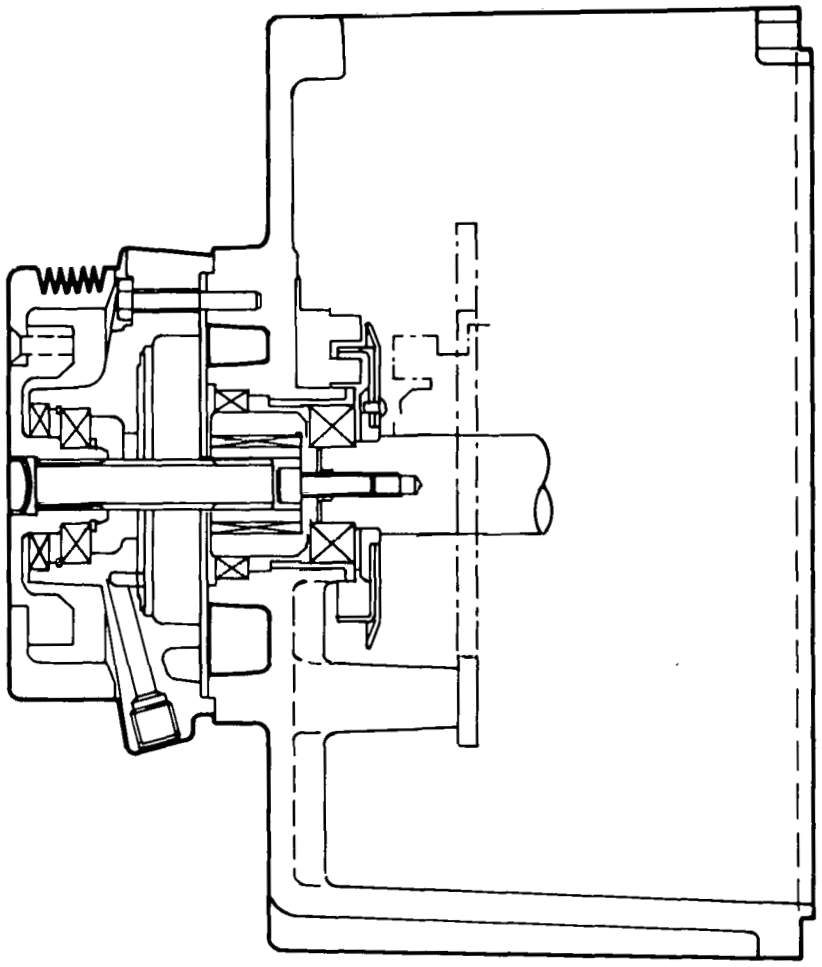

Figure 5.2-18. Sectional View of Motor - Accessory Drive and Transmission Pump

5.2.2.7 Heating, Ventilation, Air-Conditioning, and Electrical Systems

This subsection discusses the heating, ventilating, air-conditioning, electrical system, and drive electronics packaging.

Heating, Ventilating, and Air-Conditioning. The position of the battery box eliminated the possibility of using the base car system without some modification. The final design allowed use of the heater portion by relocating the heater outboard to clear the battery box. The airflow valves remain in the center of the vehicle and marry with the distribution system untouched. The air-conditioning evaporator and blower have been positioned in the front right-hand corner of the engine compartment, and ducting runs from the passenger compartment to the unit and back again to provide a recirculating system required for maximum draw down. Figure 5.2-21 shows the remote air-conditioning unit. The compressor and condenser are standard GM components as are the valves and switches. The vacuum actuated controls of the HVAC system are taken directly from the base car. The vacuum source is provided by the pump used for the engine throttle control system.

The performance required of the total heater system necessitated the use of a conventional hot water system. The hot water system makes use of heat generated by the engine when it is available.

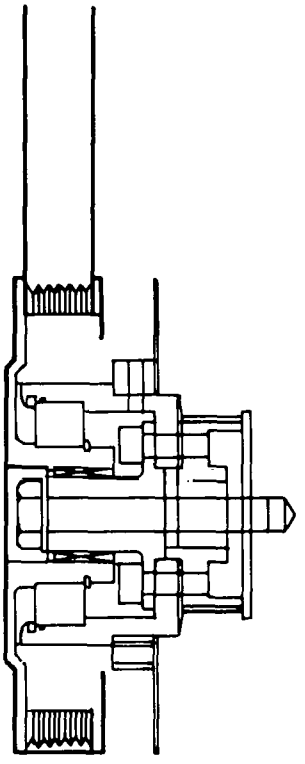

Figure 5.2-19. Sectional View of Engine Accessory Drive

Since the gasoline engine does not run continuously during normal vehicle operation and never idles, sufficient waste heat is not always available from the engine for heating the passenger compartment and providing the defrosting function. Tests on the ICE reference vehicle showed that the heater in a standard car is capable of delivering a maximum of 68,400 Btu per hour to the passenger compartment on a continuous basis. A 50,000 Btu/hr auxiliary gasoline heater is thus used in the hybrid vehicle to provide heat when the engine is not running. The heater consists of a burner, an air-to-water heat exchanger, an electrically driven fuel pump and water pump, and a control thermostat.

Figure 5.2-22 is a schematic representation of the heater system water flow. If the driver demands vehicle heating, and the water temperature is below 165 °F, the auxiliary heater will begin to operate. Should the engine not be utilized during this period, the gasoline heater will cycle on and off in order to maintain a 165 °F water temperature in the heating system. When the engine is used, the engine-cooling water will heat up and be regulated by the engine thermostat at 185 °F. This increase in water temperature will automatically shut down the auxiliary heater. Figure 5.2-23 is a drawing illustrating the operation of the combustion heater.

In order to match the air-conditioning features available in the ICE reference vehicle, the complete air-conditioning system from the standard vehicle, including cycling clutch control, is employed. This system provides 15,000 Btu/hr cooling capacity in the recirculation mode.

Electrical System. One 12 V battery is required for the vehicle and its electronic equipment power requirements. The battery is a Group 24 deep-discharge type located in the rear left-hand corner of the trunk. Filters are added to the electronic circuit to eliminate interference from the vehicle system components.

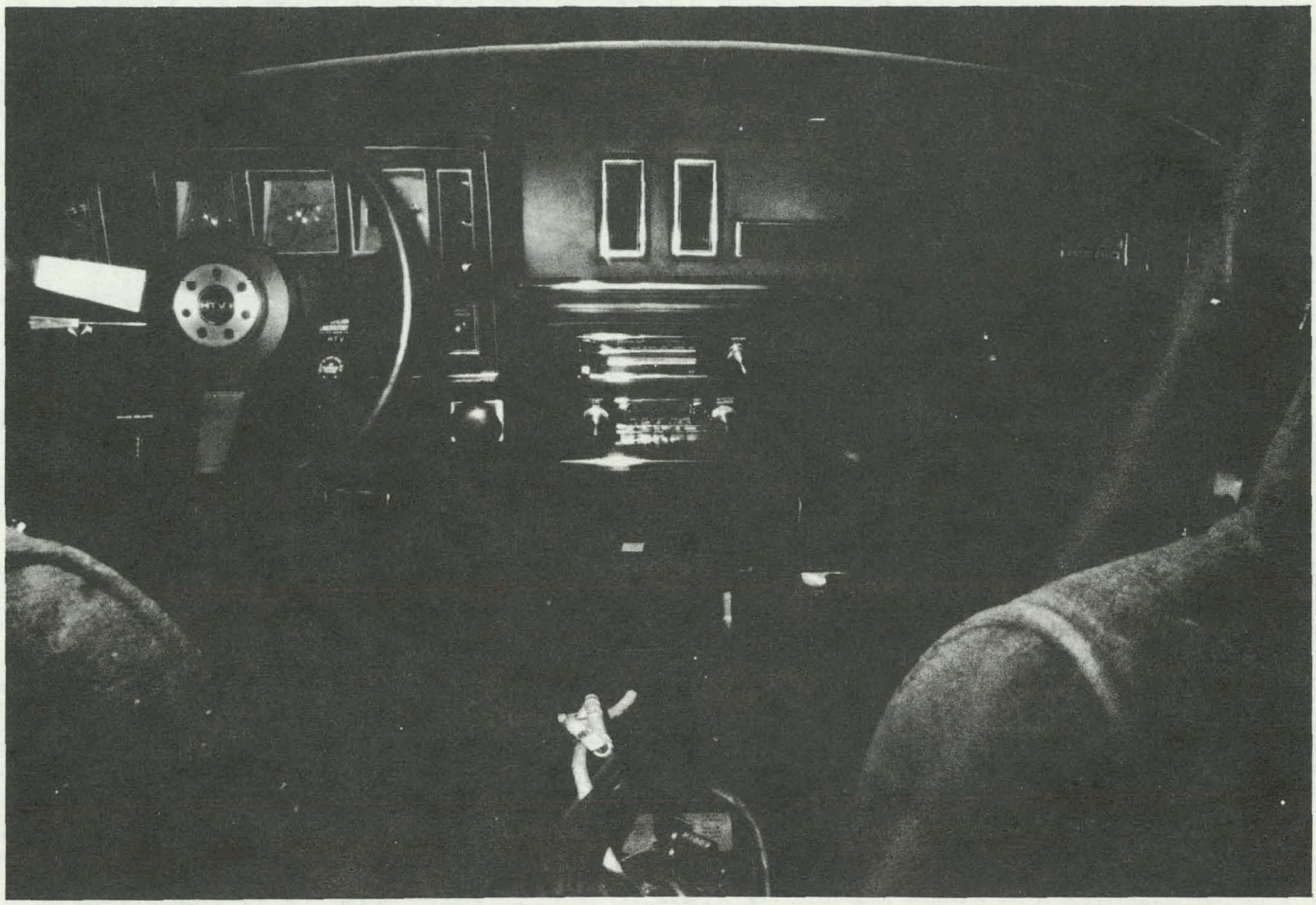

Figure 5.2-20. Instrument Panel

The 12 V battery is charged by a 100 A alternator driven by the accessory drive. Two No. 4 wires connect the battery to the alternator and power train frame. Grounding through the length of the vehicle was found to be unreliable. An analysis of the power requirements shows that 100 A is sufficient for the worst-case condition, which is a combination of all the accessories for varying lengths of time. No. 4 wire from the alternator to battery provides reasonable accessory battery voltage to maintain its state-of-charge during normal operation.

Packaging of Drive Electronics. The field chopper, the controller, and its power supply are located in the console in the passenger compartment for both environmental and space reasons. To control the temperature within the console, a blower is positioned at the front end of the compartment. Air is drawn through the rear face of the console, across the electronic components (field chopper), out an opening in the fire wall, and through the electric motor and clutch for cooling of these components. Air is available inside the passenger compartment at all times due to the forced air ventilation system in all recent GM vehicles.

The drive-motor contactors are positioned under the left front fender. Battery cable lengths, from the batteries to contactors, are minimized to reduce the power loss in the wiring. The series-parallel contactor (SPC) and the main disconnect are mounted to a bracket close to the battery box. Two Anderson connectors connect each 60 V battery bank to the

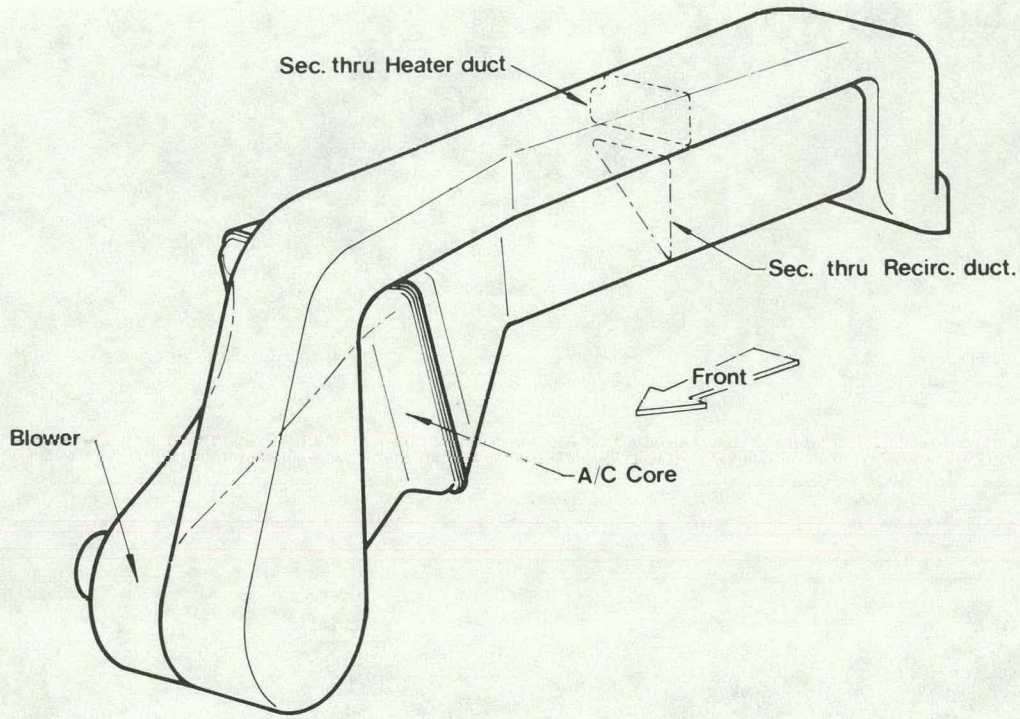

Figure 5.2-21. Sketch of Air-Conditioning Unit

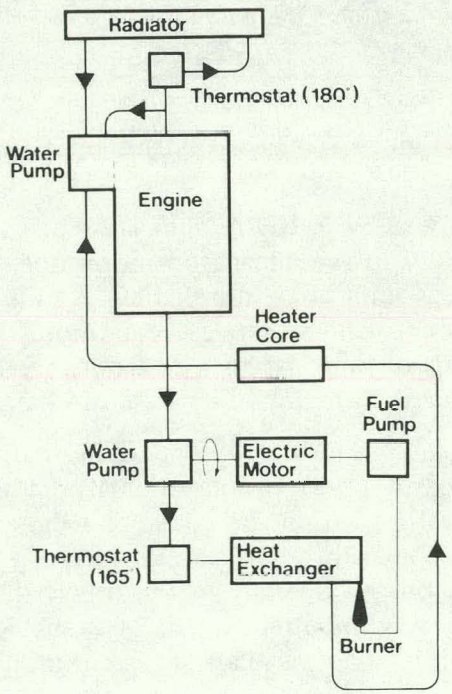

Figure 5.2-22. Schematic of Heater Water Flow

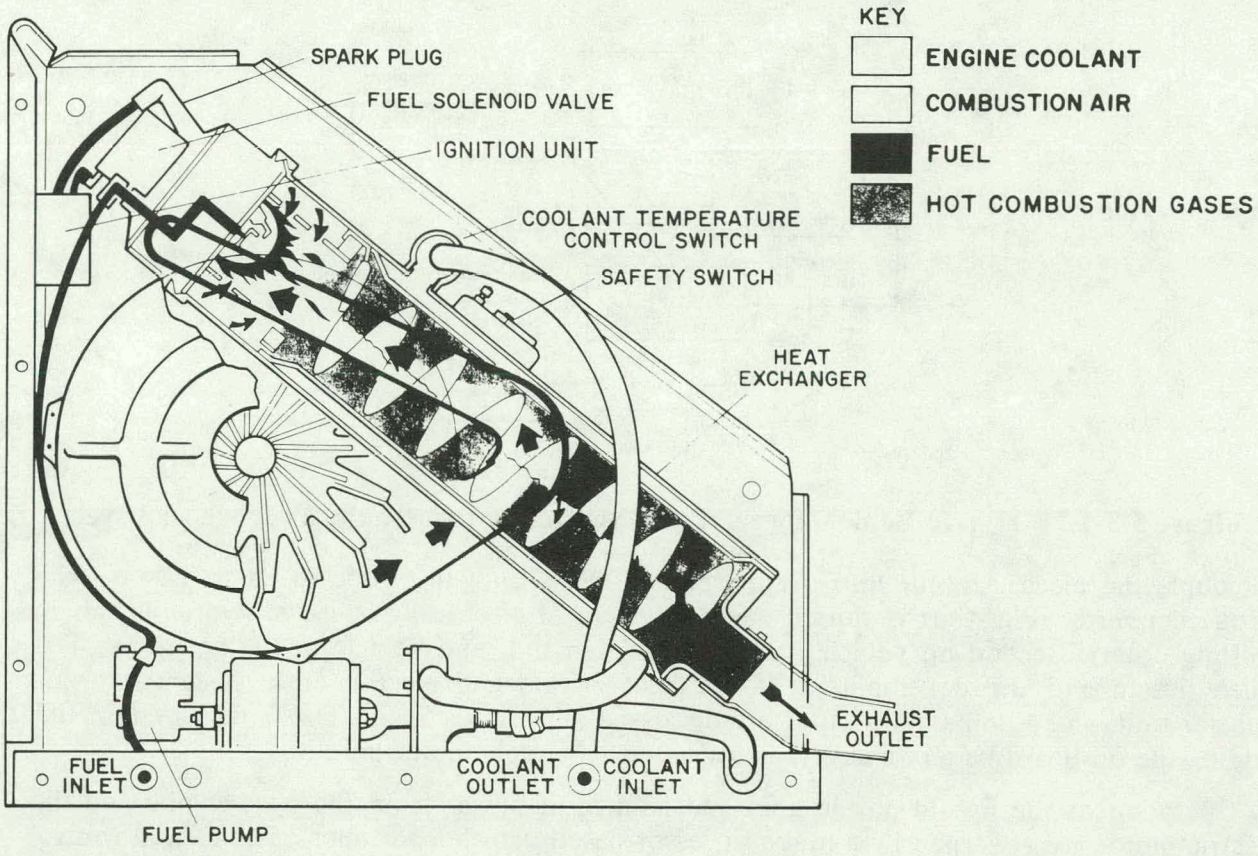

Figure 5.2-23. Combustion Heater

SPC. The motor starting resistor and its bypass contactor are mounted to the upper front structure. The resistor is located in front of the battery-cooling blower to ensure adequate air flow over it.

5.3 HYBRID PROPULSION SYSTEM

This section presents the overview and control strategy for the hybrid propulsion system. Also discussed are design details of the drive motor, the engine and engine-starting clutch, the torque transfer unit and transmission, the power electronics, the micoprocessor-based vehicle controller, the battery charger, and the sensors used in operating and controlling the vehicle. Safety, reliability, and maintainability are also discussed.

5.3.1 System Overview and Control Strategy

In this system overview, the operation of the hybrid propulsion system is described and the control strategy which was developed is explained. The heat generated by the various underhood components is considered as is the power required to drive the accessories.

5.3.1.1 Hybrid Propulsion System

The hybrid test vehicle (HTV) utilizes a parallel two-shaft hybrid power train. A schematic of the power train (Figure 5.3-1) shows that torque can be applied to the wheels using the heat engine or the electric drive separately, or using both of the drive systems together. Both the heat engine and the electric motor can be clutched into and out of the driveline as required by the vehicle operating mode. The heat engine clutch is designed for fast operation (opening or closing in less than 0.5 s). The electric motor clutch can be modulated for initiating the motion of the HTV from rest and opened/closed fast when it is necessary to decouple

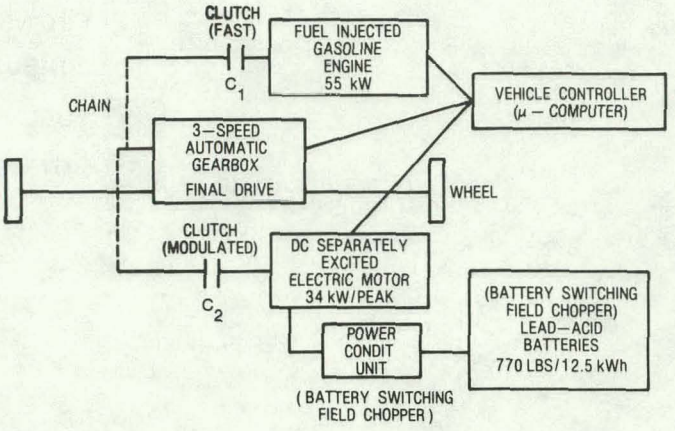

Figure 5.3-1. Hybrid Vehicle Power Train Schematic (two-shaft, front-wheel drive)

or couple the electric motor into the driveline. The automatic, three-speed transaxle (with torque converter removed) is shifted using a system of electrically operated hydraulic valves. Shifting criteria depend on vehicle speed, power demand, and vehicle operating mode. Detailed design and the development of the heat engine and electric drive systems, torque transfer unit, and automatic transaxle are discussed in Sections 5.3.4. The battery system (including the on-board battery charger) is discussed separately in Section 5.4.

Operation of the hybrid power train and control of power from the heat engine and the electric motor are governed by a microprocessor-based vehicle controller. The overall control strategy utilized in the HTV is discussed in the next section, and the detailed design of the hardware and software for the vehicle controller are discussed in Section 5.3.6. The various sensors used to obtain inputs for the vehicle controller and to determine the state of operation of the vehicle and the power train components are discussed in Section 5.3.7.

Safety, reliability, and maintainability of the hybrid power train are considered in Section 5.3.8.

5.3.1.2 Overall Control Strategy

The overall control strategy for the HTV has been devised so that the fraction of gasoline saved (compared to the ICE reference vehicle) will be maximized. This requires that the HTV utilize battery-stored electrical energy to power the vehicle whenever possible. Hence, in urban driving, the electric drive system is used alone unless the power demanded exceeds the electric drive system capability and/or the battery state-of- charge falls below 20%. In that event, the heat engine is turned on and it shares the load with the electric motor. When the power demand falls below that which can be provided by the electric motor alone, the heat engine is turned off and the HTV is driven as an electric vehicle. Hence, the heat engine is operated in an on/off mode and is on only when it is providing power. The heat engine never idles.

The two-shaft mechanical arrangement of the hybrid power train permits the electric motor to be decoupled from the driveline when it is not energized by opening the vehicle drive clutch C_2. This avoids all losses due to the motor shaft turning. Development tests of the HPTM and the HTV indicated that there were driveability problems (lags and jerks) associated with the coupling and decoupling of the electric motor into and out of the driveline when the vechicle was accelerating or braking. For that reason, the HTV as delivered does not decouple the electric motor from the driveline when it is de-energized (that is the vehicle is

operating on the heat engine only). Hence the HTV power train operates essentially as a single-shaft unit from a control point-of-view even though it is a two-shaft mechanical arrangement. The electric motor is, of course, decoupled (the drive clutch C_2 is opened) when the vehicles comes to a stop and the electric motor is idling.

The vehicle speed (V_{MOD}) at which the HTV is operated as an electric vehicle (power demand permitting) is gradually reduced as the battery state-of-charge (SOC) decreases. When the SOC reaches 20%, the V_{MOD} is set at its minimum value of 12 mph. At this condition, the heat engine is used to recharge the batteries until the SOC reaches at most 30%. The V_{MOD} is then maintained at 12 mph and the electric drive system is used primarily only at low vehicle speeds (less than 12 mph). For highway driving, the heat engine is primary with the V_{MOD} set at 40 mph. The electric drive system is used only to provide peak power for passing and to recover energy in regenerative braking. For the EPA Highway Cycle, using the electric drive system in this way (using 0.3 kWh/cycle) permits a highway range of about 300 mi before the batteries must be recharged from the heat engine*. For easy reference, the HTV power train control strategy is summarized in general terms in Table 5.3-1. The VM operating schedule as a function of battery depth-of-discharge has been given previously in Figure 4.2-8.

* Calculated using the HYVEC simulation program.

Table 5.3-1

POWER TRAIN CONTROL STRATEGY

- On/Off Engine Operation
- Regenerative Braking
- Electric Motor Idling When Vehicle is at Rest
- Electric Drive System Primary -- Battery State-of-Charge Permitting and Vehicle Speed Less Than V_{MODE}*
- Sharing of Load Between Motor and Heat Engine When Both are Needed
- Batteries Recharged by Heat Engine in a Narrow Range ($20\% < SOC < 30\%$)
- Electric Motor Dominant in Determining Shift Logic When it is Operating
- Heat Engine Primary for Highway Driving
- Electric Motor Always Used to Initiate Vehicle Motion from Rest and in Low-Speed Maneuvers (e.g., parking)

*V_{MODE} is the vehicle speed above which the heat engine is used to power the vehicle if the power demanded is less than the heat engine peak power capability. See Figure 4.2-A for the VM operating schedules as a function of battery depth-of-discharge.

The control strategy summarized in Table 5.3-1 is that for normal operation of the HTV. There are, however, a number of circumstances in which it is desirable to have the vehicle operate in special ways. Hence, a number of special operating modes have been built into the vehicle controller. These modes, which can be attained by simply positioning a knob on the outside of the controller panel, are summarized in Table 5.3-2. Some of the modes are intended primarily for test purposes (e.g., inhibiting regenerative braking) and others would be used primarily in the event of a malfunction in the power train (e.g., electric drive only). Maintenance modes are also provided to permit adjustments of the electric motor and heat engine with the vehicle at rest.

5.3.1.3 Thermal Analysis

Considerable attention was given to the thermal analysis of the various power train components and the underhood compartment in which most of the heat is released. The heat generated by the various components is summarized in Table 5.3-3. It is clear from the table that the heat engine and air-conditioner (when it is operating) generate most of the heat

Table 5.3-2

SPECIAL OPERATING MODES FOR THE HTV

No Regeneration
- Normal hybrid operation in all other respects

Electric Drive Only
- Heat engine operation completely inhibited
- With/without regeneration

Heat Engine Only (Velocity is greater than 12 mph)
- V_{MOD} set at minimum (12 mph)
- Vehicle operates on heat engine only for velocity greater than 12 mph
- Minimizes use of electric drive (used only to initiate vehicle motion)
- Can be initiated by push start if battery pack is nearly completely depleted

V_{MOD} Selector
- Auto-(V_{MOD}) max. Set at 60 mph for maximum mpg on the urban cycle
- Highway -(V_{MOD}) max. Set at 40 mph for highway driving and reduced electrical energy use on urban cycle
- See Figure 4.2-A for schedules with DOD.

Maintenance
- Transmission in neutral
- EM − 1/2 E_b (60V) operation only
- HE − engine started by electric motor which is then shut off
- Electric motor and engine speed controlled by accelerator pedal

Table 5.3-3

SUMMARY OF HTV HEAT GENERATION

Engine Compartment

- Heat Engine (18.5 kW output, 0.5 lb/bhp h)
  - Exhaust gases -- 85,000 Btu/h
  - Coolant -- 87,000 Btu/h
- Electric Motor (18.5 kW rated, 89% efficiency)
  - 6600 Btu/h
- A/C Condensor
  - 4 hp, Coefficient of Performance = 2
  - 30,700 Btu/h
- Battery Pack
  - 5300 Btu/h, 135 A rms
- Electronics Package
  - Starting resistor and contactors
  - 1000 Btu/h (300 W)

Power Electronics (front-seat console)

- Field chopper, microcomputer, power supplies
- 680 Btu/h

Battery Charger (trunk)

- Chopper control and power supplies
- 1600 Btu/h (500 W)

released and that the most severe problem occurs under the hood. The general approach taken with respect to thermal control was:

- Insulate the batteries from the high under-the-hood temperatures by placing them in a fiberglass box with an insulated cover and providing active cooling with ambient air
- Cool the electric motor and power electronics with air drawn from inside the vehicle
- Partition the under-the-hood compartment and place the power contactors and starting resistor in the airstream being drawn into the battery box
- Place the on-board battery charger in the trunk and provide for active cooling using ambient air drawn into the trunk

Much of the waste heat from the heat engine and the air-conditioning system is dissipated through the radiator. The engine is inclined forward so that most of the radiator cooling air is deflected under the car. The 1.7-liter VW engine utilizes an electric, thermostatically controlled fan to regulate the water temperature.

Special attention was given to estimating the temperature rise of the batteries and to provide adequate cooling of them. The calculated temperature rise of the batteries for continuous urban driving is shown in Figure 5.3-2. By continuous urban driving is meant that the battery pack is fully charged (state-of-charge SOC = 100%) initially and is discharged to SOC=20% after which it is charged intermittently at 145 A by the heat engine to maintain the SOC in the range 20-30%. The heat generation (Btu/hr) during discharge and charge and the periods (times) during which discharge and charge occur were determined using HYVEC and input into the battery temperature calculation. The temperature calculation was done using a

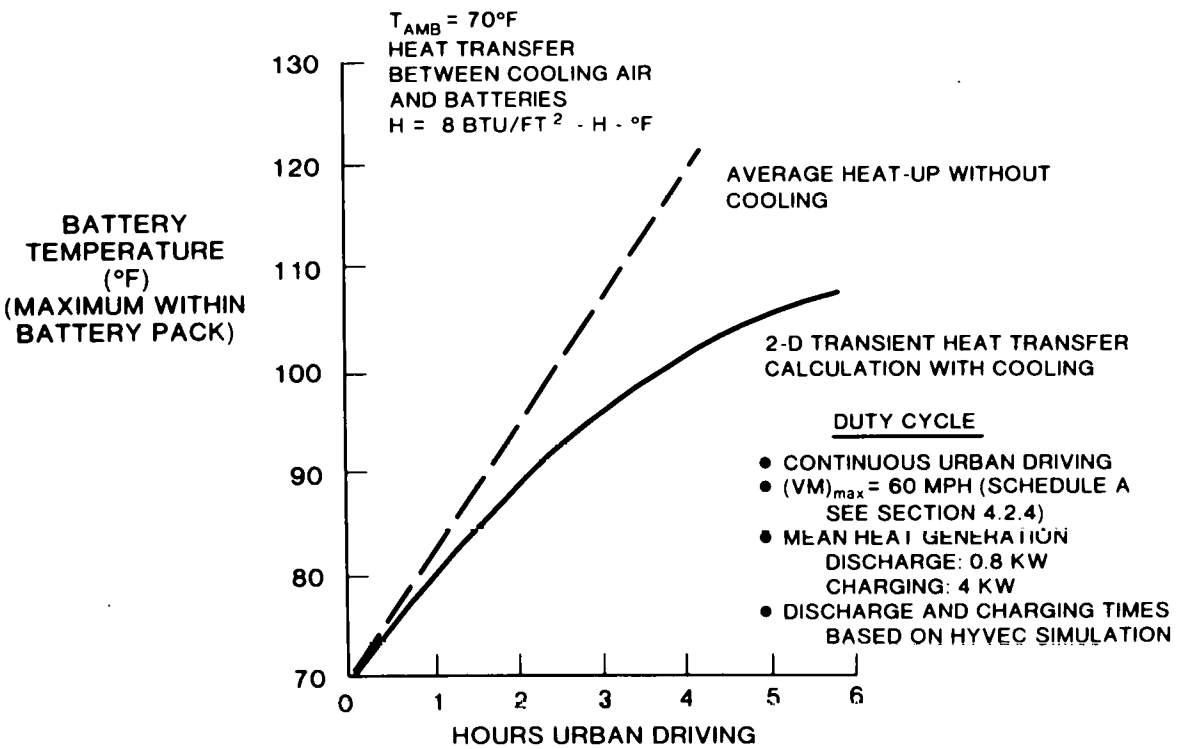

Figure 5.3-2. Calculated Battery Temperature Change in Urban Driving

finite-element approach (45 nodes). The problem was treated as two-dimensional with heat loss through the top and bottom of the batteries being neglected. Heat transfer through the sides of the batteries was included in the active cooling case. The temperature given in Figure 5.3-2 is that of the hottest node in the 45 node mesh. Based on such calculations, it was deemed necessary to cool the batteries. The battery box airflow for cooling is shown in Figure 5.3-3. Experiments were run using instrumented dummy batteries, and the blower to be used in the HTV to assure that the overall pressure drop and the airflow in the narrow passages between the batteries were as expected. The experiments indicated that the blower capacity was adequate and that the airflow distribution in the six axial channels across the battery box was reasonably uniform. Hence, it is expected that adequate cooling of the batteries has been provided.

The electrolyte temperature is sensed in one cell in each of the battery banks and the signal input into the vehicle controller. Hence data is available to track the temperature within the batteries as the HTV is operated. The battery cooling fan is turned on by a thermal switch (one in each bank) when the battery temperature reaches 90°F.

5.3.1.4 Power Train Losses and Accessory Loads

In order to simulate the hybrid power train on HYVEC, it is necessary to know the power train losses and accessory loads. The losses are primarily associated with the transmission and the torque transfer mechanisms. The accessory loads include the power required to operate the power steering and transmission pumps, the alternator, and the air-conditioner. Loss and accessory load measurements were made throughout the Phase II program on the mule vehicles as well as on the HTV.

All the loss measurements were made with the hybrid vehicle in neutral and the system being driven by the electric motor. The motor speed was varied from idle (1200 rpm) to

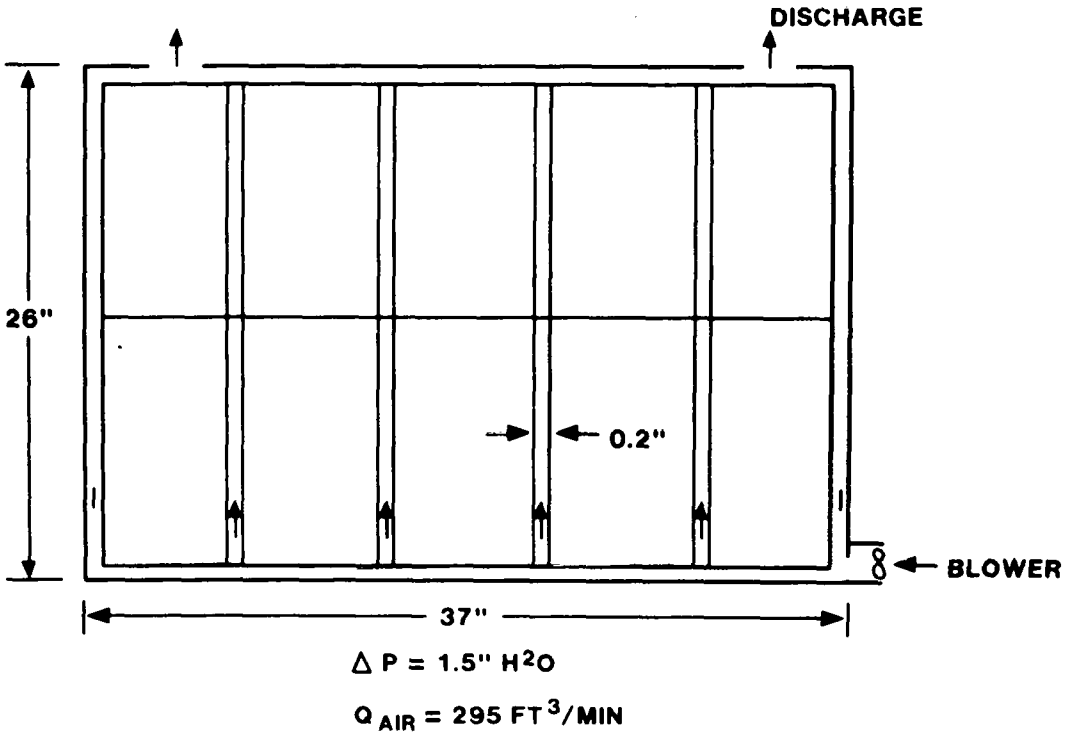

Figure 5.3-3. Battery Box Airflow for Cooling

about 5000 rpm by changing the field current. In this way steady state operating points were easily attained. Starting with the base condition (motor and transmission pump) and adding in turn each of the accessories, the power required to drive the system was determined from the vehicle controller readout P_{EM}. The torque transfer loss was determined by engaging the vehicle drive clutch with the transmission in neutral. In this configuration both the motor and engine connected hy-vo chains were turning. The losses in 3rd gear were obtained by jacking up the front (drive) wheels and operating the electric motor over the range of rpm cited previously. The final HTV loss/accessory load breakdown based on the test data is shown in Figure 5.3-4. The contribution of each of the components to the power required to drive the system at zero road load can be determined from the systematic buildup to the total accessory load. Of particular interest is the torque transfer loss from the motor and/or engine to the transmission input shaft via the clutches and the hy-VO chains (i.e., the difference between curves 1 and 2). That loss has been reduced significantly during the course of the program, but it is still much higher than expected.

The losses and accessory loads for the HTV, Hybrid Power Train Mule (HPTM), and the Test Bed Mule (TBM) are compared in Figure 5.3-5. Note that the HTV has the lowest power requirement in neutral of the three vehicles over the range of motor shaft speed (rpm). Numerous design changes including the use of a smaller power steering pump and reworking the torque transfer case lubrication and high-pressure hydraulic systems, over the course of the hybrid power train development program, contributed significantly to the improved loss/accessory load situation.

5.3.2 Drive Motor

The electric drive motor for the hybrid vehicle is a modified version of the electric motor used to drive the Electric Test Vehicle (ETV-1). See Table 5.3-4 for HTV drive motor parameters. The field has been redesigned and the voltage increased to 120 V to deliver 24 hp

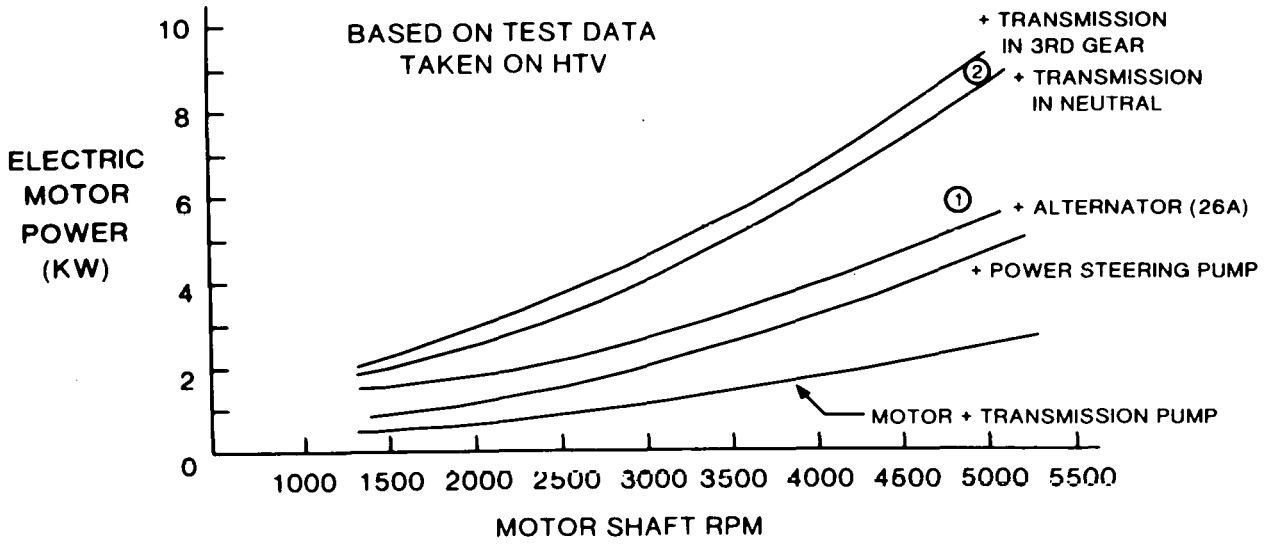

Figure 5.3-4. HTV Loss/Accessory Load Breakdown

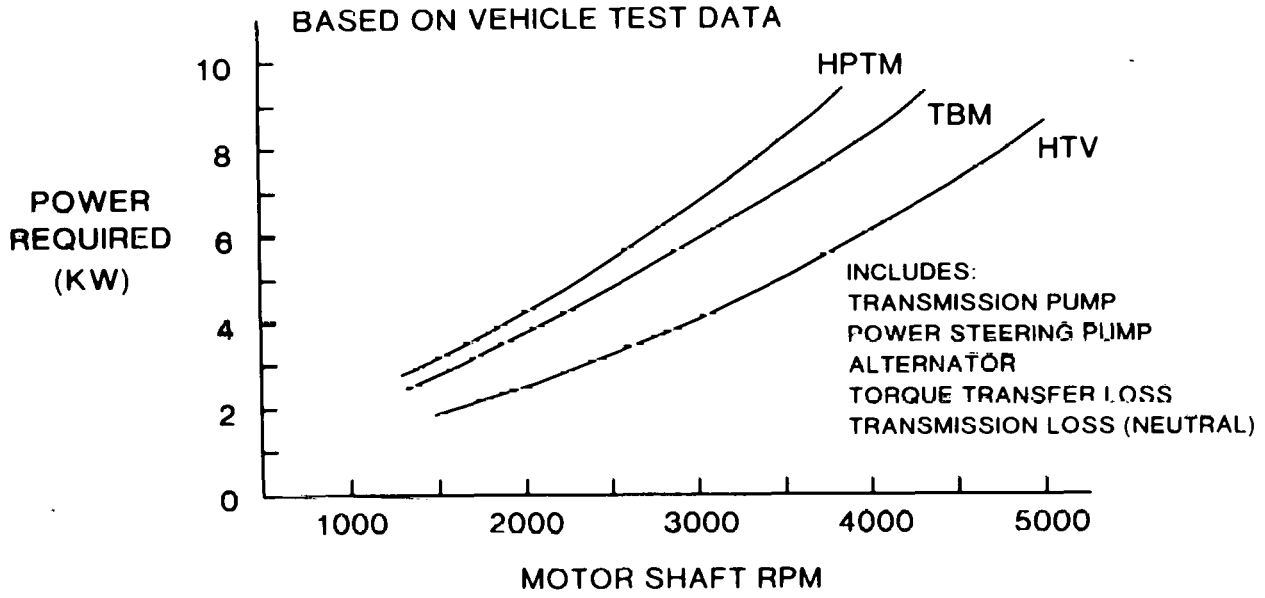

Figure 5.3-5. Power Required for HTV, HPTM, and TBM in Neutral with Accessories Operating

continuously compared with 20 hp in the ETV-1. The same armature design and frame size are used for each machine. For a short time duration (about 60 s), the HTV drive motor is capable of producing 46 hp (34 kW).

5.3.2.1 Motor Description

The drive motor was designed and manufactured by the General Electric Direct Current Motor and Generator Department (DCM&G). The motor frame size is 12 1/4 in. in diameter. Custom-designed aluminum end shields are utilized to reduce the weight. The commutator end of the motor houses an over-running clutch and the transmission hydraulic pump drive.

Table 5.3-4

HTV DRIVE MOTOR DESIGN PARAMETERS

- Continuous rating 24 hp, 112 V, 180 A, 2400/6000 rpm speed range
- Shunt wound, four-pole with commutating poles
- Totally enclosed, blower ventilated
- Shunt field

  Series/parallel external connected - 205 effective turns/pole
  Resistance - 1.69 Ω at 25 °C
  Inductance - 0.89 henry unsaturated
  Forced full field - 4950 ampere turns
- Voltage constant – 0.050 V/rpm-megaline
- Torque constant – 0.352 lb-ft/megaline-amperes
- Armature resistance – 0.0189 Ω at 25 °C
- Commutated field resistance – 0.0054 Ω at 25 °C
- Integral tachometer produces 24 pulses/revolution
- Weight – 221 lb

A custom-designed optical tachometer is mounted within the commutator end shield. Field design of this motor allows wide ranges of separate excitation, including operation at forced field, from 60 or 120 V. Figure 5.3-6 is an outline drawing of the HTV drive motor. Figure 5.3-7 illustrates the electrical connection diagram for the HTV drive motor.

5.3.3 Engine and Engine Clutch

This subsection discusses the engine and the engine starting clutch (C_1 in Figure 4.4-1).

5.3.3.1 Engine

The four-cylinder, 1.7 liter, fuel-injected (Bosch K-Jetronics-CIS) gasoline engine (Figure 5.3-8) is a modification of a production engine used in the Audi 4000. The engine produces 74 SAE hp (55 kW) at 5000 rpm. The engine modifications required in the hybrid application are discussed in the following paragraphs. In addition, a new flywheel clutch was needed because the engine is operated in an on/off mode for the hybrid application.

A new crankshaft was built for housing the bearing for the flywheel clutch and the mounting flange. The flywheel can assume any rotational position on stopping because it is not fixed to the crankshaft as in the production engine. A new top dead center (TDC) indicator was added at the front of the engine. The alternator was removed, and a change was made in the V-belt drive for the water pump. To ensure satisfactory on/off operation of the engine, changes were made in the electrical control of the fuel-injection system. For example, the engine is turned on or off by a signal from the vehicle controller rather than by the key switch in the "start" position.

Since the vertical inclination of the engine in the HTV is the opposite of that of the production car, new oil drain tubes in the lubrication system between the cylinder head and block had to be installed. Initial dynamometer tests of the engine mounted at the HTV inclination showed localized overheating in the cylinder head. This overheating was due to air pockets in the head produced by the HTV inclination. To correct this problem, four drain holes were

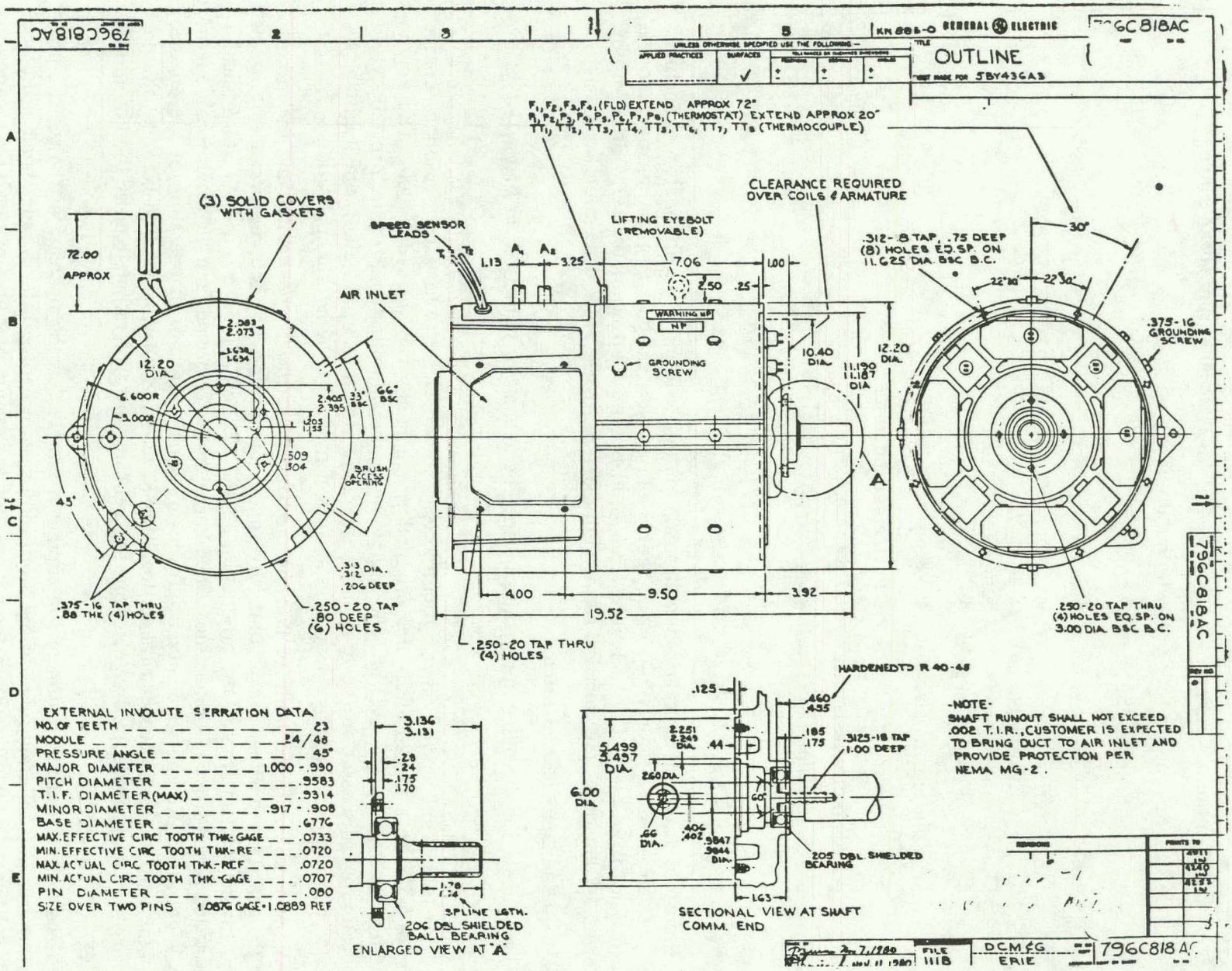

Figure 5.3-6. HTV Drive Motor

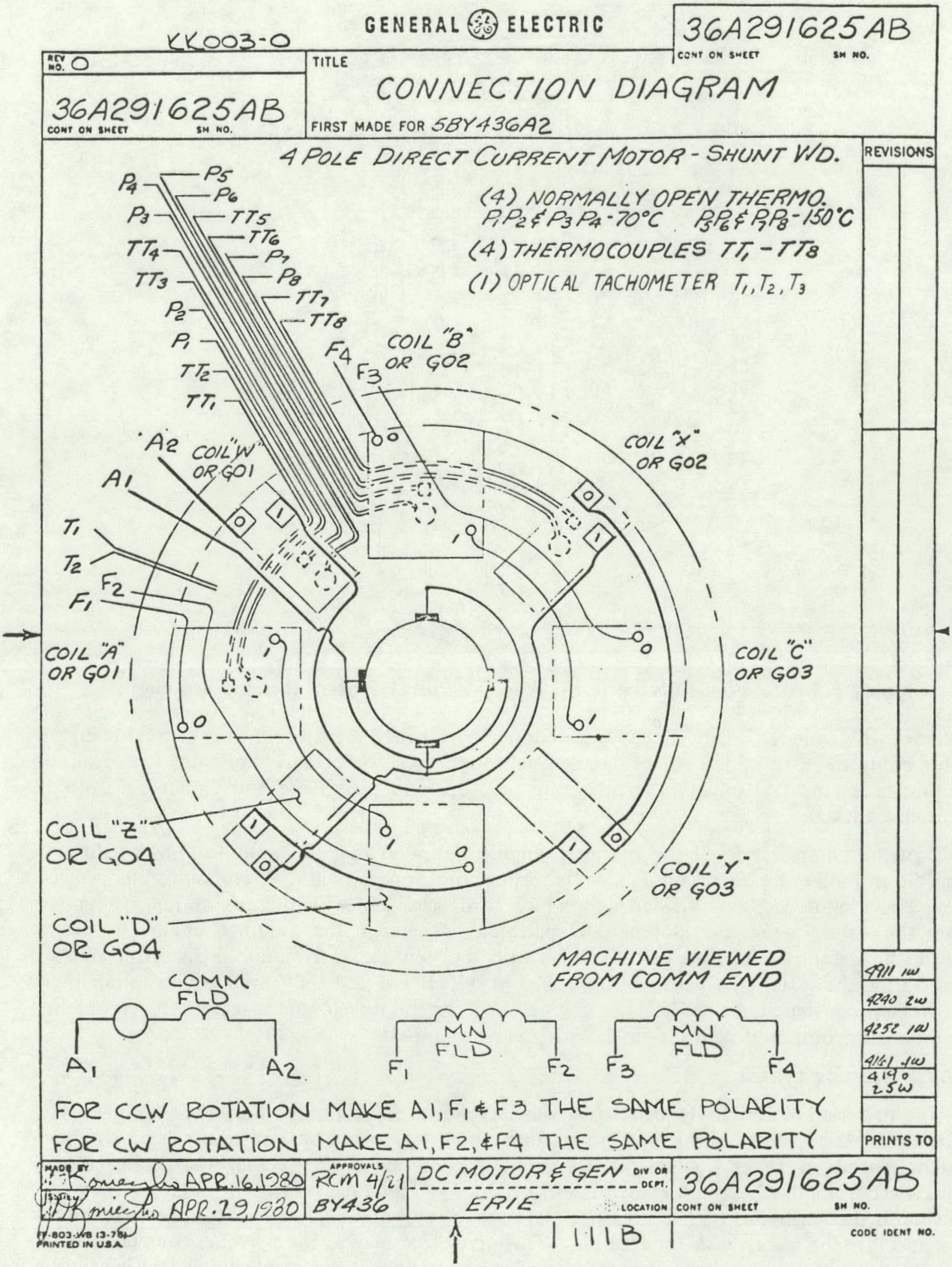

Figure 5.3-7. Electrical Connection Diagram for the HTV Drive Motor

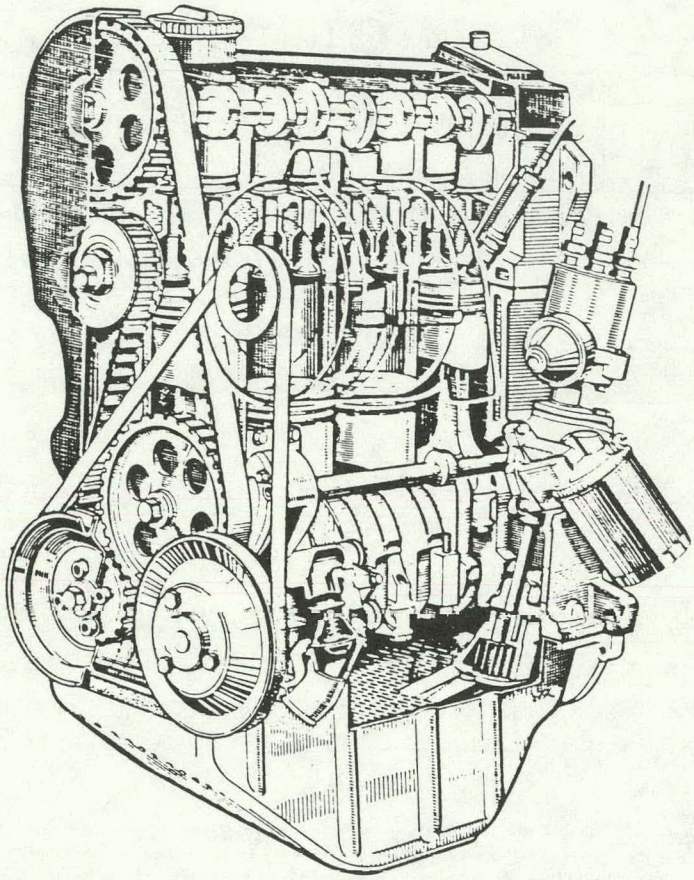

Figure 5.3-8. Fuel-injected (CIS) Audi Engine (1.7 liter) (unmodified engine)

drilled in the cylinder head. Tubes were connected through a manifold to a venturi near the water pump inlet. Engine coolant circulates through these tubes and eliminates the localized heating problem. The oilpan, the oil pump pick up, and the intake and exhaust manifolds were also altered.

Dynamometer testing of the modified engine indicated that the modifications to the engine did not affect its operation and/or its torque, fuel consumption, or emissions characteristics. The modified engine yielded data which compared well with the engine maps obtained from the Audi Engine Development Department. Tests on the modified engine were run only up to 3500 rpm because of difficulties with the new exhaust manifold distorting due to heat during the tests. Exhaust manifolds used in the HPTM and HTV are castings rather than the welded construction used for the engine used for the development testing. No problems have been encountered with the final cast exhaust manifolds.

5.3.3.2 Starting Clutch

The dry friction clutch (Figure 5.3-9) was developed especially for the hybrid vehicle program by LUK of West Germany. The starting clutch was based on VW research on flywheel clutches used in several experimental cars. Activation of the clutch to disengage the crankshaft from flywheel and transmission occurs by transferring force through a throw-out bearing to the springplate. The pressure plate moves approximately 10 mm in the axial direction and lifts the clutch disk for free play. This gives free play to the flywheel contact. Particular care was required for the special bearing configuration at the crankshaft. The bearing is filled with a special grease (lifetime filling).

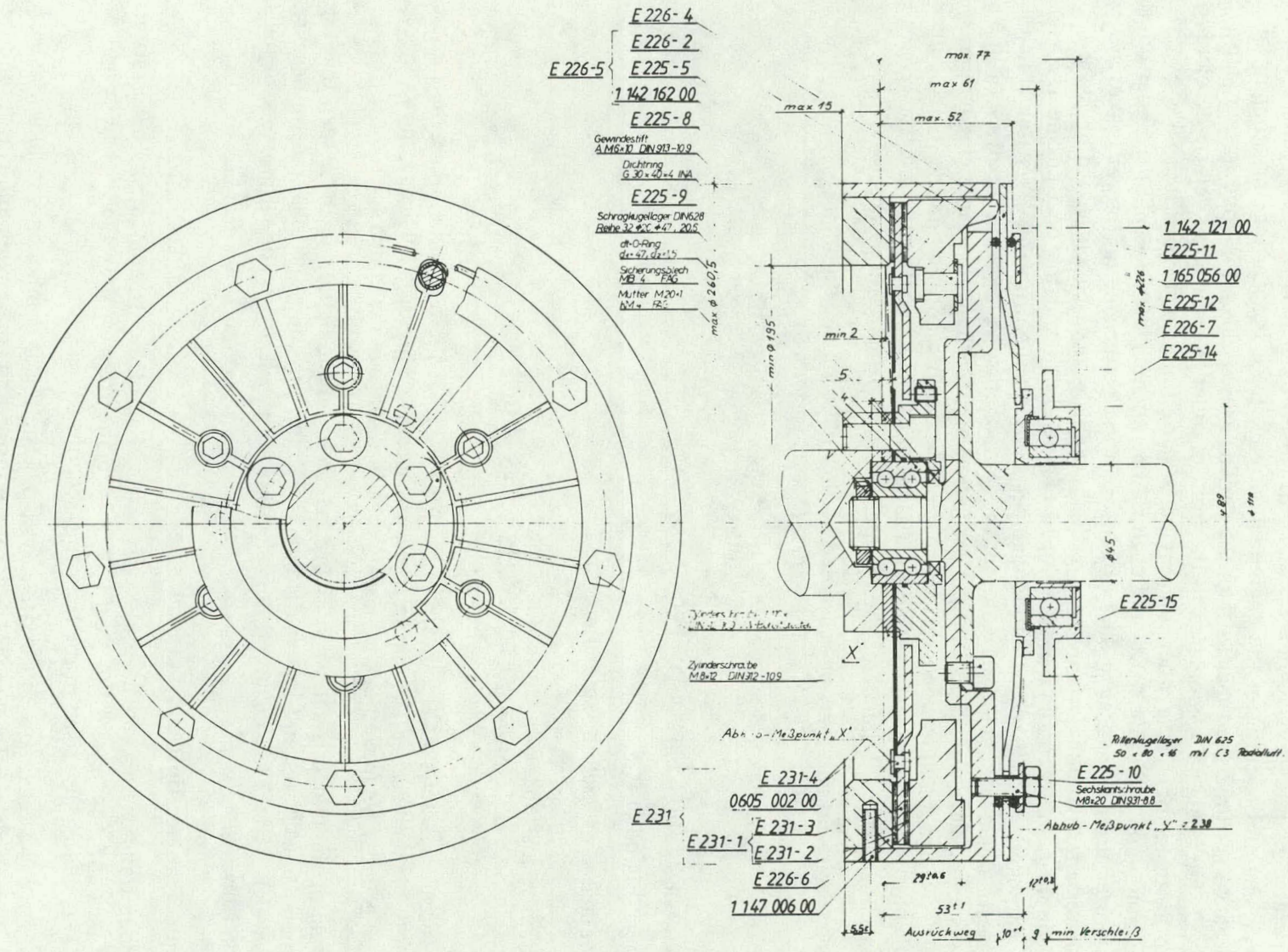

Figure 5.3-9. Engine-Starting Clutch

The engine starting clutch is opened and closed using an over-center linkage mechanism which is connected to a double-acting cylinder. The force to move the linkage is supplied by high-pressure hydraulic fluid which flows into and out of the cylinder when a set of four-way, electrically operated hydraulic valves are opened and closed by signals from the vehicle controller. The closing and opening of the engine clutch and, thus, the starting and stopping of the engine, can be accomplished in less than 0.5 s. The clutch closing is done in two steps, with the second step being slow compared to the first, in order to reduce the vehicle deceleration (jerk) to a satisfactory value when the engine is started and to decrease the stresses on mechanical components including shafts and chains. The engine clutch activation cylinder utilizes the same pressure and hydraulic fluid as is used in the power steering/power brakes systems, and shares the hydraulic accumulator with the vehicle drive clutch activation system. Mechanical coupling, between the VW developed engine clutch and the heat engine Hy-Vo chain drive sprocket, initially used torque damper components from a VW/Audi clutch. Operational tests failed the standard automotive components. A dynamic analysis of the mechanical system indicated excessive torque oscillation occurs when the heat engine clutch is closed rapidly. Design modification replaced the torque damper and automotive type spline shaft with a single piece design consisting of a large solid spline shaft with integral Hy-Vo chain sprocket. Figure 5.3-10 illustrates the integral spline shaft/sprocket assembly.

The clutch torque capacity may be calculated by the following equation:

$$Md = F \times D \times \mu$$

where

F = springplate force (closed position)

D = mean diameter

μ = coefficient of friction (special material)

The calculation yields for the clutch torque:

$$Md = 10500 \times 0.225 \times 0.45 = 1058\ Nm$$

The clutch force characteristics are shown in Figure 5.3-11. If there is clutch wear, the torque will be slightly higher because the spring force will increase. Figure 5.3-11 also shows that a force of 2100 N must be applied to the bearing area to disengage the clutch.

A drawing of the clutch is shown in Figure 5.3-9. From the figure, it can be seen that the clutch diameter is 253 mm and its axial length is 95 mm, including the axial release bearing. The clutch weight is 15.2 kg, including the release bearing, and its rotational moment of inertia is 0.14 kgf m^2.

5.3.4 Torque Transfer Unit and Transmission

The torque transfer unit and transmission consist of all of the drive elements necessary to couple the gasoline engine and the electric motor to the front drive wheels. The design of these elements will be discussed in the following sections.

Figure 5.3-12 is a schematic of the drive system. The major components include the electric motor, the vehicle starting clutch, the torque transfer unit, the engine and clutch, and the transaxle. The electric motor is connected to the drive system through a dry friction clutch which is controlled by a microprocessor. Torque from the clutch output is delivered to the transmission input shaft via a Hy-Vo chain drive with a reduction ratio of 1.393:1. Engine

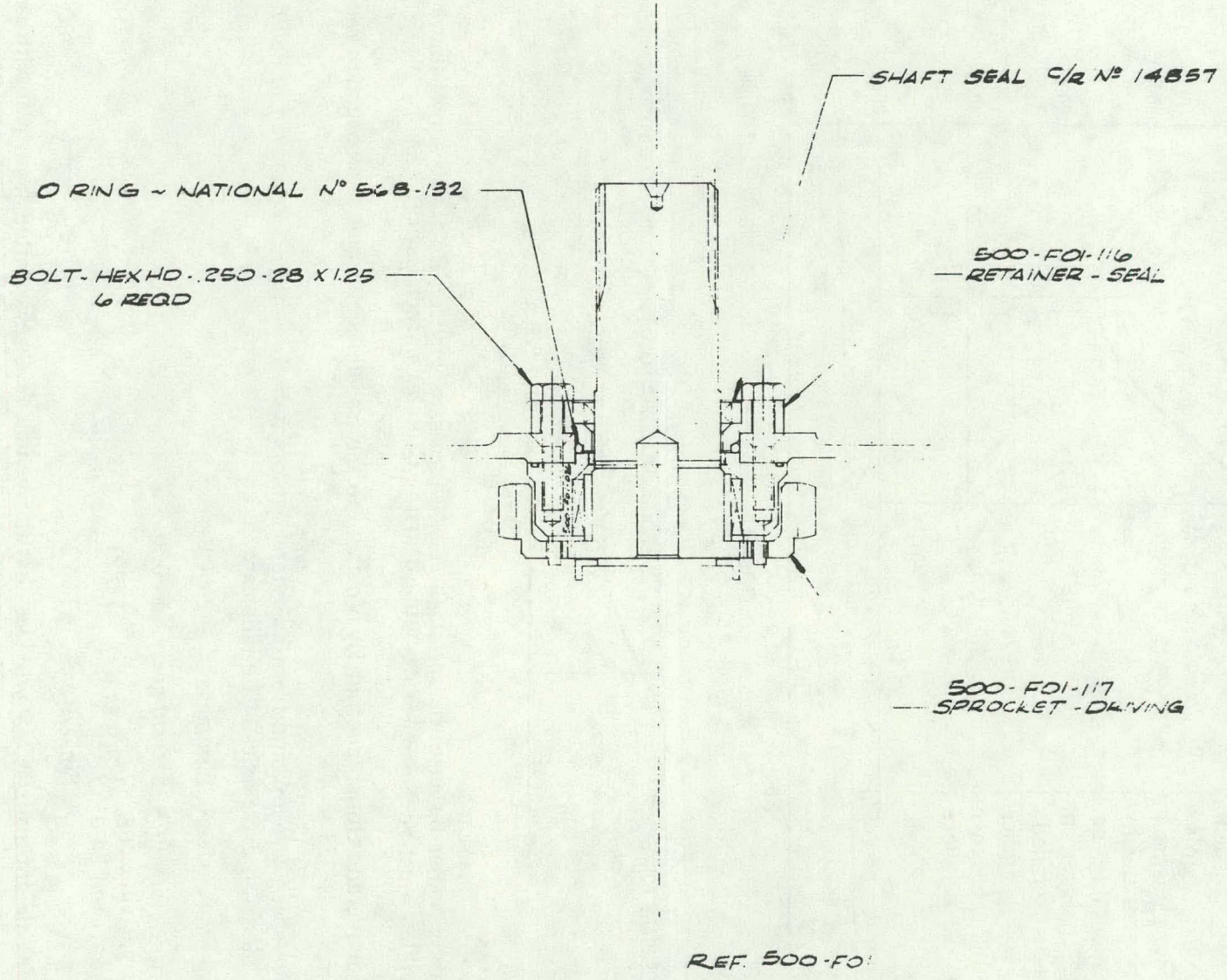

Figure 5.3-10. Heat Engine Drive Spline Shaft/Sprocket Assembly

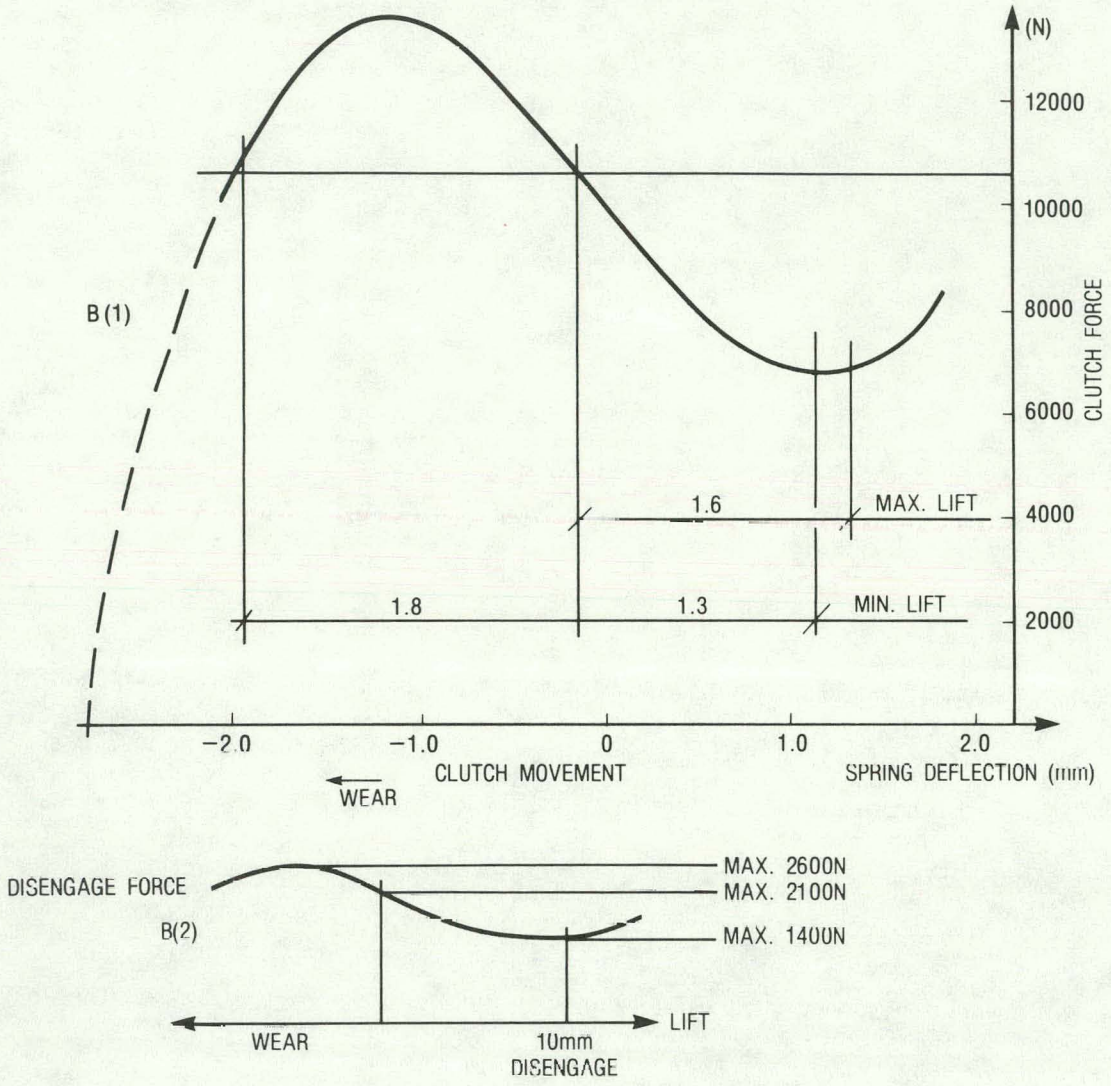

Figure 5.3-11. Engine-Starting Clutch Characteristics

power is delivered through another Hy-Vo chain to the transmission input at a reduction ratio of 1.12:1

A three-speed transmission from a General Motors X-body vehicle is employed to deliver power to the front drive axles. The ratios are

- First gear 2.84:1
- Second gear 1.60:1
- Third gear 1.00:1
- Final drive 2.84:1

The vehicle control strategy provides that the vehicle is always started from rest with the electric motor idling at its base speed at 60 V. The purpose of the drive clutch (C_2) is to smoothly modulate the flow of power from the electric motor to the vehicle drive wheels until the vehicle reaches a speed at which motor control by field weakening can begin.

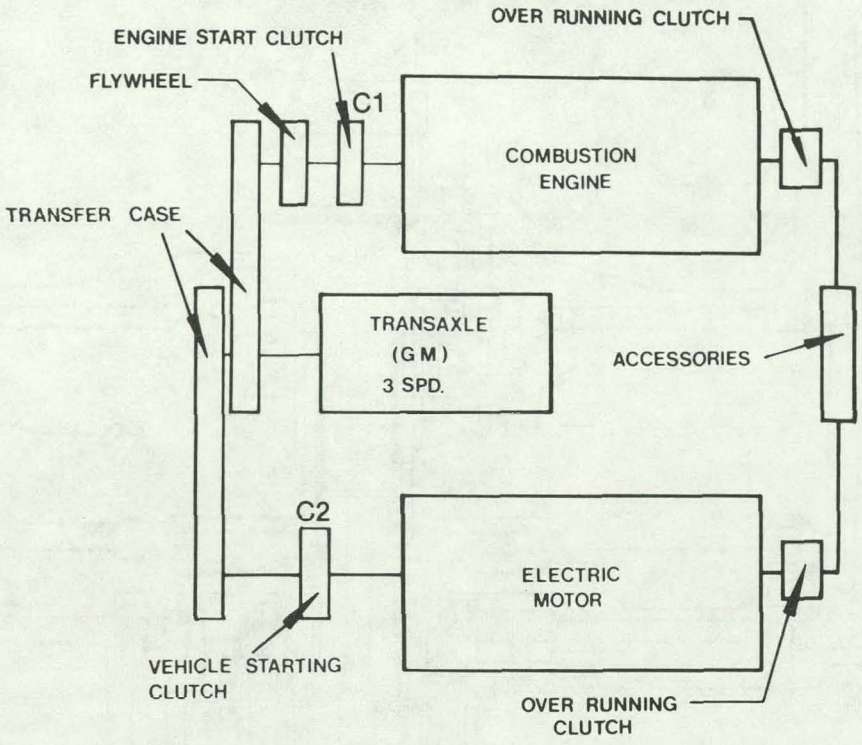

Figure 5.3-12. Schematic Diagram of HTV Drive

In order to permit a full-throttle acceleration of the vehicle from rest, the drive clutch must be capable of transmitting the full motor drive torque at maximum rated current. The drive clutch selected can transmit 220 lb-ft of torque, which is 133% of the design maximum motor torque. Additionally, the drive clutch assembly must be able to dissipate the energy necessary to maintain the current limit in the electric motor. The design philosophy employed was to add enough thermal mass to prevent the drive clutch from overheating. This requirement was established based on the heat dissipation required to allow the vehicle to climb a 30% grade for five minutes at 5 mph. This heat dissipation requirement is 6.3 Btu/sec. The drive clutch thermal mass was selected to limit the lining temperature to 900 °F during these conditions.

High-pressure hydraulics are used to actuate the drive clutch. A double-acting hydraulic cylinder applies force to a conventional clutch fork assembly. Fluid for the cylinder is delivered through a microprocessor-controlled servo-valve. The clutch modulation is controlled by the microprocessor which provides pulse-width modulated open or close signals to the servo-valve on a 5 ms time interval. The clutch loop is closed on the difference between delivered and commanded power which is a variable computed within the microcomputer. A speed difference acknowledge signal is calculated by the microcomputer using vehicle speed and electric motor speed sensors. Transition from clutch slip to electric motor feedback loop control occurs when the computed speed difference is below a given value and the clutch position microswitch indicates the clutch is closed.

The drive clutch was also designed to minimize the rotating inertia of the armature shaft in order to provide a rapid acceleration of the motor during on-off operation on the highway. This was accomplished by mounting the pressure plate assembly onto the drive housing and the clutch disc onto the armature shaft. Figure 5.3-13 is a sectional view illustrating this feature. This design requirement of minimizing the rotating inertia on the motor shaft did not prove to be necessary in the final HTV because, as noted previously, the electric motor is not

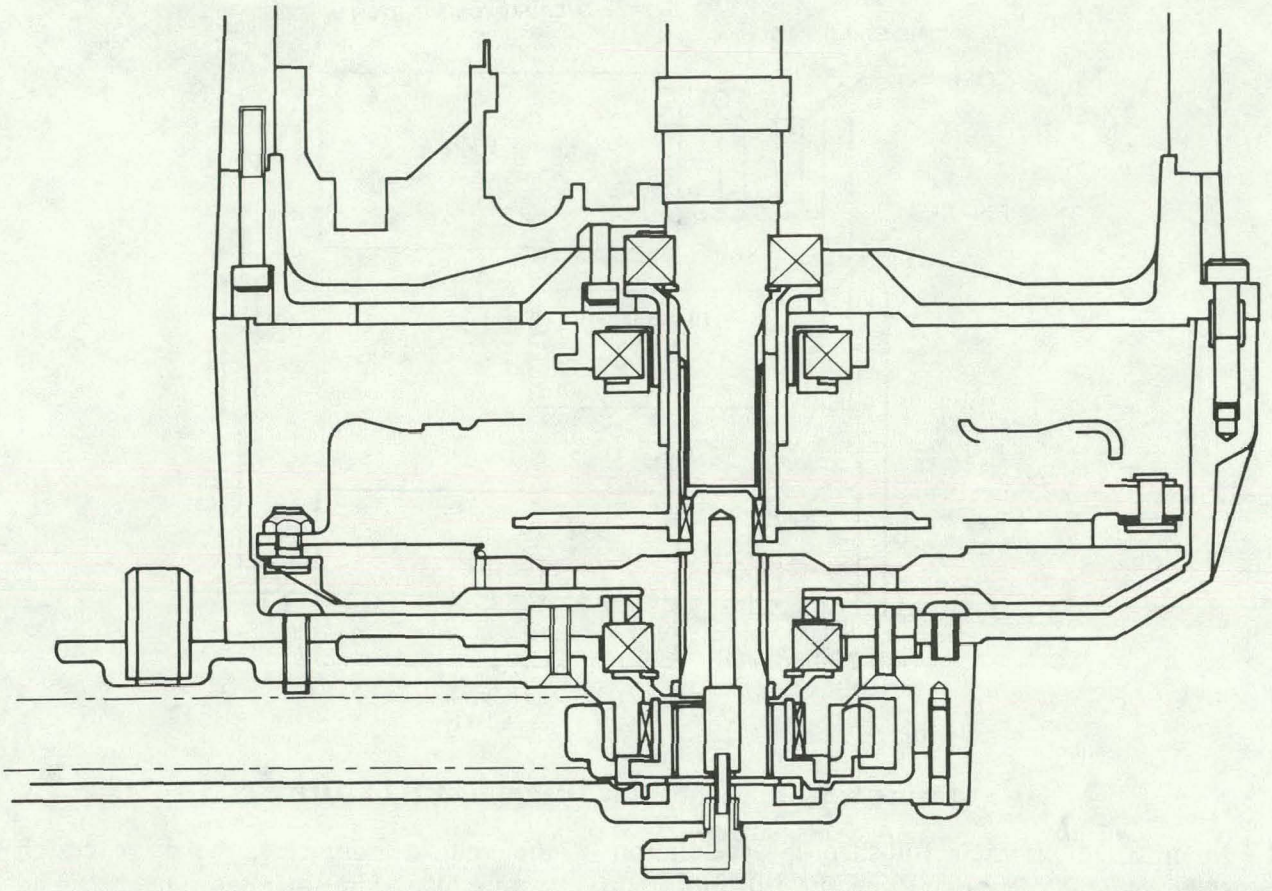

Figure 5.3-13. Sectional View of Drive Clutch (C_2)

decoupled from the driveline when it is de-energized due to driveability problems encountered in quickly restarting the motor from rest after it had been decoupled.

The transfer drive mechanisms and housings consist of those components required to transmit power from both the engine and the electric motor to the input of the transaxle. These elements were designed specifically for the hybrid application to accomodate both the mechanical requirements and the packaging constraints. The torque transfer elements selected were a pair of Morse Hy-Vo chains due to their high efficiency, low noise, and ability to handle relatively long center distances. Sprockets which run on pressure-lubricated needle bearings were designed for both the electric motor and the heat engine clutch output shafts. The design is such that all chain tension loads are reacted on these needle bearings, eliminating any bending moment from the shafts. A new tandem transaxle input sprocket was designed to replace the original singular unit.

Chains selected for this application are Morse-type 2300, 0.375 in. pitch units. This is the new chain series developed for the General Motors X-body vehicles. They have torque capacities substantially above the maximum torque of the motor or engine. The transfer drive housing replaces the original transfer case which is employed by the General Motors X-body vehicles. Figure 5.3-14 is a photograph of the transfer case with the cover removed to illustrate the Hy-Vo chain drives.

Transfer housings were fabricated from custom aluminum castings which include provision for bearing lubrication and transmission hydraulic functions. Chain lubrication is obtained by spraying oil on the inner side of the Hy-Vo chain. Sprockets and bearing retainers

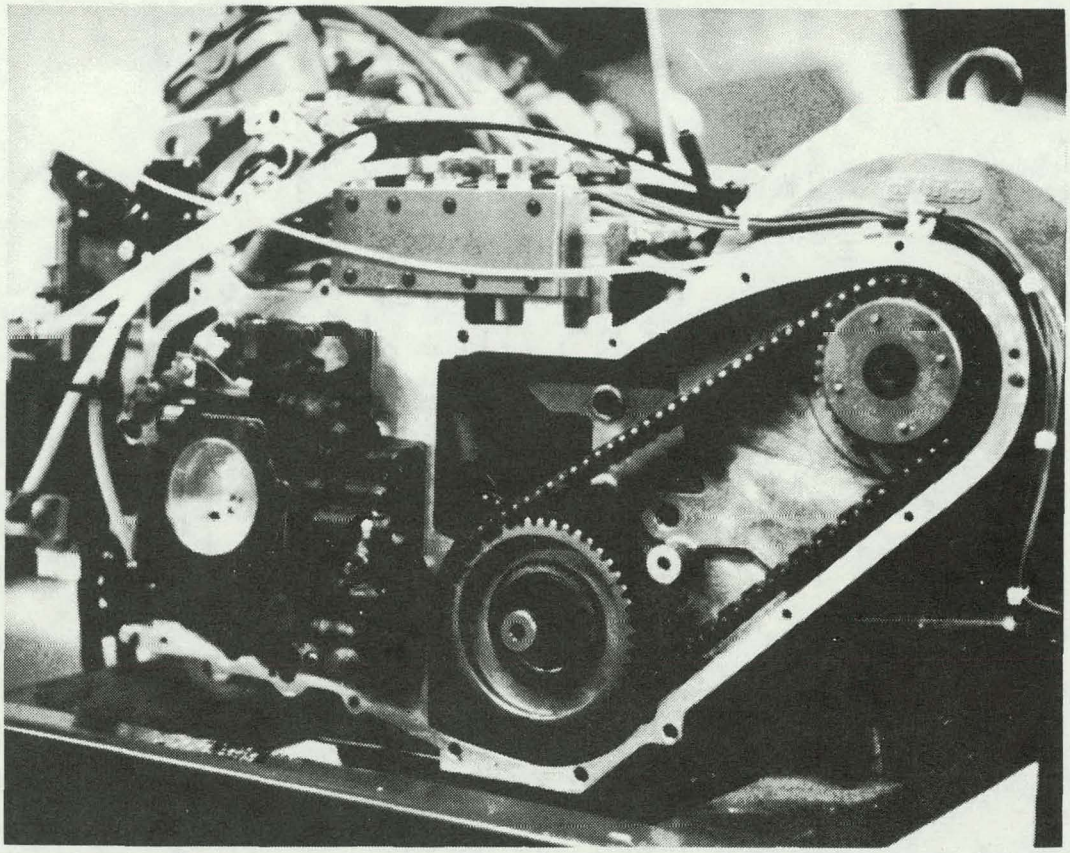

Figure 5.3-14. Transfer Case with Cover Removed

were machined from solid bar stock with splines and teeth slotted or hobbed on them where appropriate. Silicone formed-in-place gasketing techniques were employed almost exclusively on the housings.

A custom high-pressure (800-1000 psi) hydraulic system is required to actuate the heat engine and the electric motor drive clutches. Since a high-pressure hydraulic system is also required to operate the vehicle power brakes and power steering, the high-pressure hydraulic functions for the clutches were integrated with the standard automotive braking and, power steering systems utilizing production automative component where possible. Driveability tests using the HPTM vehicle show that a 2 gpm hydraulic pump provides sufficient flow to perform power steering, power braking, and clutch actuation. An Audi 4000 power steering pump was used for the HTV. Figure 5.3-15 illustrates the HTV high-pressure hydraulic system. An accumulator with provision to be periodically charged from the Audi pump was utilized to reduce accessory losses associated with the high pressure hydraulics. Accumulator charging is required due to clutch actuation and the leak rate through the servo valve to maintain it in a ready state. An electrically activated charging system was utilized to keep the accumulator pressure in range of 800-870 psi. This system has proved reliable over the range of oil temperature and servo-valve leak rates encountered in the HTV.

The transaxle is the three-speed automatic unit used in the General Motors X-body vehicles. It was chosen primarily for its packaging arrangement and adequate torque capacity. By virtue of its planetary final drive, the axle shafts can be concentric with the input shaft which

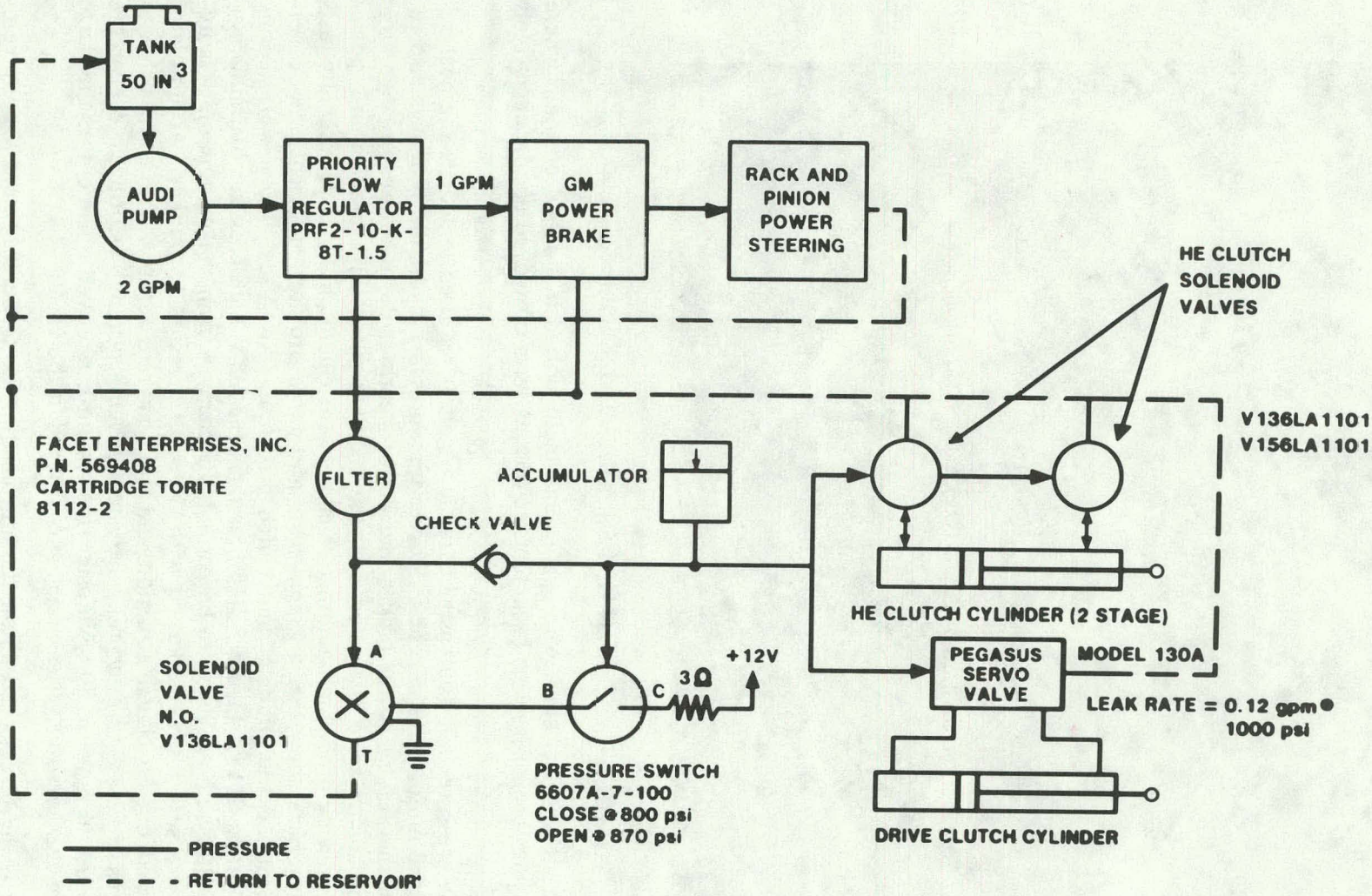

Figure 5.3-15. HTV High-Pressure Hydraulic Block Diagram

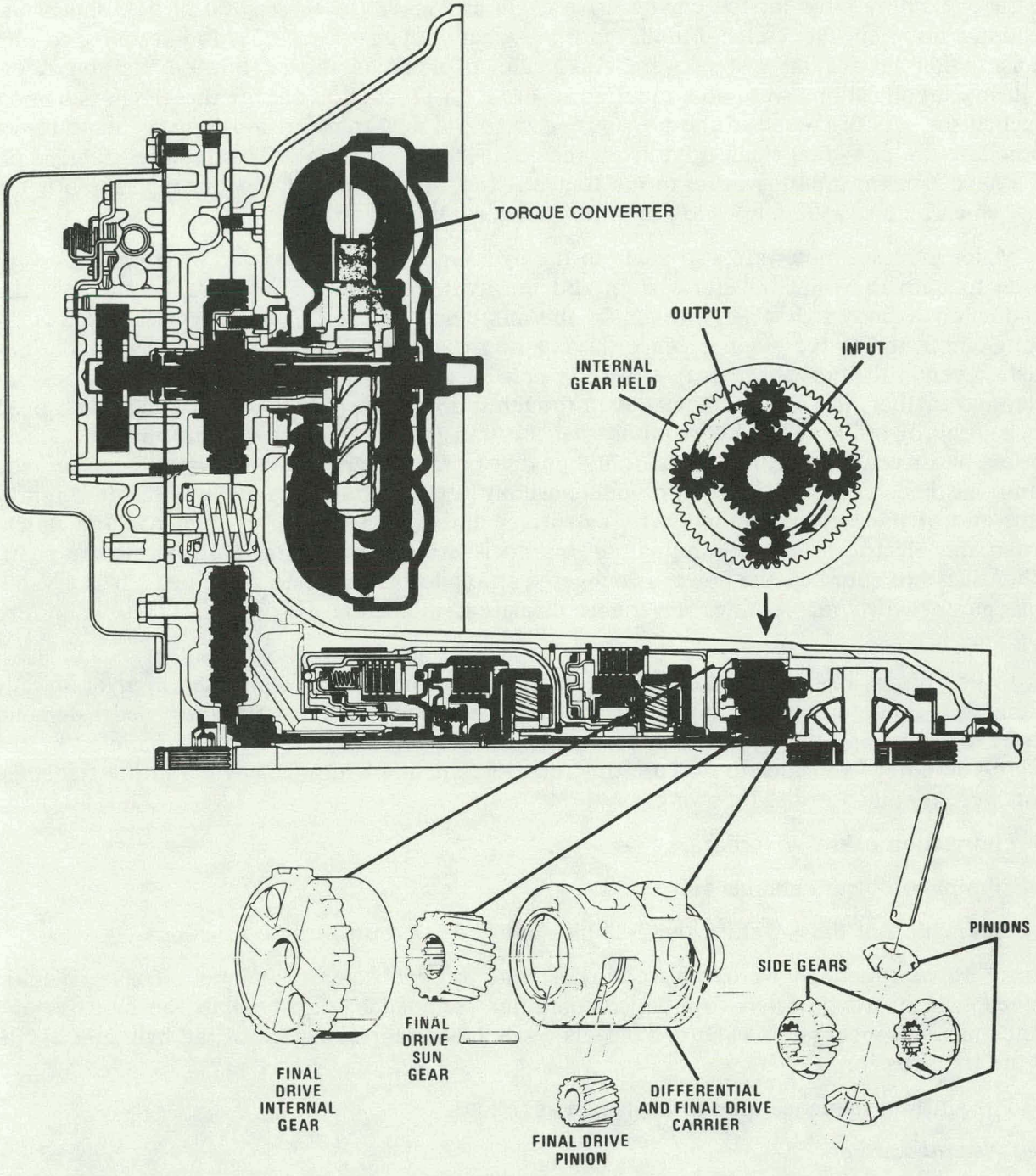

Figure 5.3-16. Final Drive

results in a highly compact unit. Figure 5.3-16 is a sectional view of an unmodified transmission assembly illustrating the planetary final drive unit and the concentric output and input shafts. The transaxle has been modified extensively mechanically and hydraulically.

The major mechanical modifications of the transaxle were the elimination of the torque converter and the addition of the tandem chain drives to the transmission input. The replacement of the torque converter by the engine starting clutch involved the fabrication of new

bearing retaining hubs for the engine drive chain as well as the fabrication of new shaft connections between the clutch output and the chain input sprocket. Modifications to the transmission lubrication system were also made to eliminate the oil flow to the converter. Housing modifications were also required in order to provide pivots for the clutch actuation mechanism. As discussed in the previous section, the new transfer housing was made to accomodate the new dual chain drive from the engine and the motor. This required fabrication of a new, tandem input sprocket to the transmission. This sprocket is wider than the original one which required the fabrication of a new, longer output shaft.

Major modifications were also made to the hydraulics of the transaxle. Modifications were made to both the fluid transfer system and the hydraulic logic. The hydraulic pump in the production X-body transaxle is driven by the pump side of the torque converter which is directly connected to the engine. Since the engine was always running, the pump ran continuously, even with the vehicle at rest. In the present application, the gasoline engine does not idle, and further, the electric motor, even though it does idle while the vehicle is at rest, need not run all of the time.* This required that the transmission hydraulic pump, like the accessories, be driven from either the gasoline engine or the electric motor. For this reason, the pump has been relocated from its original position in the hydraulic valve body to the commutator end of the electric motor where it is driven through the accessory over-running clutch. When the electric motor is running, the pump is driven directly from the armature shaft. When it is not running, the power is delivered through the accessory drive belt. It is a vane-type pump which incorporates a variable displacement feature (Figure 5.3-17) to minimize pumping losses.

In its normal application, the X-body automatic transmission is controlled by hydraulically operated logic elements which compare the engine speed and the accelerator pedal demand signal to determine the shift sequence. In the hybrid vehicle, this activity is handled by the micro-computer. In order to execute this requirement, the hydraulic circuits in the transmission were modified in the following ways:

- Elimination of the governor
- Elimination of the manual valve
- Elimination of the 1-2 shift, the 2-3 shift, and the 3-2 control valve functions.

These valve functions were replaced by a bank of five solenoid valves. These solenoid valves, which are operated from microcomputer commands, direct oil to the clutches and bands in the transmission. Figure 5.3-18 is a schematic representation of the hydraulic circuit in the transmission.

The shifting sequence may be explained as follows:

1. *Neutral and Park*

   In neutral and park, none of the solenoid valves are energized. The line-pressure ports are blocked by solenoid valves No. 1 through 5 while all of the other ports to the solenoid valves are connected to the exhaust port. All clutches and bands are released and the transmission is in neutral. From a safety standpoint, if power is lost to the solenoid valves, the transmission shifts to neutral.

---

* The original design was consistent with initial control strategy of decoupling the electric motor from the driveline when it was de-energized. The HTV does not presently utilize this capability and it functions as a single-shaft arrangement for reasons discussed previously.

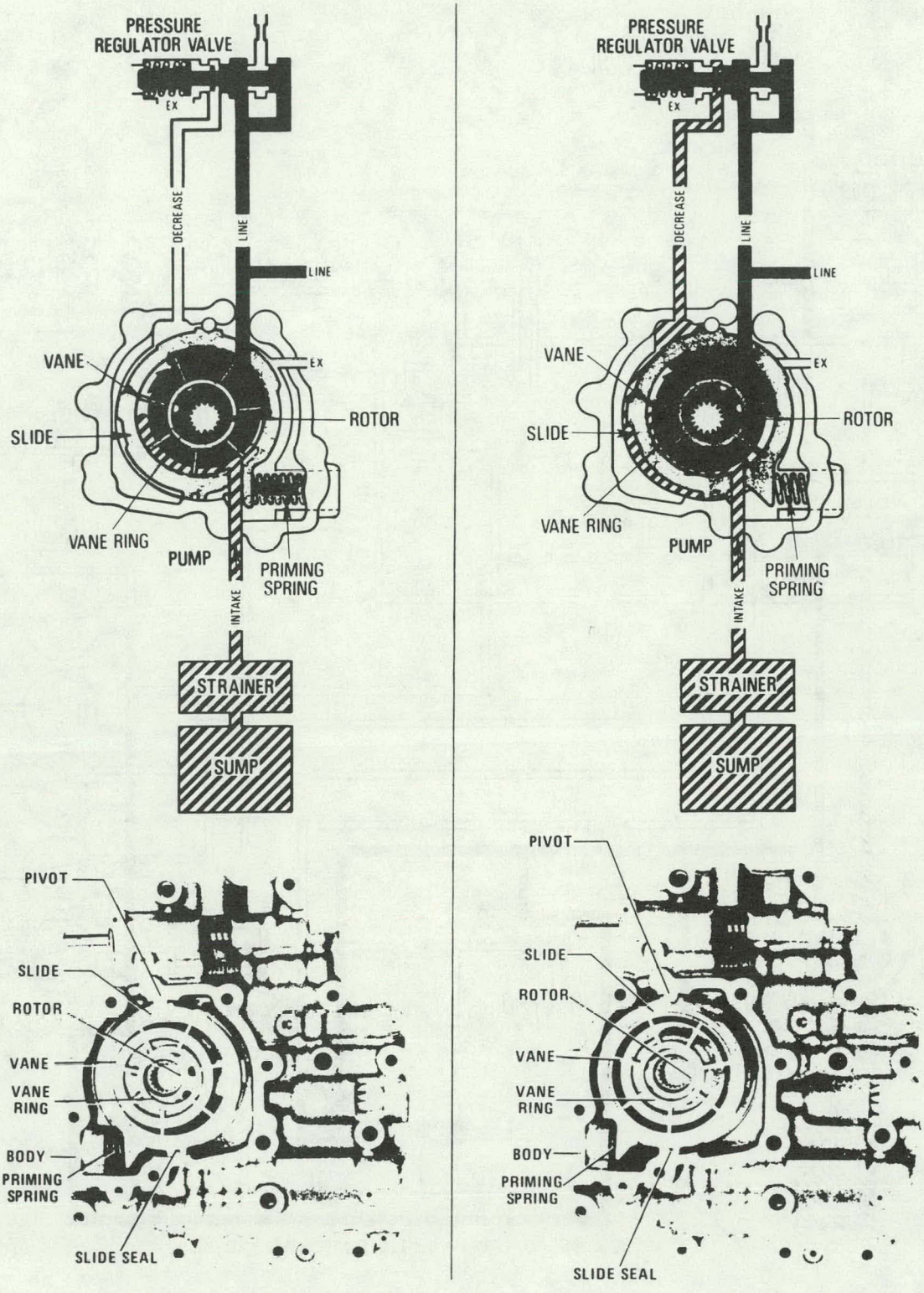

Figure 5.3-17. Hydraulic Pump

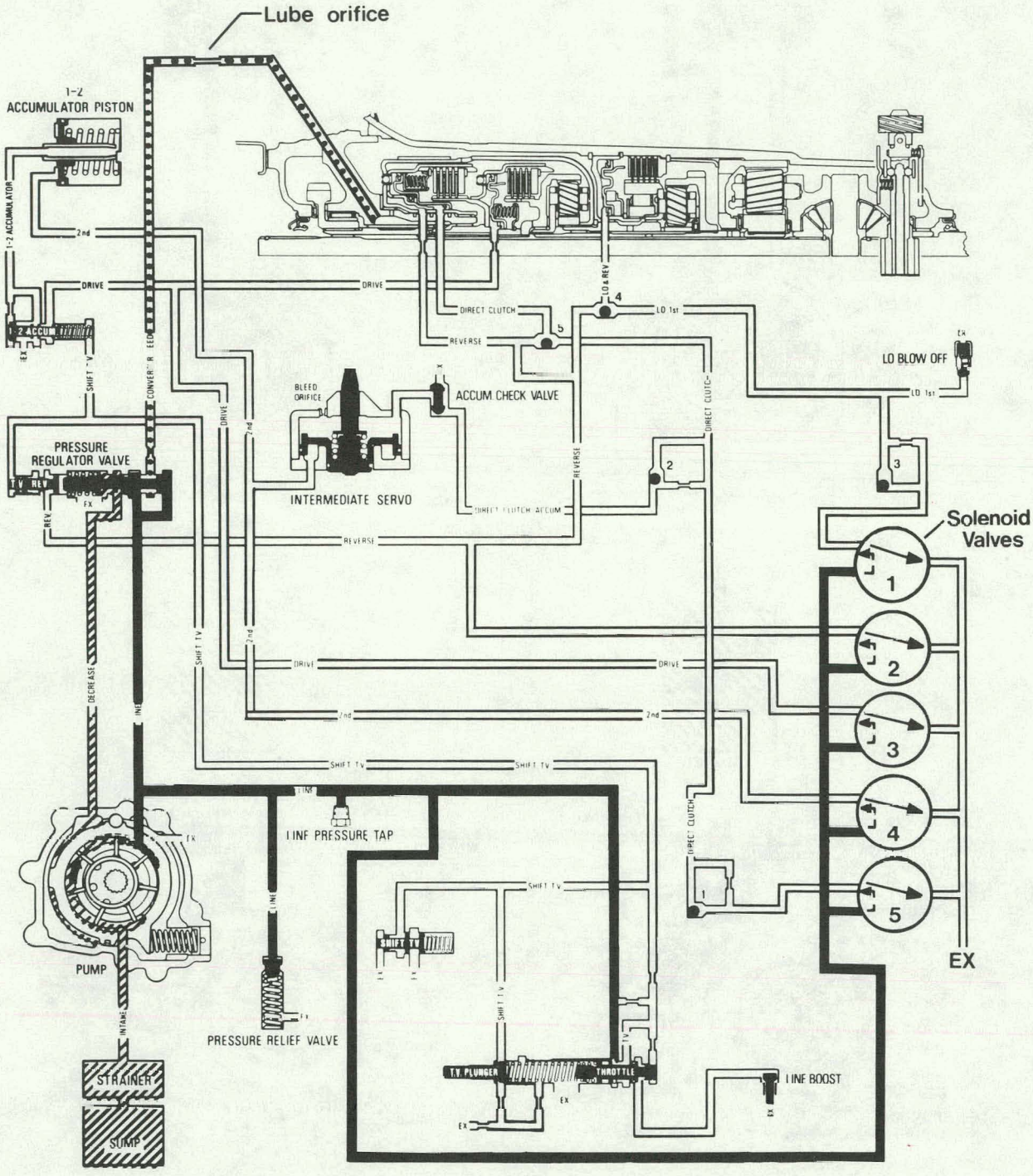

Figure 5.3-18. Schematic Diagram of Transmission Hydraulic Circuit

2. *First Gear*

To obtain first gear, valve No. 3 is energized. Since there is no regeneration in 1st gear, reverse torque reaction is not required and the Lo solenoid is not utilized.

Valve No. 3 directs line pressure to the forward clutch. When this clutch is applied, a mechanical connection is provided between the input shaft and the input internal gear of the forward planet set. This forward clutch must be engaged in all forward speeds, and is consequently utilized as the forward gear acknowledge signal to the microcomputer.

3. *Second Gear*

To obtain second gear, solenoids No. 3 and 4 are energized while Nos. 1, 2, and 5 are deenergized. Releasing solenoid No. 1 allows the oil from the low clutch to unseat check ball (3) and flow to the exhaust port, releasing the clutch. Solenoid No. 4 directs line pressure to the intermediate servo to apply the intermediate band. At the same time, this oil moves the 1-2 accumulator piston against the 1-2 accumulator spring to maintain a controlled build-up of pressure on the intermediate servo during the 1-2 shift for a smooth band apply. These actions lock the forward sun gear to the case and release the intermediate carrier.

4. *Third Gear*

To obtain third gear, solenoids No. 3, 4, and 5 are energized. Solenoid valve No. 5 allows line oil from the pump to flow past the direct clutch exhaust check ball (1) to the direct clutch and reverse check ball (5), seating it in the reverse passage, and then to the inner area of the direct clutch piston applying the direct clutch. At the same time, oil is directed past the direct clutch accumulator check ball (2) into the direct clutch accumulator passage to the direct clutch accumulator check valve, seating it; and to the release side of the intermediate servo. The pressure of the direct clutch accumulator oil combined with the servo cushion spring moves the servo piston against second oil pressure and acts as an accumulator for a smooth intermediate band release and direct clutch apply. This action locks the forward planet sun gear with the internal gear, resulting in a 1:1 ratio.

5. *Reverse*

To obtain reverse, solenoid No. 2 and No. 5 are actuated. This action seats the direct clutch and reverse check ball (5) in the direct clutch passage and oil flows to both the inner and outer areas of the clutch piston, applying the direct clutch. Reverse oil also seats the Lo and Reverse check ball (4) in this Lo first passage and applies the Lo and reverse clutch. Reverse oil also flows to the reverse boost valve to increase line pressure to about 120 psi. This "reverse" oil is also used to provide a reverse acknowledge signal to the microcomputer.

In order to execute these changes, extensive modifications were made to the hydraulic passageways in the transmission. Additional transmission modifications included: provision for lubrication, modification of chain case oil drain, and lowering the oil pan.

Since the torque converter is no longer in place, the flow through the converter feed was altered by adding a 0.040 in. orifice to the lubrication circuit to provide transmission lubrication. Oil for the chain drive bearings is provided by externally plumbed hoses.

Excessive losses in the HPTM torque transfer unit were traced to chain drag in the oil under the electric drive Hy-Vo chain sprocket. A larger than standard sprocket is used on the transmission to provide the 1.393:1 reduction. Relocating and enlarging the oil drain from the chain case plus lowering the oil pan by one inch mitigated the loss problem in the HTV power train.

5.3.5 Power Electronics

Power control in the electric drive system of the hybrid test vehicle uses a combination of battery switching and field control of the separately excited shunt-wound dc motor. Figure 5.3-19 shows the power control circuit block diagram used in the TBM, HPTM, and HTV vehicles. The microcomputer controller interfaces with each module of the power control via initiating commands and return feedback status signals.

The electric motor is operated with the two 60 V battery banks in parallel in the following situations:

- Starting and idling the electric motor while the vehicle is stationary
- Operating the vehicle at low speed and low power

The batteries are switched to the series configuration (120 V) when the electric motor power commanded is more than 17 kW or the motor speed is higher than its effective base speed.

5.3.5.1 Field Chopper

Field control of the motor is obtained via the transistorized field chopper that is under microcomputer control. Field control is used to vary the motor speed above its rated base speed in both series and parallel battery configurations.

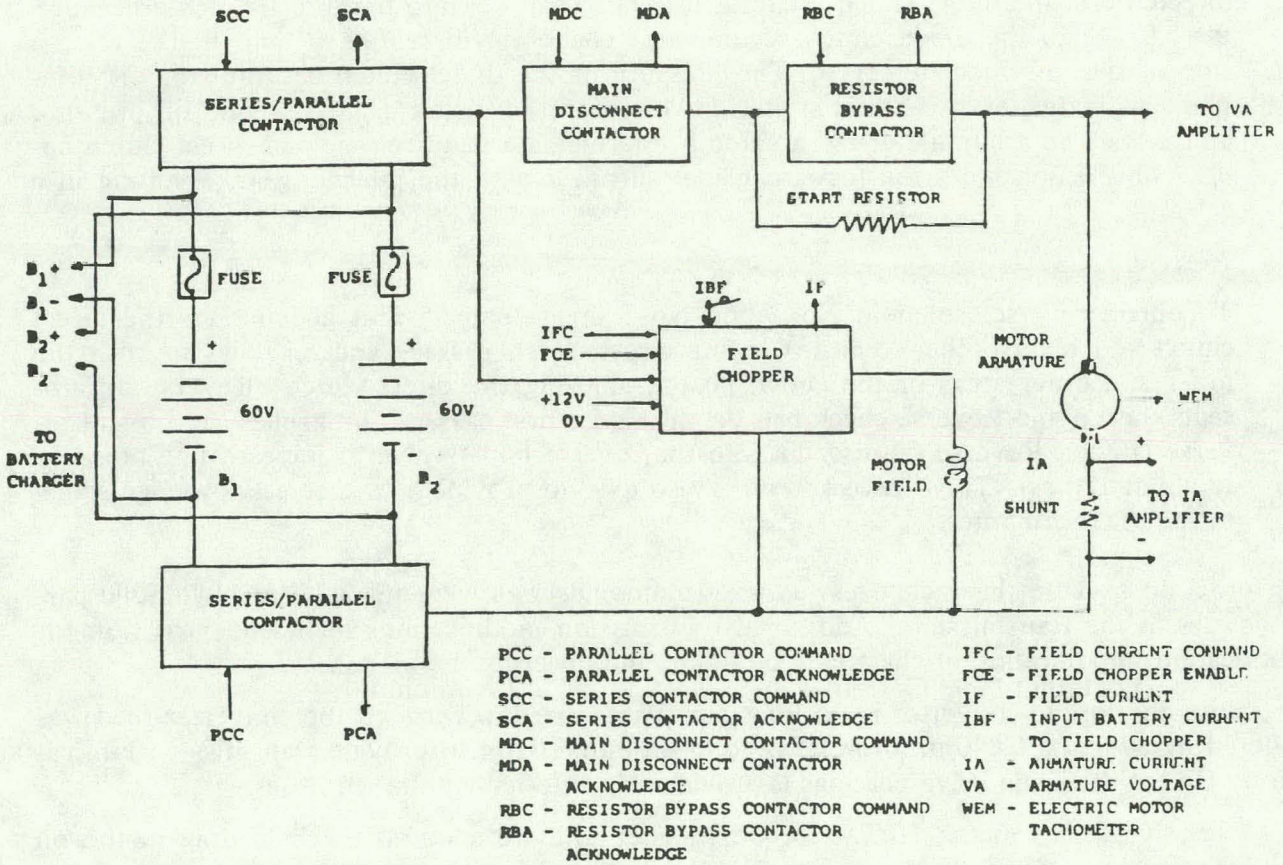

Figure 5.3-19. Power Control Circuit Block Diagram

A transistorized field chopper provides the ability to drive the electric motor field current to the level commanded by the microcomputer controller. The power circuit of the field chopper uses dc power from the main battery bank, as illustrated in Figure 5.3-19. The field chopper is designed to operate over the wide input voltage range resulting from battery switching, regenerative braking, and varying battery state-of-charge.

Identical field chopper electrical designs are used for the TBM, HPTM, and HTV vehicles. However, the mechanical packaging of the HTV field chopper has been redesigned to reduce volume and weight.

The field chopper requirements are summarized in Table 5.3-5. A photograph of the field chopper power circuit is shown in Figure 5.3-20. A down-chopper circuit is employed. The power switch transistor is protected against excessive electrical stress through careful circuit layout to minimize stray inductance and through the use of turn-on and turn-off snubbers. The input filter capacitor is sized to permit proper circuit operation during the battery switching intervals with the input current sensing resistor providing adequate damping to prevent "ringing." Field current sensing of both average and instantaneous values is provided by components that are designed for low-inductance and low-temperature coefficients. Isolated local power is provided to the base driver, logic, and current sense circuitry by dc-to-dc converters powered from the accessory battery.

The control logic, current regulation, and power switch base driver printed circuit board are shown in Figure 5.3-21. The field current "measured" by a sensing resistor in the power circuit is compared against the microcomputer-commanded current reference voltage, thus generating an error voltage which is fed to the pulse width modulation (PWM) circuit, which generates the required duty cycle for the power transistor to achieve the commanded field current. The operating frequency of 2 kHz ($T_{on(max)}$) was chosen to permit the very wide dynamic range of controlled current to be achieved (40:1). The preset times $T_{off(min)}$ and $T_{on(min)}$ (created by OR'ing the outputs of the power chip) provide proper resetting of the power circuit snubbers.

Base driver cicuitry provides appropriate interface between the control circuit and the power switch transistor. A time delay (generated by the time delay circuit and effected by a

Table 5.3-5

FIELD CHOPPER REQUIREMENTS

Chopper Input Voltage	45 V minimum 160 V maximum
Logic Power Supply Input Voltage	10.5 V minimum 14.6 V maximum
Chopper Load Characteristics	R_f = 1.69 Ω nominal L_f = 0.90 h unsaturated
Output Field Current	2.0 A minimum 10.8 A FF 25.0 A maximum FFF
Output Field Current Resolutions	25 mA (goal)
Field Current Command	0-10 V optoisolated signal from microcomputer

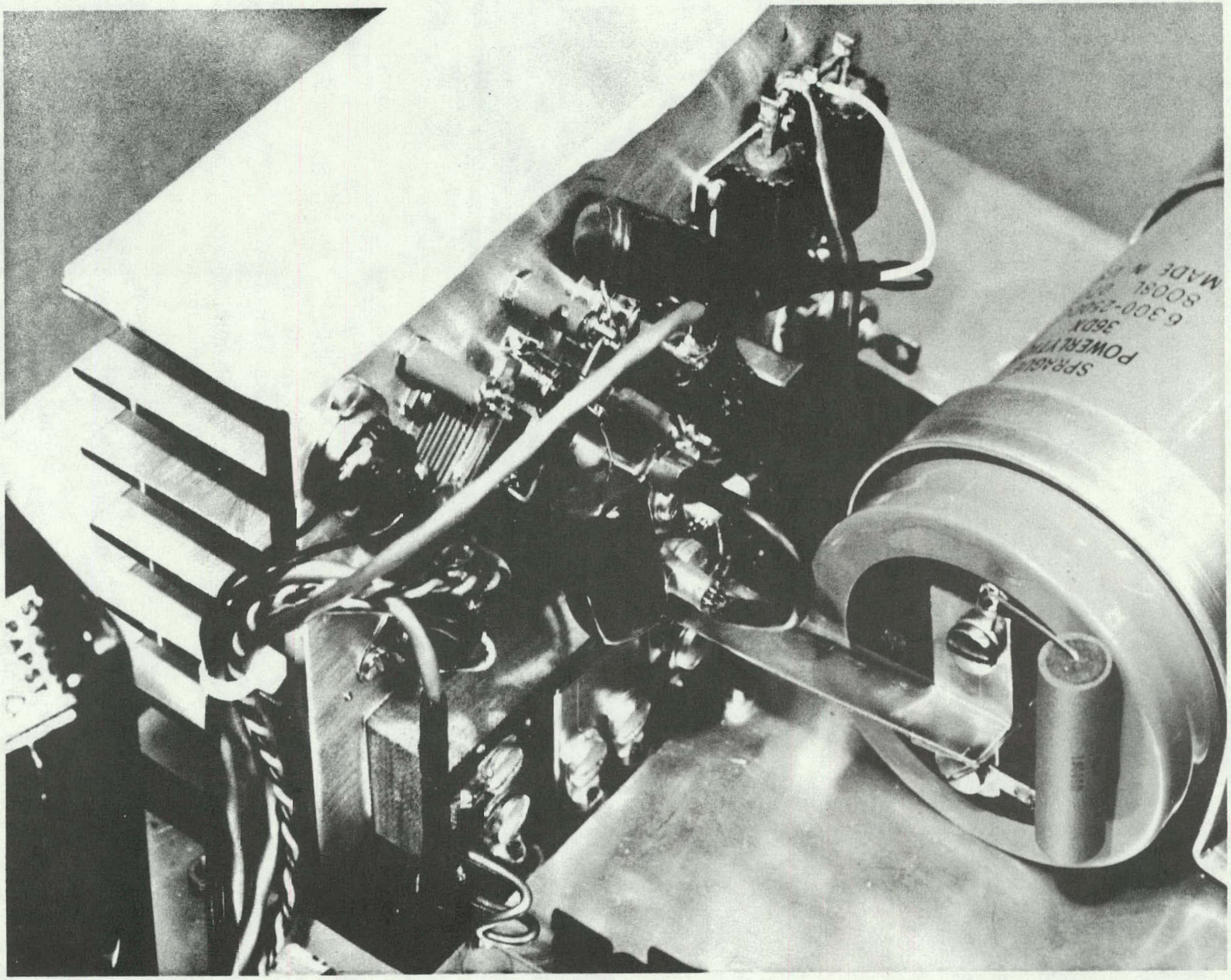

Figure 5.3-20. Field Chopper Power Circuit

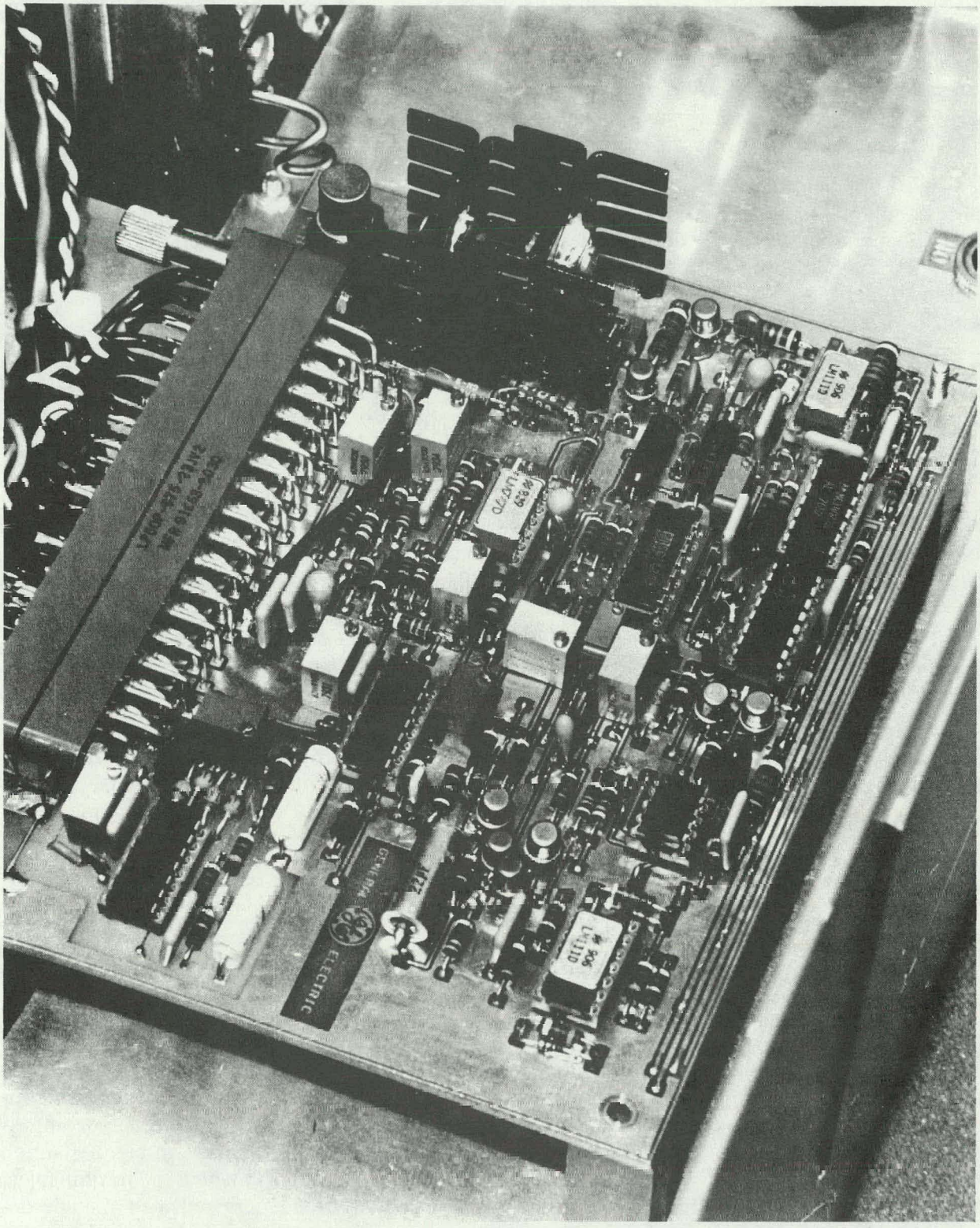

Figure 5.3-21. Field Chopper Logic/Base Drive Circuit Board

relay) inhibits the base drive to the power switch transistor during power-up and power-down to prevent improper circuit operation.

The other circuits perform the following functions: convert a field current voltage signal to a frequency signal for the microcomputer, provide a low local power supply voltage shutdown signal to the logic, OR'ing of the control signals (including the heatsink overtemperature and enable signals), and convert the chopper input current (derived from a sense resistor) to a frequency signal for use by the microcomputer. Also, all input and output control signals are isolated from the microcomputer.

Two TBM field choppers were fabricated and tested. Printed circuit boards were functionally tested and calibrated, using the field chopper logic/base drive card exerciser. Both TBM field chopper modules were bench tested and used for electric drive integration on the dynamometer in the laboratory. Both field choppers met or exceeded all design requirements. Field chopper No. 1 was successfully integrated into the TBM and is currently operating in the vehicle. Field chopper No. 2 was integrated into the HPTM vehicle.

The HTV field chopper is located within the console area in front of the microcomputer controller. Forced ventilation within the console area is provided by the drive motor ventilating fan. A photograph of the HTV field chopper is shown in Figure 5.3-22.

Battery Switching. Armature voltage control is obtained by a combination of battery switching and momentary insertion of a starting resistor into the circuit.

The series/parallel contactor (SPC) is a mechanically interlocked, normally open contactor assembly with two coils. Energizing of the parallel contactor coil (PCC) connects the two 60 V battery banks in parallel, producing nominally 60 V. Energizing the series contactor coil (SCC) connects the two 60 V battery banks in series, producing nominally 120 V. If neither the PCC nor the SCC is energized, the contactor is normally open, and there is no current to either the armature or the field chopper power circuit. Batteries are switched from parallel to series or from series to parallel without opening the main disconnect contactor.

The main disconnect contactor (MDC) is a normally open contactor. Energizing the MDC coil closes the circuit between the SPC and the armature through the start resistor and its resistor bypass contactor (RBC). Two normally open contactors, SPC and MDC, provide redundancy and safety in the event that one of these contactors "welds closed." Emergency circuitry de-energizes both the SPC and MDC coils.

The resistor bypass contactor (RBC) is a normally closed contactor that bypasses the start resistor. A normally closed contactor is selected to reduce coil dissipation. The RBC coil is energized less than 1% of the time.

The start resistor is sized in order to limit the armature current to 500 A during electric motor startup and battery switching. The resistor is 0.070 Ω in resistance and is fabricated from 5 GA nickel-chrome wire.

The dc power contactors were commercially available and purchased with the proper coils and transient suppression components. Control of the dc power contactors via the microcomputer required a coil driver interface. Contactor coil command signals from the microcomputer controller are all optically isolated to prevent any ground loop problems. An eight-channel, general-purpose coil driver, printed circuit provides necessary optical isolation, inhibit logic, and current amplification. Inhibit logic allows all the coils to be deenergized with a single optoisolated logic signal. Figure 5.3-23 illustrates a typical block diagram and circuit layout of the coil driver printed circuit card. Figure 5.3-24 is a photograph of a coil driver board. One of these cards was used in the TBM, two in the HPTM, and three in the final HTV.

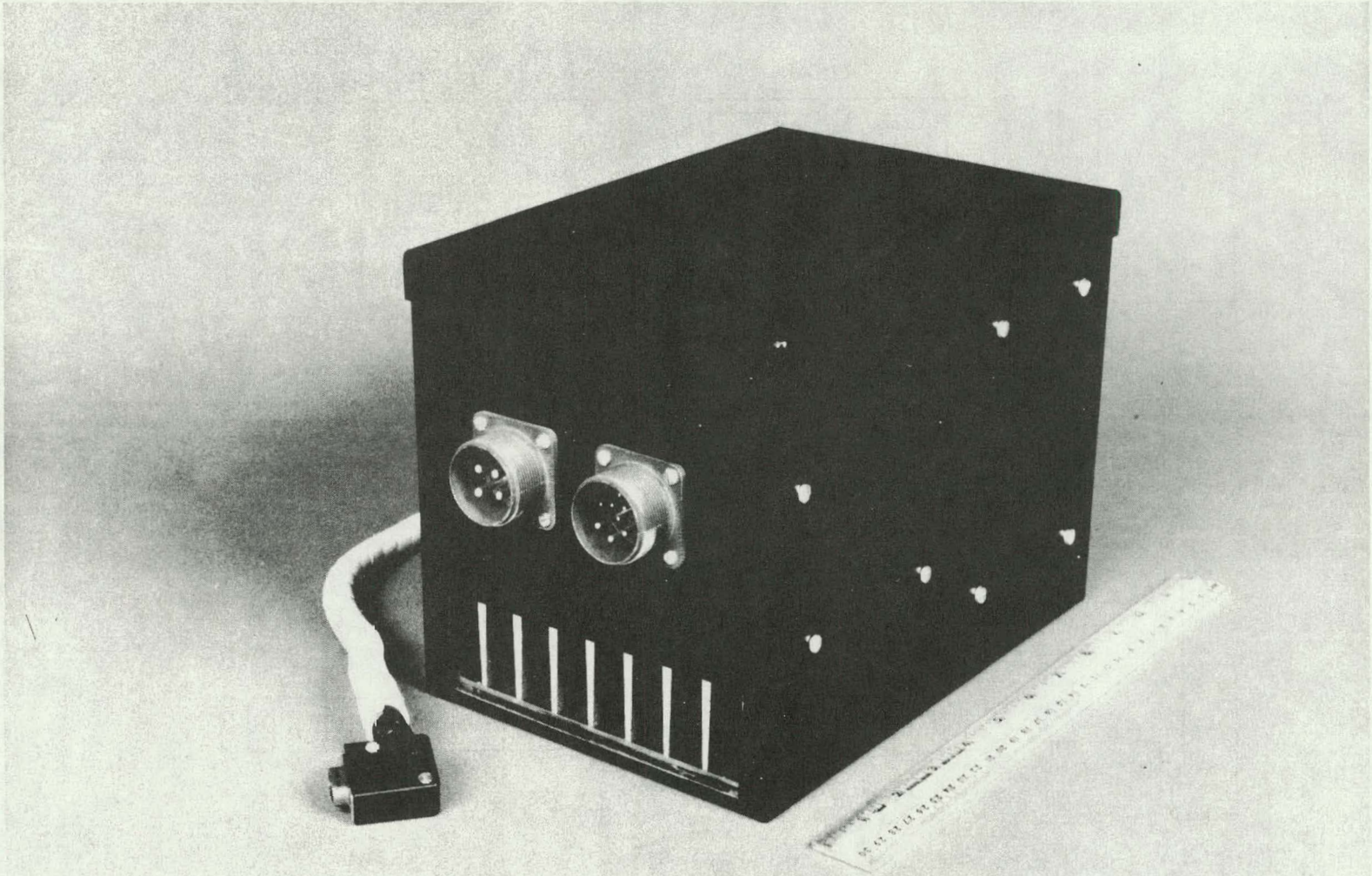

Figure 5.3-22. HTV Field Chopper

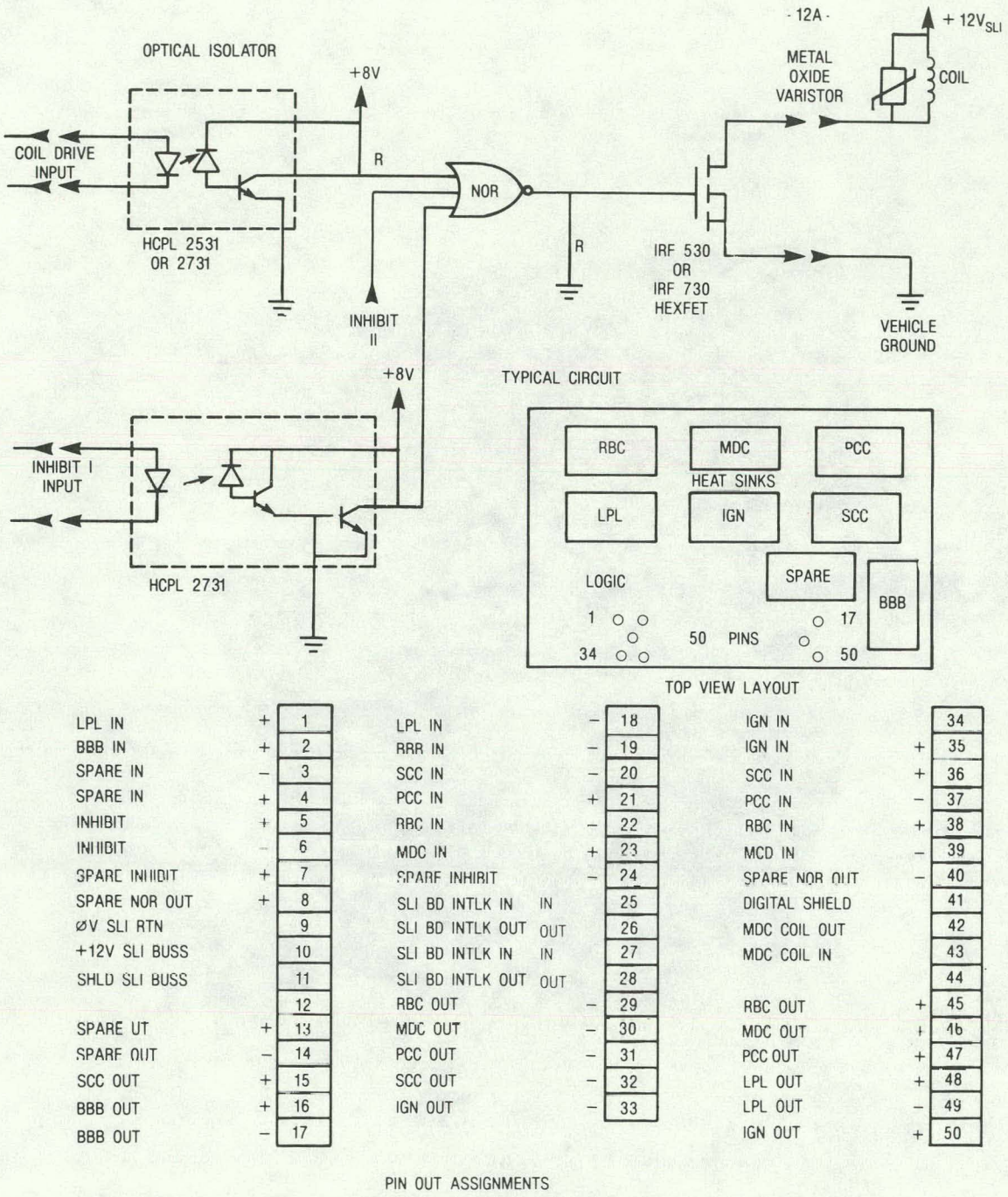

Figure 5.3-23. Block Diagram of Printed Circuit Coil Driver

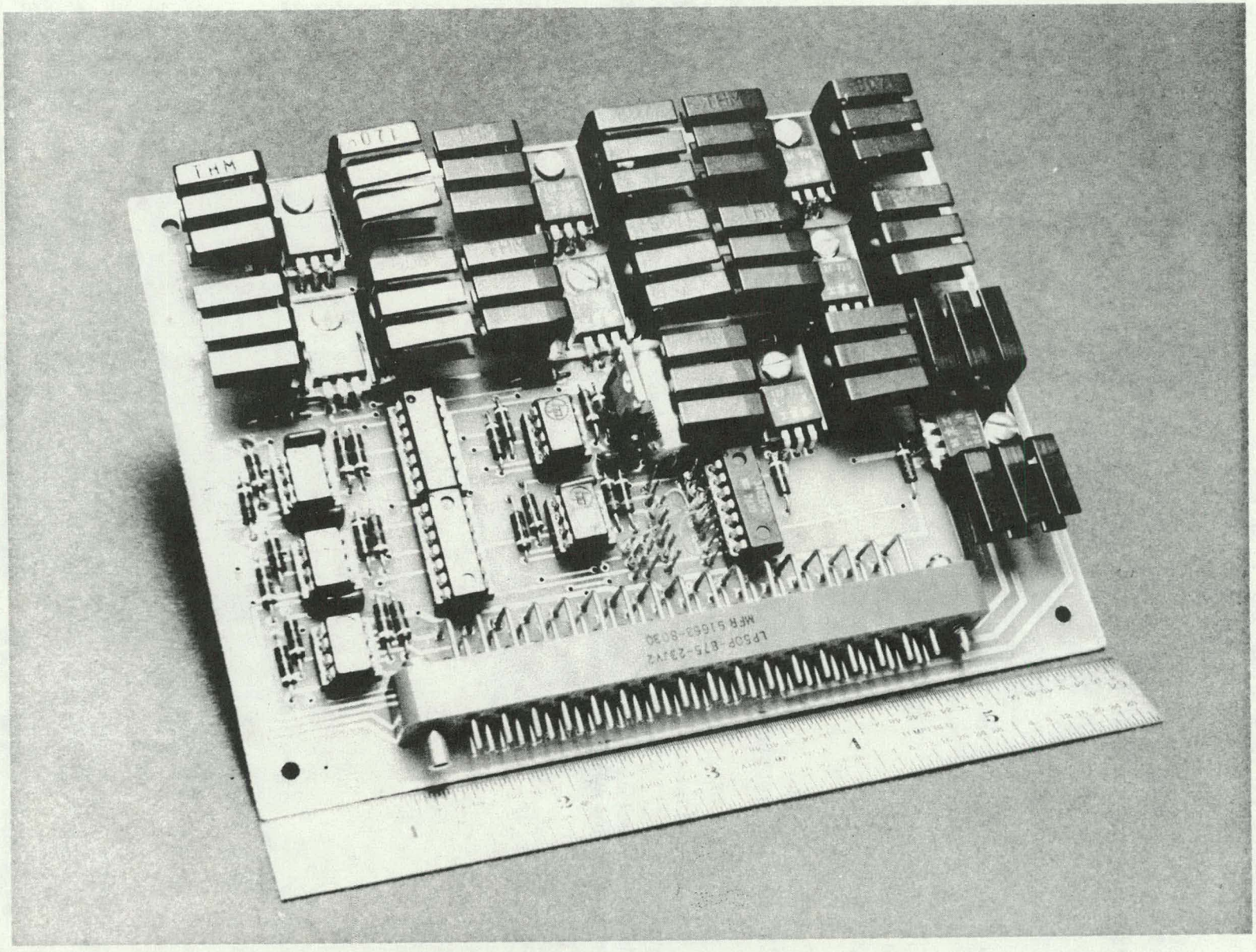

Figure 5.3-24. Coil Driver Printed Circuit

Identical battery switching and start resistor electrical hardware is used for the TBM, HPTM, and HTV vehicles. However, mechanical packaging of these components is different in the three vehicles. The dc power contactors and start resistors for the TBM and HPTM were packaged in a custom-built aluminum chassis. Motor and contactor interface circuits were also mounted in this same package. In the HTV, the dc contactors and start resistors are mounted inside the left front fender. Motor and contactor interface circuits, including three coil driver printed circuit cards plus one armature current/armature voltage card, are mounted in a custom interface box, located above the contactors under the hood. Figure 5.3-25 illustrates this interface box with the cover removed.

5.3.6 Controller

The propulsion system shown in Figure 5.3-26 is controlled by an Intel 8086-based microcomputer system. The microcomputer is responsible for propulsion unit feedback control, propulsion system sequencing, clutch and transmission control, battery charger control, power train status warning displays, and diagnostics.

The microcomputer regulates the shaft power of the heat engine and the electric motor with closed-loop control. Motoring power demand by the driver is received from the accelerator potentiometer and is then distributed to the engine, the motor, or both, depending on the magnitude of the demanded power. Regenerative braking from the electric motor is commanded by the brake potentiometer.

A simplified propulsion sequencing diagram is shown in Figure 5.3-27. The vehicle starts in motor mode with the two battery banks configured in parallel (60 V) and remains in this mode for idling, motoring, and regeneration in the low-speed range. The motor also acts as a starter for the engine, and, therefore, engine operation is transitioned through the 1/2 E_b mode for high-power, low-speed requirements. As the vehicle speed increases, battery switching to series configuration occurs (full battery voltage 120 V). At a high speed, depending on the battery state-of-charge, the engine takes over the vehicle propulsion. If the

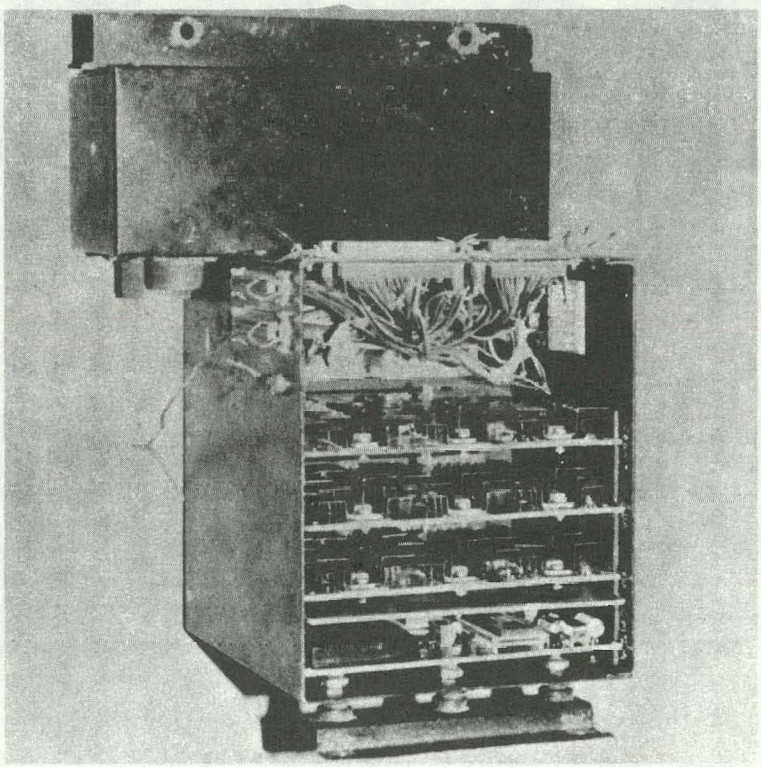

Figure 5.3-25. HTV Electrical Interface Box

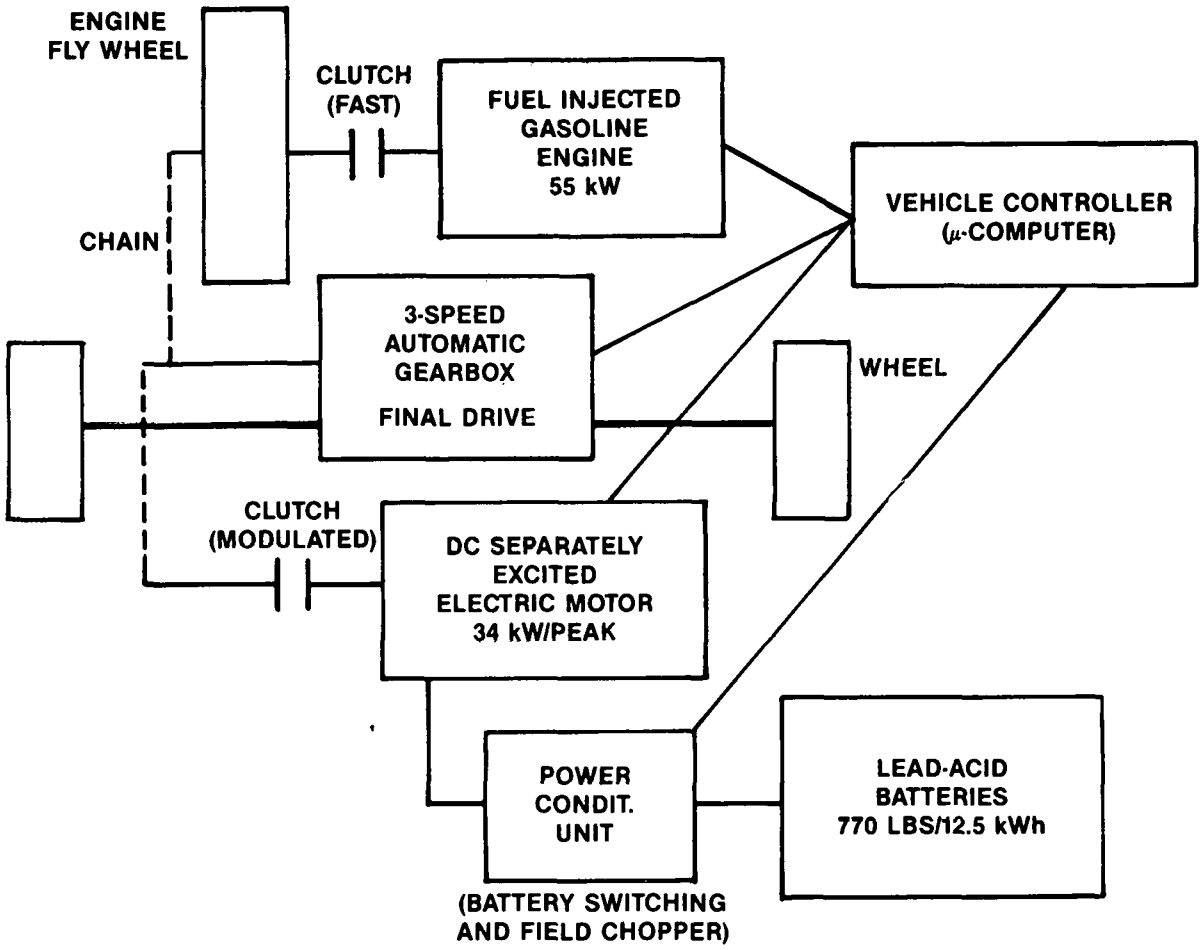

Figure 5.3-26. Schematic of the HTV Propulsion System

commanded power exceeds the capacity of either the engine or the motor, both propulsion units come into operation. If the battery state-of-charge falls below a specified value (20%), the engine charges the propulsion batteries with the electric motor acting as a generator.

The engine clutch is opened/closed fast for on-off engine operation, but the main drive clutch is modulated to permit smoothly starting the vehicle from rest. The microcomputer is responsible for shifting the three-speed automatic transmission. Transmission up and down shifting is controlled as a function of the shaft power demand and the engine/motor speed. Operation in reverse is limited to the 1/2 E_b (60 V) electric motor mode only. The transmission acknowledge signal is derived from a computation of the gear ratio from the measured vehicle speed and the shaft speed of the electric motor or the heat engine.

A block diagram of the motor feedback control system is shown in Figure 5.3-28. Shaft power is controlled in the outer loop and armature current in the inner loop. The feedback power is computed from the measured values of armature voltage and armature current. Command power is clamped to positive and negative maximum values. Maximum available power is a function of the battery state-of-charge and whether the batteries are connected in series or parallel. The maximum command current in the inner loop is limited to +480 A for motoring and −200 A for regenerative braking, irrespective of the battery configuration. The motor feedback control was modeled by transfer functions using the Bode diagram technique.

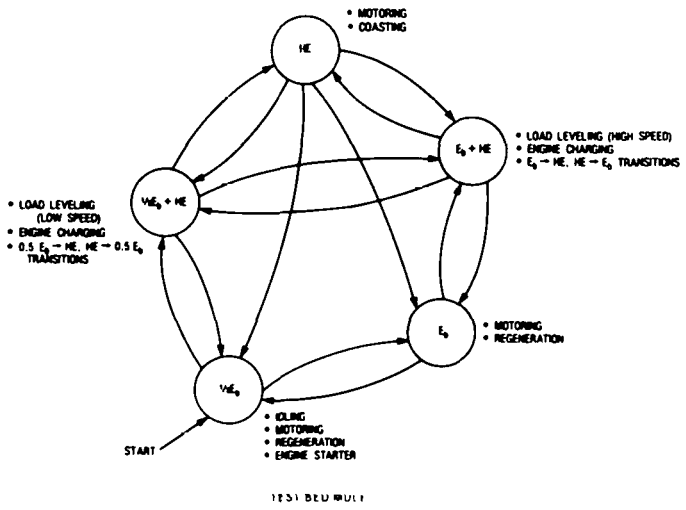

Figure 5.3-27. Simplified Propulsion Sequencing Diagram

Analysis and electric drive system tests were used to determine the gain and compensator parameters. Performance under static and dynamic conditions was investigated in detail.

A block diagram of the engine feedback control system is shown in Figure 5.3-29. The shaft power control loop establishes the command throttle angle θ^* (*indicates command signal). The throttle actuator, which utilizes a vacuum-controlled analog feedback loop, sets the throttle angle for control of the engine. Engine output power is computed from the engine speed and manifold pressure. A correction is made to the steady-state power calculated to obtain the power value which is used as the feedback signal. Power error is multiplied by a programmable gain (function of power fraction and speed) and a lag compensator to generate the throttle angle command. The feedback control system has been modeled by transfer functions. A Bode analysis was made to determine the control parameters. The system was simulated on a digital computer to study the static and dynamic performance. Figure 5.3-30 shows the simulated dynamic response of the heat engine with feedback control.

5.3.6.1 HTV Controller Hardware

HTV microcomputer controller hardware consists of three custom-designed wire-wrap boards contained in a sealed metal enclosure with connectors mounted on the enclosure exterior. Two of the boards are microcomputer-based and the third board provides signal conditioning between the microcomputer boards and the external systems. Each computer board consists of a commonly designed section consisting of a core computer system based upon the INTEL 8086 16 -bit CPU. The common hardware consists of up to 16K bytes of EPROM memory, 2K bytes of CMOS RAM memory, 24 bits of logic I/O, an interrupt controller, special diagnostic ports, a watchdog timer, and a 16 x 16 word FIFO data communication link for data communication between the two computers. Peripheral components were added to this core system in order to provide the desired I/O signals required for each board. The design includes diagnostic hardware and adequate decoupling and shielding to minimize EMI effects. Industrial or military grade components are used throughout.

A total of three HTV type microcomputer controllers were fabricated. The first controller was installed and tested in the HPTM vehicle. The second controller was installed in the

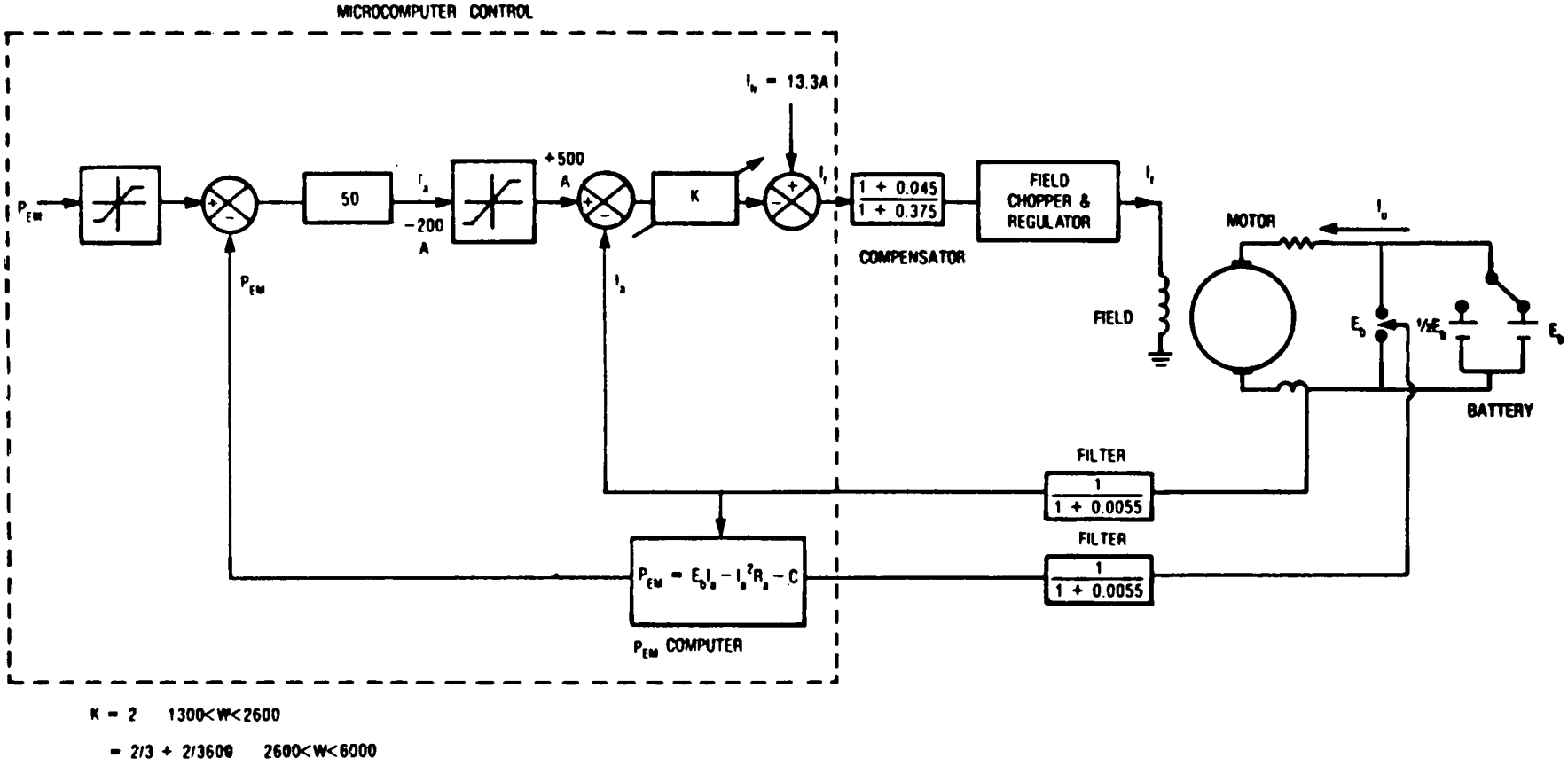

Figure 5.3-28. Block Diagram of Motor Feedback Control System

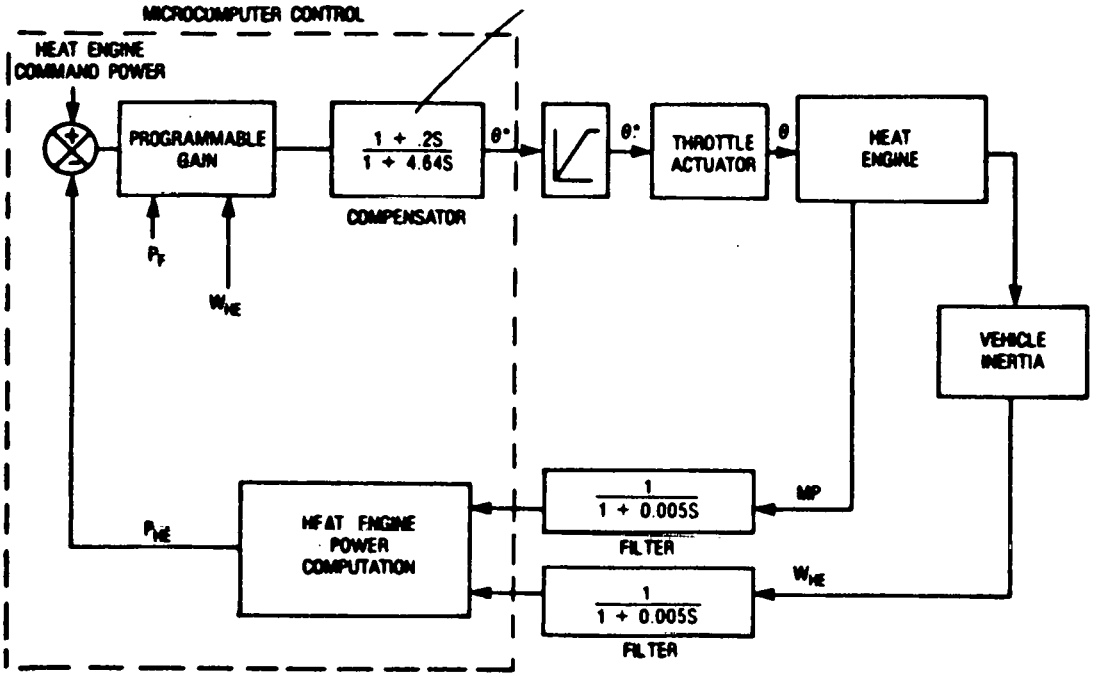

Figure 5.3-29. Block Diagram of Heat Engine Feedback Control System

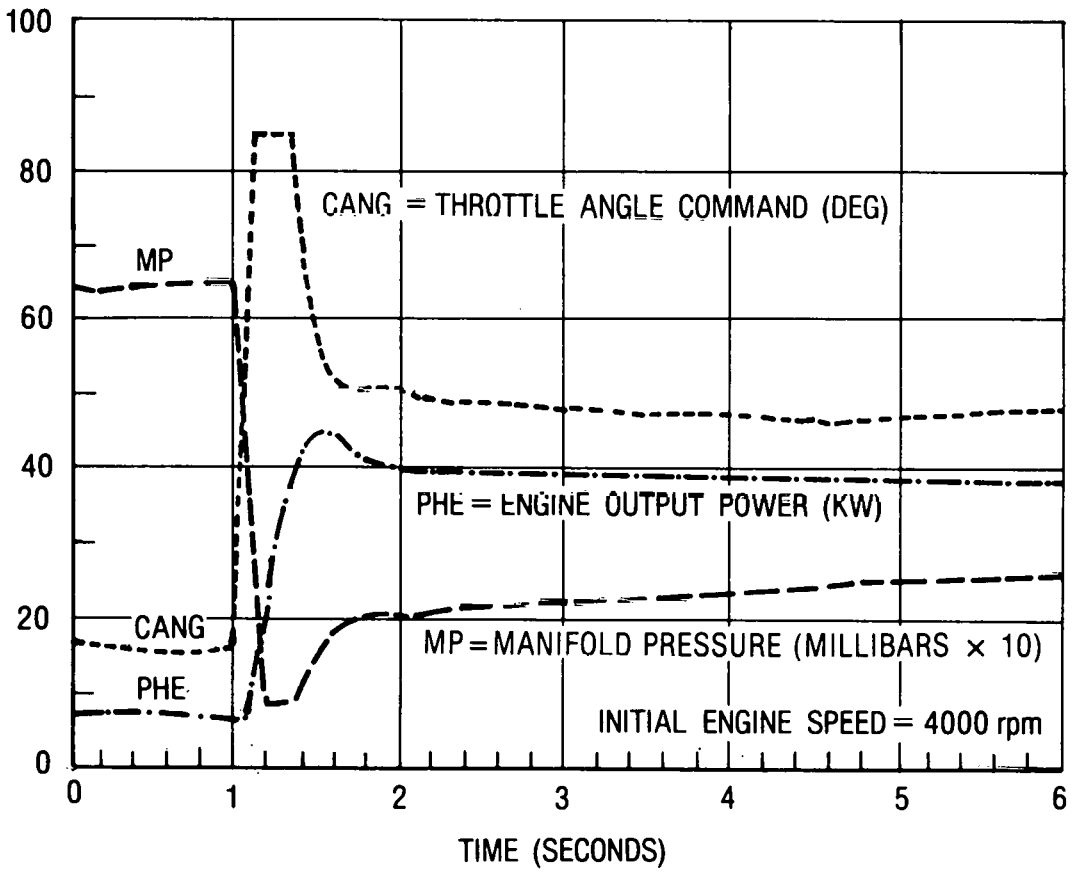

Figure 5.3-30. Simulated Dynamic Response of the Engine to a Step Change in Power Command

HTV, and the third controller is a spare. HPTM and HTV controller hardware is nearly identical; however, additional software was added for on-board battery charging in the HTV controller. Figure 5.3-31 is a photograph of the HTV microcomputer controller. Each of three boards is extended. The custom signal conditioning board is nearest the front of the controller.

5.3.6.2 Controller Software

As shown in the controller functional block diagram (Figure 5.3-32), the system is subdivided into nine major functions, each of which consists of one or more software modules. Not shown in the block diagram are the executive operating system, the diagnostic software function, or the real-time monitor. The software is implemented principally in PLM/86. Assembly language is used only where PLM/86 could not be used. The software is structured so that each function could be independently implemented and tested. The operator pedal, battery, and heat engine charging functions are unique to the HTV controller. The sequencing functions (Figure 5.3-33), which were first implemented in the TBM controller, were expanded in the HTV controller to include regenerative braking.

Expected CPU loading in the HTV necessitated the use of two 8086 computer systems with the software functions divided between the two. Both of the microcomputer systems utilize an identical real-time operating system which consists of a real-time scheduler, a FIFO data communication driver, and a data base manager. The real-time scheduler schedules each function according to its appropriate sampling interval. The FIFO data communication driver enables bi-directional communication of data between the two microcomputers. A data base manager enables the data base to be monitored and modified on-line by the real-time monitor

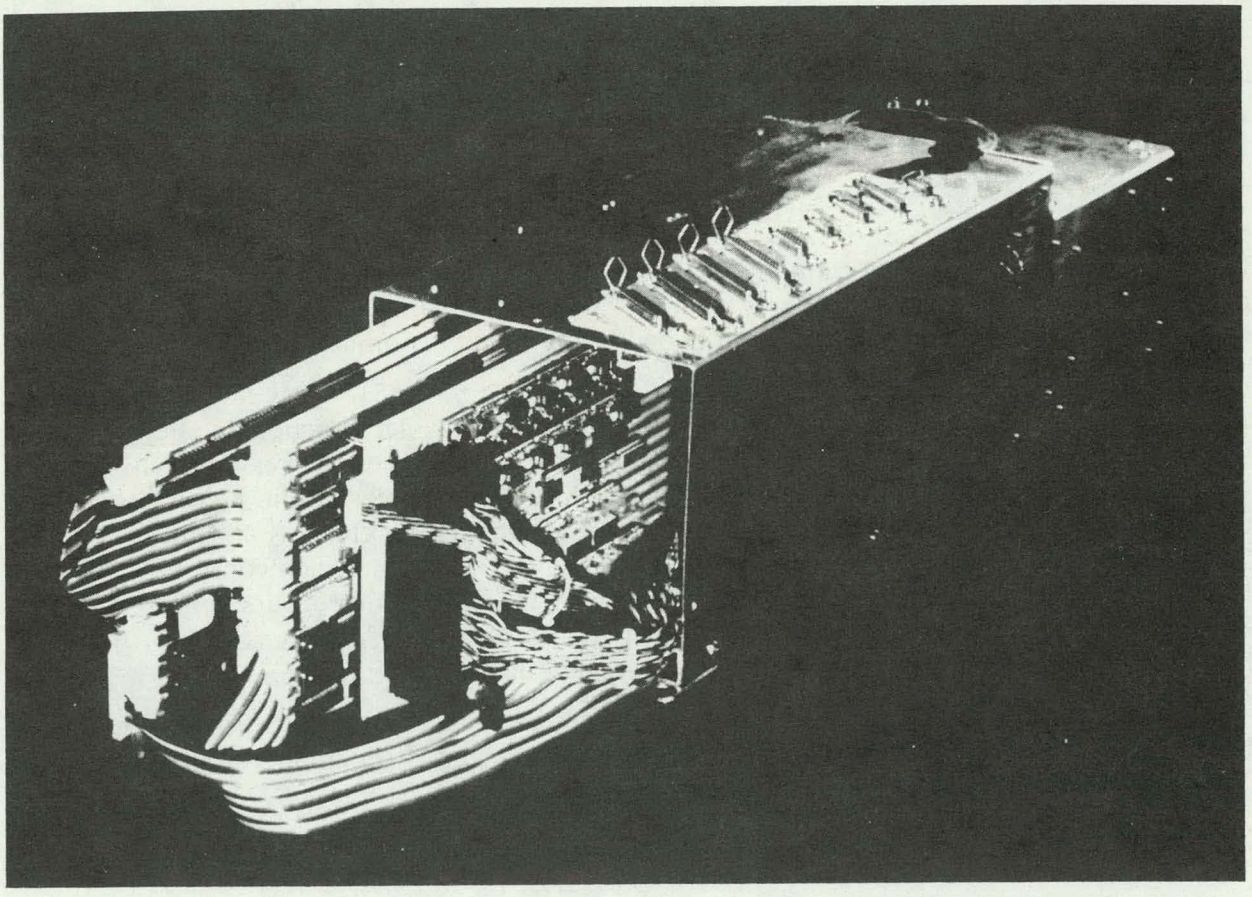

Figure 5.3-31. HTV Microcomputer Control

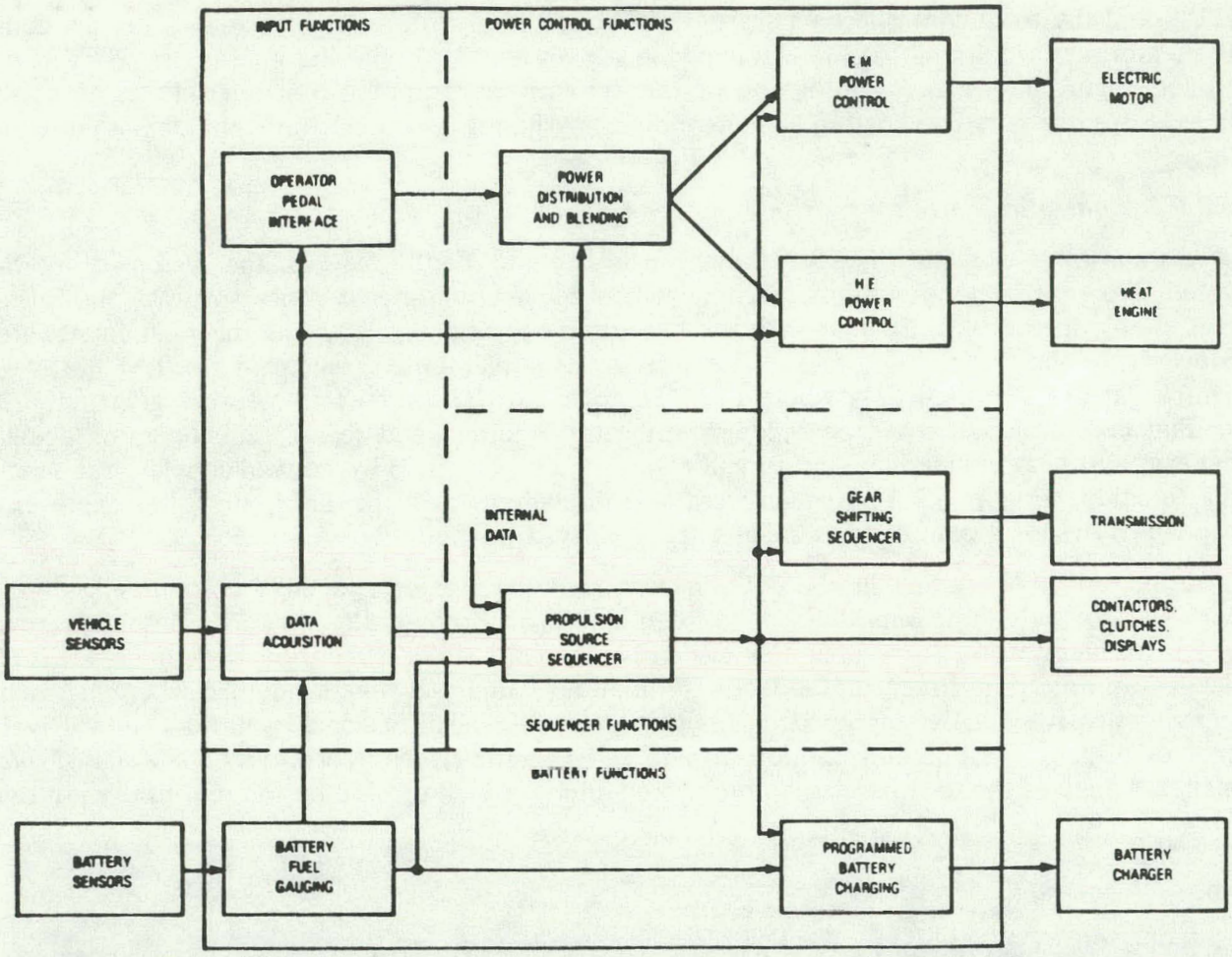

Figure 5.3-32. Block Diagram of HTV Controller Functions

diagnostic function. The I/O computer contains the input function, battery functions, and the real-time monitor diagnostic function, which communicates with the debug panel. Remaining control and sequencing functions are contained in the system computer.

The block diagram of the sequencing functions (Figure 5.3-33) shows that the propulsion source sequencer provides overall coordination of the controller functions. The propulsion source sequencer exerts control over the vehicle propulsion system either indirectly through lower level software functions, such as the gear shifting sequencer or the power distribution function, or by direct activation of external devices, such as the clutches and the contactors. Data variables identified on the diagram indicate the data paths by which control of the lower level functions is accomplished. A block diagram of the power control functions (Figure 5.3-34) shows the flow of data variables through the software modules making up the power feedback control loops. Major data variables are identified on the diagram.

Software modules were initially bench-tested using the controller exercises. Hardware/software integration and dynamic testing occurred throughout the program, using mule vehicles and the HTV on dynamometers, tracks, and roads.

5.3.7 HTV Sensors

This subsection describes the sensors used to control the power train, including the speed sensors and the current and voltage sensors.

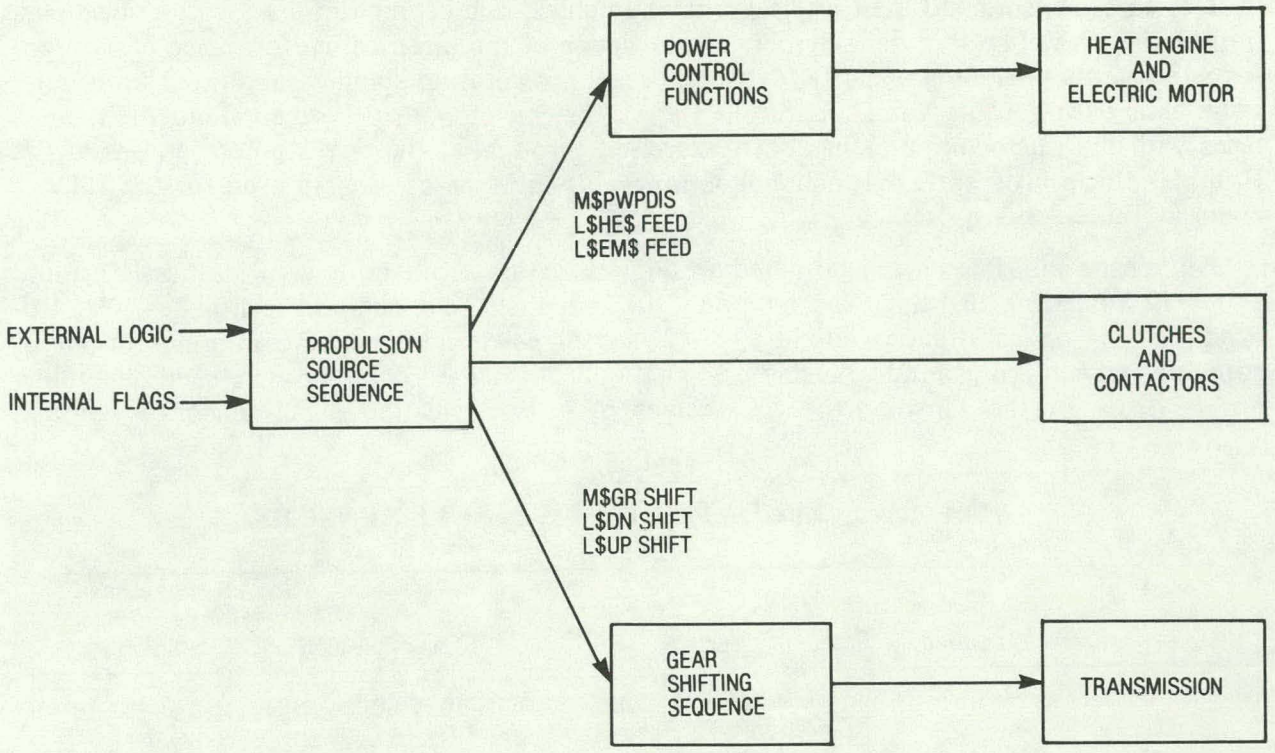

Figure 5.3-33. Block Diagram of Sequencing Functions

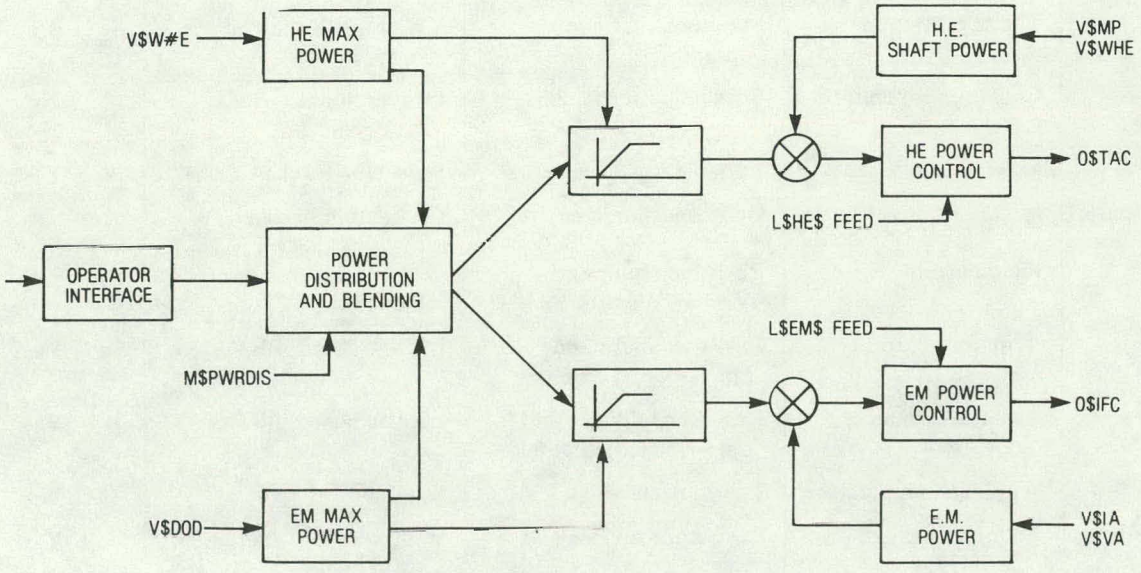

Figure 5.3-34. Power Control Functions

Design of sensors and their interfaces to the vehicle microcomputer are a very critical portion of the overall system development. Knowledge of the electrical performance of the sensor subsystems, including linearity, dynamic range, temperature stability, and noise immunity, is necessary for reliable vehicle control. Careful design of both the sensors and their interfaces with the microcomputer has been exercised throughout the development phases of the Hybrid Vehicle Program. A functional summary of the type of sensors used for the HTV is given in Table 5.3-6.

All sensor interfaces were designed to allow isolation from both vehicle chassis ground and +12 V starting, lighting, and ignition (SLI) circuits. Two isolation techniques were utilized, i.e., (1) optical isolation circuitry, or (2) sensor power and ground common with microcomputer power and ground. Analog or digital optical isolation circuitry were used depending on the form of the sensor signal. Examples of sensor isolation using sensor power and

Table 5.3-6

HYBRID INTEGRATED TEST VEHICLE SENSORS

System	Quantity to be Measured	Type	Sensor Selection	Microcomputer Controller Interface
Vehicle	Vehicle speed	Magnetic pickup with electronics	Western controls GE-01-12054	Yes
	Accelerator pedal position	Potentiometer and op-amp	10K W, BB3500	Yes
	Brake pedal position (regenerative)	Potentiometer and op-amp	10K W, BB3500	Yes
Engine	rpm	Solid state ignition pulse generator	VW ignition system	Yes
	Throttle position	Potentiometer and op-amp	VW throttle control	No
	Coolant temperature	Bi-metallic sensor	Conventional auto system	No
	Manifold pressure	Variable capacitance	Ford D9AE - 12A 680A	Yes
Electric Motor	rpm	Optical tachometer	GE custom design	Yes
	Field current	Resistive shunt and V → F converter	Within field chopper, RM4153	Yes
	Armature current	Resistive shunt and opto-isolated amplifier	IA/VA board, BB3650KG	Yes
	Armature voltage	Resistance divider and opto-isolated amplifier	IA/VA board, BB3650KG	Yes
	Windings temperature	Thermostats	Klixon	No
Battery	Terminal voltage	Resistance divider and V → F converter	Within battery charger, RM4153	Yes
	Charger current	Resistive shunt and V → F converter	Within battery charger, RM4153	Yes
	Temperature	Temperature to frequency converter	Analog devices, AD537	Yes
	State of charge	Amp-hour computer	Compucharge, BCC-200	Yes

ground common with microcomputer power and ground are the accelerator position potentiometer and brake pedal position potentiometer.

Three speed sensors are required for the hybrid vehicle i.e., (1) vehicle speed (axle rpm), (2) heat engine speed, and (3) electric motor speed. Heat engine and electric motor raw speed sensor interface format is a 1-bit digital pulse frequency modulated (PFM) waveform for which the sensor output is a digital pulse train whose frequency is proportional to the speed measured. Digital optoisolator circuits, located on the microcomputer signal conditioning board, provide the necessary isolation. Conversion of speed sensor PFM waveforms to 16-bit digital format for further processing within the microcomputer is accomplished via multipurpose 16-bit counter chips (AMD 9513). A single 40-pin counter chip is capable of converting five channels of PFM waveform to digital format. Within the microcomputer, speed (in a digital format) is obtained by using a technique that measures the time interval between adjacent pulses out of the sensor.

A GE custom-designed optical tachometer is used to measure electric motor speed. A wheel with 24 slots is mounted on the armature shaft and produces 24 pulses per motor revolution. The heat engine speed signal is obtained from the engine ignition system. Two pulses per revolution are obtained for the four-cylinder, four-cycle engine.

The vehicle speed sensor is a precision permanent magnet analog tachometer, driven by a parallel speedometer cable. After analog signal conditioning, this signal is converted to digital format by a multiplexed A/D converter. Calculations of rpm assume that the speedometer cable produces 1000 revolutions per mile and that the Goodyear tires rotate 769 revolutions per mile.

Engine manifold pressure is measured using a capacitive-type pressure sensor developed by Kavlico Corporation, Chatsworth, California, for the Ford Motor Company. The unit used in the TBM, HPTM, and HTV is a standard automotive component used by Ford since 1978 as part of the EEC-3 system on cars with three-way catalysts marketed in California. The manifold pressure unit senses the atmospheric and manifold pressures separately and yields voltage signals proportional to each pressure. The two signals are processed by the vehicle controller to determine the manifold vacuum used in the engine power calculation. Laboratory calibrations of the pressure sensor unit have shown excellent linearity, and tests of the unit in the hybrid vehicles have indicated good time response and tolerance to engine-generated electrical noise.

Engine throttle position is sensed using a gear driven precision potentiometer on the throttle. Throttle angle position is used as a feedback signal to the closed-loop, vacuum-powered throttle actuator system developed by VW. This throttle actuator is modified from a production cruise control unit. The HTV controller sends an optically isolated throttle command signal to the throttle actuator. The throttle actuator was designed to fail safe if either the supply of vacuum or 12 V power is lost.

Engine coolant temperature is sensed using the conventional automotive engine thermostat and indicator lamp. Electric motor winding temperature is sensed by thermocouples. Engine temperature and motor winding temperature are used only as driver warning and do not interface with the microcomputer controller.

The HTV contains an IA-VA (armature current-armature voltage) circuit card, which senses the electric motor armature voltage and current, correctly scales the values, and outputs the analog voltages to the system controller for further processing. Figure 5.3-35 is a functional block diagram of the IA-VA board. The voltage across the motor armature is in the range of 0 to 200 V_{DC}. A resistive divider is used to reduce this by 20:1, which scales the

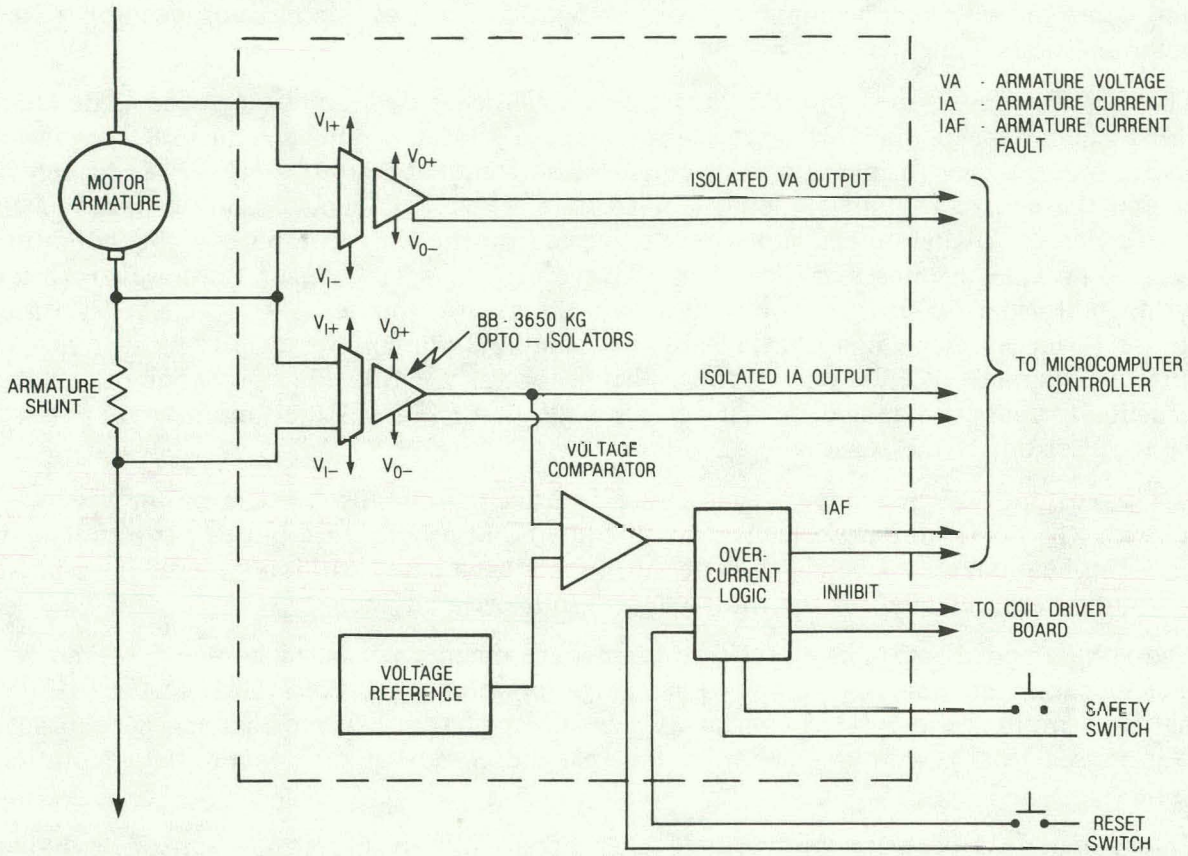

Figure 5.3-35. Functional Block Diagram of Armature Current/Armature Voltage Board

input to the IA-VA card to the range of 0 to 10 V_{DC}. The IA-VA card performs optically isolated signal conditioning of this armature voltage signal, which is then applied to the input of the system controller for analog-to-digital conversion.

Armature current is sensed by a current shunt in series with the motor armature. The resistance of the shunt is such that each ampere of armature current causes a 167 μV potential to be developed. This signal is in the range of +100 mV to -100 mV. The IA-VA card also performs optically isolated signal conditioning of this armature current signal, and provides it to the system controller for analog-to-digital conversion. Figure 5.3-36 is a photograph of the IA-VA circuit card.

Field current is sensed via a resistive shunt within the field chopper module. Shunt voltage is amplified and used as a feedback value in the field chopper PWM circuitry. The field current signal is converted to a pulse frequency signal in a voltage-to-frequency converter and transmitted to the HTV controller. A digital opto-isolator chip in the controller provides necessary isolation. An AMD 9513 counter chip, within the controller, is used to perform the frequency-to-digital conversion.

Battery sensors (one for each battery bank), including terminal voltage and charge current, are located within the HTV on-board battery charger. Resistor dividers and amplifiers are used to sense battery bank voltages. Resistive shunts with amplifiers sense the battery charger currents. Analog values of these sensed currents are used in the charger control system. Sensed battery bank voltages and charger currents are voltage-to-frequency converted

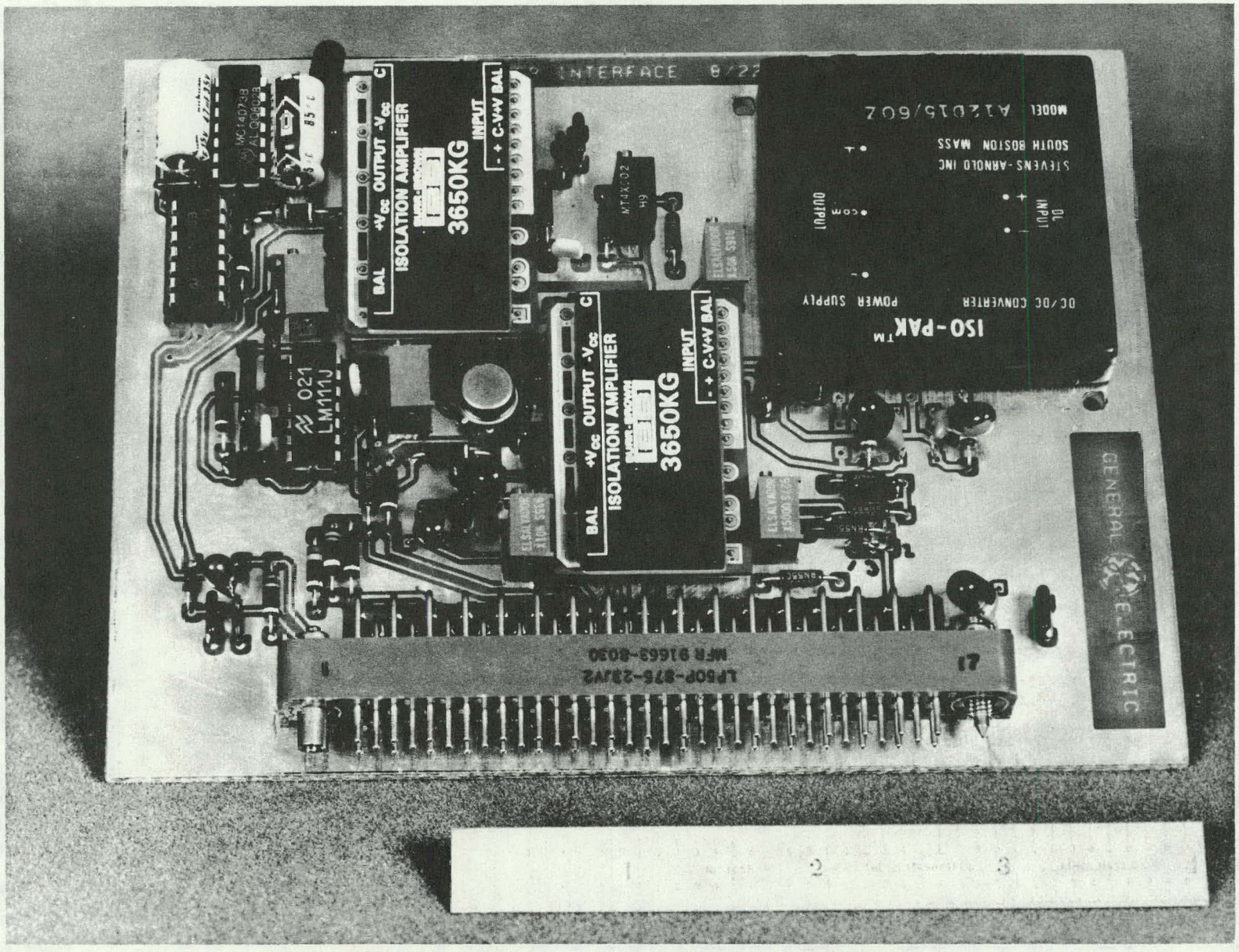

Figure 5.3-36. IA-VA (Armature Current/Armature Voltage) Circuit Board

and time multiplexed into a single channel that is transmitted to the HTV controller. Digital opto-isolators provide necessary isolation.

Battery bank electrolyte temperatures are sensed using a National Semiconductor precision temperature sensor, LM 135. This electronic temperature sensor is mounted in a custom polypropylene probe that is threaded into the top of the battery case, extending below the level of the electrolyte. Although each battery is capable of accepting the temperature probe, only a single temperature probe is installed in each of the two battery banks. Isolation is provided by the polypropylene. Sensor power is obtained by a precision 10 V regulator within the microcomputer controller. Analog signals, corresponding to electrolyte temperatures are filtered and analog-to-digital converted in the controller.

5.3.8 Safety, Reliability, and Maintainability

The hybrid test vehicle (HTV) was designed and developed with full cognizance of the importance of high levels of safety, reliability, and maintainability. The Hybrid Vehicle Program was a development project in which only one vehicle was delivered. This vehicle has many novel features incorporated in the subsystems and in their integration, sensing, and control. No formal, targeted values for safety, reliability, and maintainability were established. The vehicle as delivered however, is in compliance with contractual intent and designed for safety, reliability, and maintainability (such as compliance with all applicable FMVSS standards).

Safety, reliability, and maintainability reviews occurred throughout the contract life. Findings, analyses, and conclusions pertinent to these areas were reported in the monthly Contract Status Reports, at the various Design Reviews, and in specifically required documents (such as the Safety Report 25 September 1982).

The elements of safety, reliability, and maintainability are separately discussed in subsequent subsections.

5.3.8.1 Safety

The hybrid vehicle was designed to be a safe vehicle in a variety of ways:

- As previously indicated, the hybrid vehicle is in full compliance with all pertinent FMVSS standards for protection of occupants during and after a crash. Proof of compliance was afforded by reference to similarity with conventional current ICE practices, through engineering analyses, through testing, and by combinations of these.
- The vehicle was designed to be in compliance with all NHTSA recommended safety standards for electric and hybrid vehicles, including those for on-board batteries, charging circuitry, and electrical chassis isolation.
- Conventional, acceptable safety practices were followed wherever possible. Major items of structure, vehicle steering, and (totally sufficient) hydraulic braking may be cited.
- In overall propulsion and control, the vehicle has been designed to protect occupants and those outside the vehicle from "lurch"* modes brought about by equipment failure.
- The vehicle was also designed so that "loss-of-power" modes brought about by equipment failure were minimized. Analysis of the initial control strategy indicated that, in many instances, failure or malfunction of a sensor would have resulted in commanded system shutdown. Since sudden power loss has implications for safety, this strategy was amended

* A "lurch" mode is any sudden, unexpected, forward or reverse motion of the vehicle which cannot be controlled by the driver.

to minimize such computer-commanded shutdowns, depending instead on local protection of subsystems and equipment.

The program response to safety was documented in a safety report delivered to the Jet Propulsion Laboratory, September 15, 1982. In this report General Electric states that vehicles delivered under this program, given their limited development and the fact that they are one-of-a-kind research test vehicles, are safe when operated by knowledgeable test personnel or by others instructed by and under close supervision of knowledgeable test personnel. The conclusions reached in the Safety Report apply fully to the hybrid test vehicle (HTV), to a lesser degree to the hybrid power train mule (HPTM), and to an even lesser degree to the test bed mule (TBM). The mules are considered safe in the hands of knowledgeable personnel and when employed for their intended purposes; they had less development time than the HTV and some control functions, which are automatic (controlled by the microcomputer) in the HTV, are manual in the mules. This last statement is especially true of the TBM.

5.3.8.2 Reliability

In keeping with the developmental nature of the hybrid test vehicle, no formal numerical reliability goals or requirements were established. Many novel components, such as the modified heat engine, the externally actuated transmission, and the uniquely designed clutches, accrued operating experience in order to ensure reasonable validation of their operational characteristics. There are potential "single point" failure modes which can cause loss or significant deterioration of the vehicle's operational capability. However, enough redundancy is built into the system to allow for safe handling of such a situation (see Safety Report). A Failure Mode and Effects report was prepared (December 18, 1980), setting in greater detail the impact of equipment failures upon vehicle performance. An assessment of reliability based on operational testing of the various subsystems, the mule vehicles, and the final HTV, indicated that operational reliability is acceptable.

It is to be anticipated that any production or pre-production of hybrid vehicles will make use of a system design simpler in concept and in execution of total function, while at the same time employing additional redundancies in hardware and control logic. In contrast, this developmental contract required a more complex system coupled with a nonredundant sensing and control subsystem. Due to constraints based on developmental time and dollars, selected components and subsystems were examined for reliability during integration and signature testing.

5.3.8.3 Maintainability

Throughout the design process, it was recognized that the complexity of the total design, coupled with the limited availability of physical space in which to place all of the necessary system hardware, would require maximal attention to the questions of maintainability and easy access within the total context of the requirements for appropriate system function. This was a guiding principle throughout the system design and fabrication.

Strong diagnostic capabilities were built into the microprocessor sensing and control function. Warning labels were placed upon the equipment as required, and necessary safety interlocks on the equipment were provided. Again, interactions with safety and reliability are clear. Maintenance must be performed safely, and, to this end, appropriate procedures incorporating necessary precautions were developed. Maintenance procedures will be discussed separately in an Operations and Maintenance Manual to be delivered to JPL in November 1983.

5.4 BATTERY SUBSYSTEM

5.4.1 Battery (EV-1300)

5.4.1.1 Design and Specifications

During Phase I in the summer of 1979, three battery design options were considered. Vehicle design considerations set the energy storage (kWh) requirement and constraints on battery weight and volume. The volume (size) constraint was the most critical because the batteries were placed under the hood in the HTV. Option No. 1 utilized an existing battery container, but would only have had about 90% of the energy storage capacity desired. Option No. 2, which was selected, met the energy storage and volume requirements at some sacrifice in energy density due to the small cell size. Table 5.4-1, which is based on Option No. 2,

Table 5.4-1

HYBRID VEHICLE BATTERY MODULE SPECIFICATIONS AND CHARACTERISTICS

	Statement of Work Specifications			Characteristics of the HTV Modules*
	Minimum	Target	Maximum	
Module Voltage, V		12		12
Weight of Module, kg (lb)		34.0 (75.0)	36.5 (80.0)	33.6 (74.2)
Weight of Accessory Systems for Battery Pack, kg (lb)	4.5 (10.0)	5.5 (12.0)	6.7 (14.9)	
Module Dimensions				
Length, cm (in.)			32.38 (12.75)	32.3 (12.7)
Width, cm (in.)			18.9 (7.45)	18.8 (7.4)
Height, cm (in.)			27.43 (10.80)	26.9 (10.6)
Performance 3 h rate, to 10.5 V				
Capacity Ah	105	110		106
Energy storage, Wh	1250			1250
Energy density, Wh,kg (Wh,lb)	36.1 (16.4)			36.4 (16.5)
Power Characteristics, 15 voltage (V), 50% state of charge				
200 A pulse	10.5	10.8		10.8
300 A pulse	9.8	10.2		10.0
400 A pulse	9.0	9.5		9.6
Cycle Life at 80% DOD, 3 h Rate (cycles)		800		800

*Based on tests of final 12 V modules

shows the battery module specifications from Globe's statement of work. Of the three options, Option No. 3 was designed with the most emphasis on battery optimization. Although Option No. 3 would have resulted in the highest energy density, the nominal battery pack voltage of 96 V, which was consistent with the volume requirement, was below the desired pack voltage of 120 V.

The external dimensions of the battery were fixed on February 19, 1980, and detailed design work was initiated. The design approach for the EV-1300 battery involved the utilization of all of the Globe electric vehicle battery developments existing at the time. These included most of those in use in the Globe Improved State-of-the-Art (ISOA) battery which was developed with the assistance of DOE funding under Contract No. 31-109-38-4205 with Argonne National Laboratory.

The use of these previous developments was somewhat limited by the design constraints. The relatively low energy storage specification for the HTV pack (12.5 kWh as compared to about 20 kWh for EV passenger cars), in combination with the battery pack voltage requirement of 120 V, dictated a small cell size (106 Ah as compared to 240 Ah for the Globe ISOA design). The major impact of the small cell size was a reduction in energy density (37 Wh/kg as compared to a demonstrated 41 Wh/kg for the Globe ISOA battery). One of the main reasons that such a small cell results in a lower energy density is that the size of the electrodes must be considerably smaller than what has been determined by Globe to be ideal for EV battery electrodes. The electrodes in the Globe ISOA design are close to the ideal size. In contrast, each 15 cm x 17 cm electrode of the EV-1300 battery has only about 40% of the geometric area of an ISOA electrode. Furthermore, the height-to-width ratio of the EV-1300 electrodes is far from ideal in contrast to the ISOA design, where the ratio falls within the optimum range.

Except for the electrode differences discussed above, essentially all of the features of the Globe ISOA design have been incorporated in the EV-1300 battery. Figure 5.4-1 illustrates the battery construction and Figure 5.4-2 is a photograph of an EV-1300 battery. The thin-walled, lightweight polypropylene container and cover maximize the internal space available for active materials. The two pieces are thermally welded for a leak-free assembly. Low-resistance intercell welds, using a proprietary patented process, are made through orifices in the container cell partitions.

Globe's computer-assisted grid design program was used to design grids with minimum weight and resistance that provide for uniform current collection. Grid corrosion is reduced and active material efficiencies improved because the lead is distributed on a need basis. Three grids were designed: positive, inside negative, and a lighter weight outside negative. All three grids feature near-center lugs and radial wires. Positive grids were cast with an antimony-lead alloy and negative grids with a strontium-lead alloy.

Cell design was further improved through the selection of optimized positive-to-negative active material and electrolyte-to-active material ratios for operation at the discharge rates required. Glass mats against the positive electrodes minimize shedding of the active material. Envelope-type separators of microporous polyethylene minimize the possibility of internal shorting. The possibility of internal shorting is also reduced by an insulating coating on the electrode connecting straps. Strap lead weight is reduced by the use of straight-up (i.e., no offset) straps at the two terminal locations. Each cell element has six positive and seven negative electrodes. The sulfuric acid electrolyte has a nominal specific gravity of 1.300.

In order to achieve the cycle life goal shown in Table 5.4-1, it was decided that the battery pack would utilize an electrolyte circulation system similar to the one being used for Globe's

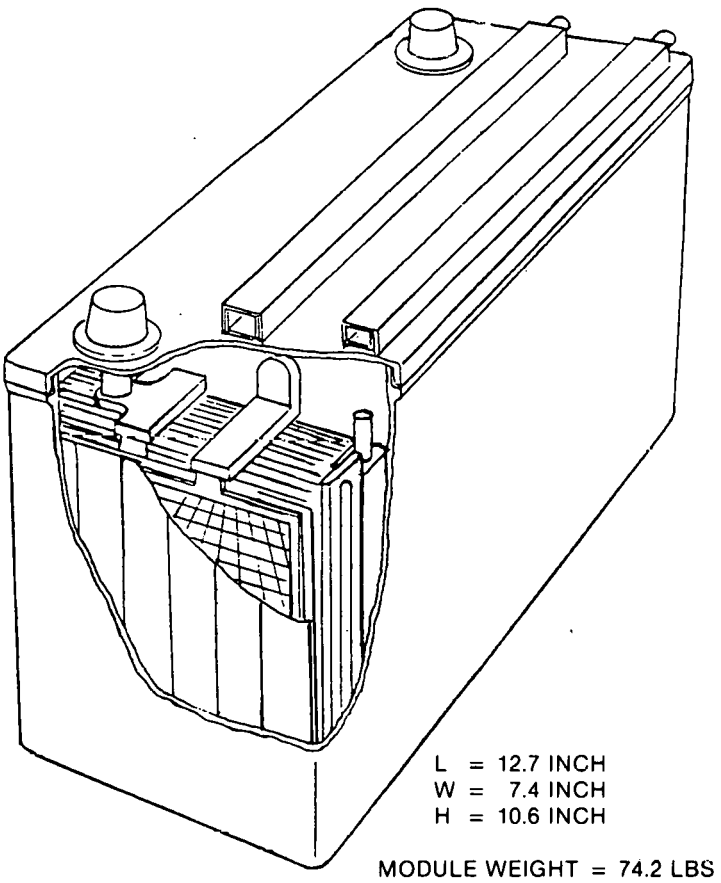

Figure 5.4-1. Cutaway View of the Hybrid Vehicle Battery Configuration

ISOA battery (U.S. Patent No. 4,221,847). Upon recharge of a deeply discharged lead-acid battery, large quantities of dense, concentrated sulfuric acid form on the surfaces of the electrodes and flow downward to collect at the bottom of the container. This causes a condition known as electrolyte stratification. Such stratification is highly detrimental to the life and electrical performance of the battery. Electrolyte stratification may be eliminated by heavy overcharge of the battery. This overcharge generates hydrogen and oxygen bubbles which agitate the electrolyte. Unfortunately, this overcharge is detrimental to cycle life since it accelerates positive grid corrosion and erosion of the active material. Reducing the overcharge factor required also increased the battery charging efficiency and thus the electrical energy costs of operating the vehicles.

The electrolyte circulation system, whose operation is illustrated in Figure 5.4-3, was developed by Globe. It is simple and efficient and works as follows. A small polypropylene insert pump, which has no moving parts, is located within each cell of the battery. These insert pumps, which are filled with electrolyte, are intermittently pressurized with a pulse of low-pressure air. This causes a flow of electrolyte from the insert pump to the upper region of less dense electrolyte in the cell. Upon termination of the pressure pulse, more dense electrolyte is forced into the insert pump from the lower region of the cell by the differential pressure head between the cell and insert pump electrolyte levels. The compressed air pulse is controlled to prevent the entry of air from the insert pump into the cell. No electrolyte is exchanged between cells. The compressed air for the entire battery pack is supplied by a small air pump using a dc motor and an air reservoir. A simple electronic circuit and two

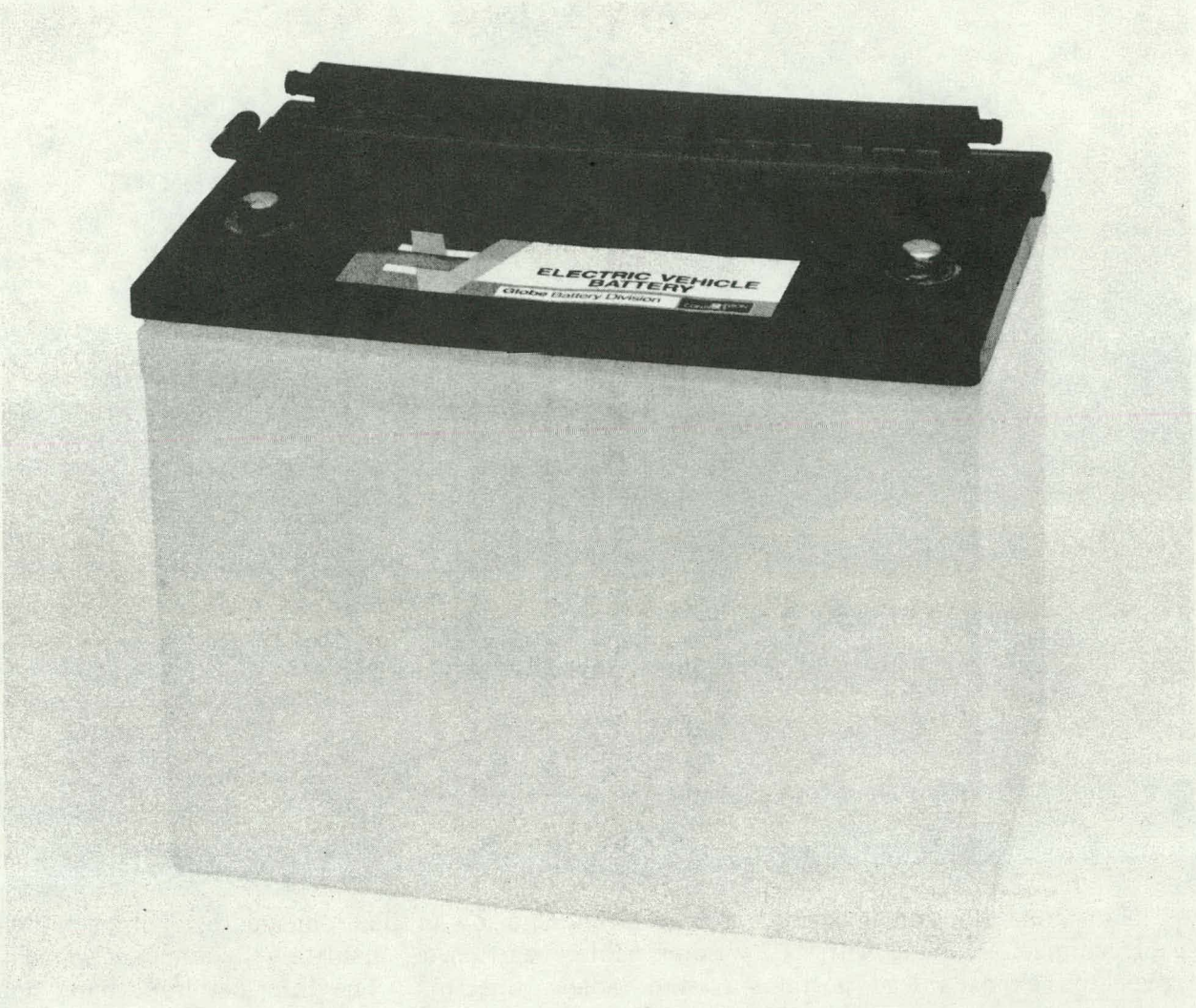

Figure 5.4-2. EV-1300 Battery

valves control the air pulses. The total weight of the electrolyte circulation system for an entire battery pack is only 3.8 kg. The system is active both during charge and discharge. During discharge, it is powered by the battery pack, but the average power drain for the 12.5 kWh pack is only 11.5 W. This parasitic drain and the extra weight are more than offset by improved capacity.

The advantages of the electrolyte circulation system are

1. Increased cycle life
2. Improved charging efficiency resulting in increased round-trip energy efficiency and decreased water loss and hydrogen generation
3. Improved power density at low states of charge
4. Improved energy density
5. Improved thermal management

The EV-1300 battery also features a single-point watering system which significantly reduces maintenance time. This system also provides for venting of the hydrogen and oxygen gases through a pair of flame arrestors located on the hood of the HTV.

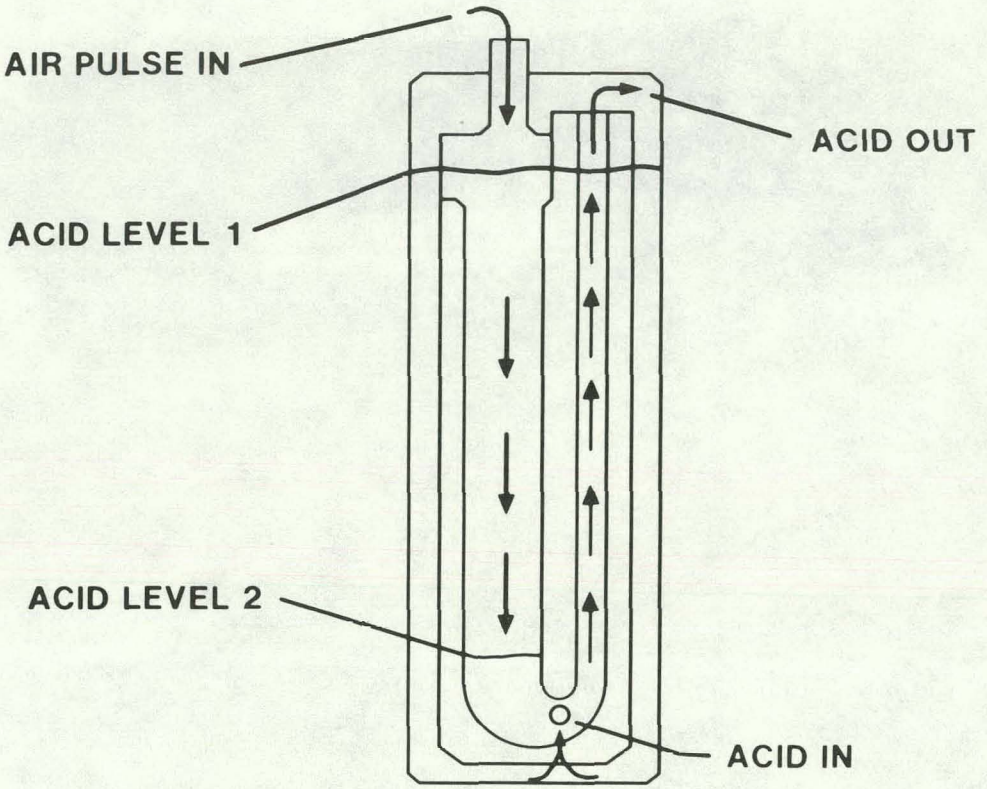

Figure 5.4-3. Acid Pump Schematic

Nonstandard terminal posts, which accommodate low-profile, "burned-on," inter-battery cable connectors made with 1/0 welding cable, were used. Insulating "connector shields" cover the exposed lead portions of the cable connectors. The inter-battery cabling and plumbing (for watering/venting and electrolyte circulation) were designed to avoid routing any cables or tubing over the top of the batteries to keep the vehicle hood profile as low as possible.

The battery pack consists of ten modules as shown in Figure 5.4-4. The pack has two strings, each of which has five modules wired in series. The two strings can be connected in series or in parallel. This is controlled by the vehicle microprocessor. Two of the ten modules in the pack (one in each bank) have temperature probes which provide measurements of electrolyte temperature. In addition, each battery bank contains thermostats that control operation of the battery pack cooling fan.

5.4.1.2 Fabrication

The EV-1300 battery was designed to be compatible with proven Globe mass production techniques. However, due to the small number of batteries needed for this project, "pilot shop" equipment was used. Injection molds were purchased for the container, cover, water/vent manifold, and air manifold. Molds were also procurred for the insert pump, three grid types, connector, and connector shield. Other tooling, such as that required for grid trimming, pasting, cast-on-strap, heat sealing, and pressure testing, was manufactured or purchased.

Test Cells. Fabrication of the first three test cells was completed November 25, 1980. Fabrication of an additional six test cells was completed December 22, 1980. The full-size test cell

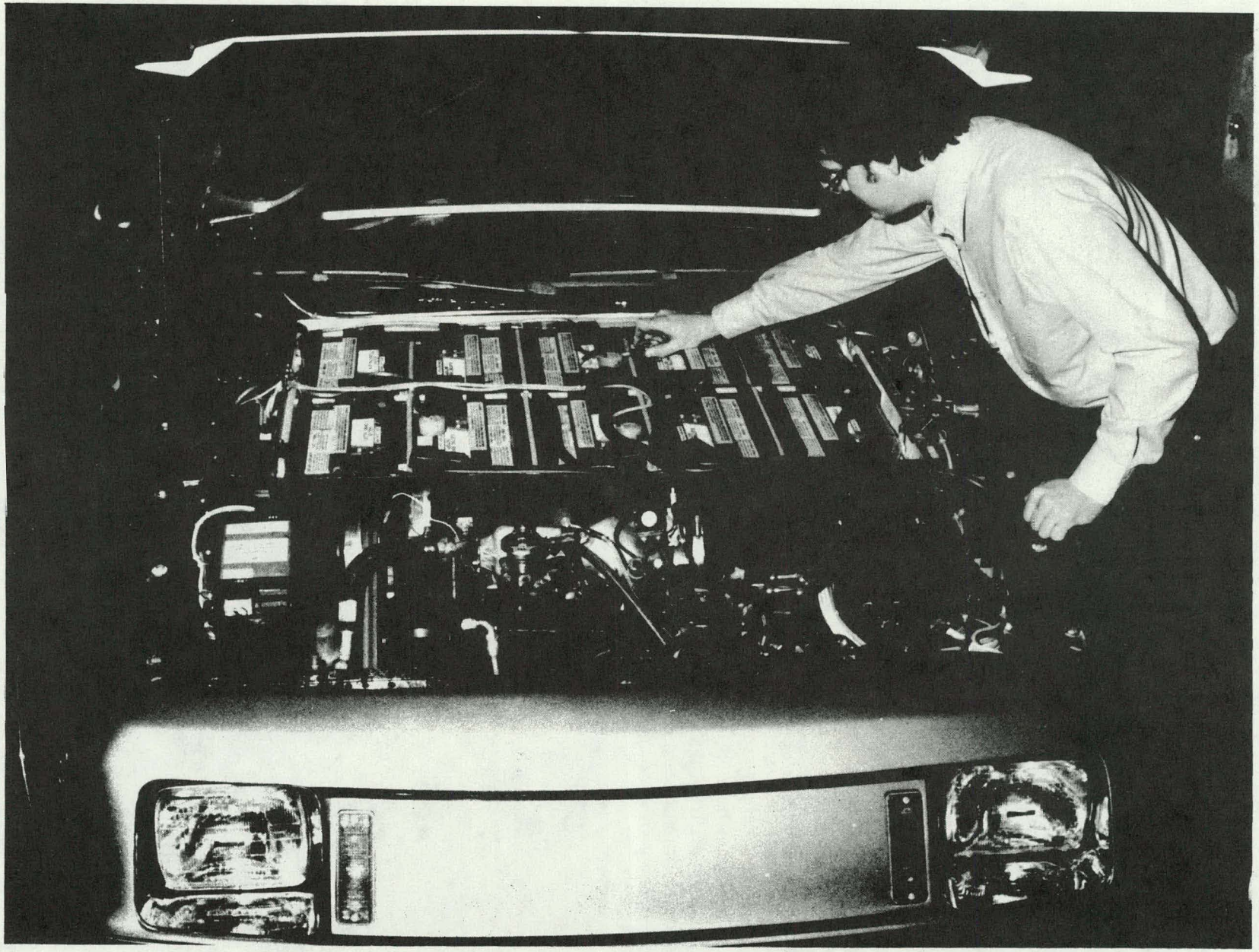

Figure 5.4-4. Battery Pack Mounted in HTV

elements, which were assembled in polycarbonate containers, were made with the same materials and processes to be used for the final batteries. Three breadboard electrolyte circulation systems were assembled to allow the testing of three groups of cells.

Battery Packs. Fabrication and testing of the first batch of 24 12 V modules were completed by early November 1981. The batteries met or exceeded all the minimum performance specifications given in Table 5.4-1. A complete battery pack (10 12 V modules in a fiberglass box with the electrolyte recirculation and watering systems installed and connected) was received by General Electric in November 1981 for use in the dynamometer testing of the hybrid power train mule (HPTM).

The fabrication and testing of a second batch of 28 12 V modules was completed by early February 1982. Two additional battery packs were assembled and plumbed and shipped to General Electric for use in testing the HPTM and the HTV. The second batch of batteries also met or exceeded all the minimum performance specifications given in Table 5.4-1.

In summary, a total of 60 12 V modules were fabricated under this contract. Three complete battery packs (10 12 V modules) were assembled for use in testing the HTV and the various hybrid mule vehicles. A photograph of a complete battery pack is shown in Figure 5.4-5.

5.4.1.3 Battery Testing

Prototype cells were tested at Globe prior to the fabrication of the 12 V modules. The 12 V modules have been tested by Globe, General Electric, and the National Battery Test Laboratory at Argonne. The complete battery pack has been tested by General Electric during dynamometer tests of the HPTM and HTV. The various test results will be discussed in the following subsections.

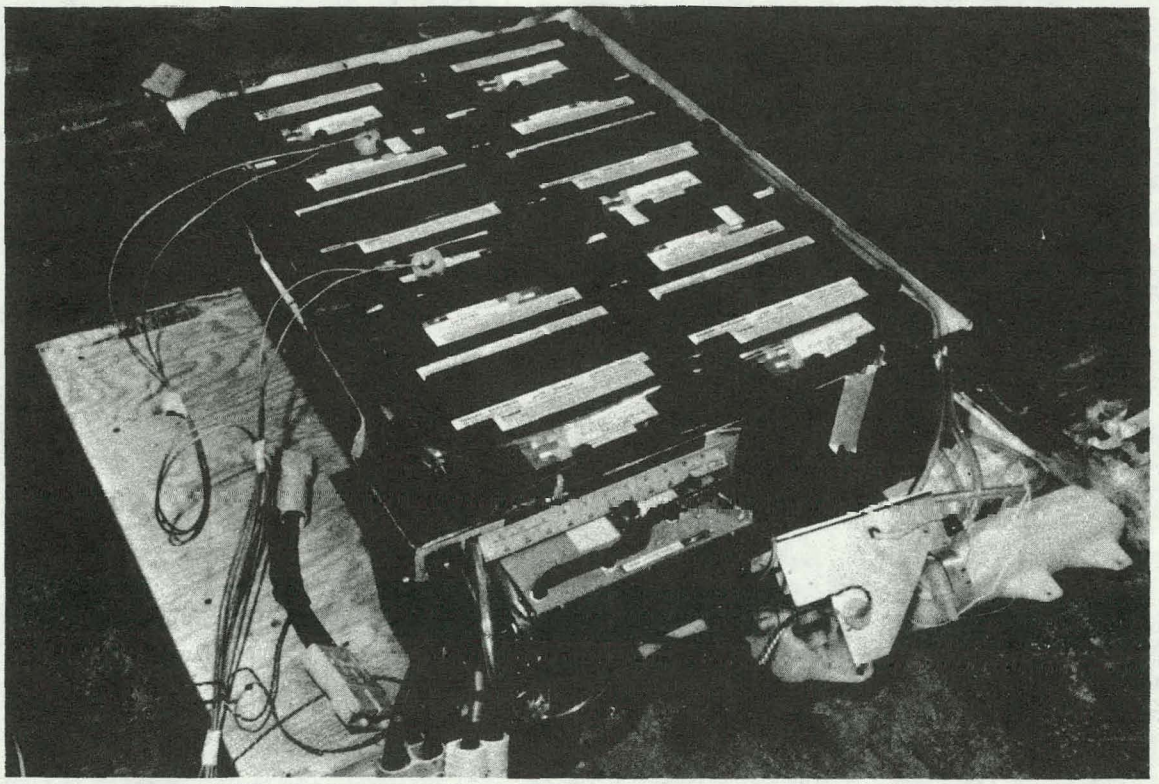

Figure 5.4-5. Battery Pack and Accessory Systems

Cell Tests. Cell performance tests were performed at Globe in December 1980 and January 1981. The first three test cells were used for all tests. Each test was performed on two cells. A summary of the constant-current discharge tests is shown in Table 5.4-2.

Pulse-power discharge tests were also run. For this test, the cell was discharged at a base rate of 35 A or 50 A. During this discharge, the cell was periodically subjected to a high-rate discharge of 15 s duration. The high-rate discharge was done at selected currents between 200 A and 500 A. The results are summarized in Table 5.4-3.

Table 5.4-4 is a comparison of the cell test data and the statement of work specifications. Performance of the test cells exceeded the specified minimum values in all cases. The test cells performed significantly better on the pulse power tests than Globe had anticipated, based on the testing of EV-1000 (formerly called EV2-13) batteries. The difference between the projected values and the actual values was larger at the greater depths of discharge. This significant improvement at low states-of-charge is attributed to the electrolyte circulation system, which maintains more concentrated electrolyte near the electrodes during discharge than would be present without the system.

Charging tests were also performed by Globe using the test cells. Tests were run for a range of initial charging currents (8 A-32 A), depths of discharge before charging (20%-100%), and battery temperatures (30 °F-110 °F). In all the tests, the charging was done using a constant initial current until a temperature-dependent clamp voltage was reached, after which the current was tapered maintaining the constant clamp voltage. Charging was terminated after a prescribed overcharge (104%-125% of the discharged Ah) was returned to the cell. A summary of the charge test data is given in Table 5.4-5. A prime objective of the charging tests was to determine the overcharge factor required for daily and equalization charges to maintain the cells at their nominal C/3 capacity for repeated discharge cycles. The data obtained in the charging tests was used to develop the algorithms included in the HTV controller for charging the battery pack. Based on the cell charging tests, a daily charge is terminated when 105% of the prior discharged Ah have been returned to the batteries and an equalization charge is terminated when 110% of the prior discharged Ah have been returned to the batteries. Cycle performance of the test cells using this type of charge termination criteria and a equalization charge after 13 daily charges is shown in Figure 5.4-6. Using the over charge factors indicated the cells maintained their nominal performance over 30 simulated daily discharges and 2 equalization charge periods.

Table 5.4-2

CELL CONSTANT-CURRENT DISCHARGES

Rate	1.75 V_{Cutoff}		1.30 V_{Cutoff}	
	(Ah)	(Wh)	(Ah)	(Wh)
35 A (3 h)	106	209	109	214
50 A (1.9 h)	95	186	98	191
100 A	66	126	71	134
200 A	40	75	56	100

Note: Results are average of two test cells.

Table 5.4-3

CELL PULSE POWER TESTS

Base Discharge Current (A)	Depth of Discharge Based on 3 Hour Capacity at Base Current (%)	Cell Voltage* After Specified Pulse			
		200 A	300 A	400 A	500 A
35	0	1.88		1.73	1.64
	30	1.86		1.68	1.59
	50	1.81	1.67	1.60	1.50
	60	1.78		1.55	1.41
	70	1.73		1.46	1.28
	80	1.68		1.28	<1.00
50	0	1.88		1.74	
	56	1.80		1.59	
	78	1.71		1.36	
	89	1.60		<1.00	

*GE HV data is average of two calls -- 15 seconds

Table 5.4-4

CELL TEST SUMMARY

Characteristic	Statement of work Specifications		Test Data
C/3 Discharge 1.75 v/cell cutoff	Target	Minimum	
Ampere-hours (Ah)	110	105	106
Watthours (Wh)	–	208	209
Pulsed (15 S) Power Tests Pulse Current, A	Target	Minimum	
200	1.80	1.75	1.81
300	1.70	1.63	1.67
400	1.58	1.50	1.60
500	–	–	1.50
All tests performed after cells were charged/discharged 30 times after fabrication.			

Table 5.4-5

EFFECTS OF CHARGING CONDITIONS ON CHARGING TIMES FOR THE HTV BATTERY

DOD[1] %	Initial Charging Current A	Battery Temperature °F	Time to Voltage Clamp hr	Additional Time (hr) 4% O.C.[2]	10% O.C.[2]
100	16	80	6.10	1.60	3.9
80	14	80	5.70	1.30	—
20	16	80	1.10	0.60	1.2
100	16	110	7.00	1.00	5.8
100	15	52	4.60	1.70	3.2
100	15	33	4.50	0.90	—
80	32	80	2.40	0.80	2.0
20	32	80	0.55	0.75	1.3
80	8	80	10.30	0.70	2.7

(1) All discharges were at 35 A; DOD is depth of discharge before start of charging.
(2) O.C. means overcharge factor.

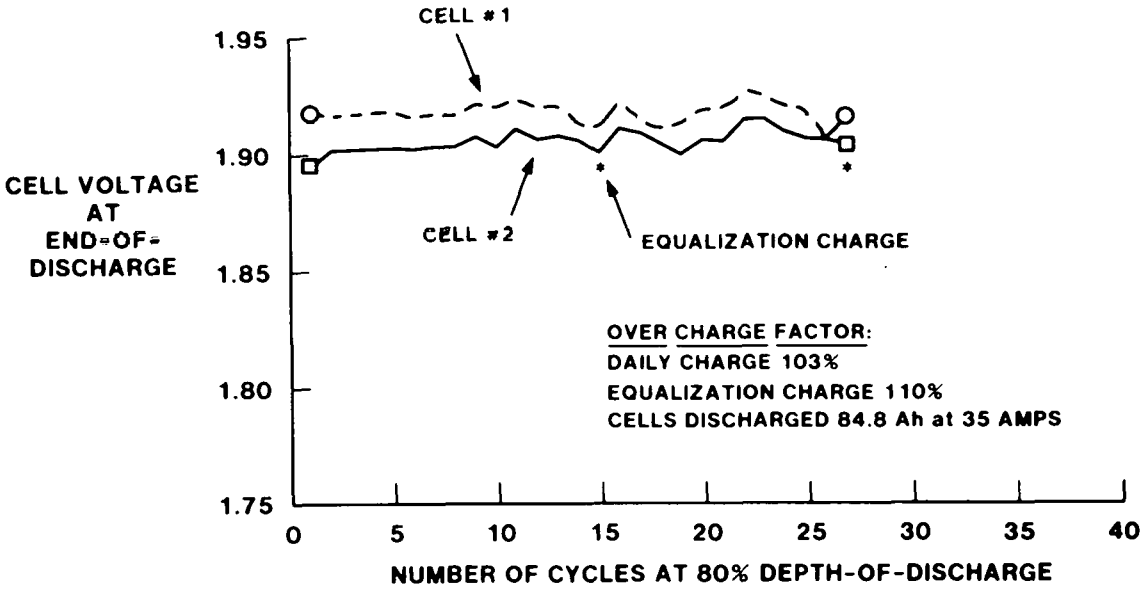

Figure 5.4-6. Cell Cycle Performance Test Data

Module Tests. Tests of the 12 V modules to be used in the HTV battery pack were performed by Globe, General Electric, and the National Battery Test Lab (NBTL) at Argonne. In those cases in which comparable tests were performed by the three groups, the results were consistent.

As noted previously, the battery specifications given to Globe by GE were expressed in terms of the C/3 capacity and the battery terminal voltages after a 15 s high current pulse at 50% DOD during a 35A constant current discharge. The objectives of the specifications were to ensure a HTV battery of a specified capacity having a high power density expressesed as specified voltage droops at high pulse currents. High power density is critical for the hybrid vehicle application in which the battery weight is limited by design and high currents are required. All the tests of the HTV battery modules showed a C/3 capacity in excess of 100 Ah (using a 1.75 V/cell cut-off) and often in excess of the 106 Ah nominal design value. In addition, the HTV modules have exhibited high power density meeting the pulsed current voltage specification set. Peak power tests of two modules at NBTL using their standard test procedure for a 30 s sustained duration of peak power yielded the following results:

DOD (%)	W/Kg
0	193
20	193
50	164
80	135

These results indicate that HTV battery is indeed a high power density, lead-acid battery exceeding the DOE battery program specific power design goal of 104 W/kg by a substantial margin. Hence, it can be concluded that the HTV batteries met the design goals for performance as set forth at the outset (Phase II) of the program.

Many additional tests of the HTV batteries have been performed. Included in these tests have been the determination of capacity (Ah) as a function of constant discharge current (see Figure 5.4-7), and the effect of unsteady, pulsed discharge profiles on the battery capacity (see Table 5.4-6). The scatter in the data increases significantly at high discharge rates, but all the data available shows a rapid decrease in Ah capacity with increased discharge current and pulse currents. As indicated in Figure 5.4-8, the decrease in Ah capacity with discharge currents was greater than expected based on the extrapolation of data from other Globe lead-acid batteries (e.g., EV-213 designed for use in the ETV-1). It was thought at the outset of the Hybrid Vehicle Program that a high power density battery would also be "stiff" relative to its droop in capacity with discharge rate. Clearly this has not been the case. The reason for this difference is not yet understood.

Laboratory tests of the HTV battery cells and modules were made using nonuniform, pulsed discharge profiles to simulate the battery duty cycle in the HTV. During these tests the average discharge current as well as the magnitude and time-spacing of the high-current pulses were varied. Pulsed discharge tests of the HTV battery were done by Globe, GE, and Argonne NBTL. The results are summarized in Table 5.4-6. The data shows a significant decrease in effective battery capacity with increasing average discharge current and peak pulse current. The NBTL HTV simulation (last entry in Table 5.4-6) which most closely matches the duty cycle in the HTV yielded only a 33-43 AH capacity. The difference of 10 AH in the module capacities (two modules were tested) adds to the uncertainty in estimating the HTV battery pack capacity where ten (10) modules are connected in series.

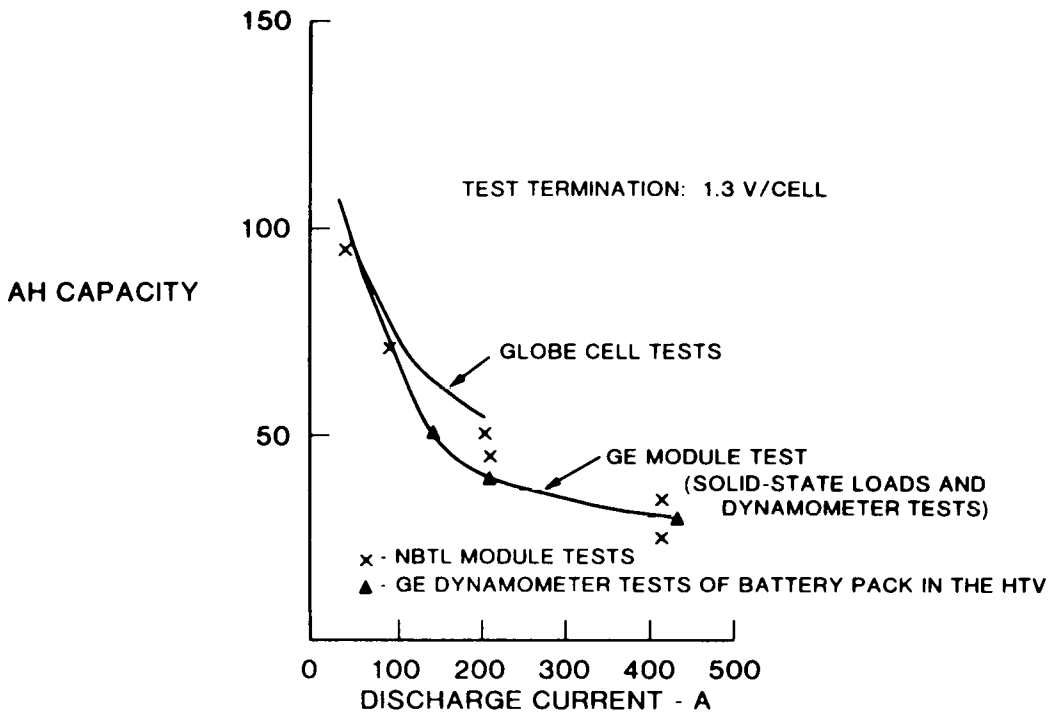

Figure 5.4-7. Constant-Current Discharge Characteristics of the HTV Battery

Preliminary tests of the HTV ($V_{MOD-MAX}$ = 40 mph, Schedule B) indicated an average discharge current about 70 A over the EPA urban cycle (1372 s) with a maximum battery (10 modules) pack capacity of 35 AH before the HTV could no longer follow the driving (velocity vs. time) profile. At this condition, the battery cell voltages drooped below 1.3 V/cell. The 35 AH capacity was much less than the expected capacity of about 65 AH based on the following interpretation of Globe cell tests: For an average discharge current of 70 A, the AH capacity would be 82 AH (see Figure 5.4-7); according to the Globe pulsed discharge data given in Figure 5.4-9, the battery can sustain a 400 A pulse for 15 s with a terminal voltage of 1.3 V/cell; the usable battery capacity would be 0.8 x 82 AH or 65 AH. This is much greater than the 35 AH capacity experienced with the HTV even though the HTV controller software reduces the allowable peak currents to 200 A as the indicated depth-of-discharge increases to 80%.

Since the fuel economy of the HTV is high (90 mpg) only while the battery state-of-charge is above 50% (i.e., VM $\approx$ VM $_{MAX}$), the lower than anticipated usable battery capacity significantly reduces the gasoline savings projected using the HTV compared to the reference ICE passenger car.

5.4.1.4 Battery Charging

Globe has specified the following battery charging guidelines:

a. Utilize independent chargers or control circuits for each 60 V bank

b. Maintain $I_{peak}/I_{avg} < 3$

c. Charge daily after use. Perform an equalization charge after 13 daily charges. Charge once per month if vehicle is not used.

Table 5.4-6

PULSED PROFILE DISCHARGE CHARACTERISTICS OF THE HTV BATTERY

Discharge Profile	Average Current (A)	Peak Current (A)	Time Between Peak Currents	Ah Capacity*	Testing Group
5 s current pulse followed by steady discharge	58	300	60 s	51	GE
5 s current pulse followed by steady discharge	88	300	60 s	57	GE
5 s current pulse followed by steady discharge	123	300	60 s	49	GE
SAE "D" simulation of ETV-1 with regen.	33	135	120 s	67-80	NBTL**
Special cycle to simulate the HTV on the EPA urban cycle	56	170	200 s	67-80	NBTL
Special cycle to simulate the HTV on the EPA urban cycle	85	255	200 s	47-61	NBTL
Special cycle to simulate the HTV on the EPA urban cycle	102	306	200 s	33-43	NBTL

*Test terminated when battery voltage droops to 1.3 V/cell during peak current pulse.

**NBTL tested two 12 V modules

d. Limit maximum charging voltages dependent on temperature.

e. Maintain constant voltage during current taper.

f. Terminate charge on the basis of an ampere-hour input value determined from prior discharge history using an overcharge factor of 1.04 for daily charges and 1.1 for equalization charges.

5.4.1.5 Battery Maintenance

Globe recommended the following procedures for the frequency of water addition to the battery pack for various battery use patterns.

Battery Use Pattern	Frequency of Water Addition
Moderate Use. Battery pack is discharged to 50% or less on	Add water after every three equalization charges. If vehicle

the average. Equalization charge is performed after every 13th daily charge.	is used daily, this corresponds to every six weeks.
Heavy Use. Battery pack is discharged between 50% and 80% on the average. Equalization charge is performed after every 13th daily charge.	Add water after every two equalization charges. If vehicle is used daily, this corresponds to every four weeks.
Severe Use (e.g., during testing using the electric drive only) Battery pack is consistently discharged to a low state-of-charge and every charge is an equalization charge.	Add water after every 15 equalization charges.

5.4.2 Battery State-of-Charge

This subsection describes the methodology, hardware, and testing of the battery state-of-charge unit.

5.4.2.1 Methodology

The battery state-of-charge (SOC) is needed by the vehicle controller to calculate V_{MOD} and to initiate and terminate charging of the battery by the heat engine. High accuracy (that is to within several percent) of the SOC is not needed, but it is important that the inferred SOC vary systematically and not reflect the transient behavior of the battery current and voltage. For these reasons, the coulombic approach is used to determine SOC in the HTV. In principle, this is done by integrating the battery current during both battery discharge and charging modes to obtain a net ampere-hour value for the battery since the last charge from

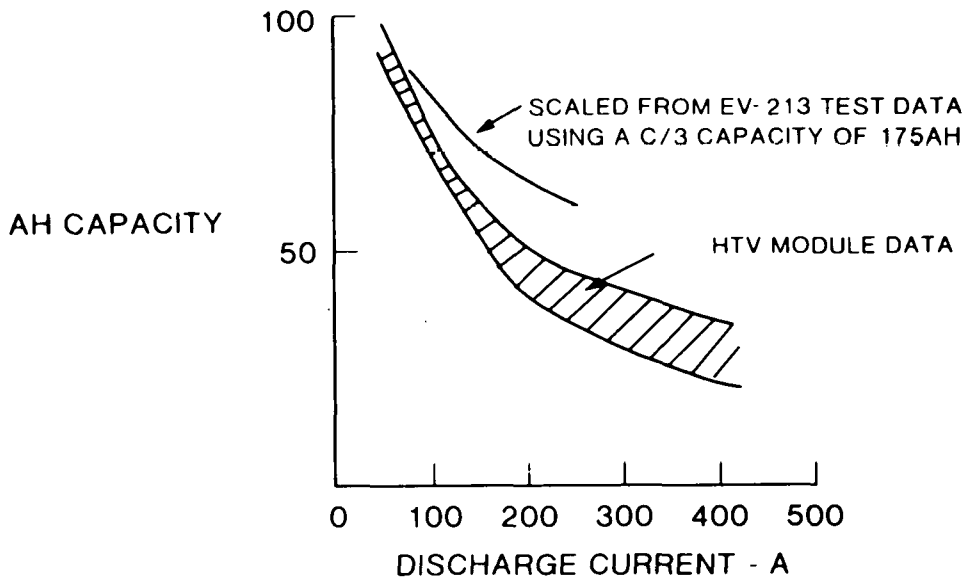

Figure 5.4-8. Comparison of Expected and Measured Constant-Current Discharge Characteristics of the HTV Battery

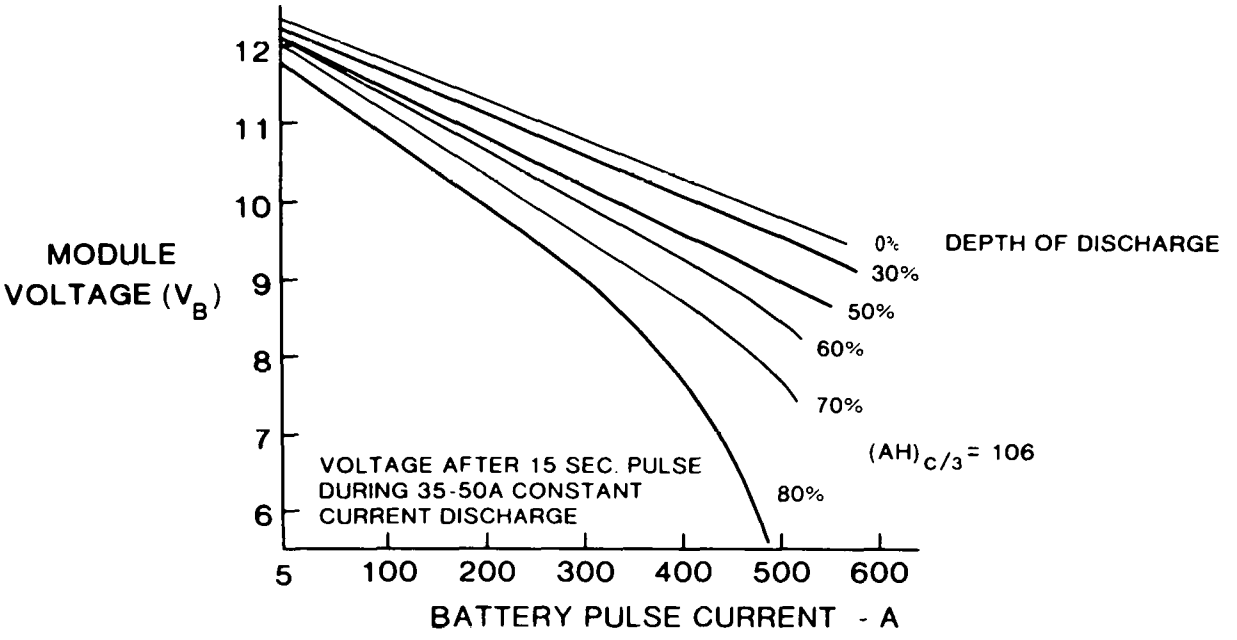

Figure 5.4-9. Pulsed Power Characteristics of the HTV Battery

the wall-plug. The depth of discharge (DOD = 1-SOC) is then calculated by dividing the net ampere-hour value by the effective battery ampere-hour capacity corresponding to the discharge profile during electric drive system operation. Determination of the effective battery capacity for the hybrid application has proven difficult because of the large ratio between the peak pulse currents and the average discharge current and, in addition, the effects of battery aging and temperature changes.

5.4.2.2 State-of-Charge Unit and Its Use in the HTV

The battery state-of-charge (SOC) unit used in the HTV is a Compucharge BCC-200 supplied by LES Industries, Montréal, Canada. The unit, shown in Figure 5.4-10, is microprocessor-based (8-bit Cpu). Its software, to the degree that available data would permit, was tailored to the characteristics of the HTV battery. The BCC-200 system was designed to utilize a resistive shunt placed in the battery circuit. The sensed voltage is then used by the microprocessor to compute the charge withdrawn from the battery for each increment of time and the net integrated charge (AH) withdrawn since the battery was last charged from the wall-plug. The microprocessor then uses the net AHs withdrawn and the inferred effective battery capacity (AH capacity at the average battery current is determined from the stored Peukert curve) to compute the state-of-charge. The voltage output of the BCC-200 is used to drive an SOC-meter displayed to the driver, to provide input to the vehicle controller for use in calculating V_{MOD} and to initiate battery charging by the heat engine.

In the HTV application, a separate battery current shunt to obtain an input to the BCC-200 is not used. Instead the vehicle controller calculates the battery current from inputs from the IA/VA sensors. A voltage signal proportional to the battery current is sent from the vehicle controller to the BCC-200. As discussed in the next section, the inferred battery current is multiplied by a factor dependent on its magnitude in order to account for the effect of high peak pulse currents on the effective capacity of the HTV battery. In all other respects, the BCC-200 unit functions in the same way as it was originally designed by LES Industries.

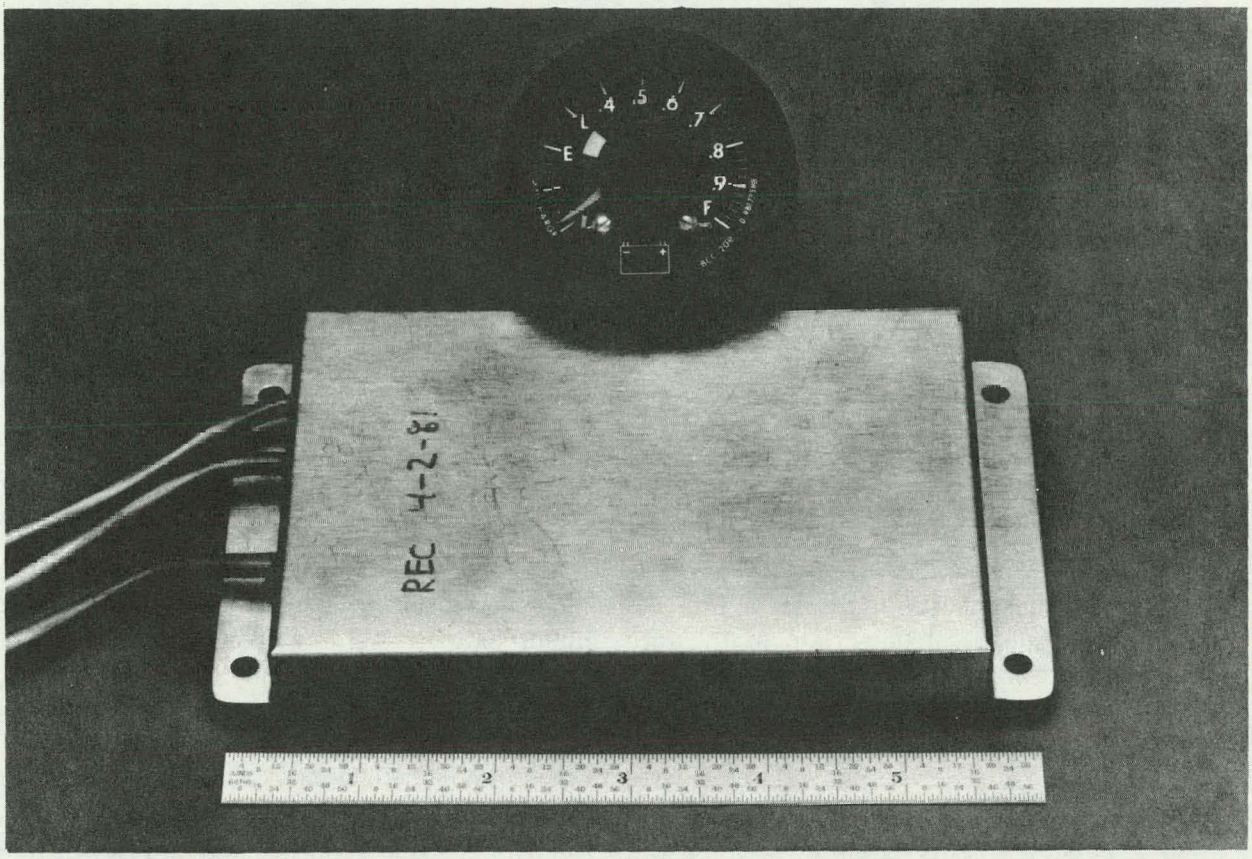

Figure 5.4-10. Battery State-of-Charge Meter and Microprocessor

5.4.2.3 Testing of the SOC System

Bench tests of the SOC system were done early in the program using HTV modules (12 V) and later in the program on the chassis dynamometer using the complete battery pack (120 V). There was uncertainty from the outset regarding the effective capacity of the lead-acid battery in an application in which the ratio of the peak pulse current to the average discharge current was large (6:1 or 450 A to 75 A).

The bench tests of the BCC-200 system were accomplished by using a battery module(s), a Wavetek Arbitrary Waveform Generator, ACME 1000 programmable solid-state loads, a voltage recorder, and a Fluke data logger. The test equipment was connected as shown in Figure 5.4-11. Tests were run using 5 s, 300 A pulses, spaced 60 s apart, with an average current of 60 A. The test was terminated when the voltage drooped to 7.8 V during the 300 A pulse. For these tests, the BCC-200 registered SOC = 41% at test termination. For the corresponding steady current discharge at 60 A, the BCC-200 registered SOC = 0%. The corresponding AH capacities were 50-55 for pulsed discharge and 85-90 for steady discharge at the same 60 A average current. These results indicated that the effective capacity of the HTV battery would be less than expected and significantly less than the C/3 rated 106 Ah.

In order to have the BCC-200 register about SOC = 20% when the battery voltage drooped to 1.3 V/cell during high currents (>400 A), it was decided to multiply the actual sensed battery current by a factor of two, when the current exceeded 100 A. This would have the effect of increasing the average current fed to the BCC-200 and result in a more rapid indicated discharge of the battery. This approach has been used in the HTV, and prelimi-

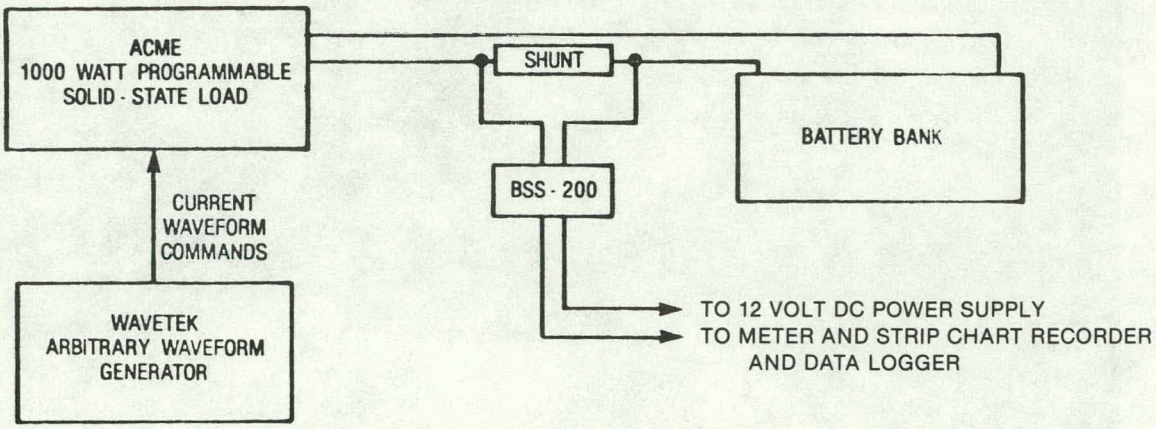

Figure 5.4-11. Battery State-of-Charge Test Setup

nary dynamometer tests of the HTV indicate that it works reasonably well as far as maintaining sufficient electrical power up to the initiation of battery charging from the heat engine. The effective battery capacity on the EPA urban cycle was found to be only about 35 Ah.

5.4.3 HTV On-board Microcomputer-Controlled Battery Charger

The microcomputer-controlled, on-board, transistorized battery charger operates from either a 120 V or 240 V service line and provides temperature compensated charging of the two independent 60 V battery banks. As shown in Figure 5.4-12, the charger is comprised of two charging circuits sharing a common ac input. This dual charger concept, where each charger is independently controlled by the microcomputer, was selected over alternate approaches, which included charging both banks in parallel from a single charger, or configuring the batteries in series (120 V) and charging from a single complex charger consisting of both an up-chopper and a down-chopper to satisfy the dual ac input voltage requirement. Features of this dual battery charger include better equalization of the batteries during charging, lower power transistor stresses for improved reliability, improved efficiency while operating from a 120 V ac line, and redundant charging capability in the event of a failure in one of the power circuits.

Ground-to-neutral continuity detection is used to provide operator safety for the high-frequency battery charger. In the event the ac receptacle fails to provide a third wire "ground" to the vehicle, the ground continuity detector inhibits the charging circuits.

Microcomputer-to-battery charger interface is digital, with opto-couplers in the controller to provide necessary isolation. Battery charger current commands are pulse width modulated signals. Charger sensor signals, including battery voltage and charger output dc current, are pulse frequency modulated by V→F converters, time multiplexed, and transmitted to an opto-coupler in the microcomputer controller.

Logic and microcomputer power is provided from the 12 V accessory battery. A separate ac-dc converter "trickle charger" supplies power to maintain the state-of-charge of the accessory battery while charging the propulsion batteries from wall-plug electricity.

Maximum charger current, under the command of the microcomputer, is determined by the ac input line. Table 5.4-7 shows the three charge rates and maximum battery recharge currents.

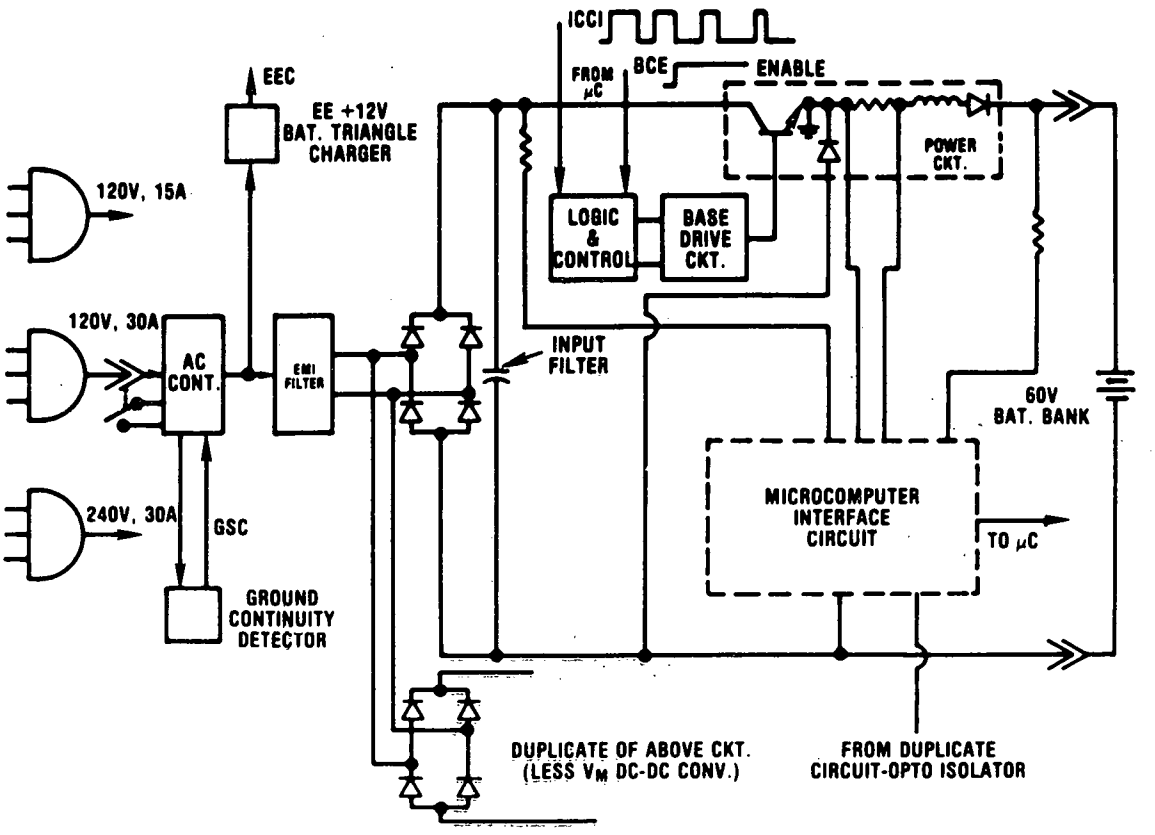

Figure 5.4-12. Dual HTV Battery Charger Block Diagram

Table 5.4-7

HTV ONBOARD BATTERY CHARGER RATINGS

60 Hz AC Input Power	Charge Rate	Battery Voltage Clamp (Each Bank) V_{CLAMP}*(V)	Maximum Average Battery Charge Current (A, Each Bank)
120 V, 15 A	Low	80	5
120 V, 30 A	Medium	80	10
240 V, 30 A	High	80	20

*V_{CLAMP} = 80V, at battery temperature of 80 °F

5.4.3.1 Battery Charger Design

The battery charger power circuit for one 60 V battery bank is shown in Figure 5.4-13 A down-chopper circuit topology was used for its simplicity and reliability. The power switch transistor, a GE D67DF7, was chosen as best suited for this application. Careful circuit lay-out for minimum stray inductance and the use of both turn-on and turn-off snubbers minimize the electrical stress placed upon the power switch. The input filter capacitor bank is

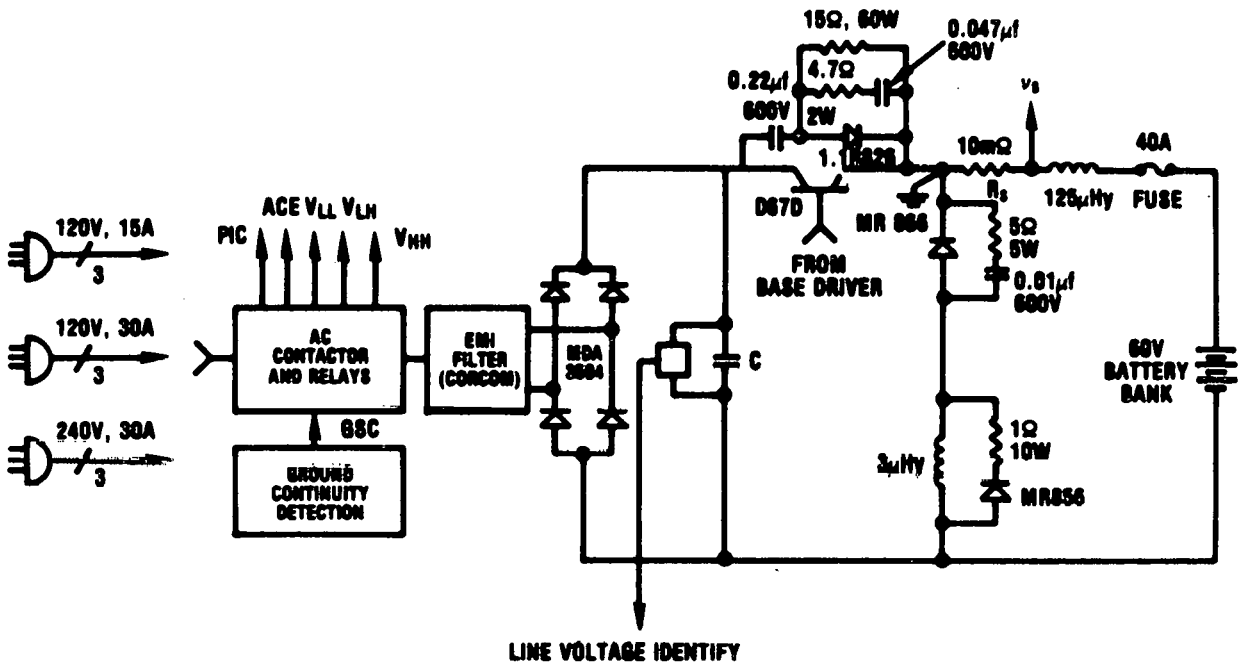

Figure 5.4-13. HTV Battery Charger Power Circuit

sized to handle the peak ripple currents in a minimum volume. Current sensing resistors are used for their simplicity, with the input sense resistor also placing a limit on input surge current. EMI filtering and transient suppression (MOV) are also included.

Control logic, current sensing, and current regulation circuits are shown in Figure 5.4-14. The instantaneous battery current "measured" by the sense resistor in the power circuit is amplified differentially by the sense amplifier whose output is delivered to the comparator and error amplifier. The average value of this signal is compared with the microcomputer commanded reference signal, thus generating an error voltage which is fed to the comparator. In this way, the instantaneous peak value of the battery current is controlled to produce the required average value. The battery current is allowed (via the hysteresis designed into the comparator) to have sufficient peak-to-peak ripple to permit a relatively small, lightweight coasting inductance design and allows a very large dynamic range of the average charging current with small front end filtering. The peak current limit amplifier protects the power switch transistor against excessive peak collector current. Preset times, $T_{on}(min)$ and $T_{off}(min)$, permit proper power switch snubber operation over the wide dynamic range of the charger. The OR function provides proper interface to the power switch base drive circuit (not shown).

Additional functions of the control circuit are heat sink over-temperature shutdown, short circuit (output) shutdown, low logic supply voltage shutdown, and enable and ground continuity detection. Also provided is a provision for operating safely on either a 15 A or 30 A service with active rms line current limiting in either case.

Ground-to-neutral continuity detection is accomplished as shown in Figure 5.4-15. The purpose is to provide operator protection by ensuring that the vehicle is solidly connected to house ground (usually at service entrance). Continuity between ground and neutral is sensed

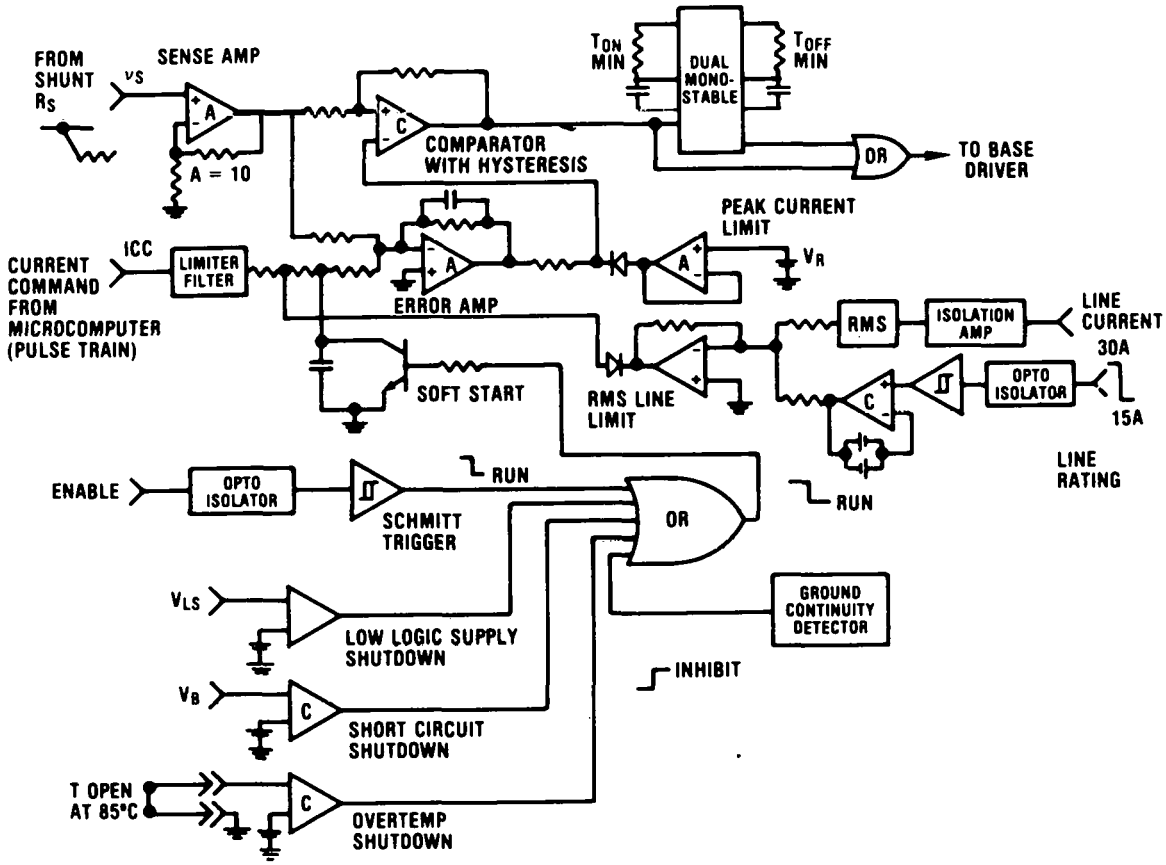

Figure 5.4-14. HTV Battery Charger Control Circuit

by two independent means. The presence of a voltage between ground and neutral or the absence of dc current produced by the dc-to-dc converter independently notify the microprocessor that continuity does not exist. The microprocessor thus acts to prevent the initiation of charging or terminates a charging condition as necessary.

The HTV battery charger packaging is illustrated in Figure 5.4-16. Electronic circuit cards for control and sensing are mounted on the hinged door, providing easy access for calibration. Dual power circuits are contained on separate vertically mounted heat sinks. Cooling air is drawn downward over heat sinks and exhausts near the rear bumper. The ac input power cable, from the receptacle in back of the vehicle license plate, interfaces to the safety contactors located behind the heat sink.

5.4.3.2 Charger Control Strategy

The software control algorithms for the HTV on-board battery charger are implemented in one of the 8086-based microcomputers in the HTV controller; this microcomputer (IOC) also serves to unload the vehicle control computer by performing I/O activities as well as providing diagnostic and monitoring functions. The IOC also maintains a record of net ampere-hours; this information is stored in CMOS RAM powered by an unswitched connection to the vehicle accessory battery. The ampere-hour net is reset to zero (full charge) upon normal charger termination.

Since the HTV charger is really comprised of two separate chargers, one for each 60 V bank, the charging software is executed twice each sample interval. The I/O variables relating

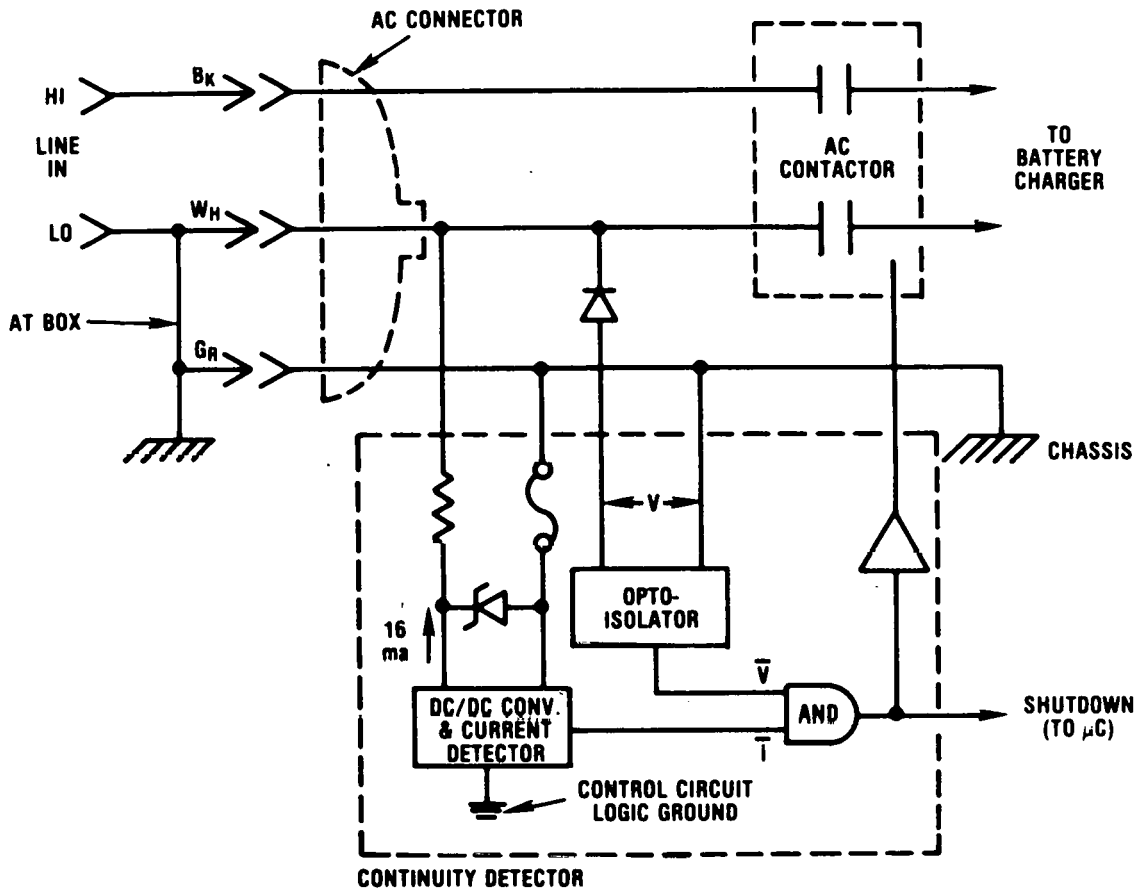

Figure 5.4-15. Battery Charger Ground Continuity Detector

to battery charging are stored in contiguous memory locations so as to allow a simple index increment to access the data associated with the second battery bank. This software multiplexing scheme provides completely independent charging of each bank while maintaining efficient code memory utilization.

Upon initiation of charging, the number of ampere-hours to be input (Ah target) is calculated:

Ah Target = Ah Net * 1.05 (normal charge, 105%)

Ah Target = Ah Net* 1.10 (equalization charge, 110%)

The software control algorithm for charging is subdivided into two modes — constant current and constant voltage. During both modes, the controller sums the value of charger feedback currents to maintain ampere-hour net and ampere-hour charge. The constant current mode is active until

Battery Voltage > 89.6 − (0.12*BT); where BT = Battery Temperature (°F)

This voltage is maintained during the constant voltage mode by decrementing the command current. The slope of the command current versus time is calculated by dividing the change in current by the time interval between decrements.

The operator can terminate charging at any point in the cycle and the value of ampere-hours net will reflect the present state of charge. The controller detects full charge and automatically terminates charging when one of the following conditions is satisfied:

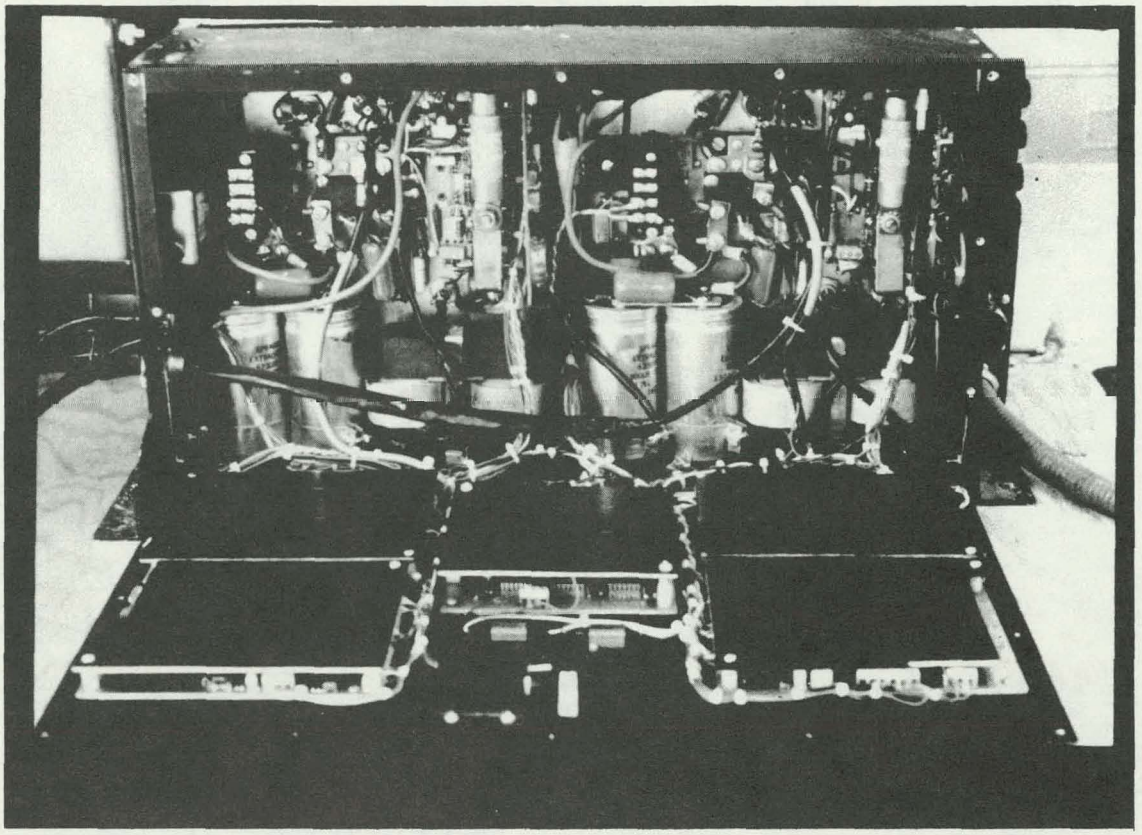

Figure 5.4-16. HTV Battery Charger

Ah Charge $\geq$ Ah Target, and Slope of Current $<$ f(Ah Overcharge)

Ah Charge $\geq$ Ah Target + 2 Ah, and Slope of Current $<$ 0.2 A/min

Slope of Current $<$ 0.1 A/min

The charge termination criteria was based on the Globe cell tests of the HTV battery (see Section 5.4.1).

Since a sensor malfunction could result in excessive overcharging of the batteries, extensive checking of sensor inputs is done while charging. Sensor checks are summarized below:

BAT TEMP $<$ 10 °C
BAT TEMP $>$ 40 °C
BAT VOLTS $<$ 52 V
BAT VOLTS $>$ 90 V
ABS (feedback current - command current) $>$ 4 A
ABS (BAT BANK 1 VOLTS - BAT BANK 2 VOLTS) $>$ 20 V
ABS (BAT BANK 1 TEMP - BAT BANK 2 TEMP) $>$ 10 °C

If any of these conditions is true for more than 6 s, the chargers will be shut off.

5.4.3.3 Battery Charger Operational Tests

During HTV performance and road tests, the on-board battery charger was routinely used to charge the batteries from varied depths of discharge. Low and medium charge rates (120 V), as well as high charge rates (240 V), were tested.

Figure 5.4-17 illustrates a battery charge operational test. Initially 17.73 Ah was removed from the propulsion batteries. On-board battery recharge, using the high rate of charge

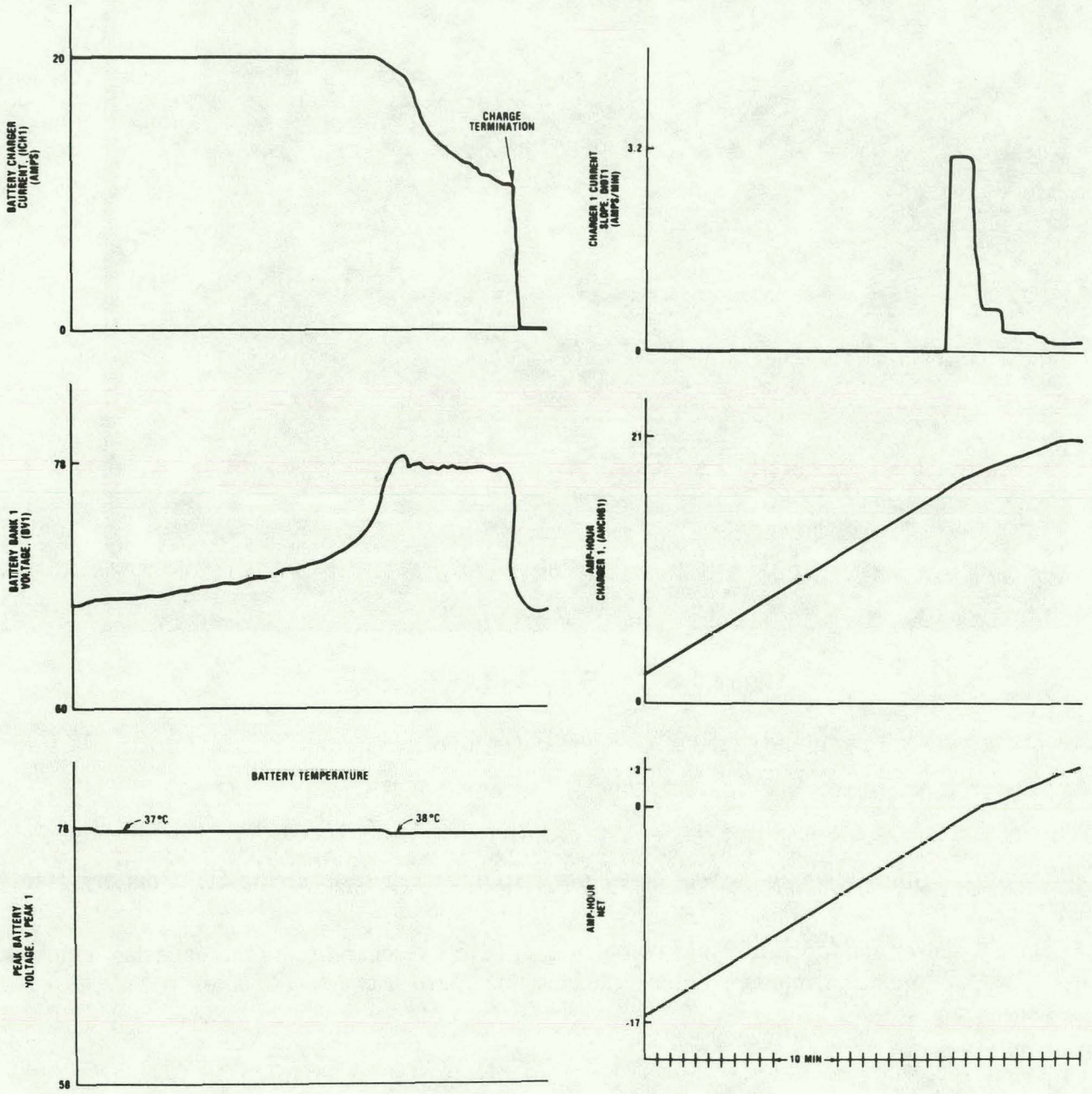

Figure 5.4-17. HTV Battery Charger Test

(240 V ac, 30 A line), was started. The initial temperature of Battery Bank No. 1 was 36 °C; therefore, the value of the peak voltage clamp is 78 V. During the early portion of the re-charge cycle, the charger operated in a constant current mode. Approximately 5 min into the test, the battery temperature increased to 37 °C and the peak voltage clamp decreased to 77.8 V. When the battery voltage first equaled the clamp voltage, the charger transitioned from a constant current mode to nearly a constant voltage mode and the current decremented appropriately. Once the current began to taper, the current slope calculation was enabled. Charger No. 1 automatically terminated when the ampere-hours exceeded the target by 2.0 Ah and the output current slope was less than 0.2 A/min. After normal termination of the second bank, the following events occurred: AHRNET was reset to zero, the state-of-charge meter was set to 100%, and finally the microcomputer turned off its own logic power supply.

5.5 MULE PROGRAM

The mule program consisted of two mule vehicles—(1) the Test Bed Mule (TBM), which was an Audi 5000 modified to accept the single-shaft, longitudinal hybrid power train, and (2) the Hybrid Power Train Mule (HPTM), which was an Oldsmobile Toronado in which the two-shaft HTV hybrid power train was first tested.

5.5.1 Test Bed Mule

This subsection presents the TBM vehicle design and description, propulsion system design and fabrication, controller, throttle control system development, and power train/controller/vehicle integration and test.

5.5.1.1 Test Bed Mule Vehicle Design and Description

Vehicle Description. The TBM (Figure 5.5-1) is a modified Audi 100 Avanti, which is the hatchback model of the Audi 5000, marketed in the U.S. This vehicle was chosen because it is a five-passenger car with front-wheel drive, and could be made comparable to the HTV in weight and dimensions. The decision to use a right-hand drive was made because the electric motor protruded through the firewall on the left side of the car. This would interfere with the pedals in a conventional left-hand drive car. The weight breakdown of the TBM is shown in Table 5.5-1. The curb weight is 1745 kg with a resulting test weight of 1882 kg.

The layout of the components, which have been installed in the TBM, is shown in Figure 5.5-1. The heat engine, clutch, and electric drive components used in the TBM are essentially the same as those to be used in the HTV. The power train configuration in the TBM is

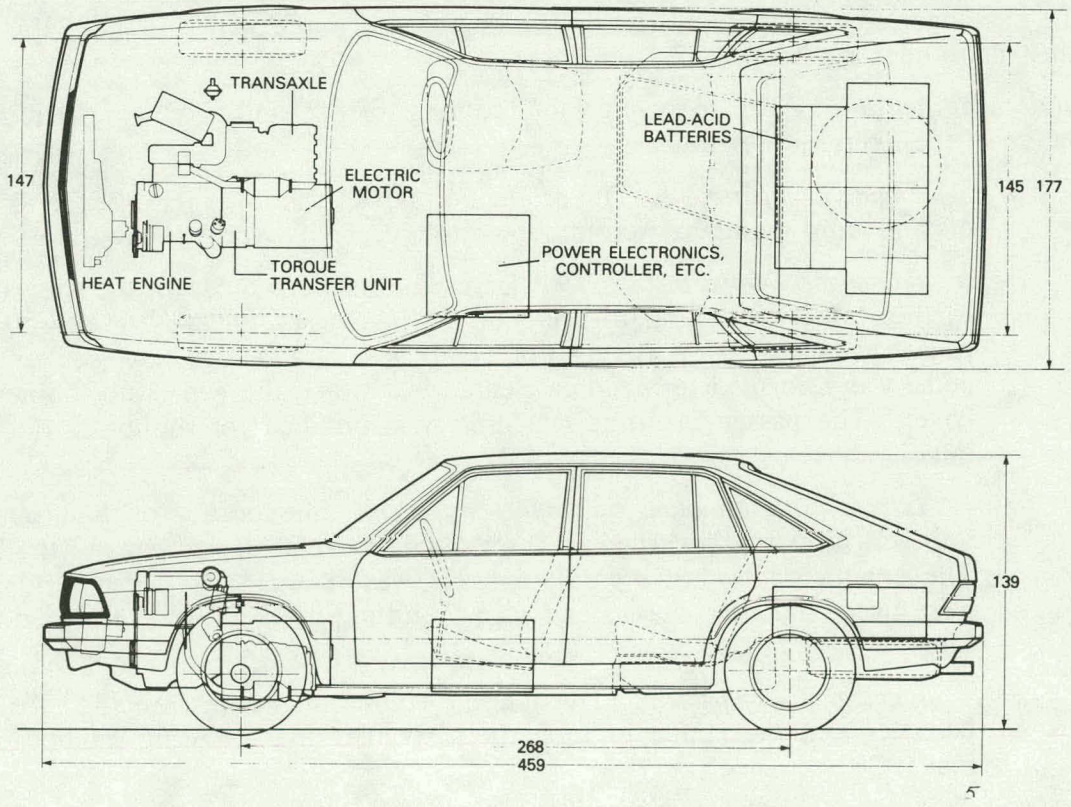

Figure 5.5-1. Test Bed Mule – Audi 5000

Table 5.5-1

TEST BED MULE WEIGHT BREAKDOWN

	Weight (kg)
Curb Weight (car only and engine/transmission)	1130
Electric Motor and Contactor Box	135
Controller and Field Chopper and Box	30
Mechanical Components (clutches, chain and housing)	65
10 Batteries and Housing	350
Auxiliary Battery and Sensors	14
Miscellaneous Materials	20
Curb Weight (TBM)	1744 kg
Test Weight	1882 kg

single-shaft, longitudinal, as compared with two-shaft, transverse in the HTV. In addition, much less attention was given to compact packaging in the TBM. The batteries are placed in the luggage compartment in a special container, which is ventilated to keep the air/hydrogen concentration low. The contactor box is placed under the battery compartment in the spare wheel housing. The field chopper and the vehicle controller are mounted in a cabinet placed in the passenger area beside the driver. The engine, starting clutch, and all of the auxiliaries are installed under the hood.

Vehicle Modifications. The following modifications to the Audi 5000 were required for installation of the hybrid power train.

Engine Compartment. The production power train was removed, and the brackets and front members were modified to accept the hybrid power train.

Passenger Compartment. Two large cutouts were made in the firewall adjacent to the tunnel to permit intrusion of the electric motor and the gearbox into the passenger space. New covers were fabricated and welded into place. The clutch pedal was reformed to maintain clearance between the pedal and the new gearbox cover. The passenger front seat area was modified for mounting the controller box.

Location and Mounting of Propulsion System. The location of the propulsion system was primarily governed by the existing drive shaft centers and the hood line. The engine slant of the production car was retained. Series mounting rubbers were used, but new chassis and unit mounting brackets were designed and fabricated.

Luggage Compartment. The luggage compartment was modified to accept the batteries and the contactor box. In particular, the following modifications were made:

- A large T-shaped box containing 10 batteries was fabricated: length -- 406 mm, height -- 229 mm, width -- 171 mm, and weight -- 350 kg

- Detachable battery box cover sealed by rubber strip and retained by clips
- Battery box venting system
- Contactor box was mounted in removable housing under battery box

Other modifications which were made included:

- Alternator driven from pulley on gearbox main drive shaft
- Main drive clutch -- golf cart-type clutch cable and lever end
- Engine start clutch, vacuum-actuated using power brake system pump and accumulator
- Gearbox dipstick repositioned and reformed
- Modified mechanical linkage between selector lever and gearbox
- New exhaust down pipe and catalyst
- New radiator position -- fabricated tubes
- Potentiometer was mounted on the accelerator pedal to provide signals to vehicle controller
- Microswitches were mounted on the accelerator pedal and gear selector
- Front passenger seat was cut down to base frame and a flat platform, to which the controller was bolted, was added
- Clutch pedal was added for actuation of drive clutch

5.5.1.2 Propulsion System Design and Fabrication

The Test Bed Mule (TBM) propulsion system was designed to minimize the special tooling required for its fabrication, since this was the only drive line of this type to be built. Figure 5.5-2 is a photograph of the components employed in the TBM drive.

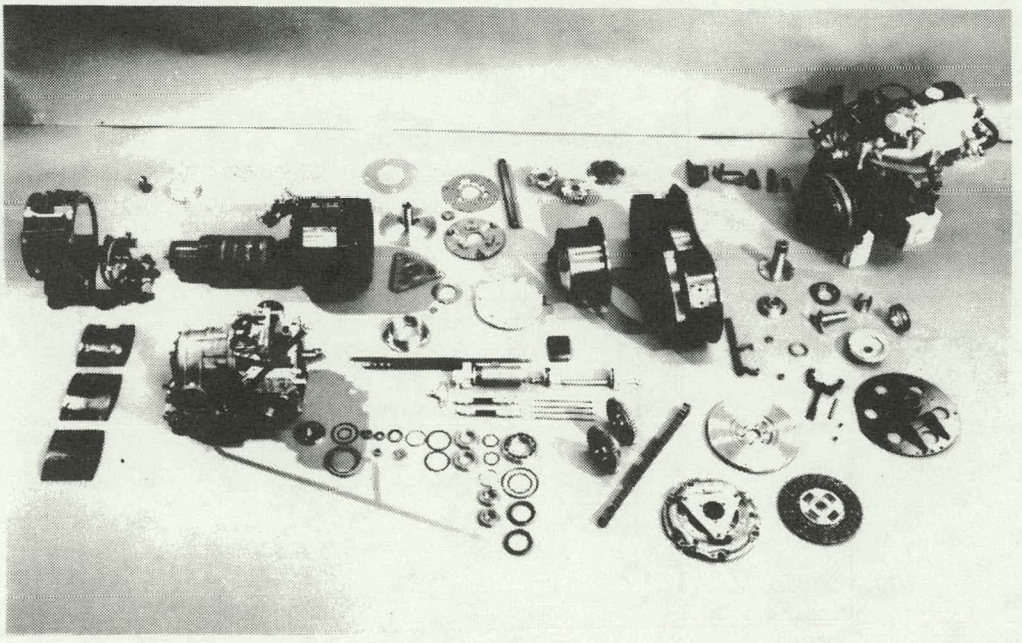

Figure 5.5-2. Drive Components of Test Bed Mule

The primary differences between the TBM and the HTV driveline can best be understood by referring to Figure 5.5-3, which is a schematic diagram of the TBM driveline. The most obvious difference is the fact that the engine and the electric motor are on a common shaft. The purpose of this arrangement is to utilize the inertia of the electric motor armature as a supplement to the engine flywheel inertia. For packaging reasons, the assembly is installed into the vehicle in a longitudinal fashion as opposed to the transverse arrangement employed in the HTV configuration. This requires a transaxle, which incorporates a right-angle drive. A further difference is that the electric motor cannot be declutched from the driveline. Later modifications to the HTV software resulted in the HTV being operated as a single-shaft unit.

In order to facilitate rapid starting and stopping of the engine for on-off operation, the standard engine flywheel was removed and a new clutching member was designed and fabricated by VW. This clutch is unique in that the disc section of the clutch is connected to the crankshaft of the engine in order to minimize the rotating inertia of the engine. The flywheel inertia, not directly a part of the engine, is then the sum of the clutch pressure plate and the motor armature inertia. In order to serve as an effective flywheel for the engine, the connection between the clutch pressure plate and the motor armature must be torsionally very stiff. This requirement is complicated by the fact that there is considerable distance between the engine and the motor, as dictated by the position of the driveaxle shaft. Additionally, packaging considerations require that the transfer drive from the engine/motor combination must be located between the two prime movers.

Dimensional tolerances on the distance between the rear face of the case of the engine and the motor posed some difficulties due to the large number of individual components/parts between them. This tolerance problem was solved by the utilization of a

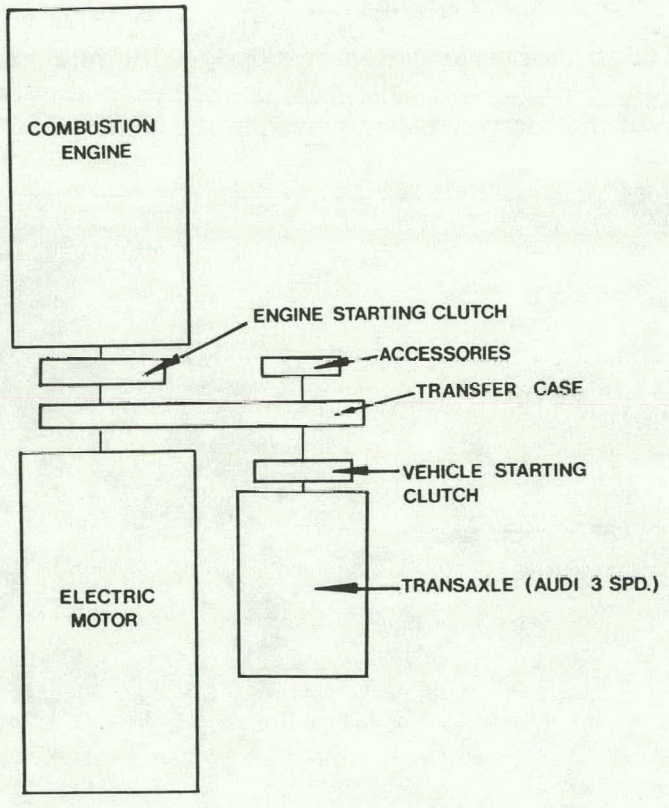

Figure 5.5-3. Schematic Diagram of Test Bed Mule Driveline

Figure 5.5-4. Torsional Damper Components

"flex plate" drive between the engine and the motor. Figure 5.5-4 is a photograph of the components which comprise this assembly. The triangular flex plate tolerates axial dimensional variations while connecting the engine to the motor in a torsionally stiff manner. In order to minimize the possibility of fretting in the splined connections, all of the splines are press fit.

Figure 5.5-5 is a sectional view through the drive housings, illustrating the location of the major components. Power is transmitted from the engine and the motor to a torsional damper located between the engine and the motor. This element provides some torsional flexibility in the drive system, as well as some damping, in order to smooth the torque pulsations transmitted to the chain and eventually to the transaxle.

The output torque is then transferred to the transmission input shaft via a Type 2300 Hy-Vo chain drive. The unit has a 0.5033 in. pitch and is 0.75 in. wide. An overall ratio of 1.025:1 (41/40 teeth) is employed in order to utilize at least one prime numbered sprocket. The chain and its bearings are pressure lubricated by the transmission pump, which is shared with the transfer drive housing. Figure 5.5-5 illustrates the components in the torsional damper, while Figure 5.5-6 depicts the chain, sprockets, and housing.

The vehicle drive clutch is located on the transmission input shaft centerline and is driven by the chain. The clutch-driven disc is connected to a new transmission input shaft. The pressure plate and disc are supported by their own bearing set, which is driven by the smaller chain sprocket. Clutch actuation is manual with the release forces applied through an unusual fingered cup to accommodate the accessory drive. A General Motors X-body clutch is employed, but the pressure plate has been modified to include provision for the accessory drive. Figure 5.5-7 illustrates the vehicle starting clutch components, as well as the accessory drive flex plate, which is bolted to the clutch pressure plate. Torque is transmitted from the accessory drive hub to the accessory drive pulley. Additionally, the center of the hub is splined to accept a new, longer, oil pump drive shaft for the transmission.

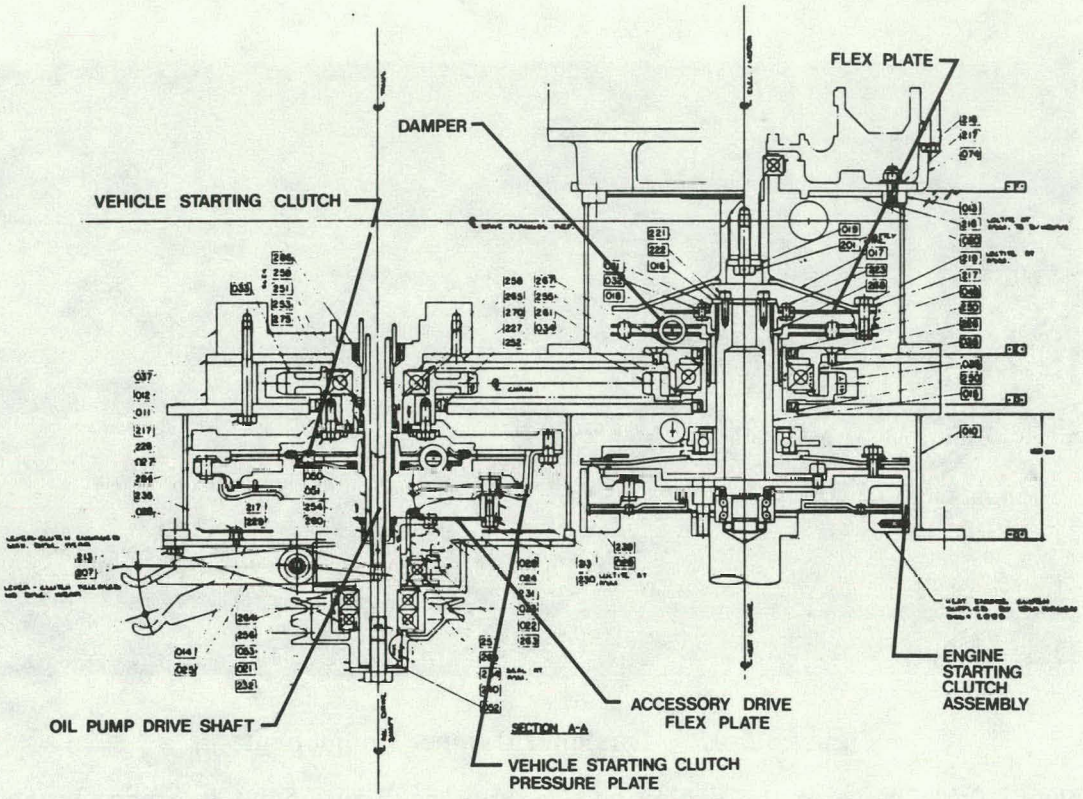

Figure 5.5-5. Sectional View of TBM Transfer Drive Unit

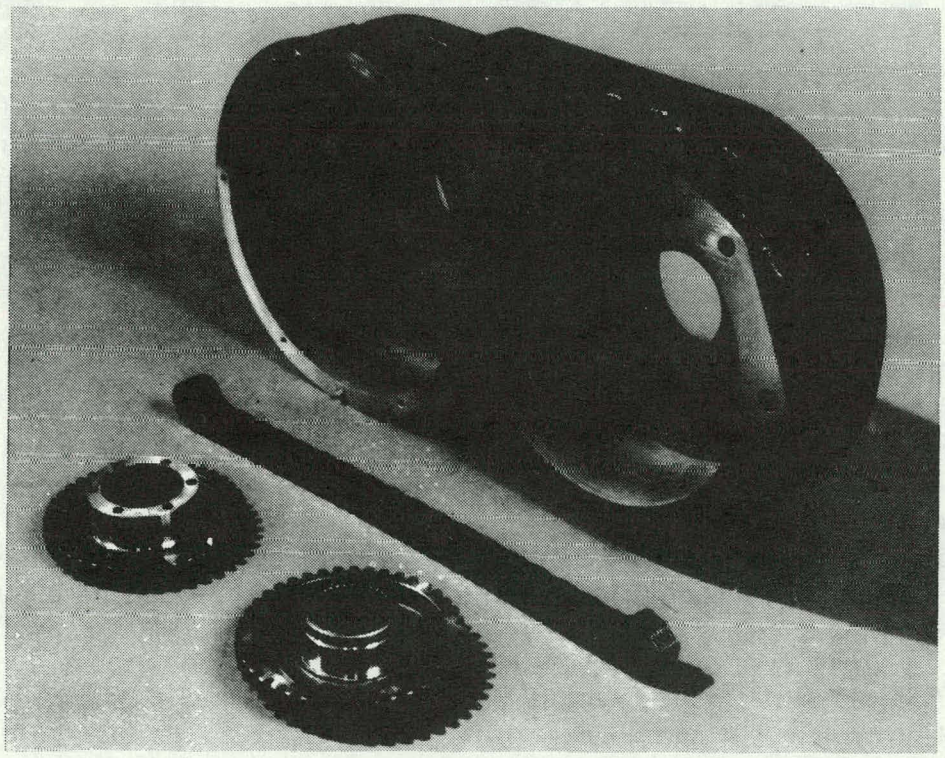

Figure 5.5-6. Transfer Drive Chain, Sprockets, and Housing

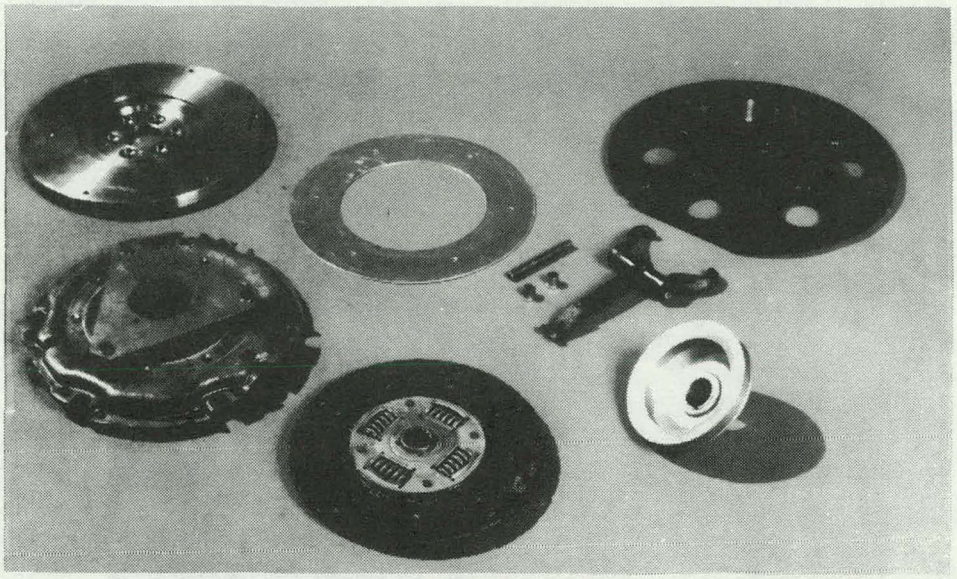

Figure 5.5-7. Vehicle Starting Clutch, Accessory Drive Flex Plate

A modified Audi 5000 transaxle is used in the TBM. The Audi 5000 transaxle modifications include:

1. Removal of the torque converter
2. Elimination of the torque converter housing
3. Fabrication of a new final drive pinion housing
4. New input shaft to accept the clutch input, incorporating revised oiling passages
5. New oil pump drive shaft
6. Elimination of the governor
7. Revised oil pan for shared lubrication with the transfer drive housing
8. Revised lubrication system to eliminate converter oil flow and to restrict lubrication flow
9. Revised hydraulic logic to permit manual shifting

Figure 5.5-8 is a photograph of the modified transaxle. A new axle shaft extension with flanges was also fabricated.

The engine starting clutch is actuated by a double-acting vacuum actuator operating from a series of vacuum accumulators. The required vacuum pressure is maintained by the same pump which provides vacuum for the brakes. In order to prevent inadvertent application of the engine starting clutch during the startup sequence of the electric motor, the linkage employed to operate the clutch has an over-center feature. Once the clutch has been released, the linkage will hold it in that position until the vacuum actuator force has been reversed.

5.5.1.3 Test Bed Mule Controller

The Test Bed Mule propulsion system is shown in Figure 5.5-9. The propulsion system is controlled by a single-board INTEL 8086/12 microcomputer. The microcomputer controls the operation of the electric motor, the heat engine, the heat engine clutch, and the optimum shift points for the transmission. The output power of both the heat engine and the electric motor are controlled by the microcomputer, using feedback control. The total power demand is dependent on the accelerator pedal position. When both power sources are operating, the

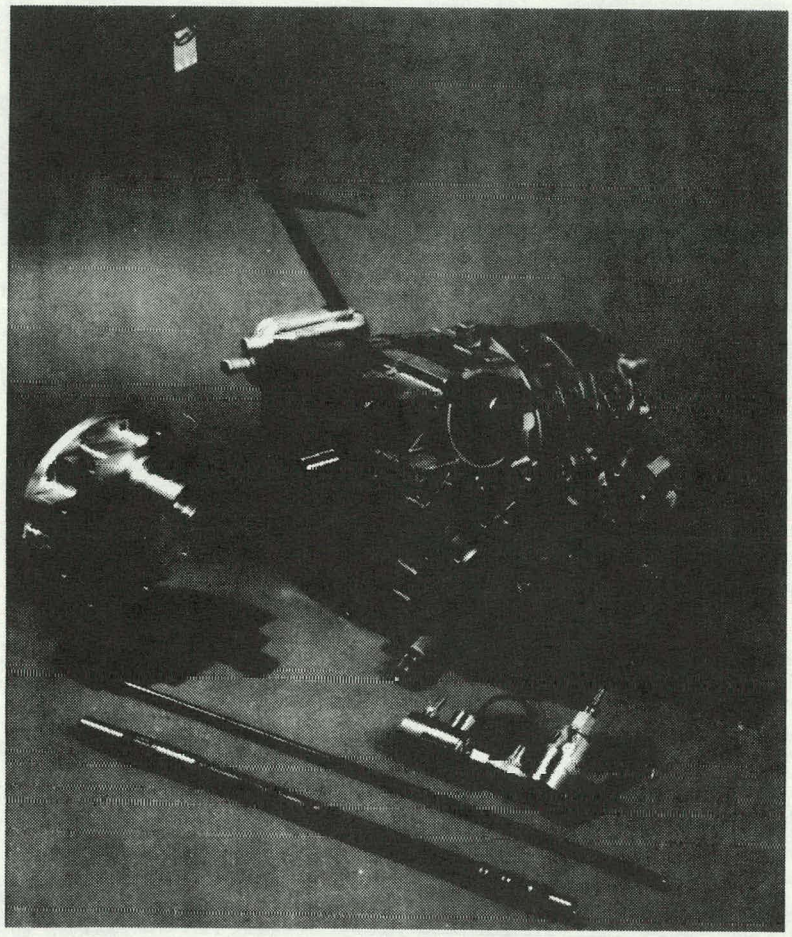

Figure 5.5-8. Modified Transaxle

output of each machine is proportional to its capability. The heat engine is used primarily for highway operation and for city operation only when the power demand exceeds the capability of the electric motor and/or the battery state-of-charge is low.

The similarities between the TBM controller and the HTV controller make it possible to consider the TBM controller a subset of the HTV controller. Figure 5.5-10, a simplified TBM/HTV propulsion sequencing diagram, identifies the commonality and differences between the propulsion sequencing for the controllers. In the TBM, unlike the HTV, the heat engine is not used to charge the batteries when the battery state-of-charge goes below 20%. Also, no regeneration is allowed in the TBM controller. The main drive clutch (or electric motor clutch) in the TBM is manually controlled by the driver in contrast to that of the HTV, which is modulated automatically by the microcomputer. The battery charger for the TBM is an offboard component and not under microcomputer control. The transmission for the TBM is a manually-shifted three-speed automatic transmission. The shift points are determined by the microcomputer, which displays to the operator the upshift/downshift commands and the present gear. The operator uses this information for gear shifting. These differences between the TBM and the HTV controllers result in a simpler controller for the Test Bed Mule.

The heat engine and electric motor power feedback control systems are identical for both the TBM and the HTV. System analysis and design of the heat engine and electric motor feedback control systems have been described in detail in Section 5.3.6.1.

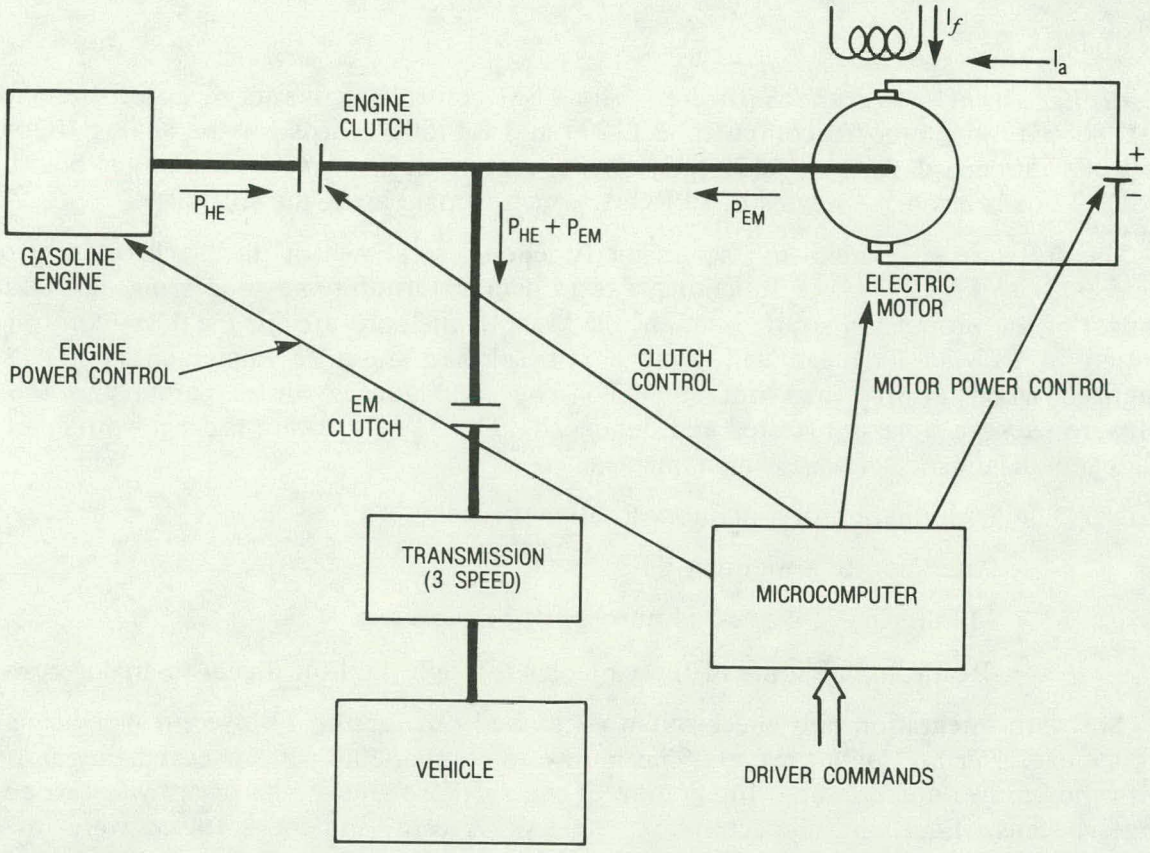

Figure 5.5-9. Test Bed Mule Propulsion System

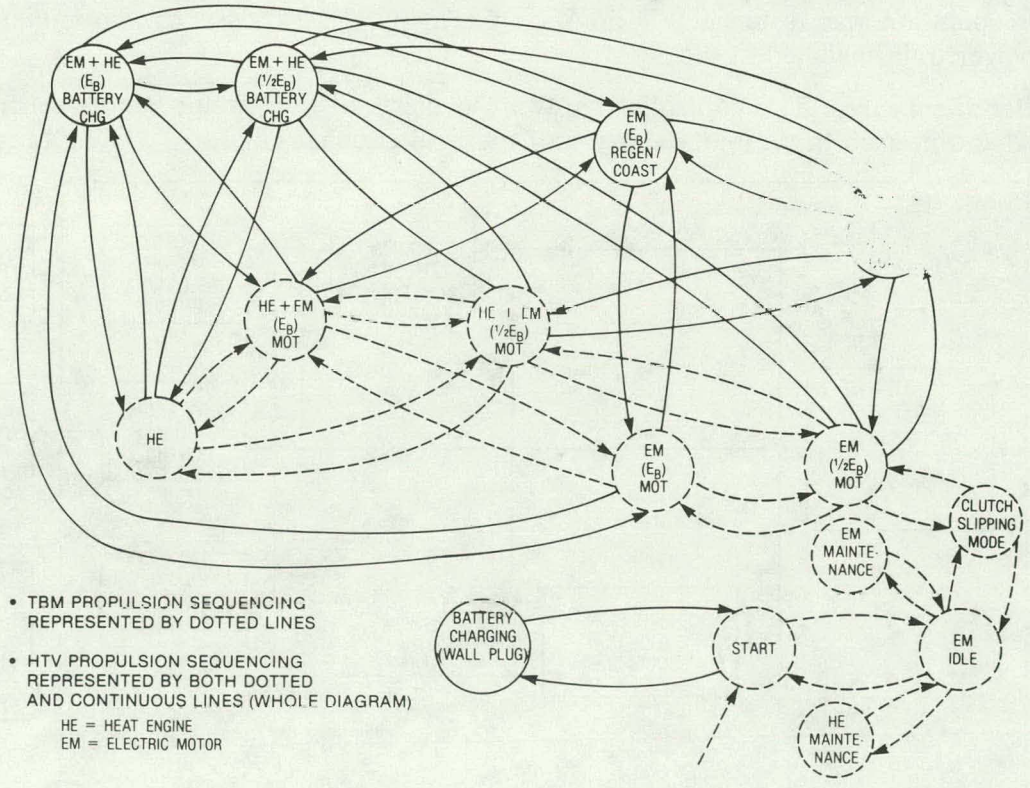

Figure 5.5-10. Simplified TBM/HTV Propulsion Sequencing Diagram

Controller Architecture and Software. The TBM controller consists of an off-the-shelf INTEL 8086/12 single-board computer, RT1200 and RT1201 boards for the analog I/O signals, an SBC 556 board for the logic I/O, and a custom-built signal conditioning board. The 8086/12 board has 4 x 4 kbytes of EPROM, which contain all of the software.

The software is divided into six major functions, as shown in the block diagram of Figure 5.5-11. All of the major functions, except data acquisition and processing, are under the control of the propulsion source sequencer. Most of the software for the TBM controller was written in PLM86 language with only a few selected modules implemented in assembly language when PLM86 was not suitable. The individual modules comprising the TBM software package were unit-tested and debugged. The TBM software package contains the debug panel diagnostic software which enables:

- Examination of a memory location charter
- Alteration of a memory data
- Monitoring of a selected number of variables
- Recording of some of the variables through the four digital-to-analog converters

Software integration and check-out were carried out for the TBM controller using a controller exerciser and debug panel. The hardware components were checked out individually with the hardware exercisers. Integration of the software and the hardware was carried out in several steps. First, the contactor box, the IA/VA card, and the software were integrated. Next, the field chopper was tested under microcomputer control. After all of the sensor signals were checked out, the microcomputer sequencing functions relating to operation of the electric motor were checked out with the electric motor on a dynamometer. The heat engine mode of operation was tested at VW in West Germany, on a chassis dynamometer with the hybrid power train installed in the TBM.

Controller Hardware. The controller hardware consists of five circuit boards set in an Intel card cage and housed in a cabinet along with the field chopper circuitry, cooling fans, isolated

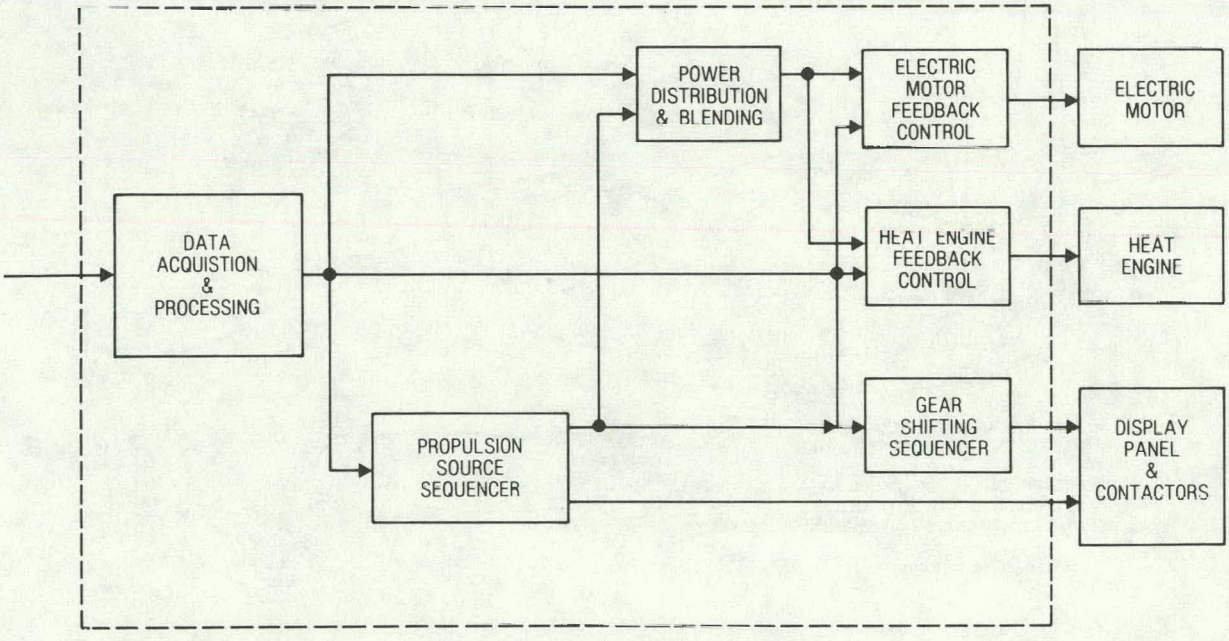

Figure 5.5-11. Functional Block Diagram of TBM Controller Software

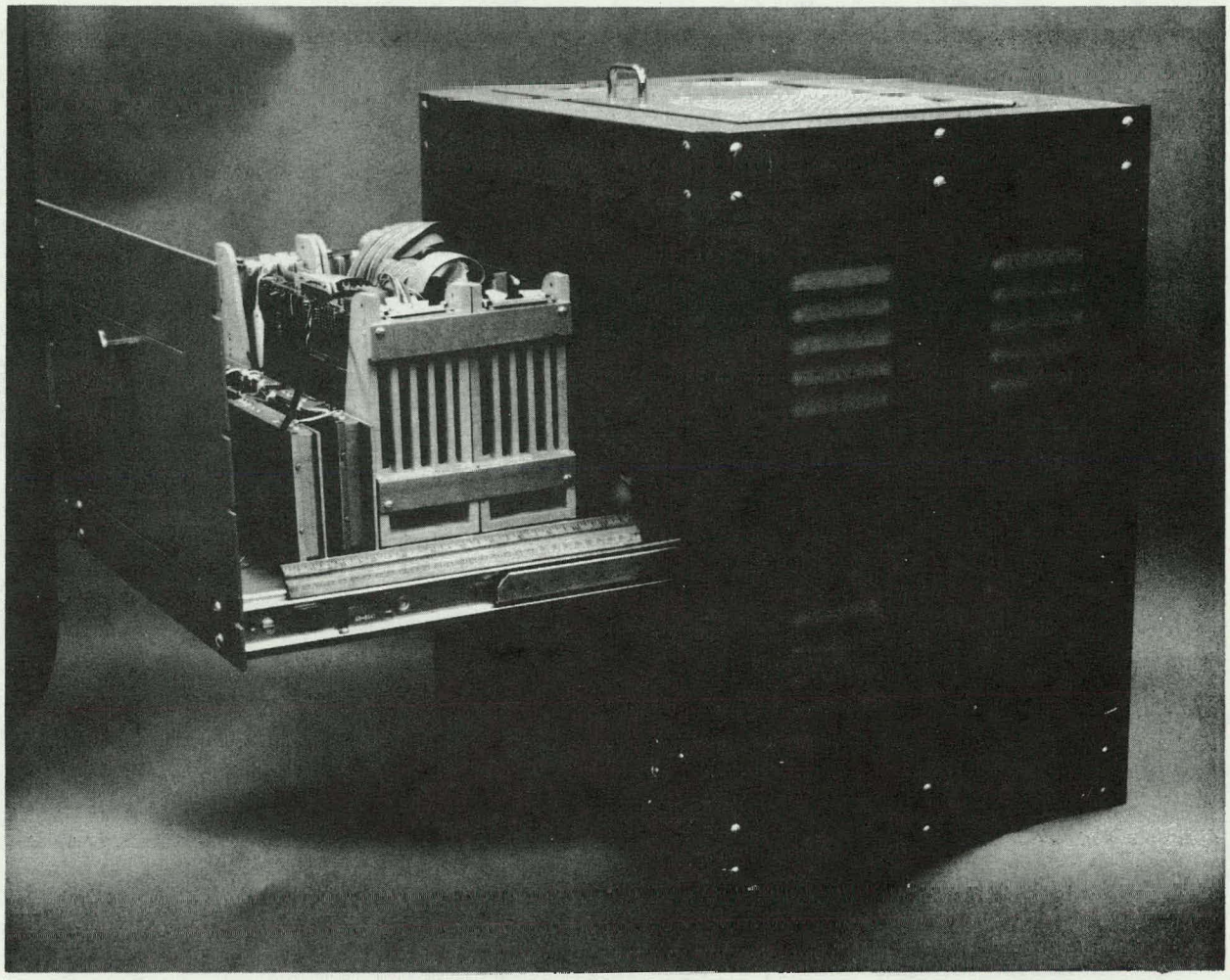

Figure 5.5-12. Controller Hardware Mounted in a Cabinet

power supplies, and support wiring (Figure 5.5-12). Of the five boards, four are commercially produced, and one is a custom board designed and built by General Electric. The commercially available ones are: the iSBC-86/12 microcomputer board, which performs the data manipulation and control functions by executing programs resident in on-board ROM memories; the RTI-1200 and RTI-1201 boards, which perform all analog-to-digital and digital-to-analog conversions; and an iSBC-5S6 board, which provides opto-isolation of digital input signals. The custom board (Figure 5.5-13) provides isolation for analog input and output signals, debounces the switch inputs, interfaces the debug panel to the controller, and provides signal conditioning for pulse-frequency-modulated inputs.

5.5.1.4 Engine Throttle Control System

This subsection describes the engine throttle control system and its bench and vehicle testing.

System Description. This system (Figure 5.5-14) employs a pneumatic servo for mechanical operation of the throttle. When vacuum is applied to the servo, a rubber diaphragm operates the throttle via a linkage. An electronic control unit regulates the vacuum supplied to the servo by closing or opening electromechanically controlled valves. The vacuum itself is created by a small electric pump, which evacuates a plastic container when the key switch is turned on. The pump is turned off by a switch when a vacuum of 0.6 bar is achieved in the container. The system also achieves vacuum by tapping the intake manifold of the engine.

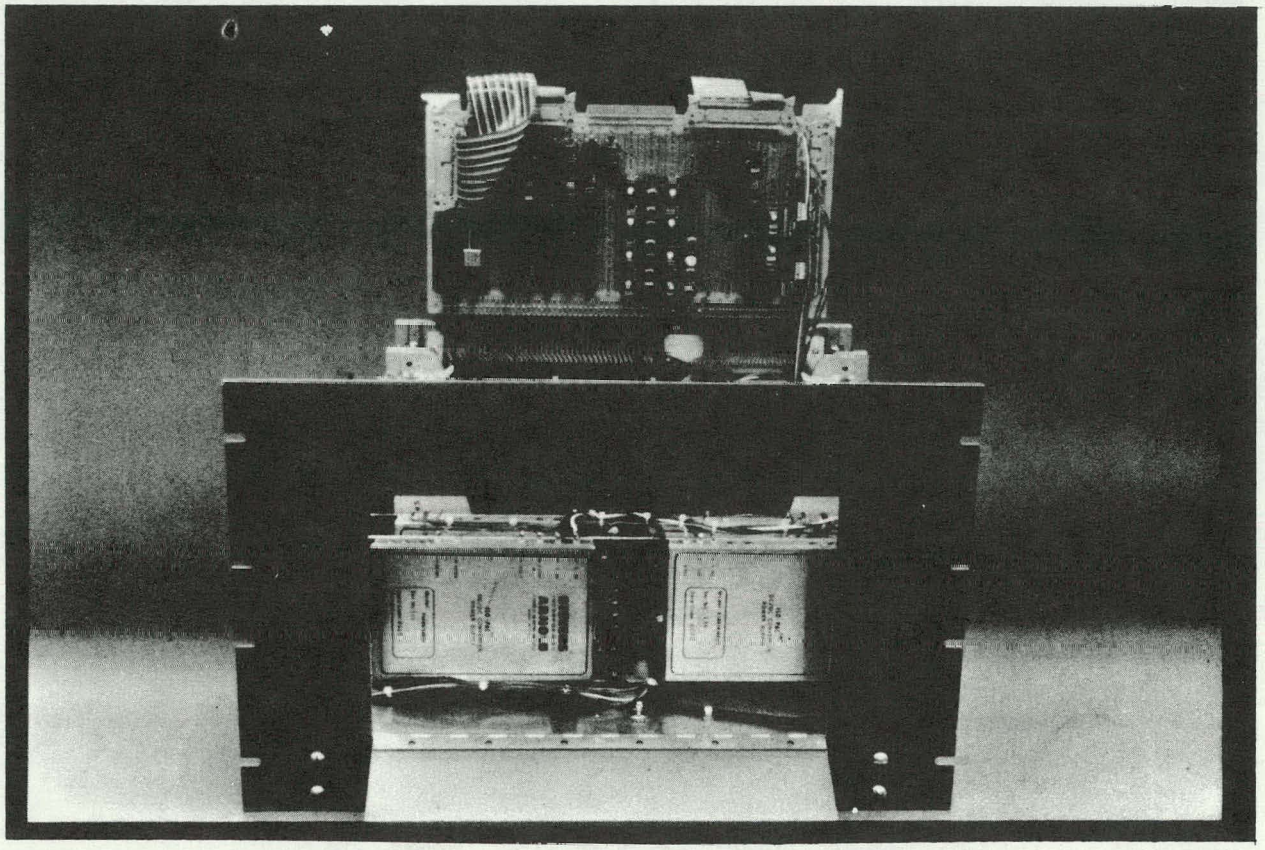

Figure 5.5-13. TBM Custom Signal Conditioning Board

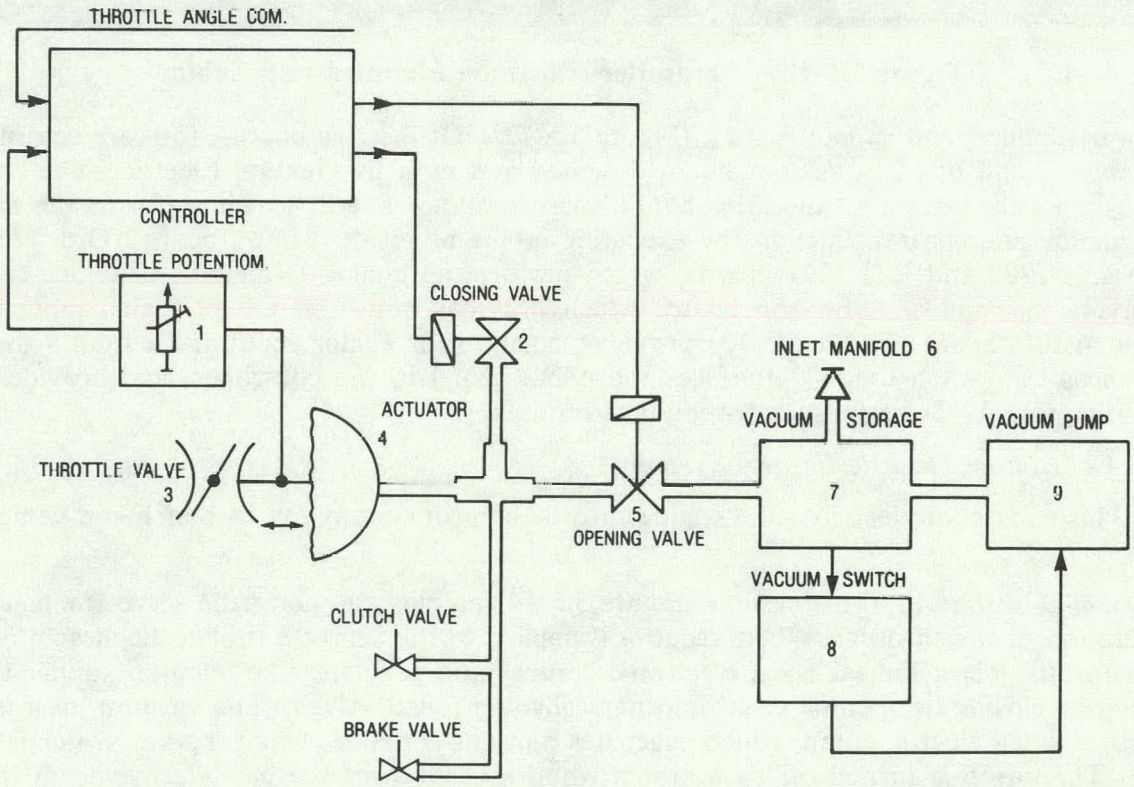

Figure 5.5-14. Block Diagram of Engine Throttle Control System

The reason a vacuum-actuated system was used rather than a stepper motor was because the four-cylinder gasoline engine causes significant vibration and shock loads. The vacuum servo is very simple and can withstand this environment. The throttle control unit used on the TBM is a modification of the production cruise control system used on the Audi 5000 and is built to withstand the automotive environment.

Bench and Vehicle Testing. A breadboard of the throttle control system was constructed for development testing in the laboratory. Photographs of the experimental setup are shown in Figures 5.5-15 and 5.5-16. After some development work, the throttle control unit exhibited the fast response shown in Figure 5.5-17. With a maximum vacuum of 0.5 bar, an opening time of 0.25 s and a closing time of 0.3 s were achieved. For those cases, the throttle was opened in 85 steps and closed in 105 steps. The response of the unit to more gradual accelerator pedal transients is shown in Figure 5.5-18.

After bench testing, the throttle control unit was installed in a VW Rabbit with a K-Jetronic fuel system. The car was driven on the road for about 500 km. After some initial difficulties with soldered connections on the throttle valve potentiometer, the unit functioned reliably. The only operational problem encountered in testing the throttle control unit in the VW Rabbit was that the throttle did not close rapidly enough during a downshift. This was solved by adding two mechanically operated valves, which were actuated when the clutch pedal or the brake pedal was depressed.

5.5.1.5 Power Train/Controller/Vehicle Integration

Integration and checkout of the hybrid power train, the power electronics, and the controller hardware and software in the Test Bed Mule were started in early December 1980. By the

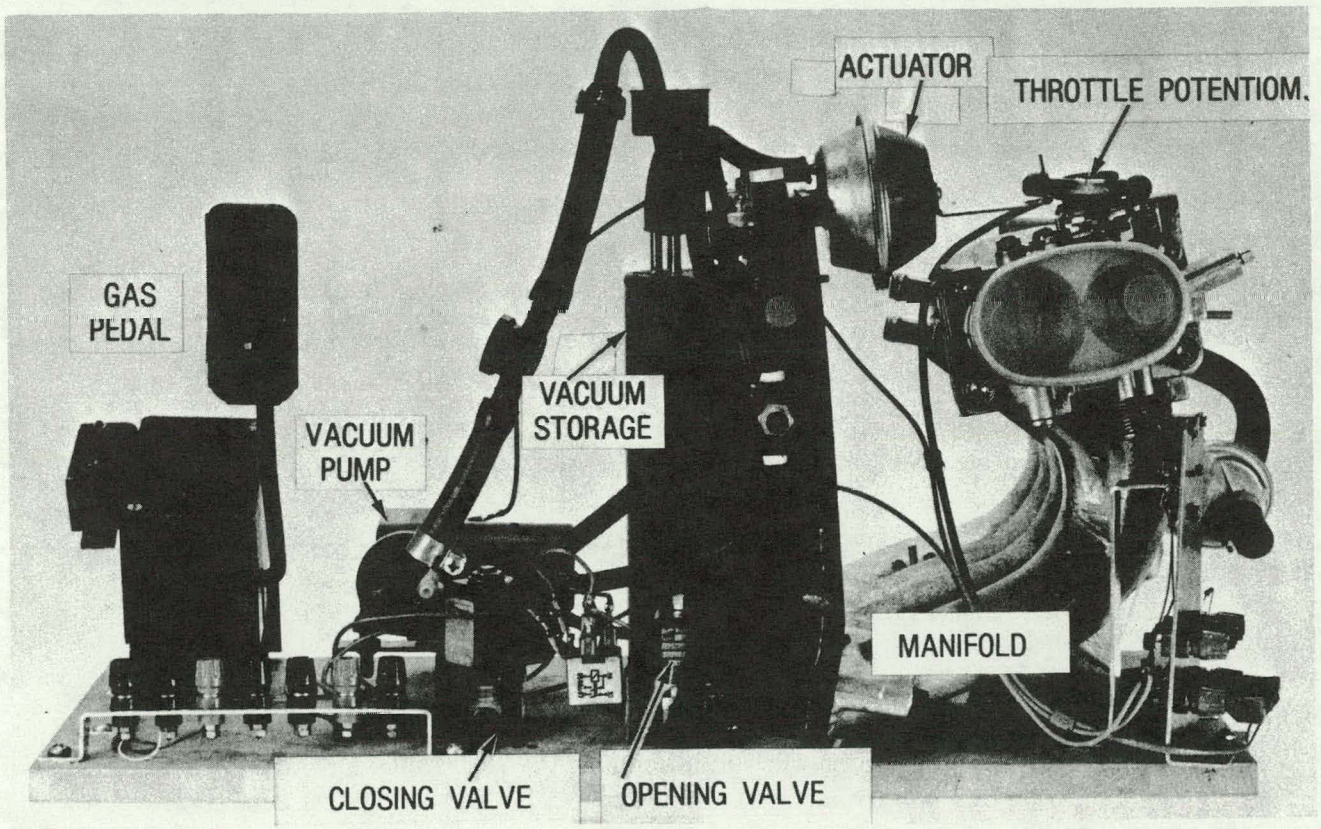

Figure 5.5-15. Throttle Control Bench Test (front view)

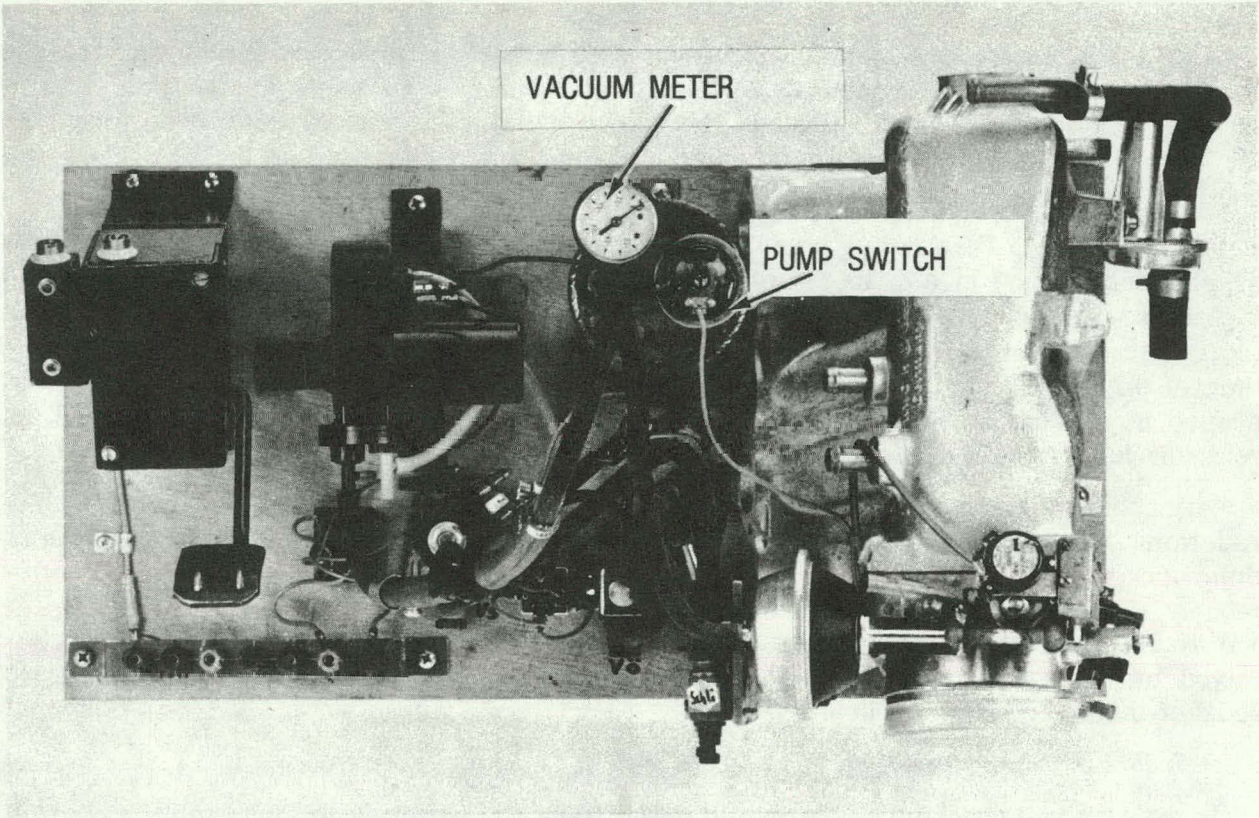

Figure 5.5-16. Throttle Control Bench Test (rear view)

end of February 1981, integration and checkout were completed and the TBM was functioning satisfactorily on a chassis dynamometer in the Electric/Hybrid Vehicle Laboratory at VW, Wolfsburg, Germany. The checkout effort included:

- Static and transient calibration and response tests of all of the sensors in the vehicle
- Verification of the electric drive system sequencing from key turn-on through motor idle and battery switching
- Transient tests of the stability and response of the heat engine feedback control system
- Verification of the accuracy of the computed gear ratios and the reliability and correctness of the controller-determined shift and clutching signals
- Tests of power train sequencing during blending of the outputs of the electric motor and the heat engine for the complete range of battery state-of-charge (V_{MOD} varied from 15 mph to 75 mph)
- Functional check of the complete power train/controller by performing rapid vehicle accelerations by making step-changes in the accelerator pedal position

5.5.1.6 TBM Vehicle Tests

The Test Bed Mule (TBM) was tested on a chassis dynamometer and the track at Volkswagon in Wolfsburg, West Germany between February and September 1981. Additional tests on a chassis dynamometer were conducted at the Jet Propulsion Laboratory in Pasadena, California, between December 1981 and May 1982. The TBM test results are given in References 6 and 7.

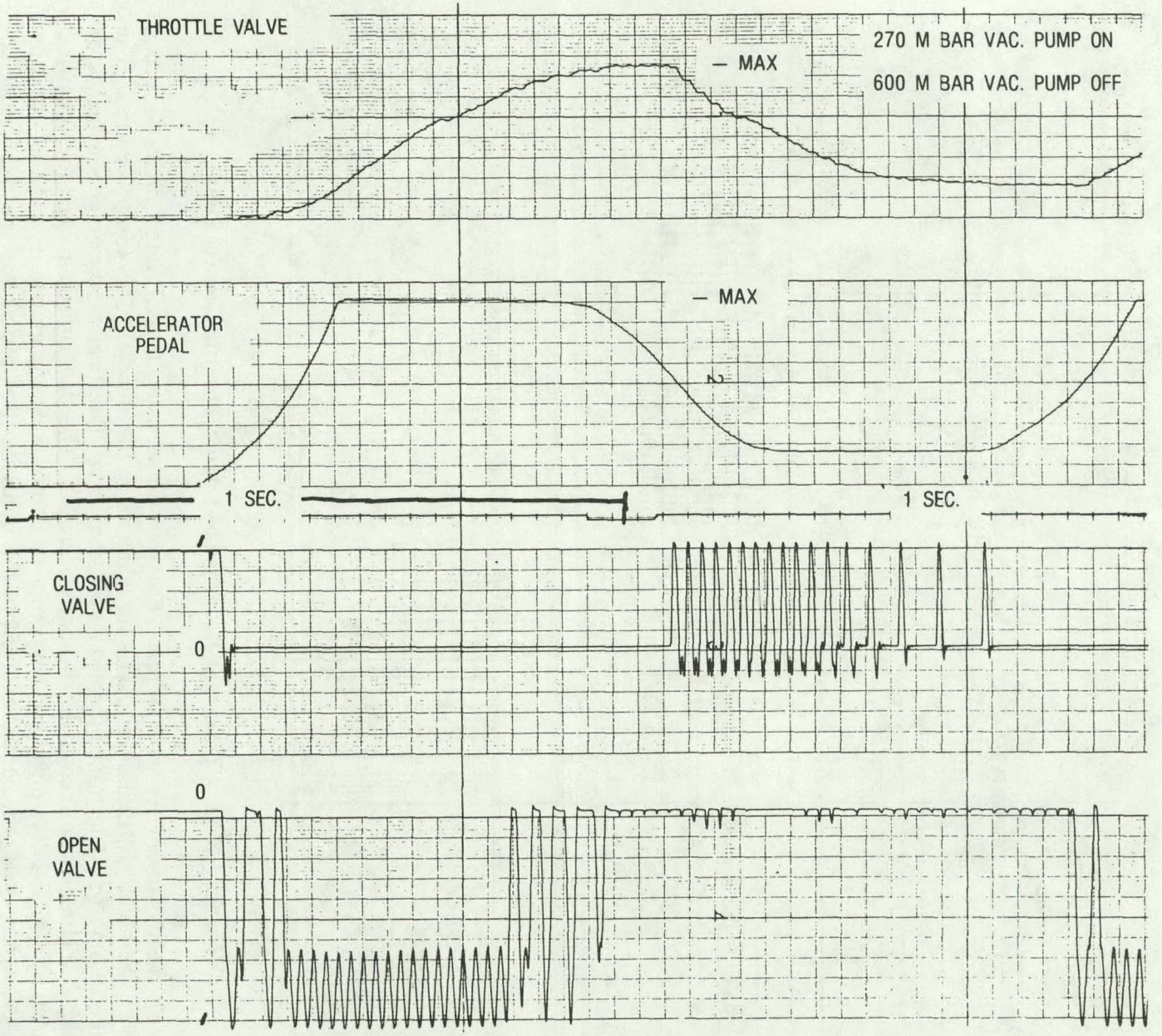

Figure 5.5-17. Response of Engine Throttle Control Unit to Step Changes in Acceleration Pedal

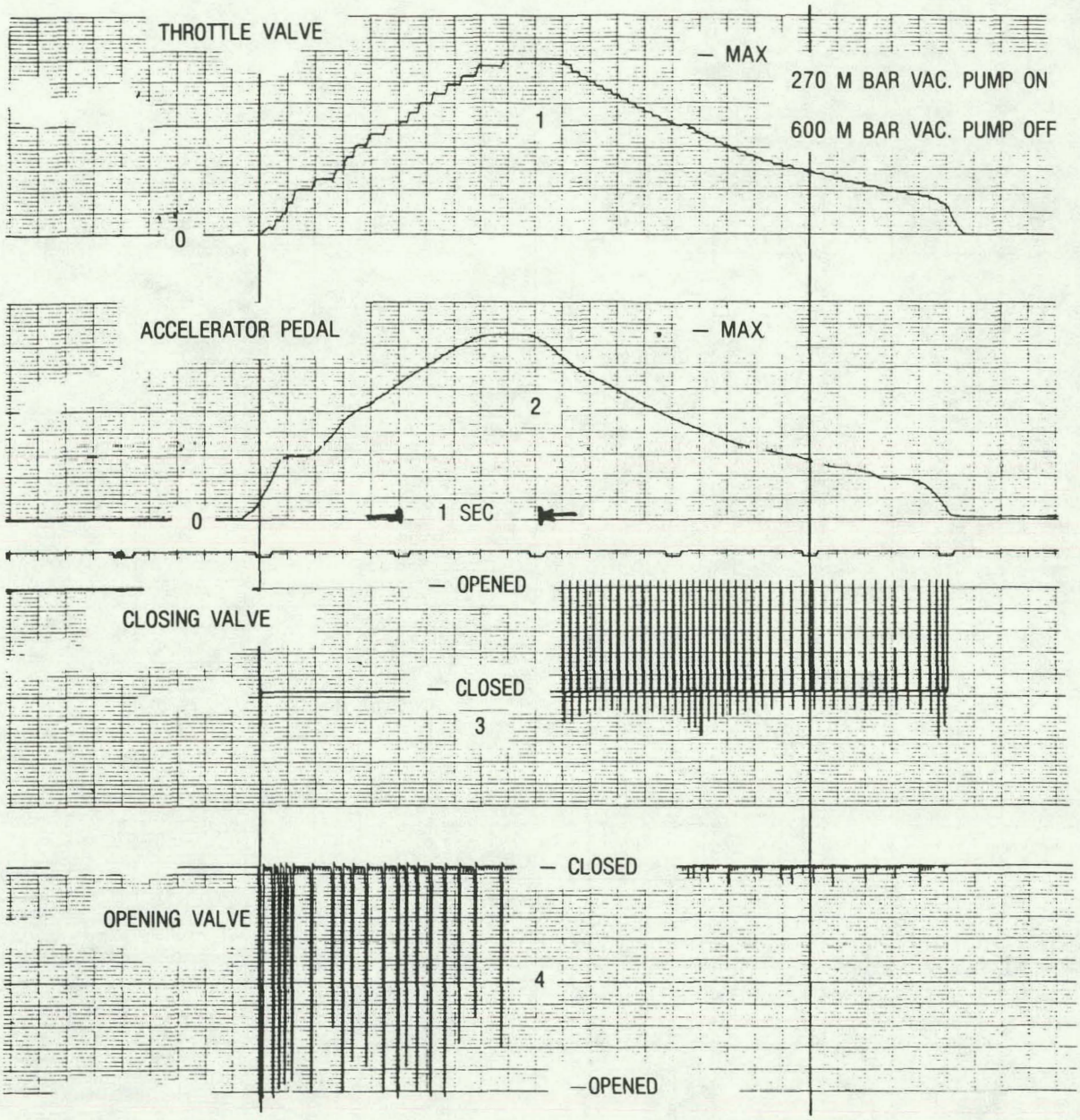

Figure 5.5-18. Transient Response of Engine Throttle Control Unit

All the dynamometer tests of the TBM were done using the EPA test cycles — urban (FTP) and highway. Emissions data were taken using the standard CVS test procedures. The fuel economy was determined from the emissions data. Electrical energy usage was measured using a WH-meter connected in the battery circuit. The data obtained were the following: gm/mi HC, CO, NO_x, mpg, and kWh/mi. In determining the emissions and fuel economy for the urban cycle, the contribution from the transient (first 505 s) and the stabilized (505-1372 s) portions of the cycle were added and then divided by the total distance (7.5 mi) of the cycle. For the hybrid vehicle, the contribution of the transient portion was not obtained by averaging cold transient and hot transient tests as is done for a conventional ICE vehicle, because the battery states-of-charge would be different if the cold and hot transients were run in the usual manner (that is, cold transient, stabilized, and hot transient run in succession).

The control strategy of the hybrid power train in the TBM can be varied from test-to-test by setting (turning a knob) different values of V-mode on the control panel of the vehicle controller. In the TBM tests, V_{MOD} was varied from 20 mph to 70 mph. In the later case, the TBM operated as an electric vehicle except when the power demand exceeded the maximum (30 kW) capability of the electric drive system. When that occurs, both the heat engine and the electric motor are operated and the TBM uses both gasoline and electricity. It was of particular interest in the TBM tests to determine how the emissions and fuel economy changed with V-mode and how the measured values compared with the computer predictions obtained using HYVEC.

The TBM test results are summarized in Table 5.5-2 taken from Reference 6. Comparisons between the test results and the HYVEC predictions are given in Figures 5.5-19 and 5.5-20. The agreement between the test data and the predictions is quite good over the complete range of V-mode. The comparisons are made using the hot-start test data because the effect of the cold start on engine operating characteristics is not included in the HYVEC computer simulation.

The TBM fuel economy test results show good promise for gasoline savings using hybrid vehicles. For a V-mode of 70 mph, the measured fuel economy was 109 mpg on the EPA urban cycle for a cold start and 59 mpg for a V-mode of 45 mph. This compares to 24 mpg for the 1982 Audi 4000 (I_w = 2500 lb) and 19 mpg for the 1982 Audi 5000 (I_w = 3000 lb). The highway fuel economy of the TBM was about 33 mpg compared with 32 mpg for the Audi 4000 and 28 mpg for the Audi 5000. Hence, if the effective electric range (that is the daily driving distance for which the V-mode can be kept at 45 mph or higher) of the TBM were in excess of 20 mi, it would be possible to save a large fraction (at least 50%) of the gasoline used by a conventional Audi by utilizing the hybrid power train. The limited testing done on the TBM indicates that the effective electric range of the TBM using the Yuasa lead-acid batteries is only 10-12 mi. This is due primarily to the fact that the effective energy density of lead-acid batteries at relatively high discharge rates is quite low (certainly less than 10 Wh/lb).

Table 5.5-2

TBM TEST RESULTS-CYCLE EMISSIONS AND FUEL ECONOMIES

Cycle	V-Mode (mph)	Engine Start Temp[2]	Fuel Economy (mpg)	Elec.[1] Eff. kWh/mi	Emissions (gm/mi) HC	CO	NO_x
Urban (7.5 mi)	70	Hot	145	0.63	0.16	0.34	0.13
		Cold	109	0.67	0.59	4.3	0.25
	45	Hot	75	0.55	0.12	0.24	0.13
		Cold	59.1	0.55	0.52	2.84	0.47
	20	Hot	24.7	0.29	0.31	1.2	0.13
		Cold	23.9	0.21	0.88	5.9	0.34
Highway (10.1 mi)	45	Hot	32.9	0.038	0.24	1.16	0.30

(1) Wall plug output - battery and charger efficiency assumed at 75%.
(2) Cold means about 70 °F, hot means warmed to > 122 °F.

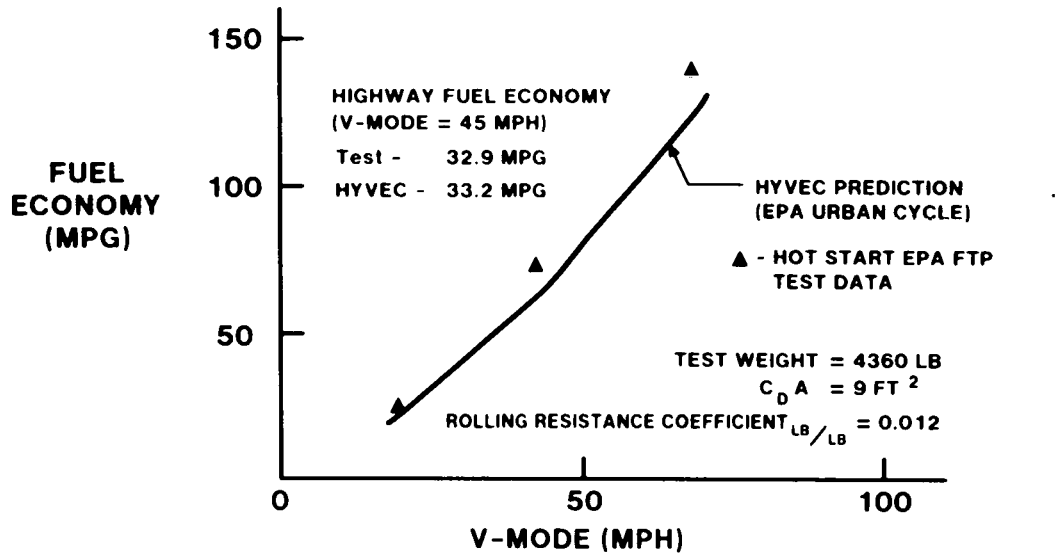

Figure 5.5-19. Comparison of TBM Fuel Economy Test Data and HYVEC Predictions for the EPA, Urban, and Highway Cycles

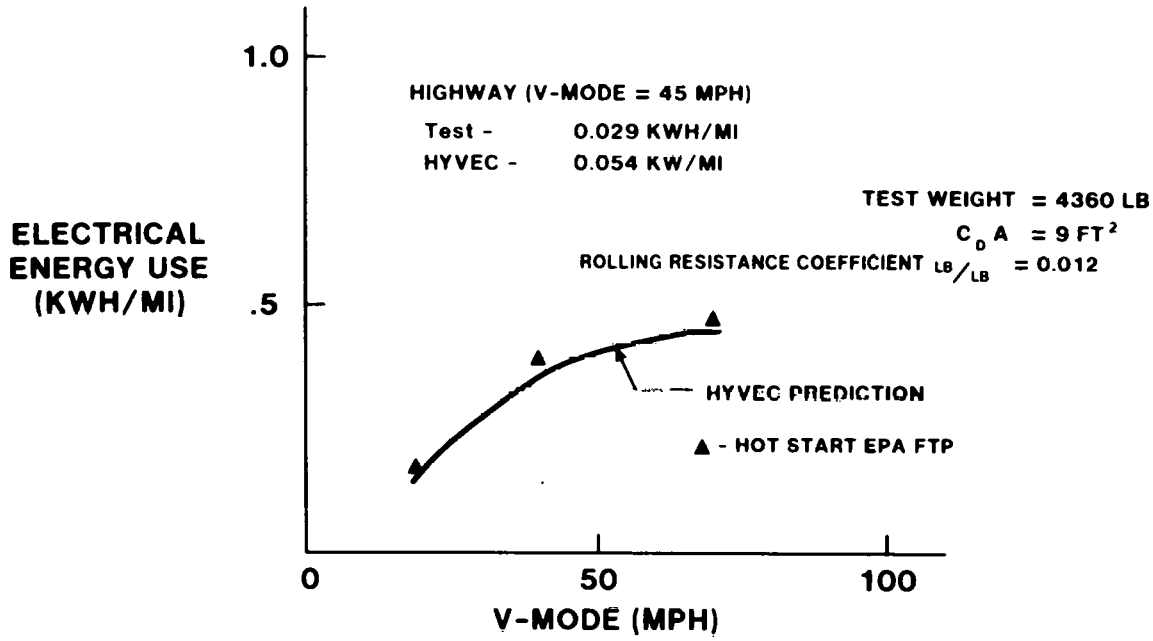

Figure 5.5-20. Comparison of TBM Electrical Use Data and HYVEC Predictions for the EPA, Urban, and Highway Cycles

The TBM emissions data indicates that the on/off operation of the engine does not result in high emissions. With little or no development effort to reduce emissions, the TBM emissions were quite close to the 1981 emission standard of 0.4 gm/mi HC, 3.4 gm/mi CO, and 1.0 gm/mi NO_x. The NO_x emissions were quite low (less than 0.4 gm/mi for nearly all cases). The HC and CO emissions were sensitive to cold-start and enrichment procedures on which little work was done as part of the present program. Hence, the TBM emissions data

indicate that emissions should not be a problem in utilizing the hybrid power train concept. The procedure for utilizing EPA cycle emissions data for calculating the effective average emissions of a hybrid car, such as the HTV, operating over a variety of modes (i.e., high VM, low VM, battery charging, etc.) has not been determined as yet by EPA (no need for such a regulation exists). Hence emissions data from the TBM and HTV are useful only for engineering purposes and for rough comparisons with conventional ICE vehicles.

5.5.2 Structural Mule

The structural mule provided an opportunity to evaluate the overall crash performance of the hybrid vehicle structure with sufficient leadtime to be beneficial to the final HTV design. The construction of the structural mule was a design check for component fabrication, packaging, and interfacing with the 1980 General Motors A-body occupant compartment. The mule structure was to provide the basis for material selection and structural fabrication techniques which were unique to the hybrid vehicle design.

The front structure and packaging of the hybrid vehicle is different from conventional vehicle systems. Therefore, there was no real precedent to follow in the design of the HTV crash structure. Hence, careful analysis and component testing was necessary to provide design direction early enough in the program to affect the final HTV configuration.

5.5.2.1 Base Vehicle Selection

The structural mule was based on a modified 1980 General Motors A-body automobile (Buick Century). The mule was structurally identical to the HTV design and maintained intact the occupant compartment of the GM A-body. Although the structural mule was not to be operable, all of the front compartment masses were installed. The mule front structure firewall and underbody were constructed to the HTV preliminary design specifications.

The structural energy absorption components, the battery containment provisions, and the main load bearing members reflected the most advanced design achievable through crash analysis and static testing.

5.5.2.2 Body and Chassis Design

A Buick Century body was sectioned, and the main occupant compartment was used to construct the mule prototype. The suspension system used the General Motors E-body configuration for the front and used modified General Motors X-car rear components. An all-new steel fabricated underbody and firewall were integrated into the remaining A-body shell.

The structural mule was built following the HTV design. The body panels obtained from the hybrid test vehicle clay model included the most recent flanging and attachment provisions dictated by the HTV final design goals. The panels primarily provided exterior body surfacing and did not contribute to vehicle structural requirements. However, their influence in both road load and crash structural requirements has been analyzed. The body panels consisted of hand layed-up fiberglass and epoxy resin. Their mechanical attachment to the underbody structure represented the functional and durability requirements of the final design, while providing the structural crash requirements necessary for collision energy management of the external body skins.

The structural mule chassis components and substructural elements were representative of the final HTV design. The A-body vehicle was sectioned and modified to accept the complete HTV front and rear suspension systems. The complete floor panel and firewall panels were removed and modified to the HTV design.

An all-new front structure and rear structure were integrated into the existing A-body-in-white. These components were designed and evaluated extensively during the static and dynamic crashworthiness phases. The fabrication techniques and material selections were based on component testing and computer analysis.

5.5.2.3 Drive Components

The structural mule was to be a nonfunctional vehicle system. The drive line components were represented by either nonoperating hardware or simulated structural masses. A nonoperative Volkswagen engine was coupled through the hybrid vehicle drive case and the X-body transmission to a fabricated electric motor housing. The drive-line components were mounted to the structural mule chassis through the HTV design mounting systems. All of the drive-line clearances were maintained in order to ensure correct dynamic responses during the barrier collision. The HTV battery subsystem was to be simulated by Globe Group 27 batteries and lead weights, which duplicated the correct battery dimensions and weights of the final Globe HTV battery design. The battery box was a hand layed-up fiberglass construction with steel cross members bolted to the chassis structure. Batteries were wired and contained as in the HTV design. The watering system and the electrolyte air distribution hardware were not present. Therefore, the Group 27 vent caps were installed, and the battery cells and crash performance of the battery system were to be based upon currently available hardware.

5.5.2.4 Fabrication Methods

The mule structure was fabricated according to the final HTV design. Subsystem assembly and attachment procedures followed the guidelines established during static crush component testing. The materials utilized and the welding procedures incorporated were identical to those used on the static test mule and subsequently to be used in the final HTV construction.

5.5.2.5 Scheduled Tests

The structural mule was scheduled to undergo a series of nondestructive structural tests. These tests would have included evaluation of overall vehicle chassis torsional stiffness and beaming. The resultant vertical and angular displacement was to be recorded and analyzed for comparison to the base line General Motors A-body. Equivalent or comparable results would have provided insight into the HTV handling and ride characteristics.

The construction of the structural mule was nearly completed when the decision was made by DOE and JPL to utilize that vehicle for the final HTV in order to reduce the cost and scope of the Phase II program (Contract Modification 17). Since the structural mule was structurally and chassis-wise identical to the HTV, this decision was relatively easy to implement. As a result of the decision, the scheduled non-destructive and 30 mph-barrier crash tests of the structural mule were cancelled.

5.5.3 Mechanical Components Mule

The Mechanical Components Mule allowed an early look at the function and fit of the components which make up the suspension, steering, brake, drive train, heating, ventilating, and air conditioning (HVAC), and hydraulic system, and their respective control. Development of these systems on a breadboard-type vehicle was economical. Updated design based on these early tests was implemented in the final HTV.

5.5.3.1 Base Vehicle Selection

A base vehicle which required a minimum of conversion time was the prime requirement. The General Motors E-body Oldsmobile Toronado filled this requirement, since it is a front-wheel drive vehicle and uses the same front suspension. In addition, the distance from the

front wheels to the dash panel was sufficient so that no major changes were necessary to that area. Modification of the rear suspension and the wheelbase presented less of a problem than did changing the body front end.

5.5.3.2 Body Modification

Body modification was restricted to three areas. The body was shortened to produce a 108.1 in. wheel base. This required the removal of five inches which were taken from the 'B' pillar area, where the fore and aft sections are almost parallel to the vehicle centerline. This allowed the rejoining of the parts without mismatch. Figure 5.5-21 shows where the body was sectioned. The second modification was required to the hood in order to clear the battery container. The third modification provided clearance for the rear suspension, which changed from an independent system to a beam type.

5.5.3.3 Frame Modification

Frame modifications were quite extensive. In addition to the removal of 5 in. to reduce the wheelbase to 108.1 in., major rework was necessary to fit the front and rear suspensions, steering, and power train. To provide an early look at those most important structural members, it was decided to include in the revision the HTV suspension mounting and power train support cross members. As the design of the HTV evolved, it became evident that space within the frame structure was at a minimum. This space limitation forced the modification of the frame from the front to the dash panel. Figure 5.5-22 shows the front end and Figure 5.5-23 shows the rear end of the modified frame.

5.5.3.4 Chassis Components

The Mechanical Components Mule, when completed, contained chassis components to the HTV level in the following areas:

- Front suspension

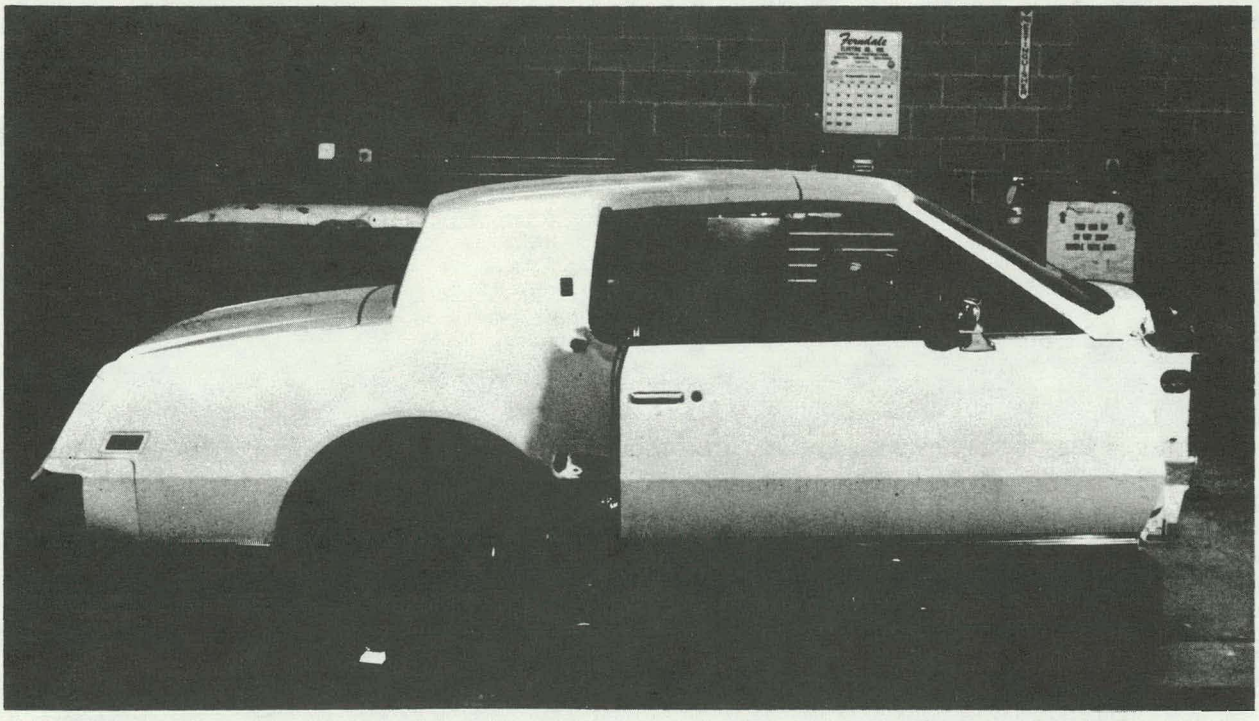

Figure 5.5-21. The Shortened Body of the Mechanical Components Mule

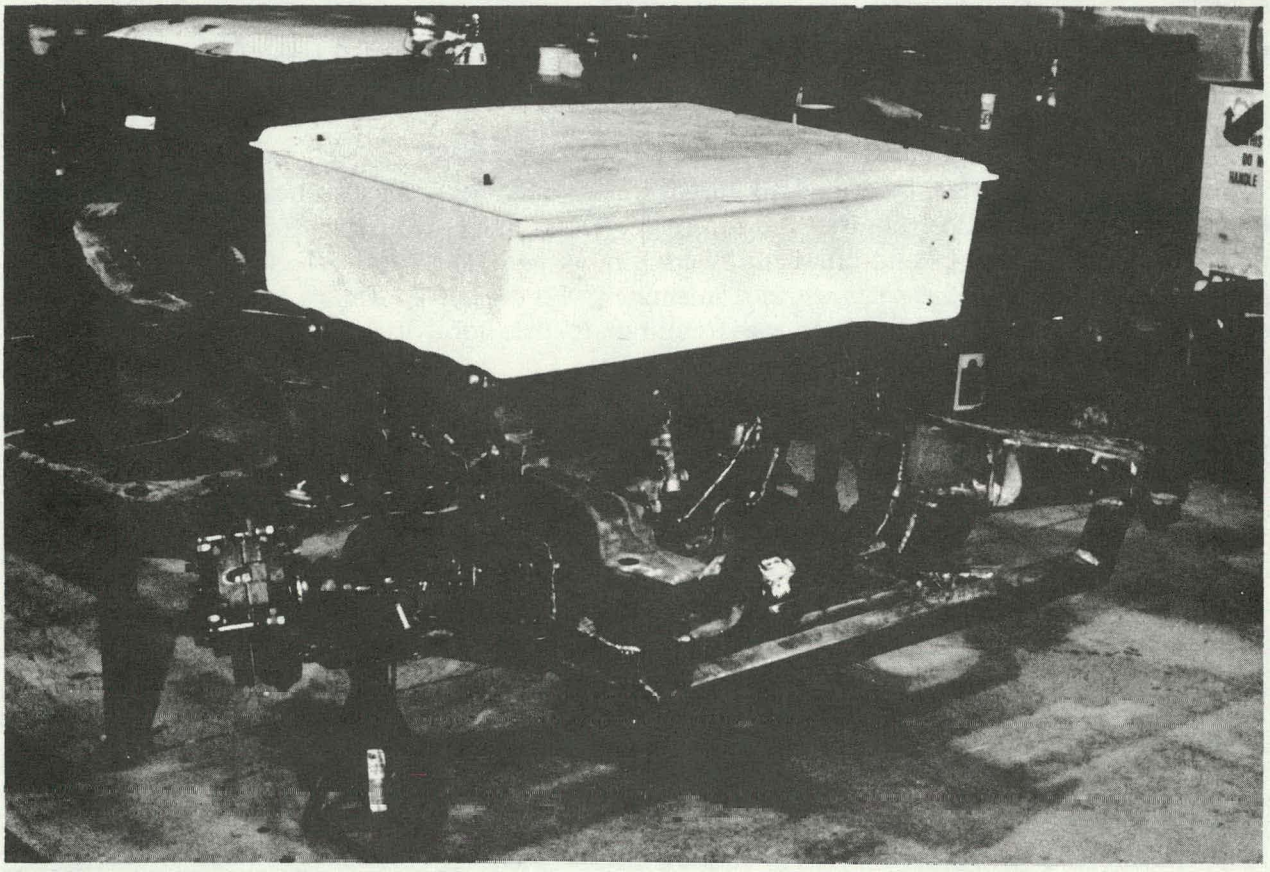

Figure 5.5-22. Front Structure and Battery Box of the Mechanical Components Mule

- Rear suspension
- Steering gear and linkage
- Brakes
- Exhaust
- Cooling
- Wheels and tires
- Power train mounting
- Traction battery container

Other systems required to operate the vehicle or support those intended for testing were modified versions of available components. Figure 5.5-24 shows the rear suspension arrangement.

5.5.3.5 Heating, Ventilating, and Air-Conditioning (HVAC)

Duplication of the HTV HVAC system on the Mechanical Component Mule would have required extensive revision to the Toronado structure, dash panel, and instrument panel. Therefore, a close approximation of the system was employed. The evaporator was placed in the same location, and ducting was routed to and from the passenger compartment, similar to

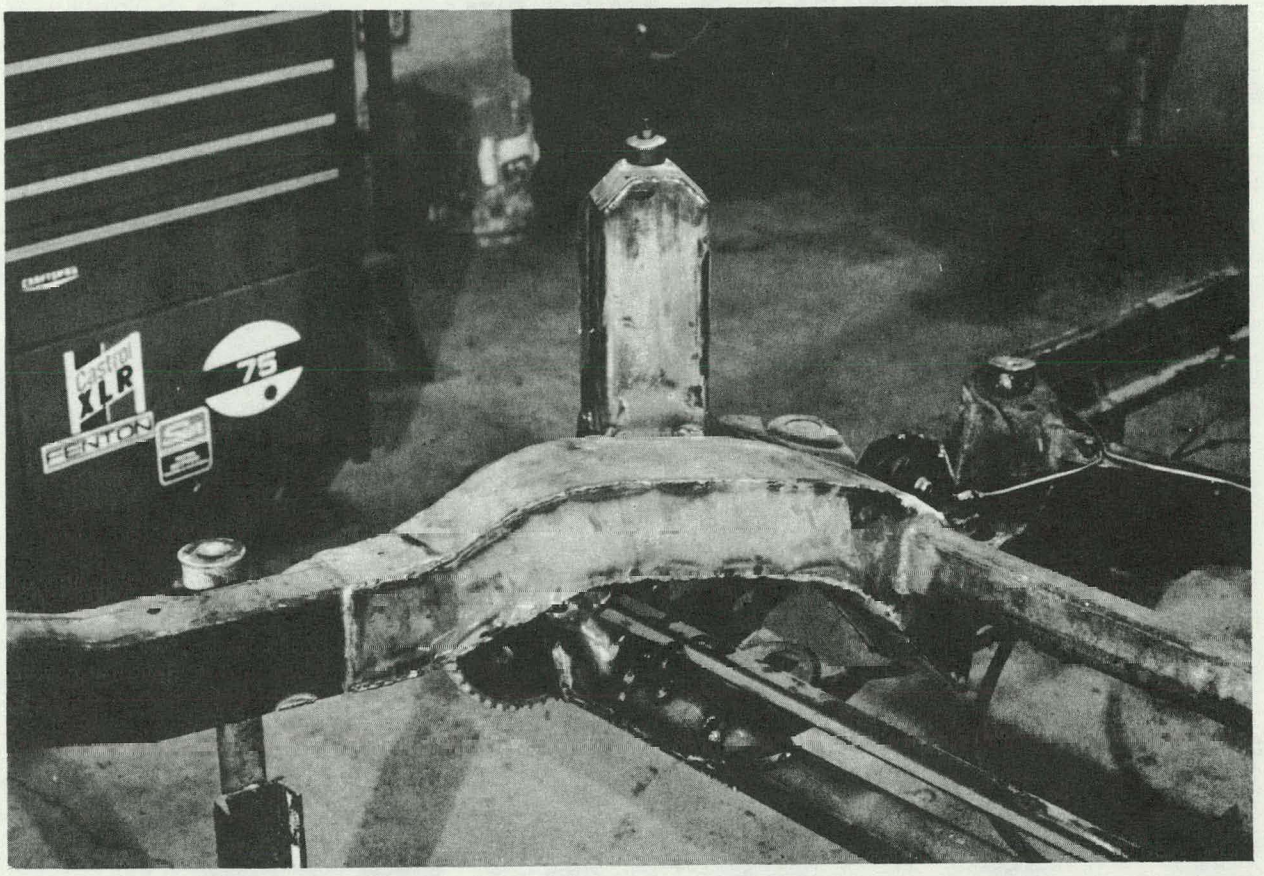

Figure 5.5-23. Rear Structure of the Mechanical Components Mule

the HTV. The blower was mounted remotely. However, this did not affect system performance. The auxiliary water heater was mounted in the trunk. This allowed access for development. Figure 5.5-25 shows installation of the auxiliary heater.

5.5.3.6 Fabrication Methods

Design layouts were made of the front suspension, the rear suspension, and the power train mounting. This was accomplished by overlaying the HTV designs and the Toronado frame. Where changes to the frame were considered to affect its structural integrity, replacement structure was added.

Design drawings were made of body modifications only for the shortening of the wheelbase. All other body modifications were made on an as-required basis as the building program evolved. When HTV components were to be used, the parts were fabricated from the HTV design drawings. No special tooling was required for the fabrication. Only the propulsion battery container required a tool. However, since the design was used on all of the vehicles built and the static crush module, the tool was reused later in the program.

The Toronado was disassembled, allowing the frame to be set up on a surface plate for rework. The body was cut at the prescribed point and mounted to the frame as two separate pieces. The two parts were welded back together using the frame as a fixture, thereby ensuring correct alignment. The total weight and the weight distribution were controlled by ballasting, where necessary. Lead spacers were added to the Group 27-type batteries to simulate the HTV battery, which was not available for the Mechanical Components Mule.

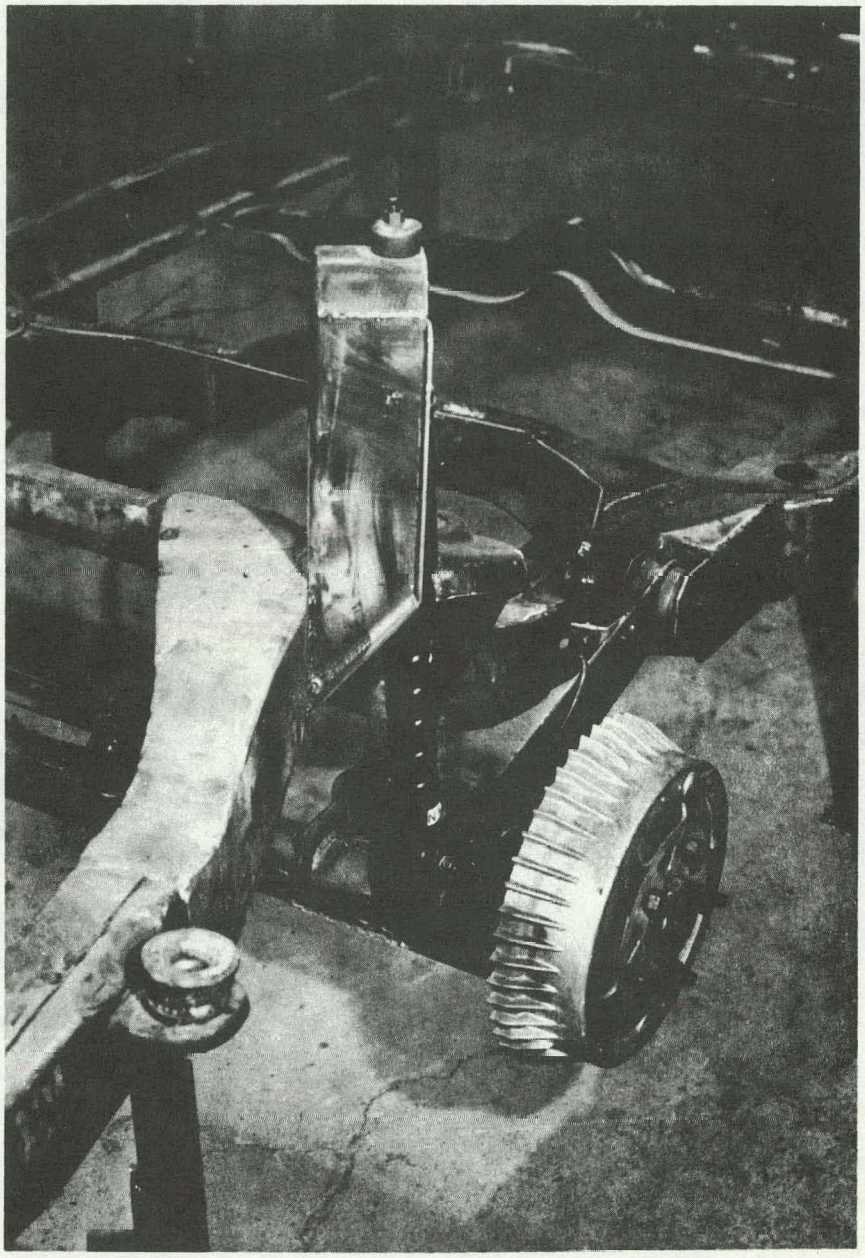

Figure 5.5-24. Rear Suspension of the Mechanical Components Mule

5.5.3.7 Instrumentation

The Mechanical Components Mule was instrumented to provide visual as well as recorded information regarding operation of the systems in the vehicle. Pressure gauges were employed to indicate the state of the hydraulic systems.

Direct reading meters were utilized for temperature measurement. Tachometers measured the speed of the engine and the motor. Appropriate electrical meters monitored the electrical system. In addition, an eight-channel, light beam oscillograph was mounted in what was once the rear seat for measuring voltages, acknowledge and command signals. A fifth wheel was also available for the measurement of vehicle speed.

Figure 5.5-25. Auxiliary Heater Installation in the Mechanical Components Mule

5.5.3.8 Transmission Development

The transmission development phase of the program was centered around the sizing of orifices and accumulators within the hydraulic system in order to obtain the appropriate shifting feel. This was done by subjective evaluation while driving the vehicle in typical situations. Work was required in the area of power downshift control in order to ensure a smooth downshift feel.

5.5.3.9 Clutch Development

The most important development activity affecting drivability of this vehicle was the development of the vehicle starting clutch. This was a complex development activity since it involved the combination of hydraulic, mechanical, and microcomputer systems.

Preliminary development activities were carried out utilizing a small microcomputer, which closed the loop on armature current as opposed to delivered power. Early development activities centered on smoothness of modulation and preciseness of control.

5.5.3.10 Ride and Handling Development

In order to accurately evaluate ride and handling, the preliminary ride and handling tests were postponed until the final controller design was fabricated and installed in the Hybrid Power Train Mule. These tests are described in Section 5.5.4.2.

5.5.3.11 Drive Train Mounting Development

The drive train mounting development consisted of subjective evaluation of the noise and vibration transmitted to the passenger compartment.

5.5.4 Hybrid Power Train Mule

The Hybrid Power Train Mule (HPTM) vehicle was the second mule vehicle delivered to JPL. During the initial part of the development phase, this vehicle was referred to as the Mechanical Components Mule. Its design and fabrication were described in Section 5.5.3. Initial plans were to install the prototype HTV power train components in this vehicle using a very simplified controller. During that phase, the vehicle would have had limited performance for preliminary dynamic low-speed testing of the transmission and vehicle drive clutch.

Per Contract Modification 17, the decision was made to install and interface a prototype HTV microcomputer controller in the Mechanical Components Mule vehicle. At this time, the mule vehicle was redesignated the Hybrid Power Train Mule (HPTM). The HPTM became the workhorse for the development and integration of the hybrid power-train hardware (electrical and mechanical components) and microcomputer controller software. Dynamometer, track, and road tests, and numerous demonstrations were conducted with the HPTM vehicle.

5.5.4.1 HPTM Development and Integration

Preliminary wiring and plumbing activities on the HPTM were initiated in April, 1981 at Triad Services. The HPTM vehicle was delivered to GE in Schenectady on May 26, 1981.

After power train and engine compartment wiring was completed, prototype HTV controller interface tests were started. Initially, the HTV controller, field chopper, and contactor assembly (modified spare TBM field chopper and contactor assembly) were mounted on a movable bench with umbilical cables connected to the vehicle. Sensors, acknowledge, and control signals were interfaced and tested. A soft starting technique for the electric drive was implemented in the microcomputer software. Soft starting the electric drive was necessary based on Mechanical Components Mule failure of accessory drive components including overrunning clutches and torque dampers.

Preliminary HPTM controller and power train interface testing concentrated on electric drive operation at light loads. Transmission shift logic and drive clutch operation were verified. The heat engine maintenance mode was used to verify correct engine and engine clutch operation. This mode allowed the engine speed to be varied with the transmission in neutral. Initial operator inputs were interfaced to the microcomputer via the controller system exercisers.

After electrical interfaces were verified, HPTM dynamometer testing began. Initial dynamometer tests were run to verify the controller propulsion source sequencing, transmission sequencing, and drive clutch modulation algorithms. Problems with mechanical components, including the high-pressure hydraulic system, transmission pump, and engine clutch mechanism required the power train to be removed numerous times from the vehicle for repair. Figure 5.5-26 shows the parallel shaft hybrid power train used in the HPTM and HTV.

In order to facilitate HPTM power train development activities, a custom power train test stand was designed and fabricated. Figure 5.5-27 illustrates this test stand, referred to as the "Rickshaw." Interface of the Rickshaw to the vehicle was via a set of umbilical electrical cables, gas lines, and vacuum hoses. The battery box was mounted on the Rickshaw to provide the necessary weight for traction on the dynamometer.

After replacing failed mechanical parts, dynamometer testing of the power train using the Rickshaw was started. Redesign of the engine clutch mechanism and high-pressure hydraulic unloading valve system was undertaken. Full load dynamometer testing was performed for both acceleration and regenerative braking. Mechanical adjustments and engine tuning, and numerous software updates were performed during this test phase.

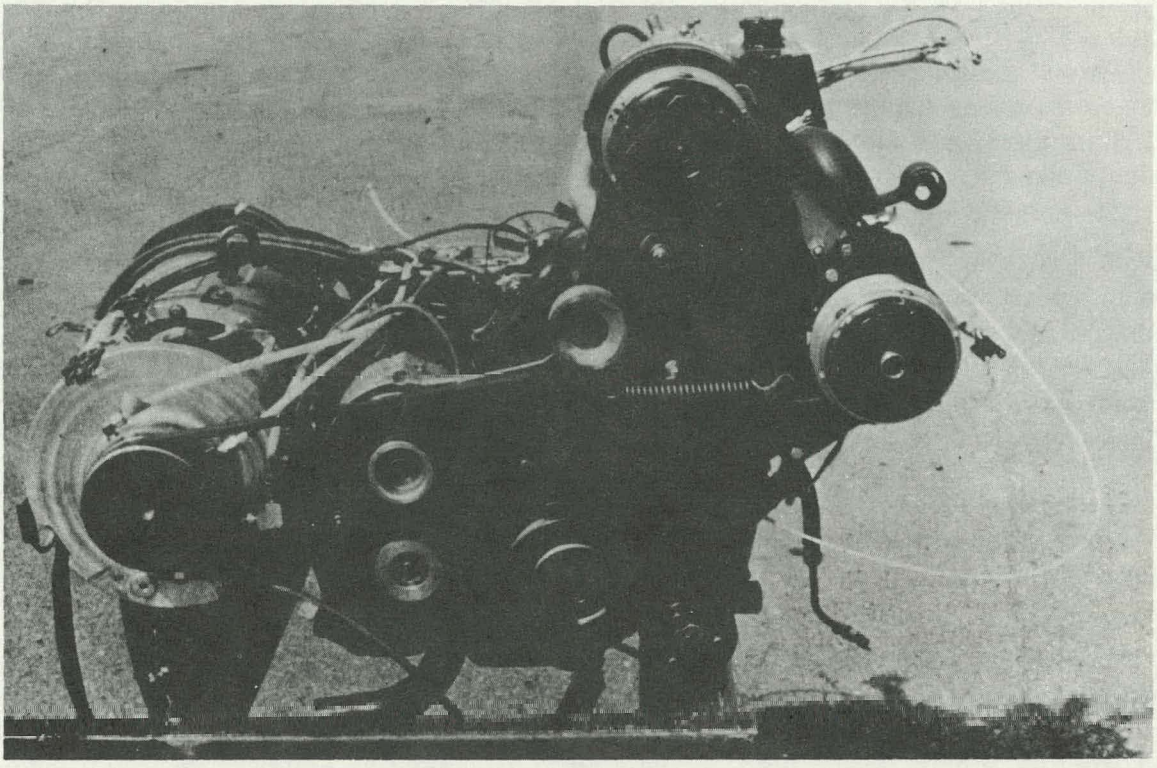

Figure 5.5-26. HPTM Parallel Shaft Hybrid Power Train

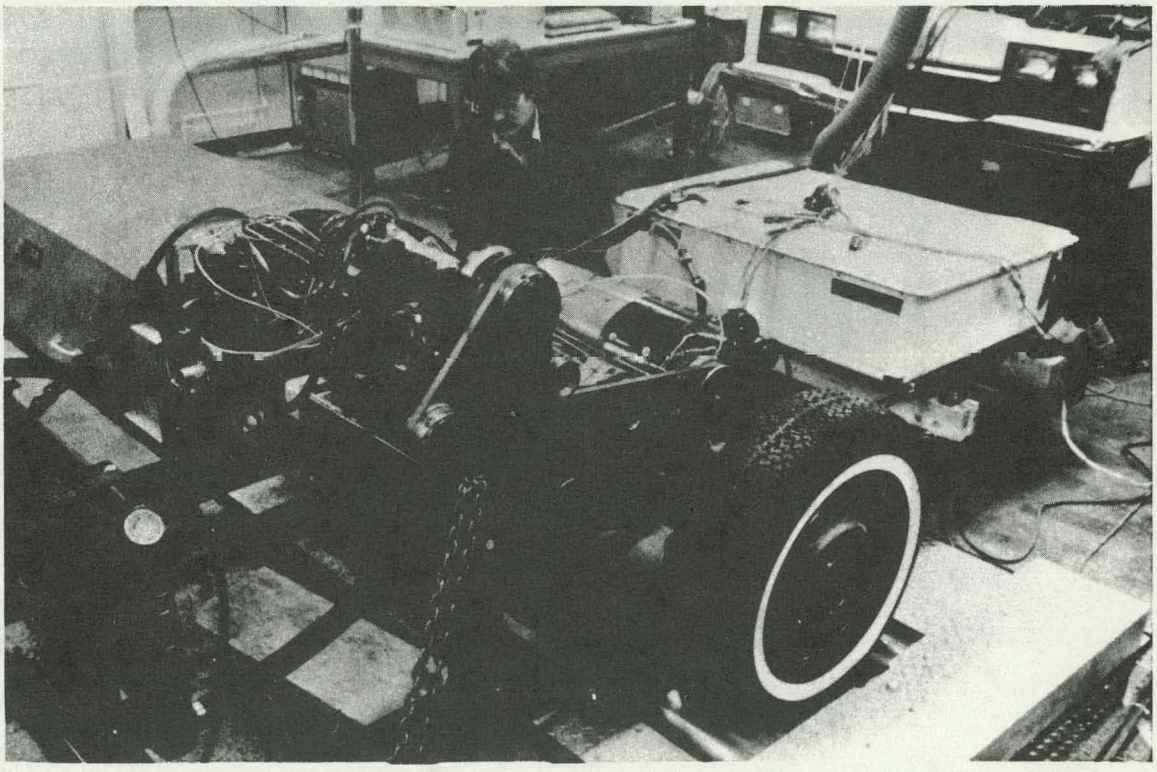

Figure 5.5-27. Hybrid Power Train Test Stand (Rickshaw) on the Dynamometer at General Electric

After full powered acceleration and braking tests, a transmission problem was encountered. Shift times, especially during downshifting from 3rd to 2nd during regeneration, initially were too long. Localized heating failed internal transmission bands and clutches. The transmission was rebuilt and hydraulic modifications were made to reduce the shift times. In addition, a software modification was made to limit the regenerative braking power during the actual downshift.

After reliable operation of the hybrid power train was achieved on the Rickshaw, the power train was installed in the HPTM vehicle for additional dynamometer and road tests. The microcomputer controller, field chopper, and contactors were mounted in the HPTM trunk as shown in Figure 5.5-28. Operator interfaces, including the accelerator and brake pedal commands, key switch and forward/reverse switch, were interfaced to the controller. The HPTM engine compartment is shown in Figure 5.5-29.

5.5.4.2 HPTM Vehicle Tests

The HPTM vehicle was tested on the GE chassis dynamometer, the track at TRC of Ohio, and private and public roads in Schenectady. The objectives of the tests were to develop and refine hardware and control software and to assess ride quality, handling, and braking.

HPTM parking lot tests started in January 1982. Although the all-electric range was limited, due partly to the use of commercially available marine-thype batteries, useful data was collected on tape by the on-board data acquisition system for analysis. Based on analysis of the data obtained, software updates were developed that improved the smoothness and drivability of the vehicle during both acceleration and regnerative braking. Software update also improved acceleration performance.

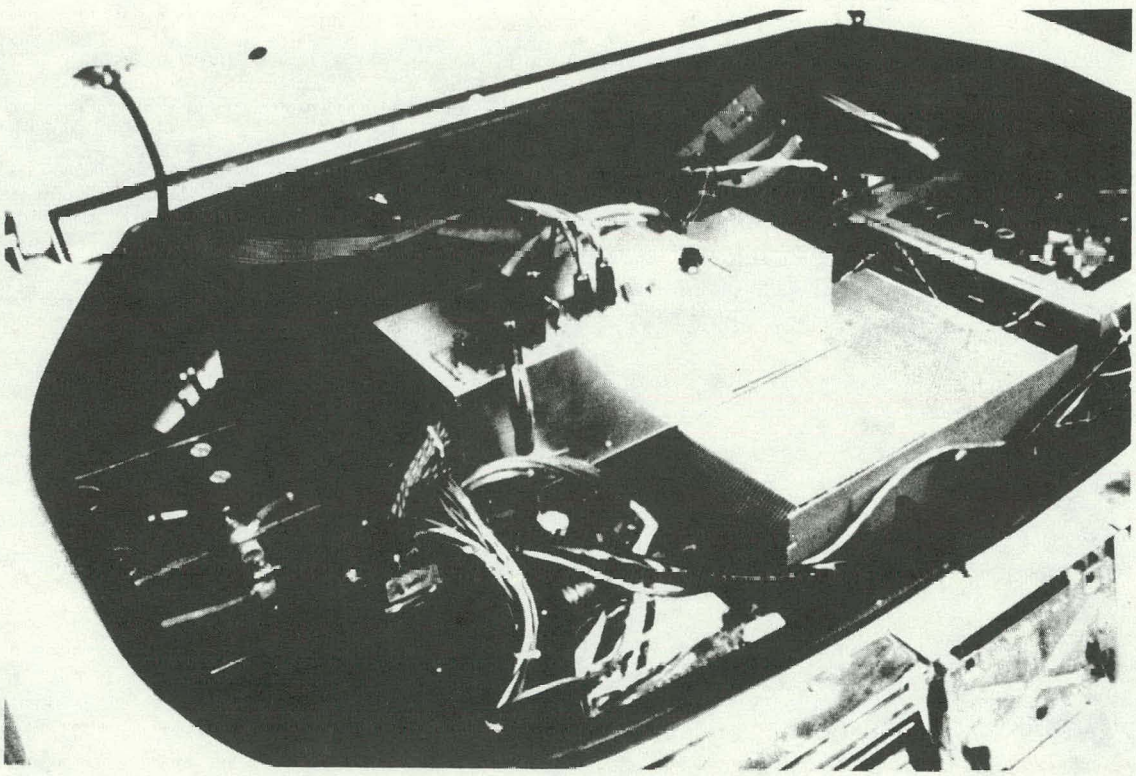

Figure 5.5-28. The Electronics and Vehicle Controller Packaged in the Trunk of the HPTM

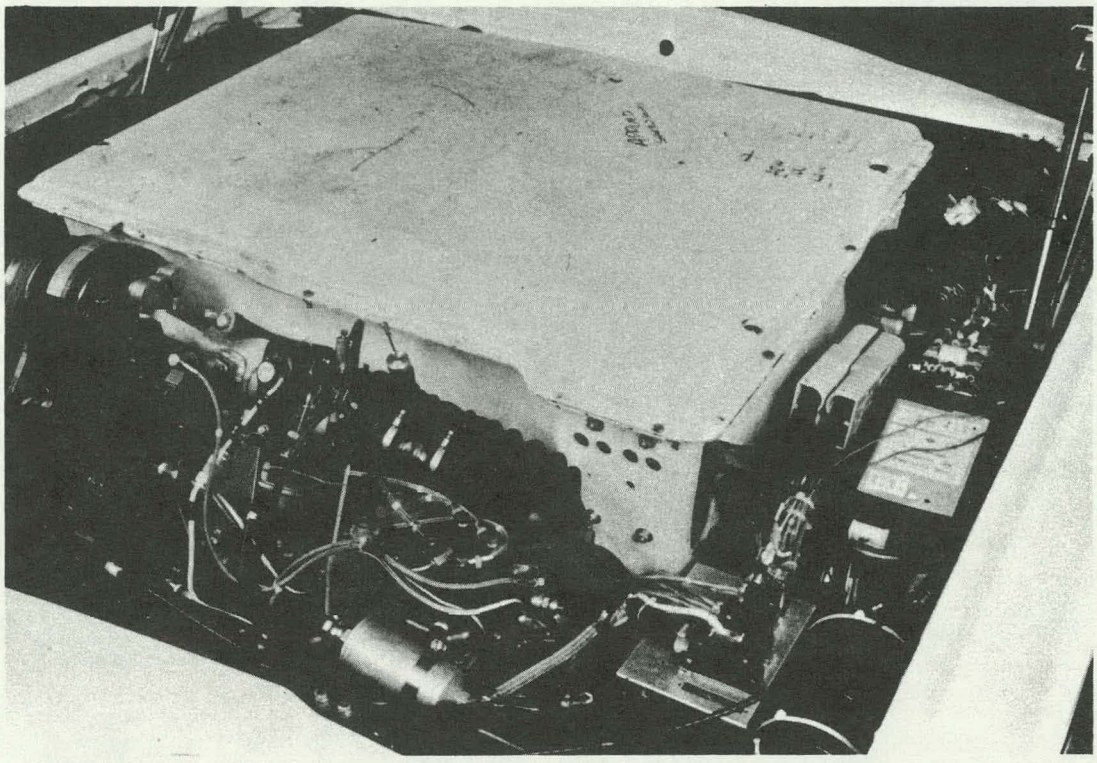

Figure 5.5-29. The Engine and Battery Box under the Hood of the HPTM

In February 1982, the HPTM was taken to the Transportation Research Center of Ohio (TRC) for detailed vehicle handling tests. Instrumentation, including a three-axis gyroscope, strip chart recorders, and associated power supplies, were mounted in the backseat area. Steering angle sensors, as well as a special steering wheel to facilitate the required step steering input, were installed on the vehicle. Results of these handling tests showed that the handling of the vehicle was quite close to calculated (see Section 5.2) and the HPTM was better in all respects than the baseline 1980 Buick Century.

HPTM ride quality tests were conducted on public roads near Schenectady in April 1982. A jury comprised of JPL, TRIAD, and GE personnel rode and drove the HPTM, the reference 1980 Buick Century, and a Buick Riviera over a course with various quality of paved roads, including numerous potholes. Results indicated ride quality comparable to the Buick Century but slightly below that of the Buick Riviera.

FMVSS brake tests were run on the HPTM in April 1982 near Schenectady. Required brake pedal forces were well within allowable ranges (15 lb required, maximum allowable force is 75 lbs) and there was no indication of any brake fade.

System loss measurements on the HPTM were performed to quantify power train component, accessory, and subsystem loads. Based on these HPTM loss accessory measurements which indicated higher than expected loads, modifications including a redesign of the chain lubrication system, relocation of transmission oil drain passages, lowering of the transmission oil pan, and reducing the capacity of the high pressure hydraulic pump were undertaken. The result was a substantial reduction in the loss accessory load in the HTV as compared to the HPTM.

Section 6

HTV TEST AND EVALUATION

6.1 INTRODUCTION

The tests reported in this section were performed prior to the HTV Hardware Review in February 1983. The objectives of the tests were to determine how well the vehicle performance conformed to the program objectives set forth in the contract. In addition, the vehicle tests were performed to verify design calculations, predictions, and characterization of the components and subsystems, and to establish a baseline of HTV performance for later comparison.

Testing of the Hybrid Test Vehicle (HTV) and its associated electronic and mechanical components was a critical part of the entire development program. HTV hardware and software development relied heavily on prior testing and evaluation performed on the TBM and HPTM mule vehicles, described in Section 5.5. Software algorithms tested in the HTV, that were not included in either of the mule vehicles, included the on-board battery charger, battery state-of-charge unit, and updates in propulsion source sequencing to improve drivability and reduce system losses.

HTV vehicle performance tests were run on the GE electromechanical chassis dynamometer (AESI).* On-road tests of the HTV were performed with both GE and JPL personnel driving the vehicle.

6.2 TEST DESCRIPTION

Tests performed on the HTV included performance tests, signature tests, and system loss and accessory load tests. The vehicle performance tests included full-throttle acceleration, gradeability, and continuous cruise tests. In addition, operational tests of the on-board battery charger were performed.

Performance tests were run on the GE chassis dynamometer. Vehicle parameters used for setting the dynamometer for testing are summarized in Table 6.2-1. HTV emission and fuel economy tests will be performed on the chassis dynamometer at the Jet Propulsion Laboratory at a later date. Parameters for the fuel economy and emission tests at JPL will be determined from HTV vehicle coastdown data obtained by JPL prior to their dynamometer tests.

Dynamometer load capacity limited actual gradability testing to 3% grades. Performance on higher slope grades was inferred from zero-grade acceleration data.

The objective of the signature tests was to establish a set of reproducible tests that would define the HTV "as delivered" performance. Table 6.2-2 summarizes the HTV signature tests. Those tests included measurements of the HTV response to 10, 20, 40 kW-step power commands in both the electric motor only and heat engine only mode as well as hybrid operation of the HTV during a maximum effort acceleration, battery charging with the heat engine, and over repeated EPA urban cycles.

System loss/accessory load tests were performed to quantify power train component and subsystem losses versus shaft speed. Component and subsystem losses measured included electric motor plus transmission pump, high-pressure hydraulic pump (power steering/power brakes), alternator, torque transfer unit plus transmission in neutral, and transmission in each

* Automotive Environmental Systems, Inc.

Table 6.2-1

VEHICLE PARAMETERS USED FOR GE DYNAMOMETER TESTS

- Test Weight – 4610 lb (4310 + 300 lb)
- Road Load
  - Rolling resistance coefficient 0.011 lb/lb
  - Drag coefficient C_D, = 0.45
  - Frontal Area, A_F = 22 ft^2
- Vehicle Accessories
  - Air conditioner OFF
  - Heater OFF
  - Lights OFF

Table 6.2-2

HTV-1 SIGNATURE TEST SUMMARY

A. Electric Motor Only – 100% SOC
   1. 10, 20, 40 kW-step acceleration to 56 mph (or maximum speed) – Coast to 15 mph
   2. 40 kW-step acceleration to 56 mph – Brake at BP = 0.5

B. Heat Engine Only Mode – Heat Engine Warm
   1. 20, 40 kW-step acceleration to 56 mph (or maximum speed) – Coast to 15 mph

C. Hybrid Mode – Heat Engine Warm, 100% SOC
   1. 20, 40, 88 kW (maximum effort) acceleration to 56 mph or maximum speed – Brake at BP = 0.5

D. EPA Urban Cycles – Cold Start, 100% SOC
   1. Urban cycles until battery recharge is required
   2. Heat engine recharge mode (150 s)
   3. 20 kW-step acceleration to stabilized speed – Brake to rest
      40 kW-step acceleration to 56 mph – Brake to rest

gear with front wheels elevated. Results from similar system loss tests for the TBM and HPTM helped to reduce these system losses in the HTV. Comparison of system loss data for the TBM, HPTM and HTV are presented in Section 5.3.1.

In addition to the tests described above, "on-road" tests and demonstrations were run over a period of several months throughout the HTV Development and Test Phases. During the Hybrid Test Vehicle Hardware Review, (February 9, and 10, 1983) the HTV was driven on public roads in Schenectady, New York, by DOE, JPL, and GE personnel. Although road conditions were less than ideal, i.e., snow-covered with ambient temperatures as low as −4 °F, the HTV performed very well.

6.3 HYBRID TEST VEHICLE TEST RESULTS

6.3.1 Performance Test Results

6.3.1.1 Continuous Cruise

The continuous cruise test was run on the chassis dynamometer at 56 mph for 1 hr. The vehicle was in the hybrid mode; however, the heat engine was the only propulsion source operating above 40 mph. The heat engine output power was 21-22 kW, and the engine speed was 2300 rpm. The transmission operated in 3rd gear.

6.3.1.2 Gradability

The gradability test was run on the chassis dynamometer. A 3% grade was simulated by increasing the road load coefficient (that part of the rolling resistance parameter which is not a function of velocity) to include the effect of the grade. The HTV was driven at 56 mph for a distance in excess of 1.0 km (0.62 mi). Total power required was 36-37 kW. Although the highway mode (V_{MOD} = 40 mph) was used for this 56 mph test, the vehicle correctly operated in a hybrid mode. Hybrid operation resulted because the engine was not capable of producing the required power at the operating engine speed. Heat engine power for this 3% grade test was 16-18 kW. Electric motor power was 20-21 kW.

Vehicle performance at steeper grades was calculated based on zero grade acceleration data. Figure 6.3-1 summarizes the HTV gradability results, which were obtained using the following method*. The correspondence between acceleration at zero grade and constant speed operation on a grade of angle θ follows from the vehicle equation of motion.

$$\frac{P_{required}}{W_V} = V\left[\frac{a}{g} + \sin\theta + fr + k\left(\frac{C_D A}{W_V}\right)V^2\right]$$

The term $\left[\frac{a}{g} + \sin\theta\right]$ represents the effective acceleration. The gradability ($\sin\theta$) corresponding to a particular acceleration on a flat road (or dynamometer) is then

$$\sin\theta = \left(\frac{a}{g}\right)_{flat}.$$

For example:

% Grade	Θ (DEG)	SIN Θ	a_{flat}(mph/s)
8	4.57	0.0796	1.75
15	8.53	0.1483	3.26

* The "jog" in the gradability occurs due to battery switching during which the electric motor output changes from 17 kW to 34 kW.

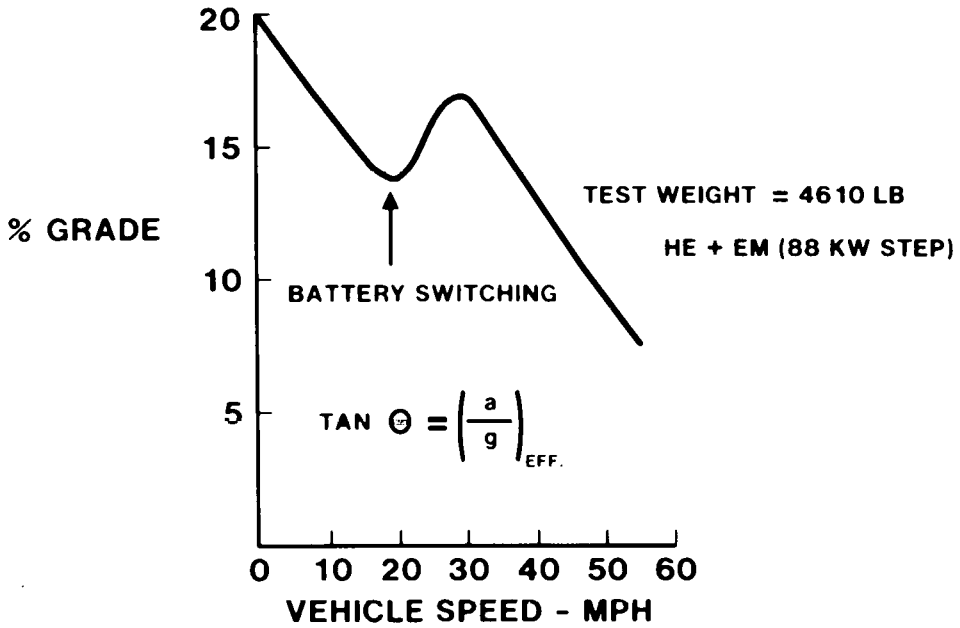

Figure 6.3-1. HTV Gradability Characteristics

25	14.03	0.2424	5.32

Gradability (%) at a specified speed (mph) would require that the corresponding acceleration (a_{flat}) be achieved at the same speed on the flat road or dynamometer. This approach is conservative in that the effect of the rotational inertia of the power train components is included in the power required in the acceleration tests but would be absent in the constant speed gradability test if that could have been performed. This error is not significant when the vehicle is in 2nd or 3rd gear, but a correction should be made when the vehicle is in 1st gear in the flat road acceleration tests and not for grades at the same speed.

6.3.1.3 Acceleration

The HTV maximum effort acceleration performance tests, i.e., 88 kW step, were run on the chassis dynamometer. Figure 6.3-2 shows the strip chart traces of this maximum effort acceleration. Accelerator pedal power command, electric motor power, heat engine power and speed of electric motor, heat engine and vehicle velocity are shown versus time. During the first four seconds, output power is limited because the switch to E_b (120 V) operation has not occured. At speeds above 15 mph, HTV acceleration is good - that is when both the electric motor (120 V) and heat engine are operating. Table 6.3-1 summarizes the HTV maximum effort acceleration test results.

A comparison of the measured maximum effort acceleration of the HTV on the chassis dynamometer and that calculated using the GE HYVEC simulation program is shown in Figure 6.3-3. The times at which the heat engine is started and battery switching occurs are indicated on each curve. In the computer simulation, it is assumed that battery switching occurs instantaneously at the earliest possible time (i.e., once motor RPM is above base speed corresponding to maximum armature current) and that the heat engine produces maximum power immediately after the engine clutch is closed. It is clear from Figure 6.3-3 that in the HTV, battery switching is delayed significantly from the earliest possible time. In addition, detailed inspection of the signature test data given in Table 6.3-4 indicates that the battery

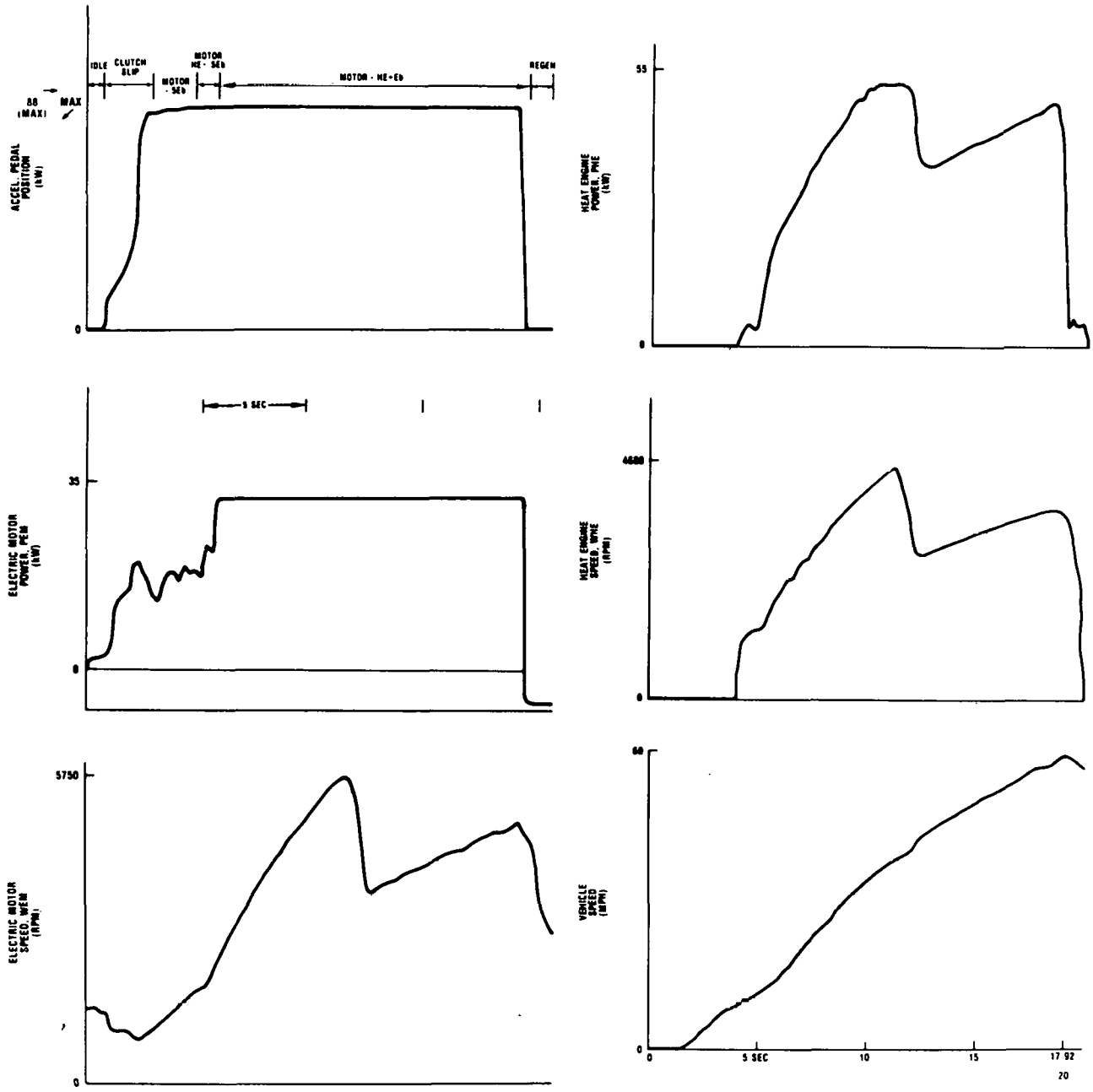

Figure 6.3-2. HTV Maximum Effort Acceleration Response

switching takes about 0.8 s to complete and the heat engine requires about 2.0 s to attain full power at its operating RPM. These lags are responsible for the sag in the HTV acceleration relative to the predicted performance in the mid-speed range. After both the electric motor and heat engine are fully operating, the HTV accelerates as expected.

6.3.1.4 On-Board Battery Charger

The microcomputer-controlled on-board battery charger operational tests were performed during the vehicle test phase of the program. After the propulsion batteries were discharged to various levels in the performance and signature tests, the on-board charger was used to re-charge the batteries. Recharge data was recorded using the data acquisition system.

Table 6.3-1

HTV MAXIMUM EFFORT ACCELERATION PERFORMANCE

Performance Test	Acceleration Time (sec)	
	Test Data	Design Goals
0-50 km/hr (0-31 mph)	8.4	5
0-90 km/hr (0-56 mph)	17.6	15
40-90 km/hr (31-56 mph)	10.7	10

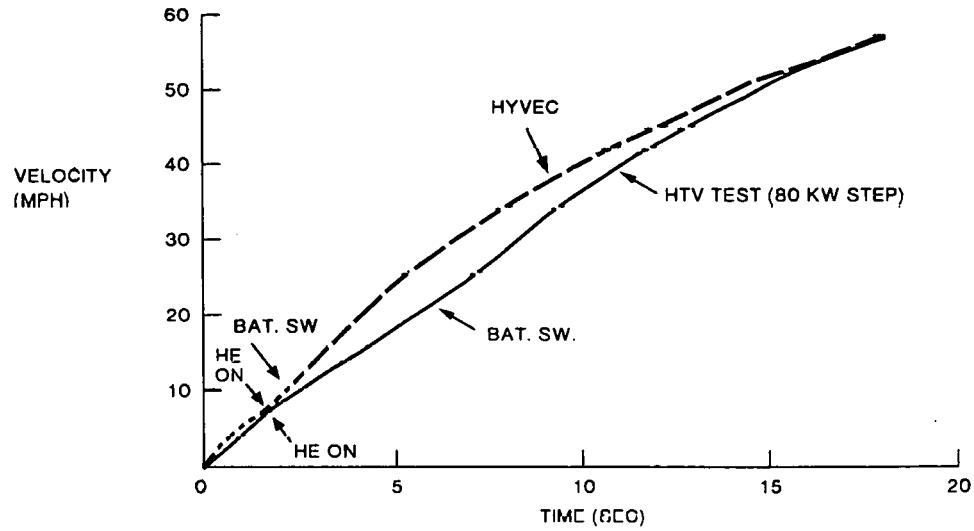

Figure 6.3-3. Comparison of Maximum Effort Acceleration in Hybrid Mode — Test and HYVEC

Battery charger tests were run operating from each of the three ac input lines, i.e., 120 V, 15 A (VLL), 120 V, 30 A (VLH), and 240 V, 30 A (VHH). Proper current taper occurred in all cases after the battery voltage reached the temperature corrected V_{CLAMP} voltage. The battery electrolyte temperature sensors functioned correctly. After normal battery charger termination, the following events occurred: the state-of-charge meter was reset to 100%, the microcomputer accummulated value of ampere-hour net (AHNET) was reset to 0.00, and finally the microcomputer turned off its own logic power supplies.

Table 6.3-2 gives selected parameters from the data acquisition output of an on-board battery charger test operating from a 240 V, 30 A ac line. Additional battery charger performance curves are presented in Section 5.4.3.

6.4 SIGNATURE TEST RESULTS

Results of signature test step responses for the electric motor only, heat engine only, and hybrid mode (tests A, B, and C described in Table 6.2.-2) are summarized in Table 6.3-3. "Heat engine only" tests used the heat engine test mode in the vehicle controller. As discussed in Section 5.3.1, the HTV in the heat engine test mode starts on the electric motor

Table 6.3-2

BATTERY CHARGER TEST SUMMARY (240 V, 30 A, AC LINE)

Time (min)	Amp-Hour Net (Ah)	Battery Bank #1 V_{CLAMP} (V)	Battery Bank #1 Voltage (V)	Battery Bank #2 V_{CLAMP} (V)	Battery Bank #2 Voltage (V)	Charger #1 Current (A)	Charger #2 Current (A)	Comments
0	−17.73	78.0	63.8	78.6	63.8	0	0	Initial Discharge - 17.73 Ah
15.00	−12.76	77.8	68.1	78.6	68.3	20.30	20.60	Battery #1 Temperature Increased 1 °C
30.00	−7.71	77.8	69.2	78.6	69.5	20.40	20.80	
45.00	−2.62	77.8	72.2	78.6	73.1	20.40	20.50	
50.72	−0.76	77.8	78.0	78.6	78.9	19.00	19.10	Charger #2 Start Taper
50.86	−0.71	77.8	78.0	78.6	79.1	18.90	19.00	Charger #1 Start Taper
60.00	+1.58	77.6	77.5	78.4	78.4	12.31	13.00	
67.52	+3.02	77.6	70.6	78.4	78.4	0	11.50	Charger #1 Turned Off
69.97	+3.24	77.6	67.2	78.4	70.6	0	0	Charger #2 Turned Off

Table 6.3-3

HTV SIGNATURE TEST STEP RESPONSE SUMMARY

		Performance			Stabilized
Test Description	Test Number	0-31 mph (s)	25-56 mph (s)	0-56 mph (s)	Speed (mph)
Electric Motor Only (EM Test)					
10 kW step	10-3	57.3	---	---	34
20 kW step	10-0	20.5	---	---	46
40 kW step	10-1	13.6	35.8	45.8	>56
Heat Engine Only (HE Test)					
20 kW step	11-0	15.6	---	---	51
40 kW step	11-1	15.8	28.9	39.2	>56
Hybrid (V_{MOD} = 40 mph)					
20 kW step	13-0	21.0	---	---	47
40 kW step	13-1	12.0	26.4	35.3	>56
88 kW step	13-2	8.4	10.73	17.63	>56

and then at speeds above 12 mph transitions to heat engine only operation regardless of power demand.

A stabilized speed of approximately 50 mph is achieved with the 20 kW step command. The stabilized vehicle speed is the same for a given power command regardless of the power source, HE, EM, or He+EM. Low power acceleration, i.e., 20 kW, in the hybrid mode is comparable to the electric only 20 kW step because the 20 kW command does not exceed the capabilities of the electric drive system, and because vehicle speeds are below V_{MOD} of 40 mph, the heat engine does not start during the 0-31 mph acceleration. Acceleration performance, 0-31 mph for 40 kW step is slightly better in the electric-only mode than the H.E.-only mode because the electric drive produces its maximum power at lower comparable speeds than the heat engine. However, the 40 kW high-speed acceleration performance in the heat engine-only mode is better than for the electric-only mode because the electric drive has a maximum power clamp of 33 kW.

Table 6.3-4 shows selected data acquisition system output for the maximum effort hybrid mode signature test. All major propulsion source sequencing and gear shifting transitions are listed. Battery, electric motor, transmission, and heat engine parameters versus time and vehicle speed are presented in the tables. Comparison of future vehicle signature tests with the documented signature tests delivered with the HTV vehicle will be valuable diagnostic tools in troubleshooting possible problems with components, subsystems or sensors.

The final HTV signature test required driving multiple EPA urban cycles (cold start) with the batteries initially at 100% SOC. These EPA cycles were driven until the battery state-of-charge decreased to 20% and the heat engine started to recharge the batteries. After stabilizing in the battery recharge mode of operation, the EPA cycle was terminated. Two vehicle accelerations were then run - a 20 kW step and a 40 kW step. Table 6.3-5 summarizes this multiple EPA cycle/step response signature test.

Table 6.3.4

HYBRID MODE SIGNATURE TEST – 88 kW STEP, BRAKE AT BP = 0.5, VMODE = 40 MPH

Test-Record	Accum. Time (s)	Transition	Vehicle Velocity (mph)	Battery		Electric Motor			
				Cell Current (A)	Net Amp-Hours (Ah)	Armature Current IA (A)	Armature Voltage VA (V)	Base Speed WB (rpm)	Speed WEM (rpm)
13-60	0/1.5	Clutch Slip	0/4.75	262	−11.5	519_{pk}	54.5_{min}	---	786
13-61	2.8/4.1	Mot. $0.5E_b \rightarrow HE + 0.5E_b$	8.7/11.5	231/220	−11.6	458/437	55.5	---	1364/1775
13-62	4.1/4.9	Mot. HE + $0.5E_b \rightarrow HE + E_b$	11.5/14.3	220/348	−11.7	437/355	55.5/103.0	864	1775/2314
13-62	6.9	Mot. HE + E_b at 25 mph	24.5	347	−11.8	347	103.5	1940	3709
13-63	8.3	Mot. HE + E_b at 31 mph	31.0	348	−12.0	348	103.0	1961	4631
13-64	10.8/12.0	Mot. HE + E_b 1st → 2nd Shift	38.8/43.8	340/367	−12.2	340/367	102.5	1914	5708/3602
13-66	17.6	Mot. HE + E_b at 56 mph	56.0	346	−12.8	346	102.5	1904	4628
13-66	19.5/20.5	Mot. HE + E_b 2nd → 3rd Shift	58.0/56.5	−49/−39	−13.0	−49/−39	126.0	2791	4412/2826
13-66	20.5	Mot. HE + E_b → Regen. E_b	56.5	−39	−13.0	−39	130.0	---	2826
13-67	20.5/21.5	Regen. E_b → Regen. $0.5E_b$	55.8/53.3	−23/−93	−13.0	−23/−188	129.0/67.0	2770/1567	2806/2705
13-69	29.2/31.0	Regen. $0.5E_b$ 3rd → 2nd Shift	31.0/26.0	−63/−86	−12.8	−125/−172	68.5/69.0	1557/1593	1565/2019
13-70	33.5	Regen. $0.5E_b$ 2nd → 1st Shift	18.8	−35	−12.7	−70	67.5	1497	1423

Table 6.3.4 (Cont'd)

HYBRID MODE SIGNATURE TEST – 88 kW STEP, BRAKE AT BP = 0.5, VMODE = 40 MPH

Test-Record	Accum. Time (s)	Transition	Vehicle Velocity (mph)	Battery		Electric Motor			
				Cell Current (A)	Net Amp-Hours (Ah)	Armature Current IA (A)	Armature Voltage VA (V)	Base Speed WB (rpm)	Speed WEM (rpm)
13-60	0/1.5	Clutch Slip	0/4.75	262	−11.5	519_{pk}	54.5_{min}	---	786
13-61	2.8/4.1	Mot. $0.5E_b$ → $HE + 0.5E_b$	8.7/11.5	231/220	−11.6	458/437	55.5	---	1364/1775
13-62	4.1/4.9	Mot. HE + $0.5E_b$ → $HE + E_b$	11.5/14.3	220/348	−11.7	437/355	55.5/103.0	864	1775/2314
13-62	6.9	Mot. HE + E_b at 25 mph	24.5	347	−11.8	347	103.5	1940	3709
13-63	8.3	Mot. HE + E_b at 31 mph	31.0	348	−12.0	348	103.0	1961	4631
13-64	10.8/12.0	Mot. HE + E_b 1st → 2nd Shift	38.8/43.8	340/367	−12.2	340/367	102.5	1914	5708/3602
13-66	17.6	Mot. HE + E_b at 56 mph	56.0	346	−12.8	346	102.5	1904	4628
13-66	19.5/20.5	Mot. HE + E_b 2nd → 3rd Shift	58.0/56.5	−49/−39	−13.0	−49/−39	126.0	2791	4412/2826
13-66	20.5	Mot. HE + E_b → Regen. E_b	56.5	−39	−13.0	−39	130.0	---	2826
13-67	20.5/21.5	Regen. E_b → Regen. $0.5E_b$	55.8/53.3	−23/−93	−13.0	−23/−188	129.0/67.0	2770/1567	2806/2705
13-69	29.2/31.0	Regen. $0.5E_b$ 3rd → 2nd Shift	31.0/26.0	−63/−86	−12.8	−125/−172	68.5/69.0	1557/1593	1565/2019
13-70	33.5	Regen. $0.5E_b$ 2nd → 1st Shift	18.8	−35	−12.7	−70	67.5	1497	1423

Table 6.3-5

SIGNATURE TEST SUMMARY
MULTIPLE EPA CYCLES FOLLOWED BY STEP ACCELERATIONS
(VM = 40 mph)

- First EPA test cycle – 1370 s, −27.7 AH, SOC = 40%
- Heat engine charging started at 1100 s on second EPA cycle, −36.0 AH, SOC = 20%
- Terminated second EPA cycle at 1253 s, −36.2 AH, heat engine charging 2.7 AH
- Step response summary
  - 20 kW step, 0-25 mph, 17.4 s, heat engine charging initiated
  - 40 kW step, 0-31 mph, 13.8 s, no heat engine charging
  - 40 kW step, 25-56 mph, 28.7 s, heat engine charging
  - 40 kW step, 0-56 mph, 42.5 s, heat engine charging
- Heat engine charging during step response test −1.2 AH final battery state-of-charge − 16%

Section 7

QUALITY ASSURANCE

Quality inspection plans were prepared by each of the major subcontractors. These plans were reviewed by General Electric and, after initial approval, were submitted to JPL. The plans prepared reflected minimum inspection requirements since the hardware produced by the individual subcontractors was built in an engineering model shop, and not in a production facility.

The quality assurance (QA)/inspection matrix (Table 7-1) was presented at the preliminary design review (PDR). It summarizes the type of inspections to be performed at the incoming, in process, and final inspection and test stages of work by each major subcontractor. At the time of the PDR, no hardware for the final HTV was being fabricated, thus the QA inspection program had not been formally implemented.

Table 7-1

QUALITY ASSURANCE/INSPECTION

	Incoming	In Process	Final Inspection and Test
General Electric	Industrial quality standards vs. completeness and condition	Each operator and certain cross inspection and monitoring (SF)	Visual Electrical continuity (PE) Subsystem tests vs. specifications (PE)
Globe-Union	Material specifications and drawings tag system	Process specifications and drawings (0) Component specifications and drawings records (PE)	Visual Electrical tests (ADE) - Open circuit - High rate discharge - Three rate discharge
Triad	Industrial quality vs. completeness and condition Sign-off system (SF)	Structural Fabrications (SE) General Machining, Fabrication, Priming and Painting (0, SF with PE monitoring)	Power systems (SF) Wiring, alignment fluids (SF) Subsystem functional tests (PE) Cosmetic (PM)
Volkswagen	Inspect quality and properties against orders, drawings, etc.	Machined parts (0 and SF)	Assemblies - Visual - Gauging

0 = Operator, PE = Project Engineer, SF = Shop Foreman,
ADE = Advanced Development Engineer, SE = Structural Engineer,
PM = Program Manager

At the interim design review (IDR), the status of the implementation of each of the quality assurance plans submitted by the subcontractors was reviewed. Implementation of the quality assurance plans again was minimal in that very little hardware for the HTV was being fabricated. At that time, JPL requested that a more formal quality assurance program be implemented with some consideration given to third party inspection. The added costs required for third-party inspections were reviewed, and a decision was made not to implement that procedure.

Section 8

SUPPORT EQUIPMENT

8.1 OVERVIEW

The following items comprised the support equipment group:

- IA/VA card exerciser
- Coil driver card exerciser
- Field chopper logic/base drive card exerciser
- Debug panel
- Controller exerciser
- Data acquisition system

Each of these units are discussed in this subsection.

The armature current—armature voltage, IA-VA card exerciser (Figure 8.1-1) provided a method of calibrating the IA and VA sensor amplifiers and checking the setpoint of the armature current fault, IAF signal. The VA input signal was provided by an external dc voltage

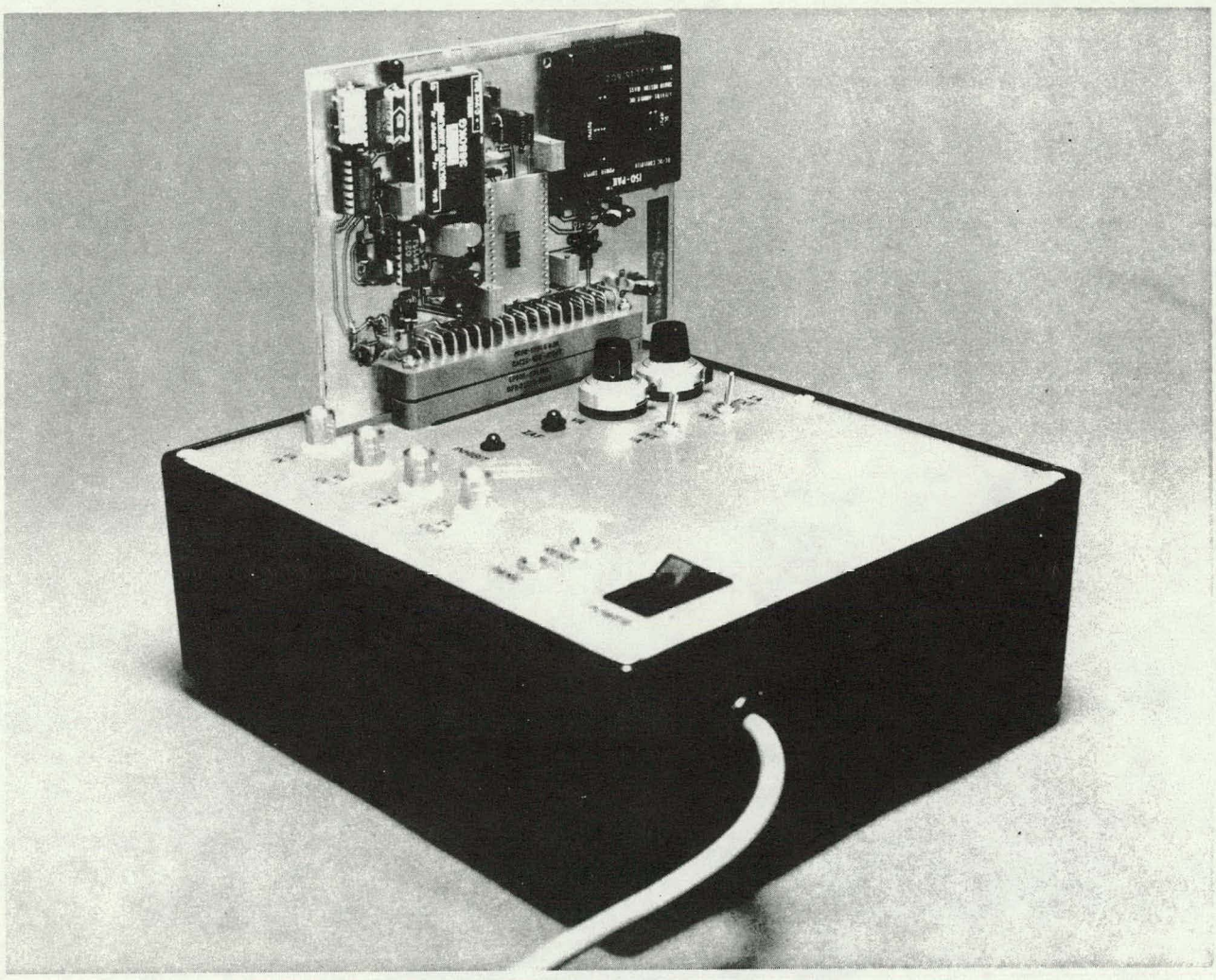

Figure 8.1-1. IA/VA Card Exerciser

supply. This voltage is switch-selectable to be either applied directly to the VA input of the card under test or to be scaled by a ten-turn potentiometer. The IA input may either be generated by a regulated supply in the exerciser or from an external source. Both VA and IA outputs are monitored by BNC connections. Two LEDs are used to monitor the IAF and INHIBIT outputs, allowing the trip point to be set. All necessary power supplies are contained in the exerciser and are powered from a single 110 volt line.

The coil driver card exerciser (Figure 8.1-2) provided the means of functionally testing each of the eight coil drivers, as well as the two inhibit functions on the coil driver card. Two switch closures apply logic-level-one voltages to the inputs of the INHIBIT 1 and INHIBIT 2 optoisolators on the coil driver card. An eight-position switch, one switch associated with each of the coil drivers, applies a logic level one to the optoisolator on the coil driver card for the selected function. The output of each of the driver FETs is applied, through a load resistor, to an LED indicator on the exerciser. If INHIBIT 1, INHIBIT 2, and the function input are all logic level one, the associated LED should light. All of the power supplies for the exerciser are self-contained and are powered from a single 110 V line.

The field chopper card exerciser (Figure 8.1-3) exercises the CLBA card of the field chopper. Three voltages simulate inputs to the card: field current command (IFC), frequency modulated signal of actual field current IF, and battery input current to field chopper

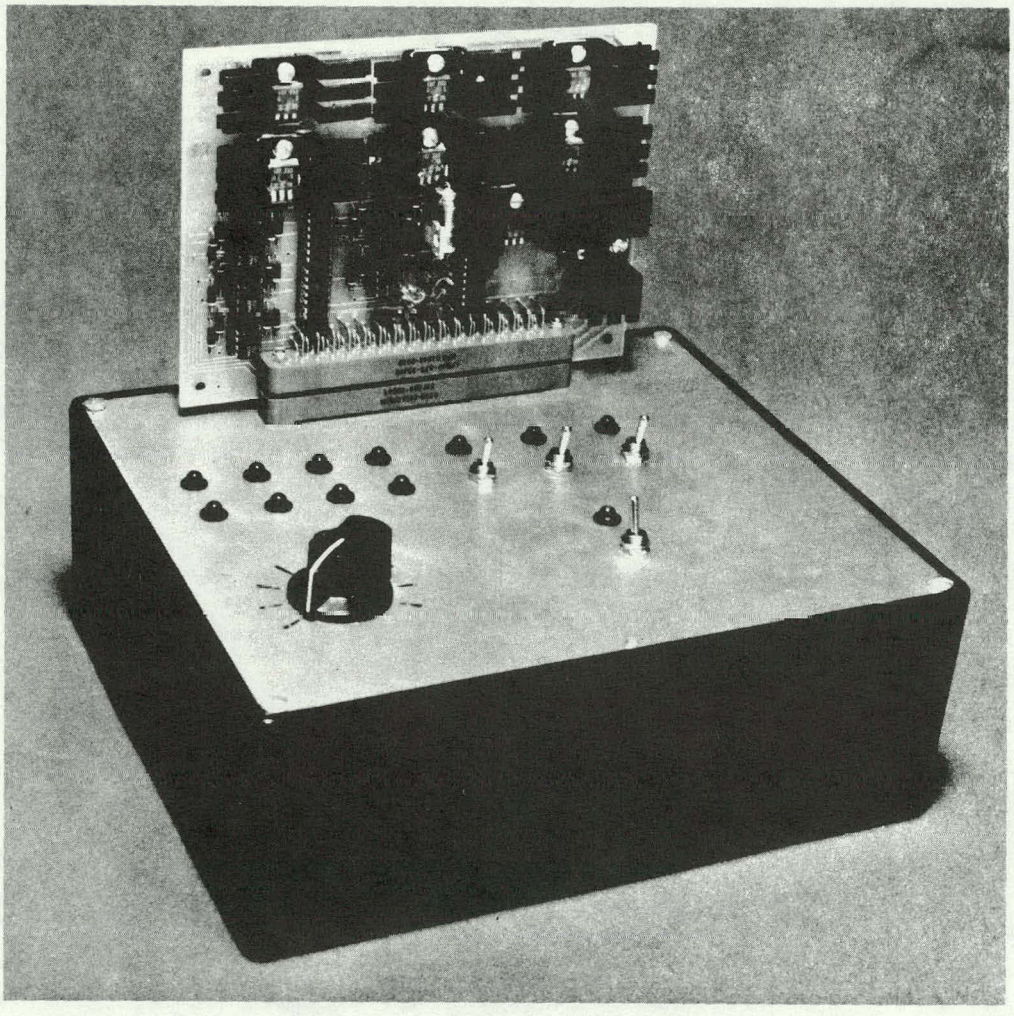

Figure 8.1-2. Coil Driver Card Exerciser

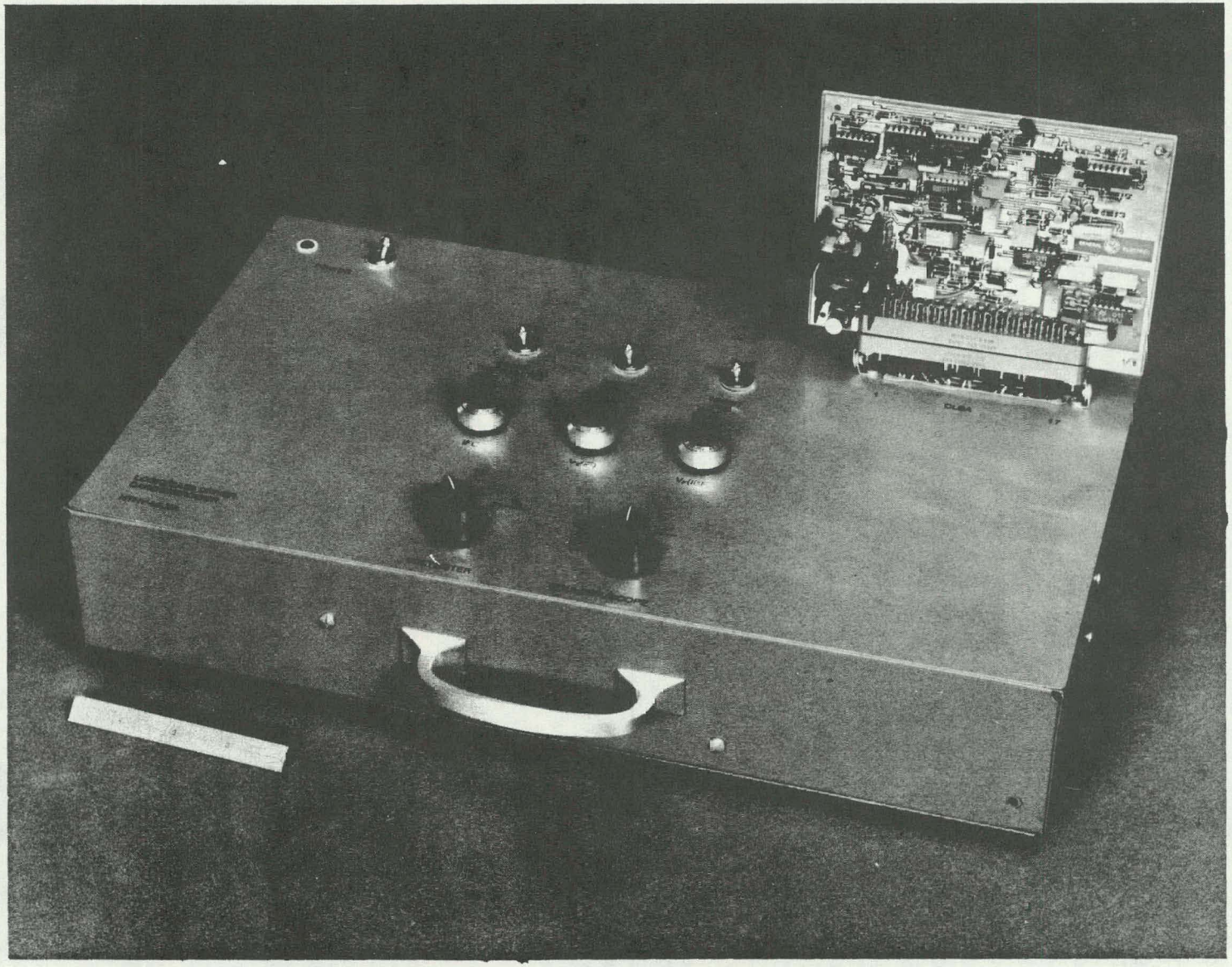

Figure 8.1-3. Field Chopper Card Exerciser

(IBF). Also, three inhibit inputs are provided as switches. A voltmeter, oscilloscope, or frequency counter may be connected to the device for calibrating circuitry of each of the above three signals. The box is approximately 2 in. high, 16 in. long, 12 in. wide, and weighs approximately 16 lb.

The debug panel is a digitally based fixture that provides access to all the microcontroller functions. It is specifically designed for human interface to the microprocessor-based controller. The functions include key pad inputs for programming and LED display outputs for observing. The device operates dynamically with the controller during the controller standby modes or during actual vehicular operation. Typically, constants, variables, programs, or any other memory locations may be observed by entering the proper commands and viewing the result on a display. Four alphanumeric displays can be programmed to output any of these parameters dynamically or statically. The key pad may also be used to change values in the microcontroller's RAMs. Sixteen individual LEDs are also included as programmable status indicators. Figure 8.1-4 is a photograph of the debug panel.

The controller exerciser (Figure 8.1-5) simulates all of the electrical signals, both input and output, of the HTV vehicle. There are a total of 71 signals in the form of switches, LED indicators, panel meters, and potentiometers that appear on the front panel. These devices feed directly to and from the microcontroller or lead to signal conditioning. Inside the exerciser is a signal-conditioning board that provides the frequency modulated signals, delays, and voltage sources for input to the vehicle controller. This board requires a ± 15 V power supply and a $+5$ V power supply external to the box. These supplies do not power the microcontroller or any other peripheral devices. Interconnection to the vehicle controller is achieved through a cable that is pin compatible with the microcomputer's main connector. This complete unit, except cables, is installed in a portable box ready for simple hookup and fast debugging.

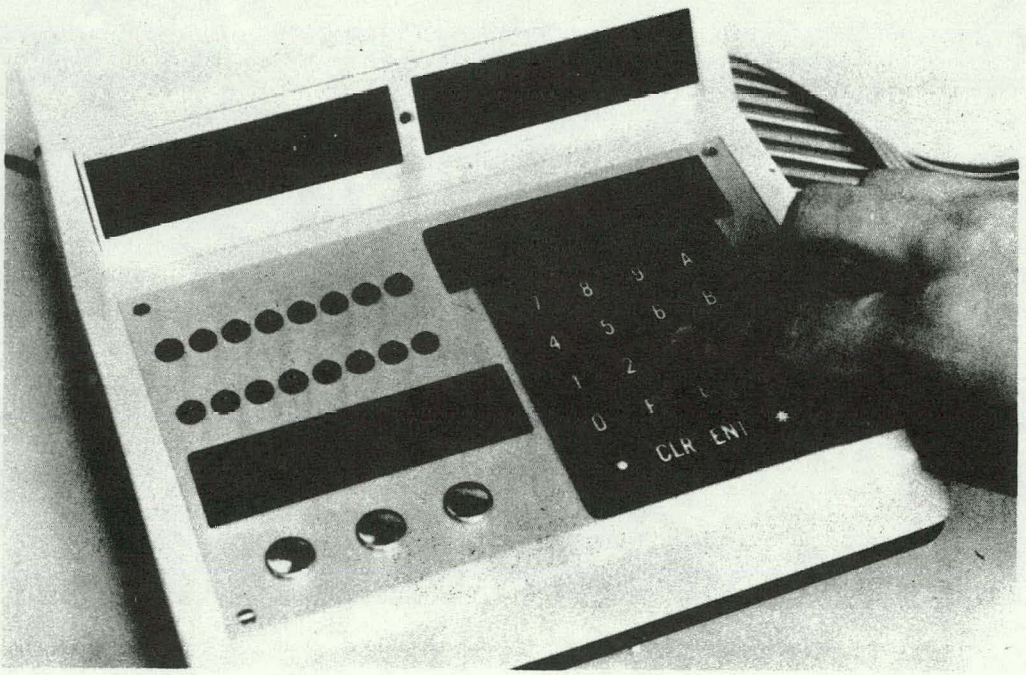

Figure 8.1-4. Debug Panel

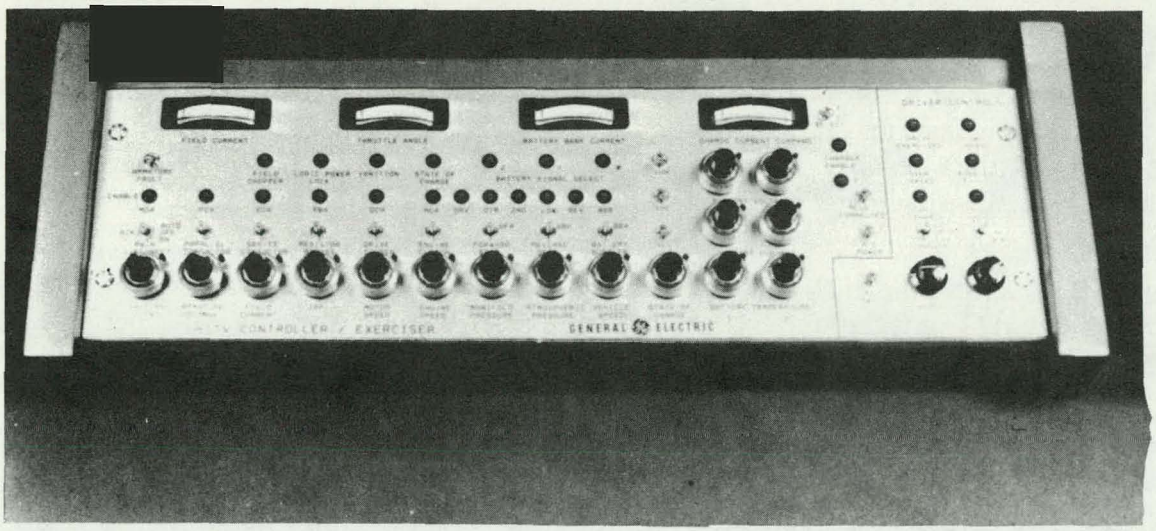

Figure 8.1-5. HTV Controller Exerciser

8.2 DATA ACQUISITION SYSTEM

A microcomputer-based data acquistion system has been developed to acquire data directly from the HTV and HPTM vehicle controller. This data acquisition system uses an Intel 8612A single-board microcomputer that contains an Intel 16-bit 8086 microprocessor. The system contains a 32K RAM buffer memory that allows continuous data acquisition.

Signal data acquired by this data acquisition system includes sensor signals [analog, logic, pulse frequency modulated (PFM), and pulse width modulated (PWM)] plus microcomputer calculated data. Example sensor signals include: armature current (IA); electric motor speed (WEM); and manifold absolute pressure (MAP). Example microcomputer calculated data includes: heat engine power command (PHEC); computed heat engine power (PHE); gear ratio (GRN); transmission gear command (TRN); and V_{MOD}.

During HTV road and track tests, data collected by the data acquisition system can be stored on a digital cassette tape. Dynamometer test data can be transmitted directly to a laboratory computer via an IEEE 488 bus. This mode of operation does not have the data storage list as in the portable mode using the digital cassette tape. In a third mode of operation, data previously recorded on cassette tape can be read to a laboratory computer via an IEEE 488 bus.

Sampling rate is programmable via front panel keys. Sampling rates can be selected from once every 32 ms to once every 4.096 s.

For operator convenience, the data acquisition system was designed to store predefined data groups, consisting of:

Group	Data Type
0	Hybrid data
1	EM only data
2	H.E. only data
3	On-board battery charging data
4	All data

Data storage time on the cassette tape is a function of the sampling interval and the data group selected. For example, sampling all data (Group 4) every 32 ms, the 450 ft tape will store approximately 1.5 min of test data. At the other extreme, a battery charger test

(Group 3) sampling at 4.096 s, the cassette tape will store approximately 10.5 hr of test data. An internal dc-dc converter allows operation directly from the vehicle 12 V accessory battery during road and track testing. Input power for the data acquisition system is approximately 10 A at 12 V dc. During dynamometer testing the data acquisition is powered from a 12 V dc power supply.

Figure 8.1-6 shows the HTV Data Acquisition System. This system was used extensively for HPTM and HTV integration tests as well as vehicle road and dynamometer performance testing.

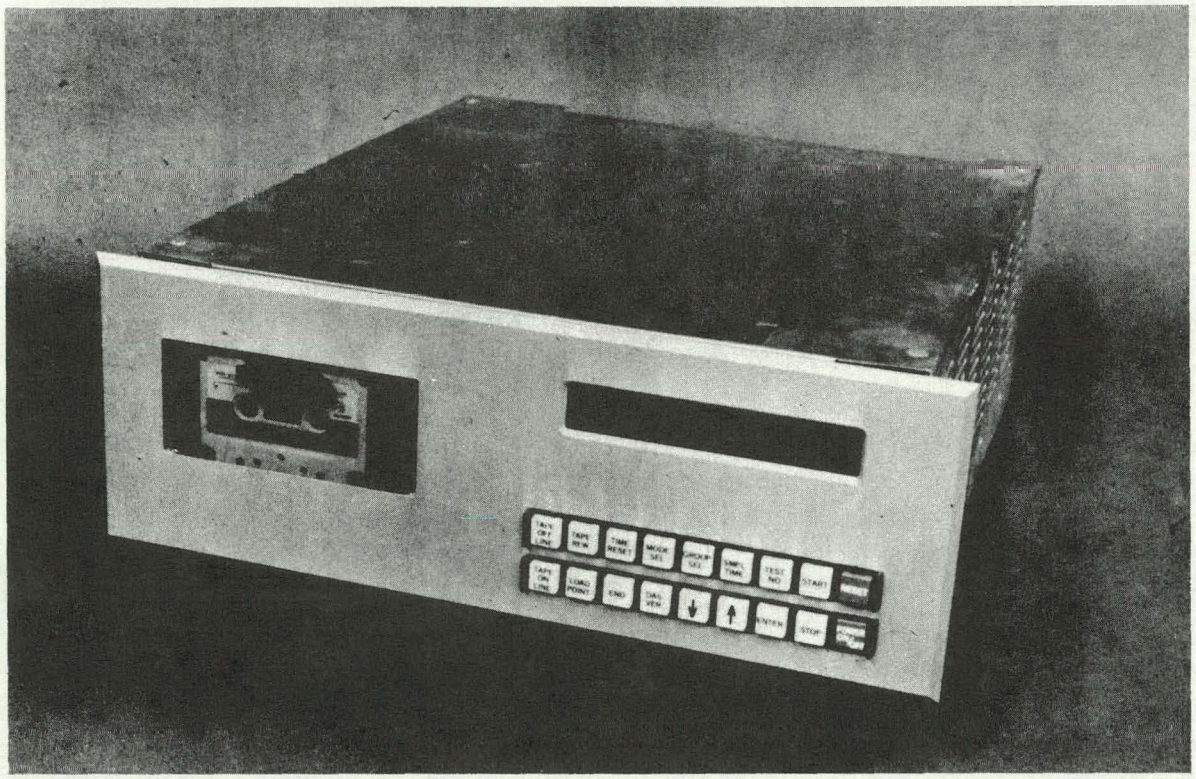

Figure 8.1-6. Data Acquisition System

REFERENCES

[1] *Near-Term Hybrid Vehicle Program, Final Report - Phase I*, SRD-134/1-7.

[2] *Near-Term Hybrid Passenger Vehicle Development Program -- Phase I, Guidelines and Assumptions*, Jet Propulsion Laboratories, received September 27, 1978.

[3] L.W. DeRaad, *The Influence of Road Surface Texture on Tire Rolling Resistance*, SAE Paper 780257, March 1978.

[4] A.F. Burke and G.E. Smith, *Impacts of Use-Pattern on the Design of Electric and Hybrid Vehicles*, SAE Paper 810265, February 1981.

[5] S.A. Velinsky and R.A. White, *Increased Vehicle Energy Dissipation Due to Changes in Road Roughness with Emphasis on Rolling Losses*, SAE Paper 790653, June 1979.

[6] M.C. Trummel and A.F. Burke, "Development History of the Hybrid Test Vehicle," *IEEE Transactions of Vehicular Technology, Vol. VT-32* (1), February 19, 1983.

[7] *Hybrid Vehicle Program Test Report - Test Bed Mule*, GE Report SRD-81-091, November 1981.

[8] A.F. Burke, *The Hybrid Test Vehicle (HTV) - From Concept through Fabrication and Marketing*, GE Report No. 82CRD174, June 1982.

[9] A.F. Burke and C.B. Somuah, *Computer-Aided Design of Electric and Hybrid Vehicles*, GE Report No. 81CRD212, August 1981.

[10] A.F. Burke, "A Family of Hybrid (Electric/ICE) Passenger Cars," EVC Symposium No. VI Proceedings, Paper No. 8144, Baltimore, MD, October 21-23, 1981.

[11] A.F. Burke and R. Miersch, "Development of a Full-Size (Electric/ICE) Passenger Car," Electric Vehicle Development Group Fourth International Conference of Hybrid, Dual Mode, and Tracked Systems, London, England, September 15-16, 1981.

[12] C.B. Somuah and R.D. King, "Development and Integration Tests of a Microcomputer Controlled Hybrid Vehicle," 1982 SAE Congress, Detroit, Michigan, February 22-26, 1982.

[13] A.F. Burke, B.K. Bose, R.D. King, C.B. Somuah, and M.A. Pocobello, ' Microcomputer Controlled Powertrain for a Hybrid Vehicle," Workshop on Automotive Applications of Microprocessors, Dearborn, Michigan, October 7-8, 1982.

[14] R.D. King, C.F. Saj, J.N. Park, and P.M. Szczesny, "A Microcomputer Controlled Hybrid Vehicle with On-Board Battery Charger," 18th Intersociety Energy Conversion Engineering Conference, Orlando, Florida, August 21-26, 1983.

[15] J.W.A. Wilson, "The Drive System of the DOE Near-term Electric Vehicle (ETV-1)" SAE Paper 8000 58, 1980.

[16] E.A. Rowland and K.W. Schwavze, "System Design of the Electric Test Vehicle (ETV-1)," SAE Paper 8000 57, 1980.